

The Synthesis of Low-Coordinate Transition Metal Complexes of the Heavier Group 13 Elements

Natalie D Coombs MChem. (Hons)

A thesis submitted to the University of Wales in accordance with the requirements for the degree of Doctor of Philosophy in the Faculty of Science, Department of Chemistry, University of Wales, Cardiff.

August 2008

UMI Number: U585148

All rights reserved

INFORMATION TO ALL USERS

The quality of this reproduction is dependent upon the quality of the copy submitted.

In the unlikely event that the author did not send a complete manuscript and there are missing pages, these will be noted. Also, if material had to be removed, a note will indicate the deletion.



UMI U585148

Published by ProQuest LLC 2013. Copyright in the Dissertation held by the Author.
Microform Edition © ProQuest LLC.

All rights reserved. This work is protected against
unauthorized copying under Title 17, United States Code.



ProQuest LLC
789 East Eisenhower Parkway
P.O. Box 1346
Ann Arbor, MI 48106-1346

Acknowledgements

Firstly I would like to extend my sincerest thanks to my supervisor, Dr Simon Aldridge for all his ideas and guidance throughout the last three years.

I would like to acknowledge the contributions made by the following people:

The people who performed the crystallography described in this thesis: Drs Li-Ling Ooi, Andreas Stasch, William Clegg, Amber Thompson, Andrew Cowley, Miss Joanna Day and Prof. Cameron Jones.

Drs Dave Willock, Andrea Rossin and Mr James Landon for all their help and guidance in showing me how to perform the theoretical calculations and also for carrying out some of the calculations described in this thesis.

Dr Debbie Kays (née Coombs) for initial syntheses of the complexes $[\text{Cp}^*\text{Fe}(\text{CO})_2]_2\text{InBr}$, $[\text{Cp}^*\text{Fe}(\text{CO})_2]_2\text{InI}$, $[\{\text{Cp}^*\text{Fe}(\text{CO})_2\}_2(\mu\text{-In})][\text{BAr}'_4]$, $[\{\text{Cp}^*\text{Fe}(\text{CO})_2\}_2(\mu\text{-I})][\text{BAr}'_4]$ and $[\{\text{Cp}^*\text{Fe}(\text{CO})_2\}_2(\mu\text{-In}\cdot\text{thf})][\text{BAr}'_4]$.

Drs Ian Fallis and Angelo Amoroso for numerous discussions (chemical and otherwise) and for allowing me to use some of their chemicals and equipment.

The technical staff – (Cardiff University) Alan, Dr Rob Jenkins, Ricky, Gaz, Robin and Jobo; (Oxford University) Dr Nick Rees.

Thanks to EPSRC National Crystallography and Mass Spectrometry Service Centres at Southampton and Swansea, respectively.

A big thank you to the members of labs 1.124, 1.125 and the Jones group (Cardiff University), and S12 (Oxford University) past and present for always sharing a laugh and for providing much entertainment, especially Debbie, Glesni, Jo, Chris, Alex, Neha, Cerys, Mark, Tom, Nat B, Dave M, Andreas, Rich, Dan, Matt and James.

A big thanks must go to my sister Dr Debbie Kays (née Coombs) not only for all the help and support she gave me as the lab post doc but also for giving me somewhere to stay during my time spent at Oxford University.

I would like to thank Mum, Dad, and brother-in law Andrew for their unconditional love and support.

Finally a special, thanks must go to my fiancé Jonny, for the immeasurable love and support he has given me over the past three years.

Abstract

This thesis describes the synthesis, structural and reaction chemistry of a number of novel gallium and indium containing species, including metal complexes featuring previously unreported gallium and indium ligand systems.

The synthesis, spectroscopic and structural characterisation of the asymmetric haloindyl ($\eta^5\text{-C}_5\text{R}_5\text{Fe}(\text{CO})_2\text{In}(\text{Mes}^*)\text{Br}$ ($\text{R} = \text{H}, \text{Me}$) and halogallyl $\text{Cp}^*\text{Fe}(\text{CO})_2\text{Ga}(\text{Mes})\text{I}$ complexes are reported herein, with $\text{Cp}^*\text{Fe}(\text{CO})_2\text{In}(\text{Mes}^*)\text{Br}$ representing the first example of structurally characterised asymmetric bromoindyl complex. $\text{Cp}^*\text{Fe}(\text{CO})_2\text{In}(\text{Mes}^*)\text{Br}$ is a versatile substrate for the synthesis of asymmetric indyl complexes via substitution chemistry, thereby allowing the synthesis and characterisation of $\text{Cp}^*\text{Fe}(\text{CO})_2\text{In}(\text{Mes}^*)\text{ER}_n$ ($\text{ER}_n = \text{OC}_6\text{H}_4\text{Bu-4}, \text{SPh}$).

The synthesis, spectroscopic and structural characterisation of the dihalogallyl complex $\text{Cp}^*\text{Fe}(\text{dppe})\text{GaI}_2$ is also reported; this synthesis was accomplished *via* photolytic displacement of the carbonyl ligands in $[\text{Cp}^*\text{Fe}(\text{CO})_2\text{GaI}_2]_2$ by dppe [1,2-bis(diphenylphosphino)ethane]. $\text{Cp}^*\text{Fe}(\text{dppe})\text{GaI}_2$ has proven to be versatile reagent in the generation of the asymmetric halogallyl species via substitution chemistry with retention of the iron-gallium bond, thereby allowing the synthesis and characterisation of $\text{Cp}^*\text{Fe}(\text{dppe})\text{Ga}(\text{Mes})\text{I}$. The diiodogallyl complex has also been implicated in the synthesis of the first structurally characterised base-free cationic gallylene complex $[\text{Cp}^*\text{Fe}(\text{CO})_2\text{GaI}]^+[\text{BAR}'_4]^-$, bearing a terminally bound GaI ligand which is valence isoelectronic with CO and N_2 . Investigations into the synthesis of molybdenum- and ruthenium-phosphine containing systems are also reported herein. Insertion of 'GaI' into metal-halogen bonds has proved to a viable synthetic route, for example in the formation of $[(\eta^7\text{-C}_7\text{H}_7)\text{Mo}(\text{CO})_2\text{GaI}_2]_2$. Further reaction of $[(\eta^7\text{-C}_7\text{H}_7)\text{Mo}(\text{CO})_2\text{GaI}_2]_2$ with dppe, however, has been shown to yield $[(\eta^7\text{-C}_7\text{H}_7)\text{Mo}(\text{CO})_2\text{GaI}_2]_2(\mu\text{-dppe})$. Investigation of 'GaI' insertion reactions involving ruthenium-halogen bonds have shown to yield the tetraiodogallate species $\text{CpRu}(\text{PPh}_3)_2(\mu\text{-I})\text{GaI}_3$ and $[\text{CpRu}(\text{dppe})][\text{GaI}_4]$.

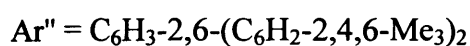
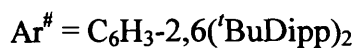
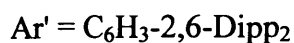
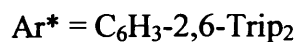
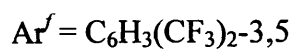
The synthesis, spectroscopic and structural characterisation of the bridging halo-indanediyl complexes $[\text{Cp}^*\text{Fe}(\text{CO})_2]_2\text{InX}$ ($\text{X} = \text{Br}, \text{I}$) are reported. The bromo-substituted species has proven to be a useful precursor in the synthesis of the cationic trimetallic system $[\{\text{Cp}^*\text{Fe}(\text{CO})_2\}_2(\mu\text{-In})]^+[\text{BAR}'_4]^-$, the formation of which has been shown to be strongly dependant on the nature of abstracting agent and on the identity of the halide. Reactivity studies of $[\{\text{Cp}^*\text{Fe}(\text{CO})_2\}_2(\mu\text{-E})]^+$ ($\text{E} = \text{Ga}, \text{In}$) involving the addition of nucleophiles has allowed the synthesis and characterisation of the three-coordinate cationic complexes $[\{\text{Cp}^*\text{Fe}(\text{CO})_2\}_2(\mu\text{-E:L})]^+[\text{BAR}'_4]^-$ ($\text{E} = \text{Ga}, \text{In}; \text{L} = \text{thf}, 4\text{-picoline}, \text{PPh}_3$).

The syntheses and metallation of sterically bulky carbazol-9-yl ligands derived from 1,8-diaryl-3,6-dimethylcarbazole are described herein. Furthermore, the synthesis and structural characterisation of the amidogallyl complexes (1,8-diphenyl-3,6-dimethylcarbazol-9-yl)gallium dichloride and (1,8-dimesityl-3,6-dimethylcarbazol-9-yl)gallium dichloride are reported by salt metathesis reactions involving gallium trichloride. Investigations of subsequent reduction chemistry using potassium metal yielded the potassium salt [1,8-diphenyl-3,6-dimethylcarbazol-9-yl]potassium.

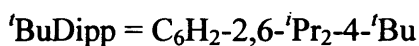
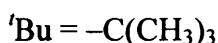
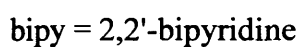
Quantum chemical investigations using Density Functional Theory have been explored to probe the electronic structure in the novel bond types. In particular, studies targeted factors affecting the degree of π back-bonding (and hence multiple bond character) within the TM-ER bond.

Notes

The following abbreviations were used in the text:



b = broad



cm^{-1} = wavenumber

cod = cyclooctadiene



Cy = cyclohexyl

δ = NMR chemical shift

d = doublet, days

dd = doublet of doublets

DFT = density functional theory

Dipp = 2,6-diisopropylphenyl, $\text{C}_6\text{H}_3\text{-}$

2,6- $^i\text{Pr}_2$

dmpe = 1,2-

bis(dimethylphosphino)ethane

dppe = 1,2-

bis(diphenylphosphino)ethane

dtbpy = 4,4'- ^iBu -2,2'-bipyridyl

dvds = 1,3-divinyl-1,1,3,3-

tetramethyldisiloxane

EI = electron impact

ES = electrospray



FT = Fourier transform

h = hours

HOMO = highest occupied molecular

orbital

Hz = Hertz

IR = infrared

LUMO = lowest unoccupied molecular

orbital

m = multiplet

md = medium

Me = $-\text{CH}_3$

Mes = mesityl, $\text{C}_6\text{H}_2\text{-2,4,6-Me}_3$

Mes* = supermesityl, $\text{C}_6\text{H}_2\text{-2,4,6-}^i\text{Bu}_3$

min = minutes

MS = mass spectrometry

m/z = mass/charge ratio

μ = bridging mode of coordination

ν = stretching mode

NHC = N-heterocyclic carbene

NMR = nuclear magnetic resonance

OTf = triflate, $[\text{OSO}_2\text{CF}_3]^-$

Ph = $-\text{C}_6\text{H}_5$

4-pic = 4-picoline

ppm = parts per million

PPN = bis(triphenylphosphoranylidene)-

ammonium

$^i\text{Pr} = -\text{CH}(\text{CH}_3)_2$

q = quartet

s = singlet

sh = shoulder

st = strong

t = triplet

tert = tertiary

thf = tetrahydrofuran

TMEDA = N,N,N',N'-

tetramethylethane-1,2-diamine

tmp = 2,2,6,6-tetramethylpiperidine

$\text{Tp}^i\text{Bu}_2 = \text{tris}(3,5\text{-di-tert-butylpyrazolyl})$

hydroborato

Trip = 2,4,6-triisopropylphenyl,

$\text{C}_6\text{H}_2\text{-2,4,6-}^i\text{Pr}_3$

Contents

	Page
Chapter One Introduction	
1.1 Introduction	1
1.2. Gallyl and Indyl Complexes	2
1.2.1 History of Gallyl and Indyl Complexes	2
1.2.2 Synthesis of Gallyl and Indyl Complexes	3
1.2.2.1 Synthesis of Gallyl and Indyl Complexes: Alkane Elimination	3
1.2.2.2 Synthesis of Gallyl and Indyl Complexes: Insertion of Metal(I) Halides	5
1.2.2.3 Synthesis of Gallyl and Indyl Complexes: Salt Elimination	7
1.2.2.4 Synthesis of Gallyl Complexes: Dehalosilylation	11
1.3 Spectroscopic and Structural Aspects of Gallyl and Indyl Complexes	12
1.3.1 Bonding in Gallyl and Indyl Complexes	12
1.3.2 Spectroscopic Features for Gallyl and Indyl Complexes	14
1.3.3 Structural Features of Gallyl and Indyl Complexes	15
1.3.4 Reactivity of Gallyl and Indyl complexes	17
1.4 Group 13 Diyl Complexes	18
1.4.1 History of Group 13 Diyl Complexes	18
1.4.2 Synthesis of Group 13 Diyls	18
1.4.2.1 Synthesis of Group 13 Diyls: Dehalogenation	18
1.4.2.2 Synthesis of Group 13 Diyls: Salt Elimination	19
1.4.3 Structure and Bonding of Group 13 Diyl Complexes	22
1.5 Group 13 Amido Complexes	23
1.5.1 Synthesis of Anionic 5-Membered Group 13(I) Heterocycles	23
1.5.2 Synthesis of Neutral 6-Membered Group 13(I) Heterocycles	26
1.5.3 Synthesis of 4-Membered Group 13(I) Heterocycles	28
1. 6 Transition Metal Complexes of Group 13 Diyl Ligands	29
1.6.1 Introduction to Transition Metal Complexes of Group 13 Diyl Ligands	29
1.6.2 Synthesis of Transition Metal Complexes of Group 13 Diyl Complexes	29
1.6.2.1 Neutral Systems	29

	Page
1.6.2.1.1 Substitution of Labile Ligands	30
1.6.2.1.2 Salt Elimination	32
1.6.2.1.3 ER Insertion	34
1.6.2.1.4 Addition of ER	36
1.6.2.1.5 Oxidation of ER	37
1.6.3 Group 13 Metalladiyl Complexes	38
1.6.3.1 Neutral Metalladiyl Complexes	38
1.6.4 Aspects of Bonding in Transition Metal Complexes of Group 13 Diyls	39
1.6.4.1 Bonding in Diyl Complexes	39
1.6.4.2 Structural and Spectroscopic Aspects of Transition Metal Group 13 Diyl Complexes	40
1.6.4.3 Theory of Bonding in Transition Metal Group 13 Diyl Complexes	43
1.6.4.4 Reactivity of Transition Metal Complexes of Group 13 Diyls	47
1.6.4.4.1 Substitution/Addition Reactions of Transition Metal Complexes of Group 13 Diyls	47
1.6.4.4.2 Bond Activation Reactions of Transition Metal Complexes of Group 13 Diyls	47
1.6.4.4.3 Formation of Cluster Complexes by Transition Metal Complexes of Group 13 diyls	48
1.6.5 Cationic Transition Metal Group 13 Diyl Complexes	49
1.6.5.1 Cationic M-ER Systems	49
1.6.5.2 Cationic M-E-M Complexes	54
1.6.5.3 Anionic M-E-M Complexes	57
1.7 Aims of this Research	57
1.8 References for Chapter One	59

Chapter Two Experimental Techniques

2.1 The Manipulation of Air Sensitive Complexes	68
2.1.1 Inert Atmosphere Techniques	68
2.1.2 High Vacuum Techniques	70
2.2 Physical Measurements	71
2.2.1 NMR Spectroscopy	71

	Page
2.2.2 Infrared Spectroscopy	71
2.2.3 Mass Spectrometry	71
2.2.4 Chemical Analysis	72
2.2.5 X-ray Crystallography	72
2.2.6 Theoretical Calculations	72
2.3 Purification and Preparation of Essential Solvents and Reagents	76
2.3.1 Preparation of Transition Metal Anions	80
2.3.2 Preparation of Transition Metal Halides	81
2.3.3 Preparation of Aryl Anions	84
2.3.4 Preparation of [1,8-diphenyl-3,6-dimethylcarbazol-9-yl]Li	86
2.3.5 Preparation of [2,4,6- ^t Bu ₃ C ₆ H ₂ EX ₂] (E = Ga, In, X = Cl, Br)	88
2.3.6 Preparation of Ga(N(SiMe ₃) ₂)Cl ₂ ·thf	89
2.3.7 Preparation of Transition Metal-Group 13 complexes	90
2.3.8 Preparation of Halide Abstracting Agents	91
2.3.9 Synthesis of Aryl Boronic Acids	92
2.4 References for Chapter Two	95

Chapter Three Asymmetric Indyl and Gallyl Complexes: Synthesis and Reactivity

3.1 Introduction	98
3.1.1 Aims of Research	101
3.2 Synthesis of Asymmetric Haloindyl and Halogallyl Species	102
3.2.1 Experimental	102
3.2.2 Results and Discussion	104
3.2.2.1 Asymmetric Haloindyl Species	104
3.2.2.2 Asymmetric Halogallyl Species	108
3.3 Synthesis of Symmetric Bridging Amido Gallyl Complexes – Attempted	111
Synthesis of Asymmetric Amino Halogallyl Species	
3.3.1 Experimental	111
3.3.2 Results and Discussion	112
3.4 Substitution Chemistry of Asymmetric Haloindyl Complexes	115
3.4.1 Experimental	115

	Page
3.4.2 Results and Discussion	117
3.5 Halide Abstraction Chemistry of Asymmetric Haloindyl and Halogallyl Complexes	121
3.5.1 Experimental	121
3.5.2 Results and Discussion	123
3.6 Trapping Reactions	128
3.6.1 Experimental	128
3.6.2 Results and Discussion	131
3.7 Conclusions and Suggestions for Further Research	137
3.8 References for Chapter Three	139

Chapter Four Phosphine Substituted Complexes: Synthesis and Reactivity

4.1 Introduction	142
4.1.1 Aims of Research	143
4.2 Phosphine-Iron Containing Systems	143
4.2.1 Synthesis of Asymmetric Halogallyl Complexes	143
4.2.1.1 Experimental	143
4.2.1.2 Results and Discussion	147
4.2.2 Halide Abstraction Chemistry of Asymmetric Halogallyl Complexes	158
4.2.2.1 Experimental	158
4.2.2.2 Results and Discussion	161
4.2.3 Reactions of $[\text{Cp}^*\text{Fe}(\text{dppe})\text{GaI}]^+[\text{BAR}^f_4]^-$	174
4.2.3.1 Experimental	174
4.2.3.2 Results and Discussion	175
4.3 Attempted Synthesis of Heavier Group 13 Analogues of $\text{Cp}^*\text{Fe}(\text{dppe})\text{EI}_2$	177
4.3.1 Experimental	177
4.3.2 Results and Discussion	178
4.4 Molybdenum Containing Systems	181
4.4.1 Experimental	181
4.4.2 Results and Discussion	185
4.5 Ruthenium Containing Systems	196

	Page
4.5.1 Attempted 'Gal' Insertion into Metal-Halogen Bonds	196
4.5.1.1 Experimental	196
4.5.1.2 Results and Discussion	198
4.6 Conclusions and Suggestions for Further Work	205
4.7 References for Chapter Four	208

**Chapter Five Trinuclear Complexes Containing a 'Naked' Bridging
Group 13 Atom: Synthesis and Reactivity**

5.1 Introduction	211
5.1.1 Aims of Research	214
5.2 Synthesis of $[(\eta^5\text{-C}_5\text{R}_5)\text{Fe}(\text{CO})_2]_2\text{InX}$ Systems	215
5.2.1 Experimental	215
5.2.2 Results and Discussion	216
5.2.2.1 Salt elimination	216
5.2.2.2 Insertion of InI	219
5.3 Halide Abstraction Chemistry	222
5.3.1 Experimental	222
5.3.2 Results and Discussion	224
5.4 Trapping Reactions	233
5.4.1 Experimental	233
5.4.2 Results and Discussion	237
5.5 Attempted Syntheses of Phosphine Containing Bridging Systems	246
5.5.1 Experimental	246
5.5.2 Results and Discussion	247
5.6 Conclusions and Suggestions for Further Research	248
5.7 References for Chapter Five	250

Chapter Six Halogallyl Amido Complexes: Synthesis and Reactivity

6.1 Introduction	252
6.1.1 Aims of Research	255
6.2 Synthesis of Halogallyl Amido Complexes	256
6.2.1 Experimental	256

	Page
6.2.2 Results and Discussion	259
6.3 Attempted Reduction Chemistry	269
6.3.1 Experimental	269
6.3.2 Results and Discussion	270
6.4 Attempted Synthesis from Metal(I) Halides	274
6.4.1 Experimental	274
6.4.2 Results and Discussion	275
6.5 Conclusions and Suggestions for Further Research	275
6.6 References for Chapter Six	277

Chapter Seven DFT Calculations of Group 13 Diyl Complexes: Structure and Bonding

7.1 Introduction	281
7.1.1 Aims of Research	286
7.2 Singlet Versus Triplet States	287
7.2.1 Results	287
7.2.2 Discussion of Results	287
7.3 EX Complexes (X = F, Cl, Br, I)	289
7.3.1 Results	289
7.3.2 Discussion of results	291
7.4 Sterically Demanding Borylene and Gallylene Complexes	295
7.4.1 Results	295
7.4.2 Discussion of Results	296
7.5 Base Stabilised Adducts	298
7.5.1 Results	298
7.5.2 Discussion of Results	299
7.6 Conclusions and Suggestions for Further Research	300
7.7 References for Chapter Seven	302

Appendix One List of Publications i

Appendix Two Crystal Structure Data CD

Chapter One

Introduction

1.1 Introduction

The possibility of forming transition metal complexes featuring two-centre two-electron bonds with group 13 elements has been the subject of intense research interest. Within this area there are a number of structural types of group 13 boron, gallium and indium complexes featuring a two-centre two-electron interaction with a transition metal centre.¹ These structural types are shown in Figure 1² of which boryl complexes are the most numerous and feature a three coordinate boron centre. Synthetically the two most commonly used routes for the preparation of transition metal boryl complexes are (i) salt elimination, typically by the reaction between an anionic transition metal fragment and a haloborane precursor (although recent developments have opened up the reverse sense of this synthetic approach, utilizing the boryl anion), and (ii) oxidative addition of a B-B, B-H, B-X (X = Cl, Br) or even a B-Sn bond to a low valent, low coordinate transition metal fragment, typically generated by the loss of a labile ligand.³ It has been well established that for gallium and indium coordination numbers of three, four, five and even six are possible, when the group 13 centre is in its most common formal oxidation state of + III. The coordination number of the species is largely dependant on the nature of the element, the ligand and in the case of some anionic complexes, the balancing cation. Aggregation is a distinctive feature of the chemistry of the group 13 metals, reflecting the electrophilicity of the metal centre in relation to its ligands. This tendency for aggregation can be curbed by the coordinating action of suitable donor species or by the steric bulk of appropriate ligands.⁴

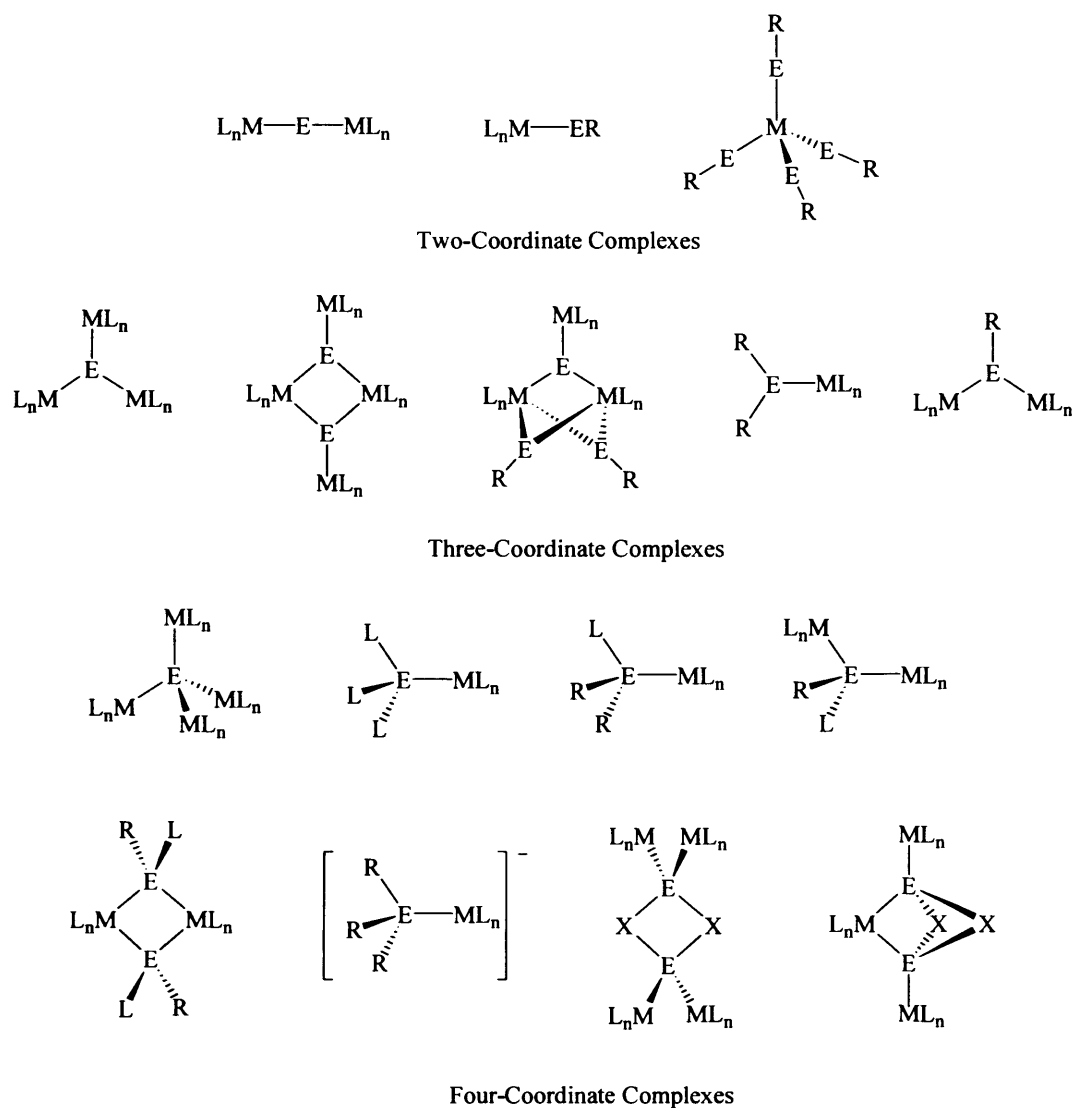


Figure 1

The chemistry of low coordinate or multiply bonded group 13 ligand systems is an area that has attracted considerable recent research interest with a view to examining the structure/bonding and reactivity of such systems.^{1b, 5-7}

1.2. Gallyl and Indyl Complexes

1.2.1 History of Gallyl and Indyl Complexes

Transition metal gallyl and indyl complexes of the type L_nMEX_2 (where $E = Ga$ or In) represent an important structural class of group 13 complexes potentially

featuring a three-coordinate gallium or indium centre. In addition, a number base stabilised derivatives of these species are known. The synthesis and chemistry of related transition metal boryl complexes has been the subject of extensive research interest; this has led to the development of a large number of structurally authenticated boryl complexes reported in the literature.^{1-3, 8} In comparison however, syntheses of analogous three-coordinate gallyl and indyl complexes are relatively rare.

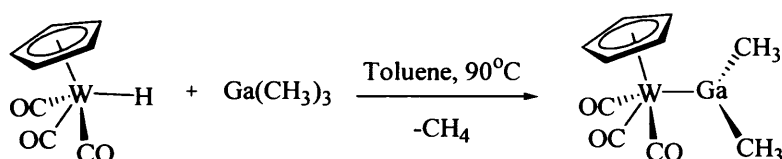
1.2.2 Synthesis of Gallyl and Indyl Complexes

A distinctive feature of gallium and indium metal chemistry is aggregation *via* bridging ligands (*e.g.* halides) as a result of the increase in the atomic radius of the group 13 atom on descending the group, and the increased polarity of bonds to gallium and indium compared to boron resulting in a much larger δ^+ charge on the group 13 metal centre. Thus, the formation of three coordinate systems is more favourable for boron compared to gallium and indium. There are a number of synthetic routes to the formation of gallyl and indyl complexes, with the most common synthetic route being salt elimination. This approach generally involves the reaction being carried out in a coordinating solvent; this is in marked contrast to the chemistry observed for boryl systems, which typically decompose in the presence of a coordinating solvent.

1.2.2.1 Synthesis of Gallyl and Indyl Complexes: Alkane Elimination

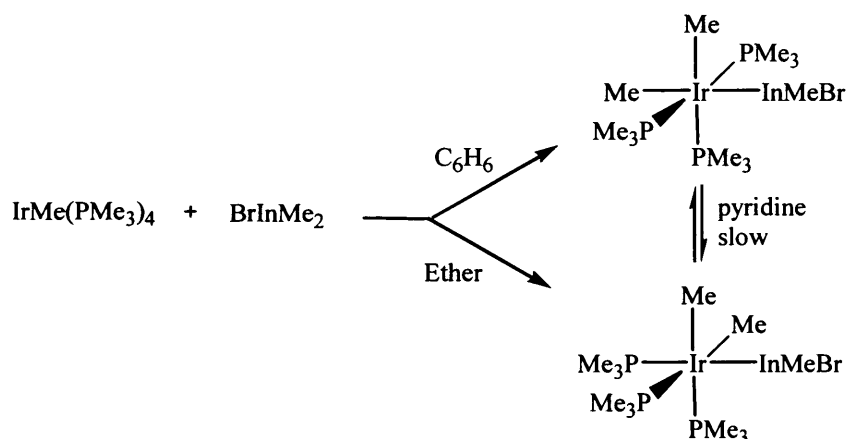
In 1977, the synthesis of the first example of a transition metal gallyl complex was reported by St. Denis *et al.* utilising alkane elimination chemistry.⁹ Reaction of $\text{CpW}(\text{CO})_3\text{H}$ with $\text{Ga}(\text{CH}_3)_3$ at elevated temperatures (*ca.* 90°C) with UV photolysis

resulted in the synthesis of $\text{CpW}(\text{CO})_3\text{Ga}(\text{CH}_3)_2$ with elimination of a single equivalent of methane (Scheme 1). It was proposed that the reaction proceeds *via* a radical mechanism. This synthetic methodology represents a rare example of alkane elimination of this type, as this chemistry is usually restricted to reactive M-H functions and sterically unhindered organometallic complexes.



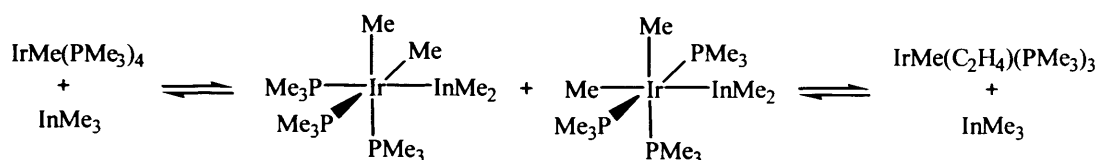
Scheme 1

Corresponding reactions are also known for indium. In 1989 Thorn and Harlow investigated reactions between methyl(trimethylphosphine)iridium(I) and alkylindium compounds, in which it was found that the reaction proceeds with alkylindium bond cleavage instead of Lewis acid-base adduct formation (Scheme 2).¹⁰ It was reported that (trimethylphosphine)methyliridium(I) compounds and the In-CH_3 bond of BrInMe_2 readily undergo oxidative addition of the In-alkyl bond in preference to the In-Br bond. The propensity of transition-metal compounds to add a main-group metal-alkyl or aryl bond in preference to a main group metal-halo bond has been reported for reactions between mixed organohalotin and -lead compounds and some $\text{Pt}(0)$ and $\text{Pt}(\text{III})$ complexes.¹¹ It was concluded that these addition reactions are probably controlled by a thermodynamic balance of energies of metal-alkyl and metal-halo compounds.



Scheme 2

Reactions of methyliridium(I) species with InMe_3 were also examined; it was found that in benzene or alkane solution both $\text{IrMe}(\text{PMe}_3)_4$ and $\text{IrMe}(\text{C}_2\text{H}_4)(\text{PMe}_3)_3$ react rapidly with the diethyl ether complex of InMe_3 to form mixtures of *fac*- and *mer*- $\text{IrMe}_2(\text{InMe}_2)(\text{PMe}_3)_3$ (Scheme 3). Ethylene reversibly displaces InMe_3 from compounds *fac*- and *mer*- $\text{IrMe}_2(\text{InMe}_2)(\text{PMe}_3)_3$, establishing an equilibrium with the compound $\text{Ir}(\text{Me})(\text{C}_2\text{H}_4)(\text{PMe}_3)_3$.



Scheme 3

1.2.2.2 Synthesis of Gallyl and Indyl Complexes: Insertion of Metal(I) Halides

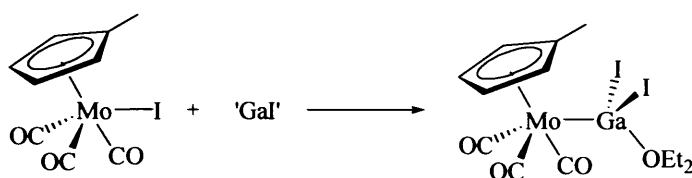
Insertion of a metal(I) halide into a metal-metal or metal-halogen bond was first utilised by Hsieh and Mays in the generation of a series of indium-transition metal complexes featuring E-M bonds.¹² It was demonstrated that insertion of indium(I) chloride into the Fe-Fe bond of the dimeric complex $[\text{CpFe}(\text{CO})_2]_2$ afforded

the diiron-indium chloride species $[\{\text{CpFe}(\text{CO})_2\}_2\text{InCl}]_x$; however no structural data was obtained and it wasn't until 1991 that Norman *et al.* structurally characterised the diiron indium chloride complex showing it to exist as the dimer $[\{\text{CpFe}(\text{CO})_2\}_2\text{InCl}]_2$ in the solid state.¹³ By analogy Hsieh and Mays found that insertion of InX ($\text{X} =$ halide), into iron-halogen bonds yielded the monoiron complexes $\text{CpFe}(\text{CO})_2\text{InX}_2$, and $\text{Cp}_2\text{Fe}(\text{CO})_2\text{InBr}_2(\text{thf})$.

In 1990, Green *et al.*, reported the novel synthesis of a compound formulated as 'GaI' by the ultrasonic activation of gallium metal with 0.5 equivalents of I_2 in toluene.¹⁴ It was found that the powder diffraction pattern of the resulting pale green precipitate differed from that previously reported by Corbett or Chadwick,^{15, 16} and from those for low-valent gallium iodides reported by Gerlach.¹⁷ It was however, similar to that prepared by Wilkinson and Worrall, which was shown to contain Ga , Ga_2I_3 and Ga_2I_4 units.¹⁸ It should be noted that the exact formulation of 'GaI' remains unknown but it has been proposed to exist as $[\text{Ga}]^+[\text{Ga}_2\text{I}_6]^{2-}$, based on Raman spectroscopic studies. Although not a homogeneous material, it has been found that this reactive pale green powder behaves in many respects as a monovalent gallium system. Its reactivity has been shown to be consistent with its acting as a source of gallium(I) *e.g.* the conversion of organometallic and organic iodides (RI) to gallyl derivatives of the type RGaI_2 . Jones *et al.* have reported the reactivity of 'GaI' with primary and secondary amines and secondary phosphines to yield a variety of gallium (II) iodide complexes of the type $[\text{Ga}_2\text{I}_4(\text{L})_2]$, ($\text{L} = \text{NR}_2\text{H}, \text{NRH}_2, \text{PR}_2\text{H}$) *via* disproportionation reactions.¹⁹ In addition other groups have seen similar reactivity of gallium sub-halides with tertiary amines, phosphines and arsines to yield gallium(I)

and (II) iodide complexes, *e.g.* $[\text{GaI}(\text{PEt}_3)]_9$, $[\text{Ga}_2\text{I}_4(\text{NEt}_3)_2]$, $[\text{Ga}_3\text{I}_5(\text{PEt}_3)_3]$ and $[\text{Ga}_2\text{I}_4(\text{AsEt}_3)_2]$.²⁰

The use of ‘GaI’ has been employed in the synthesis of a number of complexes featuring gallium-transition metal bonds *via* formal insertion of ‘GaI’ into a metal-metal or metal-halogen bond. Green *et al.* further investigated the insertion of ‘GaI’ into metal-iodine bonds.¹⁴ Reaction of $\text{CpFe}(\text{CO})_2\text{I}$ with ‘GaI’ followed by recrystallisation from diethyl ether yielded the complex $\text{CpFe}(\text{CO})_2\text{GaI}_2(\text{OEt}_2)$. Similarly, reaction of ‘GaI’ with $(\eta^7\text{-C}_7\text{H}_7)\text{Mo}(\text{CO})_2\text{I}$ or with $(\eta^5\text{-C}_5\text{H}_4\text{Me})\text{Mo}(\text{CO})_3\text{I}$ yielded similar complexes containing Mo-Ga bonds, *viz* $(\eta^7\text{-C}_7\text{H}_7)(\text{CO})_2\text{MoGaI}_2(\text{thf})$ and $(\eta^5\text{-C}_5\text{H}_4\text{Me})(\text{CO})_3\text{MoGaI}_2(\text{Et}_2\text{O})$ (Scheme 4) respectively, thus confirming the feasibility of insertion of ‘GaI’ into metal-halogen bonds in the generation of gallyl complexes featuring transition metals.

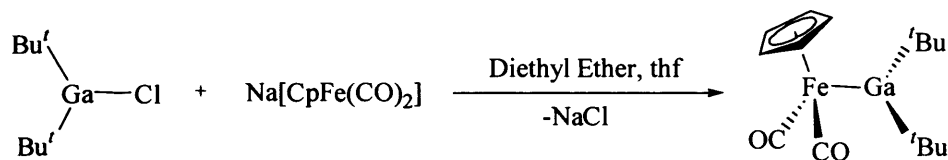


Scheme 4

1.2.2.3 Synthesis of Gallyl and Indyl Complexes: Salt Elimination

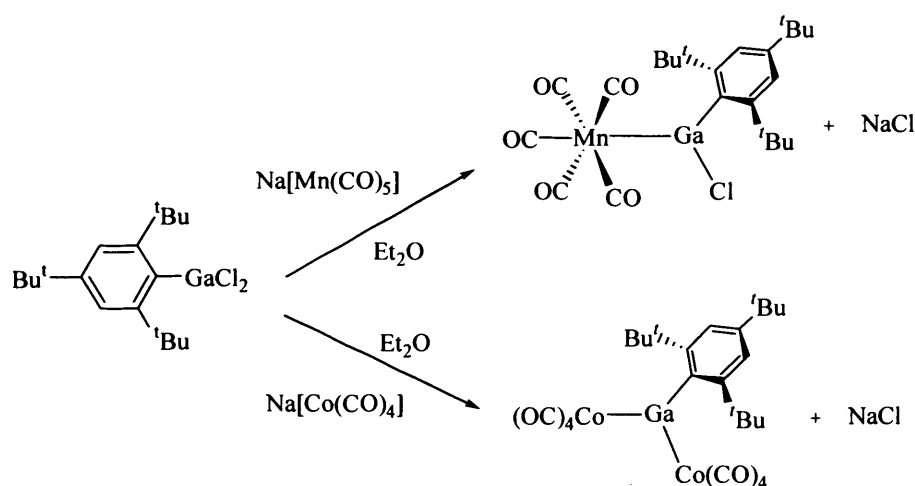
The reaction between an anionic transition metal fragment and a halogallyl or –indyl species is the most widely used synthetic route employed in the generation of gallyl and indyl complexes featuring transition metal fragments. Power *et al.* reported the synthesis of several three-coordinate organogallium-iron complexes featuring terminal alkyl groups utilising salt elimination chemistry.²¹ Reaction of $\text{Na}[\text{CpFe}(\text{CO})_2]$ with ‘ Bu_2GaCl ’ or ‘ BuGaCl_2 ’ in thf, generated the organogallium

species $\text{CpFe}(\text{CO})_2\text{Ga}^t\text{Bu}_2$, $[\text{CpFe}(\text{CO})_2]_2\text{Ga}^t\text{Bu}$, or $[\text{CpFe}(\text{CO})_2]\text{Ga}^t\text{Bu}_2[\text{CpFe}(\text{CO})_2]_2$ (Scheme 5).



Scheme 5

Cowley *et al.* subsequently utilised salt elimination chemistry in the synthesis of the complex $(\text{OC})_5\text{MnGa}(\text{Mes}^*)\text{Cl}$, featuring a gallium-manganese bond formed by treatment of $\text{Mes}^*\text{GaCl}_2$ with $\text{Na}[\text{Mn}(\text{CO})_5]$ with elimination of NaCl (Scheme 6). It was also found that the analogous reaction with $\text{Na}[\text{Co}(\text{CO})_4]$ led to the formation of the species $[\text{Co}(\text{CO})_4]_2\text{Ga}(\text{Mes}^*)$ (Scheme 6). This result was attributed to the reduced steric demands of the cobalt tetracarbonyl fragment compared to the manganese pentacarbonyl fragment.²²

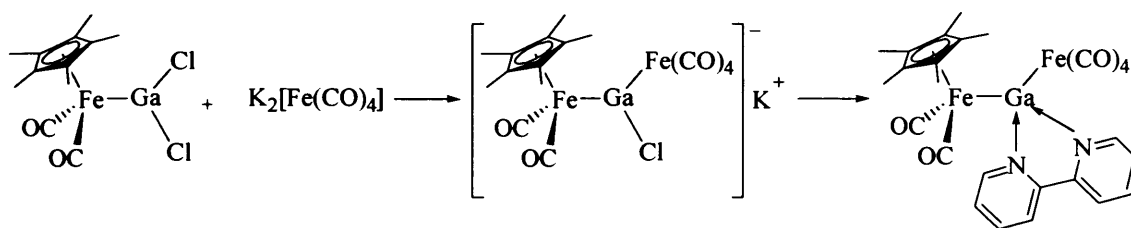


Scheme 6

Furthermore, Barron *et al.* demonstrated that the reaction between $\text{K}[\text{CpFe}(\text{CO})_2]$ and GaCl_3 is dependent on the reaction stoichiometry.²³ Reaction of

0.5 equivalents of GaCl_3 with $\text{K}[\text{CpFe}(\text{CO})_2]$ yielded the species $[\{\text{CpFe}(\text{CO})_2\}_2\text{Ga}(\mu\text{-Cl})]_n$ which is polymeric in the solid state and features bridging chlorides and pendant $\text{CpFe}(\text{CO})_2$ units. Reactions utilising 1 equivalent of GaCl_3 yielded the complex $[\{\text{CpFe}(\text{CO})_2\}\text{GaCl}_2]_n$, however this species was not structurally characterised; reaction with excess GaCl_3 generated the compound $[\{\text{CpFe}(\text{CO})_2\}\text{Ga}(\text{ClGaCl}_3)(\mu\text{-Cl})]_2$. The reactions of $\text{CpMo}(\text{CO})_3\text{H}$ with E^tBu_3 were also investigated and found to yield the monomeric complexes $\text{CpMo}(\text{CO})_3\text{E}^t\text{Bu}_2$ ($\text{E} = \text{Ga}, \text{Al}$). Furthermore, the analogous reaction of $\text{CpMo}(\text{CO})_3\text{H}$ with $(\text{BHT})_2\text{AlH}(\text{Et}_2\text{O})$ yielded the sterically hindered aryloxide derivative $[\text{CpMo}(\text{CO})_3]\text{Al}(\text{BHT})_2$.

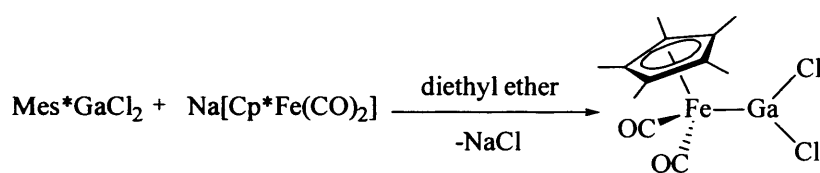
Ogino *et al.* reported the synthesis of the unstable anionic complex, $[\{\text{CpFe}(\text{CO})_2\}\text{Ga}(\mu\text{-Cl})\{\text{Fe}(\text{CO})_4\}]^-$ as the potassium salt *via* the salt elimination reaction between $[\text{Cp}(\text{CO})_2\text{Fe}]\text{GaCl}_2$ and $\text{K}_2[\text{Fe}(\text{CO})_4]$ (Scheme 7).²⁴ It was found that due to the highly reactive nature of the product, isolation could only be effected as the base stabilised species formed by reaction with 2,2'-bipyridyl.



Scheme 7

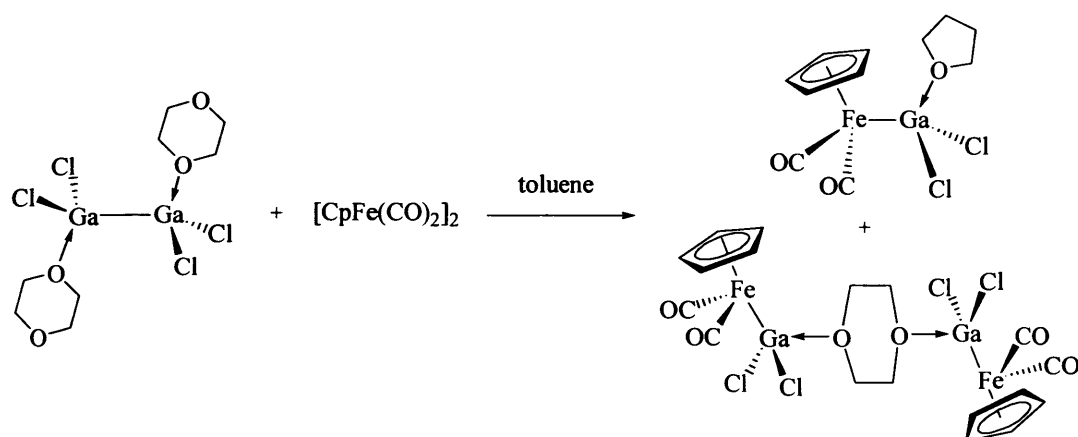
In 1997, Nöth reported the synthesis of the first tricoordinated aluminyl group bonded to a transition metal *via* the salt elimination reaction of $\text{Na}[\text{CpFe}(\text{CO})_2]$ and $(\text{tmp})_2\text{AlBr}$.²⁵ Aldridge *et al.*, have utilised salt elimination chemistry in the synthesis

of a number of boryl and gallyl species of the type $(\eta^5\text{-C}_5\text{R}_5)\text{Fe}(\text{CO})_2\text{ER}'(\text{X})$.²⁶ It was demonstrated that reaction of $\text{R}'\text{EX}_2$ with $\text{Na}[(\eta^5\text{-C}_5\text{R}_5)\text{Fe}(\text{CO})_2]$ ($\text{E} = \text{B}, \text{Ga}$; $\text{R} = \text{H}, \text{Me}$; $\text{R}' = \text{Mes}, \text{Mes}^*$; $\text{X} = \text{Br}, \text{Cl}$) yielded the corresponding boryl and gallyl species. For example, reaction of $\text{Mes}^*\text{GaCl}_2$ with $\text{Na}[\text{Cp}^*\text{Fe}(\text{CO})_2]$ in diethyl ether yielded $\text{Cp}^*\text{Fe}(\text{CO})_2\text{GaMes}^*(\text{Cl})$. In addition, reaction of GaCl_3 with 2 equivalents of $\text{Na}[(\eta^5\text{-C}_5\text{R}_5)\text{Fe}(\text{CO})_2]$ yielded $[(\eta^5\text{-C}_5\text{R}_5)\text{Fe}(\text{CO})_2]_2\text{GaCl}$ (Scheme 8).



Scheme 8

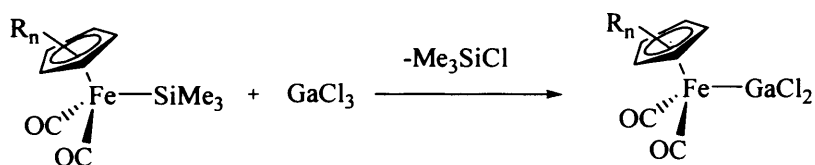
An alternative method to salt elimination is the metathesis reaction between compounds featuring Ga-Ga and Fe-Fe bonds. Linti *et al.* investigated the reactions between gallium subhalides such as $\text{Ga}_2\text{Cl}_4 \cdot 2\text{dioxane}$ and 'GaI', with $\text{K}[\text{CpFe}(\text{CO})_2]$ and $[\text{CpFe}(\text{CO})_2]_2$, respectively.²⁷ In all cases it was proposed that gallium(I) and gallium(II) compounds were formed *via* disproportionation reactions involving the formation of elemental gallium and gallium(III) halides. Several novel complexes containing tetracoordinated gallium centres of the types $\text{CpFe}(\text{CO})_2\text{FeGaX}_2(\text{L})$, ($\text{L} = \text{thf}, \text{dioxane}, [\text{CpFe}(\text{C}_7\text{H}_8)]^+\text{I}^-$; $\text{X} = \text{Cl}, \text{I}$) and $\text{CpFe}(\text{CO})_2\text{GaCl}(\text{L})$ ($\text{L} = \text{thf}, \frac{1}{2}\text{KCl}$) were reported (Scheme 9).



Scheme 9

1.2.2.4 Synthesis of Gallyl Complexes: Dehalosilylation

In 2003, Ogino *et al.* demonstrated that the complexes $\text{CpFe}(\text{CO})_2\text{GaCl}_2$ and $\text{Cp}^*\text{Fe}(\text{CO})_2\text{GaCl}_2$, first reported by Barron *et al.*, could be prepared *via* an alternative route involving the dehalosilylation reaction between $\text{CpFe}(\text{CO})_2\text{SiMe}_3$ or $\text{Cp}^*\text{Fe}(\text{CO})_2\text{SiMe}_3$ and GaCl_3 , in toluene or hexanes respectively (Scheme 10).²⁸ Both complexes were obtained in almost quantitative yields with the reaction yielding much purer compounds, according to spectroscopic measurements, than those reported by Barron.



Scheme 10

1.3 Spectroscopic and Structural Aspects of Gallyl and Indyl Complexes

1.3.1 Bonding in Gallyl and Indyl Complexes

A simplified model used to examine the bonding situation within gallyl and indyl transition metal complexes (L_nM-EX_2) ($E = Ga, \text{ or } In$) involves the sp^2 hybridised orbital on the group 13 centre forming a σ bond with an empty metal-based orbital of σ symmetry and with the gallyl or indyl substituents X shown in Figure 2. In addition, there is the possibility of supplementing the M-Ga bond order by an interaction involving π donation from a metal-based frontier orbital of appropriate symmetry into the formally vacant group 13 p orbital. This effect is in competition with π donation from the filled non-bonding orbitals of the X substituents. Thus, the extent of π back bonding is dependant on the nature of the metal (M), the ligands located on the metal centre (L) on E itself and on the E bound substituents (X). The degree of π bonding can be examined by analysis of the metal-group 13 bond lengths, the relative orientation of the gallyl or indyl fragments, and the IR stretching frequencies of the ancillary carbonyl ligands on the transition metal centre.²⁹ Generally however, the extent of back bonding in gallyl and indyl species is thought to be minimal due to the p orbital of π symmetry on the gallium or indium centres being too high in energy to be involved significantly in bonding.

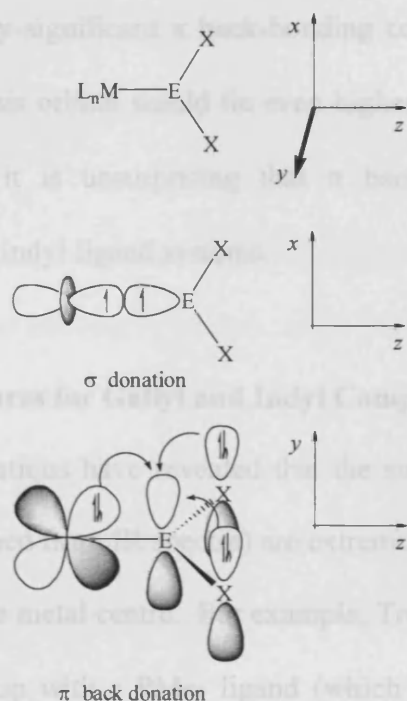


Figure 2

This 'competitive π bonding' model is, of course, also appropriate for transition metal complexes (L_nMBX_2),^{3c} and analogous to that found for Fischer carbene complexes.³⁰ For boryl systems, the degree of σ and π contributions to M-B bonding has been the subject of extensive theoretical studies^{29, 31} and generally it has been found that the π component of the covalent interaction between the metal and boron centres is minimised by strongly π donating substituents at the boron centre e.g. F. Even in the case of weaker π donors such as H or C_6F_5 , however, this component never exceeded 20%.^{3c, 32} Thus it was concluded that although modification of the boryl substituents can exert some influence on the degree of the metal to boron π bonding, π interactions represent a relatively minor contribution to the overall bonding character within the complex. This effect in turn is related to the fact that the boron-based acceptor orbital lies too high in energy with respect to the corresponding

filled metal orbital for any significant π back-bonding contribution.³² Furthermore, since it is expected that this orbital would lie even higher in energy for gallium and indium than for boron, it is unsurprising that π backbonding is of even less significance for gallyl and indyl ligand systems.

1.3.2 Spectroscopic Features for Gallyl and Indyl Complexes

Extensive investigations have revealed that the stretching frequencies of CO ligands (typically determined from IR spectra) are extremely sensitive to the effects of other ligands bonded to the metal centre. For example, Tolman has demonstrated that replacement of a CO group with a PMe_3 ligand (which is known to be a better σ donor and a poorer π acceptor than CO) causes the remaining $\nu(\text{CO})$ bands to shift to lower frequencies *e.g.* $\text{Ni}(\text{CO})_4$ (2094 cm^{-1}), $\text{Ni}(\text{CO})_3\text{PMe}_3$ ($2064, 1982\text{ cm}^{-1}$), $\text{Ni}(\text{CO})_2(\text{PMe}_3)_2$ ($1990, 1926\text{ cm}^{-1}$), and $\text{Ni}(\text{CO})(\text{PMe}_3)_3$ (1900 cm^{-1}).³³ Conversely if the ligand attached to the transition metal is a good π acceptor, competition arises, which leads to a reduction in the electron density at the metal centre, giving rise to higher CO stretching frequencies. Therefore the character of E-M bonds can be probed by examination of the stretching frequencies of the ancillary carbonyl ligands within the complex. For example, the IR spectra of $\text{CpFe}(\text{CO})_2\text{Ga}^t\text{Bu}_2$, displays two very strong absorptions at 1980 and 1928 cm^{-1} . These bands are at significantly lower frequencies than those observed for $\text{CpFe}(\text{CO})_2\text{CH}_3$,²¹ which shows bands at 2010 and 1960 cm^{-1} . These lower frequencies presumably arise as a result of the increased electron density (and increased back donation into the π^* -CO orbitals) caused by the electropositive nature of the gallium donor Ga^tBu_2 ligand. This behaviour can be contrasted with boryl species such as $\text{CpFe}(\text{CO})_2\text{Bcat}$, in which the carbonyl stretching frequencies are higher than $\text{CpFe}(\text{CO})_2\text{CH}_3$, indicating the presence of a M-

B π backbonding interaction.^{29, 31} In general, gallyl complexes are worse π acceptors and better σ donors than the corresponding boryl complexes.

1.3.3 Structural Features of Gallyl and Indyl Complexes

Whilst bond lengths and angles provide useful probes of bonding character for gallyl and indyl complexes, an added complication is the propensity of gallium/indium to increase their coordination number (typically to four) *via* bridging interactions. Thus in the absence of steric shielding, and in contrast to related boron-containing systems, poly- or oligomeric systems are sometimes observed in the solid state.

The first structurally characterised gallyl species $\text{CpW}(\text{CO})_3\text{Ga}(\text{CH}_3)_2$ reported by St. Denis *et al.* features a trigonal planar geometry at gallium in which the angles about the gallium are approximately 120° . The W-Ga bond length of 2.708(3) Å is approximately equal to the sum of the covalent radii of tungsten and gallium (*ca.* 2.72 Å) thus indicating there is minimal π back bonding within the complex.⁹ In a similar fashion, $\text{CpFe}(\text{CO})_2\text{Ga}^t\text{Bu}_2$ reported by Power *et al.* reveals a trigonal planar gallium coordination geometry with a Fe-Ga bond distance of 2.417(1) Å. Power reported that the π interactions between the iron and gallium fragments are weak as evident by the measured dihedral angles of the Cp(centroid)-Fe-Ga and C-Ga-C planes (90.2 and 88.2° respectively).²¹ A theoretical study reported by Hoffman *et al.*³⁴ supported this conclusion on the basis of orbital analyses for the $[\text{CpFe}(\text{CO})_2]^+$ fragment. It was shown that the most efficient π overlap with a π acceptor ligand, such as a carbene, involves the a'' orbital located at the iron centre. As this orbital is orientated parallel to the Cp ring plane maximum π overlap with the carbene (or by

implication, gallyl) p-orbital is observed when the plane of the ligand is perpendicular to the Cp ring corresponding to a zero dihedral angle between the Cp(centroid)-Fe-Ga and C-Ga-C planes. Thus it was concluded that for CpFe(CO)₂Ga^tBu₂, the sterically demanding ^tBu substituents may effectively prevent an orientation that would maximise π -bonding.

The asymmetric halogallyl complex (CO)₅MnGa(Mes^{*})Cl reported by Cowley *et al.* represents one of the first rare examples of a tricoordinate gallium centre featuring three different substituents.²² As with more symmetrical systems the geometry about the gallium centre is planar, and the Ga-Mn bond length is 2.495(4) Å. The large C-Ga-Mn bond angle (140.9(6)^o) observed was attributed to the large steric interaction between the aryl and Mn(CO)₅ moieties. Conversely [$\{\text{CpFe}(\text{CO})_2\}_2\text{Ga}(\mu\text{-Cl})\}_n$] reported by Barron *et al.* is polymeric in the solid state and features an infinite chain of bridging chlorides with two pendant CpFe(CO)₂ units per gallium atom. The chloride bridges are near linear (171.9(7)^o) and symmetrical, with the CpFe(CO)₂ groups positioned both above and below the plane defined by the Ga-Cl \cdots Ga-Cl chain and orientated so as to provide approximate C₂ symmetry about the gallium centre. Interestingly it was found that the Ga-Fe bond distance of 2.3654(7) Å is short when taking into consideration the four-coordinate gallium centre.²³

The structure of the monomeric complex CpMo(CO)₃Ga^tBu₂ is similar to that reported for Cp(CO)₃WGa(CH₃)₂, in which the gallium alkyl groups are orientated in the Ga-Mo-Cp centroid plane. Interestingly however, the geometries of the Mo and Ga centres feature a distinct asymmetry to the Ga^tBu₂ moiety with one of the carbonyl carbon atoms positioned very close to gallium (Figure 3). This is reported to be due

to the presence of an unusual weakly bridging carbonyl interaction as a consequence of the electron deficient nature of the gallium centre.²³

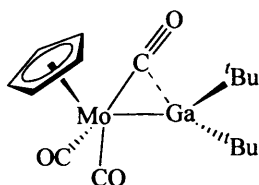


Figure 3

The molecular structure of $\text{CpFe}(\text{CO})_2\text{GaCl}_2\text{thf}$, exhibits a tetrahedrally coordinated gallium atom with the bonding parameters of the $\text{CpFe}(\text{CO})_2$ fragment in the normal range with a Ga-Fe bond length of 2.317 \AA .²⁷

1.3.4 Reactivity of Gallyl and Indyl complexes

The reactivity of transition metal boryl complexes has been the subject of extensive research interest, whereas transition metal gallyl and indyl species are relatively rare and studies of their reactivity remains relatively elusive. The majority of reactivity studies have been confined to adduct formation. For example, Green *et al.* have shown that the adducts $\text{CpFe}(\text{CO})_2\text{GaI}_2(\text{Et}_2\text{O})_n$, and $\text{Cp}'\text{Mo}(\text{CO})_3\text{GaI}_2\cdot\text{Et}_2\text{O}$, readily undergo displacement reactions of the ether group to form 1:1 adducts with the stronger donor pyridine.¹⁴

Barron *et al.* briefly investigated the reactivity of a series of cyclopentadienyliron- and cyclopentadienylmolybdenum gallyl compounds. It was reported that reaction of $[\text{CpFe}(\text{CO})_2\text{GaCl}_2]_n$ with MeCN and NMe_3 resulted in the formation of $\text{CpFe}(\text{CO})_2\text{GaCl}_2(\text{MeCN})$ and $\text{CpFe}(\text{CO})_2\text{GaCl}_2(\text{NMe}_3)$, respectively.

Conversely, attempted reduction of $[\{\text{CpFe}(\text{CO})_2\}_2\text{Ga}(\mu\text{-Cl})]_\infty$, with potassium in diethyl ether yielded gallium metal and $[\text{CpFe}(\text{CO})_2]_3\text{Ga}$.²³

1.4 Group 13 Diyl Complexes

1.4.1 History of Group 13 Diyl Complexes

Over the last decade the synthesis and chemistry of low oxidation state compounds featuring group 13 elements has been the subject of intensive research investigations. It is well known that the +I oxidation state becomes more dominant as the group is descended; while the monohalides of indium and thallium are thermally stable and their use in the syntheses of indium(I) and thallium(I) alkyls, aryls, and amides has been demonstrated, it has only been in the last 15 years that the synthesis of analogous low valent compounds of the lighter group 13 elements has developed. The reason for this in part lies with the fact that compounds containing, for example, gallium and aluminium in an oxidation state lower than +III are inherently less stable than their heavier congeners. However, through the pioneering work of Schnöckel³⁶,³⁵ and Uhl^{37, 38} a number of novel low oxidation state group 13 metal species have been synthesised.

1.4.2 Synthesis of Group 13 Diyls

It has been demonstrated that there are two main synthetic routes for the synthesis of group 13 diyls; dehalogenation (reduction) of REX_2 and salt elimination.

1.4.2.1 Synthesis of Group 13 Diyls: Dehalogenation

The most effective method in the synthesis of group 13 diyls species is dehalogenation, by reaction of the trivalent gallium or indium species with a suitable

reducing agent such as an alkali metal, Riecke magnesium, NaSi^tBu₃ and KC₈. This methodology was utilised by Paetzold and co-workers in the synthesis of the organo B(I) cluster [B^tBu]₄ by the reductive dehalogenation of ^tBuBF₂ with Na/K alloy.³⁹ Roesky *et al.* reported the synthesis of [AlCp*]₄ by reaction of Cp*AlCl₂ with potassium in toluene.⁴⁰ Similarly, Jutzi *et al.* prepared [GaCp*]₆ by the reductive dehalogenation of Cp*GaI₂ with potassium metal.⁴¹ [AlC(SiMe₃)₃]₄ was also prepared by reduction of (Me₃Si)₃CAI₂·thf with Na/K alloy.⁴²



E = Al, Ga; X = halide; M = alkali metal

Scheme 11

1.4.2.2 Synthesis of Group 13 Diyls: Salt Elimination

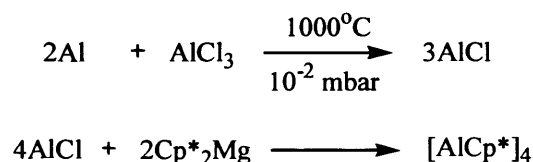
Low valent gallium and indium species can be prepared by salt elimination chemistry, this synthetic methodology generally involves the group 13 monohalide dissolved in a stabilising solvent. Examples include the preparation of InCp* by reaction of InCl and LiCp* in diethyl ether⁴³ (Scheme 12) and the synthesis of [InC(SiMe₃)₃]₄ from the metathetical reaction between LiC(SiMe₃)₃ with InCl.⁴⁴



Scheme 12

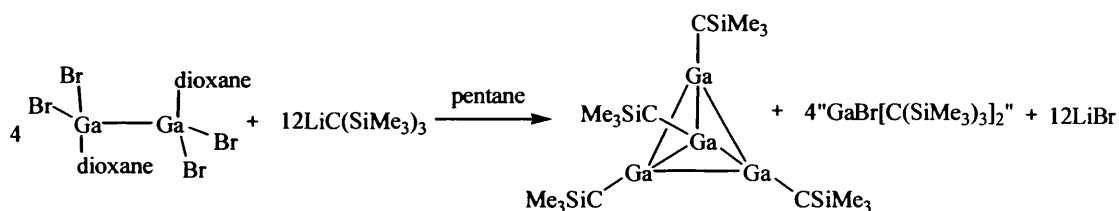
Schnöckel *et al.* demonstrated a variation on this methodology in the synthesis of the first organo Al(I) compound [AlCp*]₄, (and later the analogous [GaCp*]₆)³⁶

from metastable AlCl .³⁵ HCl gas was passed over aluminium metal at high temperature (1000°C) and low pressure (10^{-2} mbar), then co-condensed with a donor solvent to give a metastable solution of nearly pure AlCl . Addition of bis(pentamethylcyclopentadienyl) magnesium to the metastable AlCl solution then yielded $[\text{AlCp}^*]_4$ (Scheme 13).³⁵



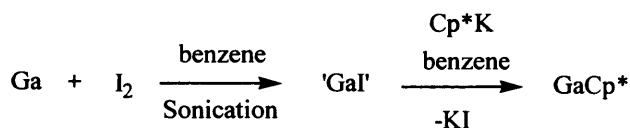
Scheme 13

In related chemistry Uhl *et al.* originally prepared $[\text{GaC}(\text{SiMe}_3)_3]_4$, in low yield, from the metathesis reaction between $\text{Ga}_2\text{X}_4 \cdot 2\text{dioxane}$ and $\text{LiC}(\text{SiMe}_3)_3$ in pentane (Scheme 14).⁴⁵

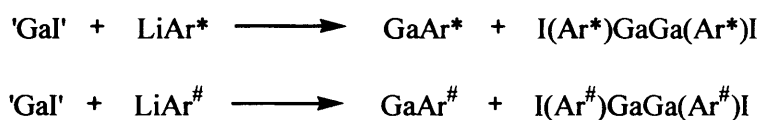


Scheme 14

Synthetic routes to group 13 diyl species which utilise 'GaI' as the reagent, often represent a more viable option to reduction reactions. Such reactions however tend to be low yielding or synthetically challenging. Jutzi *et al.* have demonstrated that GaCp^* , can alternatively be formed by treatment of 'GaI' with the potassium salt of a substituted cyclopentadienyl ligand (Scheme 15).⁴⁶ Several other Ga(I) alkyls or aryls, such as $[\text{GaC}(\text{SiMe}_3)_3]_4$ have also been synthesised by reactions with 'GaI'.⁴⁷

**Scheme 15**

Power *et al.* have utilised highly bulky terphenyl ligands in the synthesis of monomeric indium and thallium compounds of the type $\text{MC}_6\text{H}_3\text{-2,6-Trip}_2$ (MAr^* ; $\text{M} = \text{In}$ or Tl), featuring a one-coordinate group 13 centre, by reaction of the bulky terphenyllithium reagent LiAr^* with the corresponding monohalides of indium and thallium.⁴⁸ Extending this methodology to gallium systems it was found that reaction of the corresponding terphenyllithium reagents with 'GaI' yielded the first stable monovalent compounds of the type GaAr^* and $\text{GaAr}^\#$ (Scheme 16).^{7a} It was reported that the chemical behaviour of the gallium monoaryls in solution is consistent with their formulation as monomers rather than dimers. The weakness of the Ga-Ga bonding can be attributed primarily to the large energy difference between the frontier lone pair and p-orbitals of the arylgallium monomers. Thus in the neutral gallium aryls, the gallium valence electrons behave essentially as lone pairs rather than bonding pairs.

**Scheme 16**

Subsequently in 2006, with the aim of examining the bonding between heavier group 13 atoms and nitrogen, Power reported the synthesis of the first gallium(I) amide $\text{GaN(SiMe}_3\text{)Ar}''$ by reaction of $\text{LiN(SiMe}_3\text{)Ar}''$ with 'GaI'.⁴⁹

1.4.3 Structure and Bonding of Group 13 Diyl Complexes

Vital to the stabilisation of low oxidation state species, ER, is the nature of the R substituent. Both the steric and electronic properties of the substituent effect the overall stabilisation of the species. For bulky R substituents, such ER fragments are often monomeric in solution and in the gas phase but tend to aggregate in the solid state unless the R substituent is extremely sterically demanding. Thus for example, $(\text{AlCp}^*)_4$,³⁵ $[\text{Al}(\text{Si}^t\text{Bu}_3)]_4$,⁵⁰ and $[\text{EC}(\text{SiMe}_3)_3]_4$ ^{37, 38, 42, 44} (E = Ga, In) are tetrameric whereas $[\text{ECp}^*]_6$ (E = Ga, In) are hexameric^{36, 38, 51} and sterically demanding ligands of the type 2,6- $\text{C}_6\text{H}_3\text{Trip}_2$, can be utilised to enforce mono-coordination such as in $\text{Ga}(2,6\text{-C}_6\text{H}_3\text{Trip}_2)$. For oligomeric species such as Schnöckel's $[\text{Cp}^*\text{Ga}]_6$,³⁶ the $\text{Ga}\cdots\text{Ga}$ bonding within these sub-units is weak and it is considered that cluster complexes of this type are primarily formed as a result of Van der Waals interactions between the Cp^* ligands and not *via* metal-metal bonds per se. Interestingly, it was found that the metal-metal bond lengths within $[\text{GaCp}^*]_6$ (Figure 4) are slightly longer than those of the isomorphous $[\text{InCp}^*]_6$ cluster,^{6c} presumably due to the ligand packing requirements. The aggregates are however unstable in comparison with the corresponding monomers; theoretical calculations performed on the related "clusters" $[\text{AlCp}]_4$ and $[\text{AlCp}^*]_4$ have suggested that $\text{Cp}\rightarrow\text{Al}$ π back bonding is the primary reason for this.⁵²

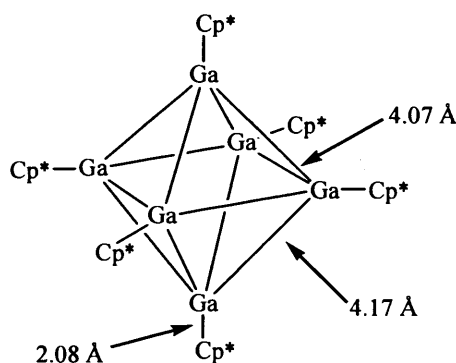
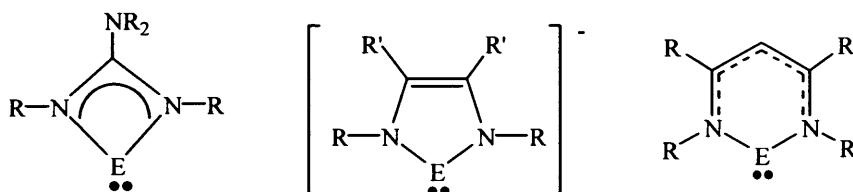


Figure 4

1.5 Group 13 Amido Complexes

The synthesis and isolation of stable carbenes based on imidazolium heterocycles (N-heterocyclic carbenes NHCs) has been the focus of considerable research interest. As with group 13 diyls, N-heterocyclic carbene ligands possess a singlet lone pair and act as strong σ -donors towards a variety of s, p and d-block metal fragments.⁵³ There has been considerable attention paid to the heavier group 14 analogues of N-heterocyclic carbenes (E = Si, Ge, or Sn) and the valence isoelectronic phosphorous and arsenic cationic analogues (E = P or As).⁵⁴ Conversely, the synthesis of anionic group 13 heterocycles has only recently been developed. In addition related neutral 6-membered aluminium, gallium, indium and thallium heterocycles have also been reported (Scheme 17). These systems can be viewed, in effect, as base-stabilised amido-diyl complexes.⁵⁵ In 2005 Jones *et al.* reported the synthesis of a series of monomeric four-membered group 13 metal heterocycles of the type $[:E\{\eta^2-N,N'-N(R)C(R')N(R)\}]$ (Scheme 17).⁵⁶

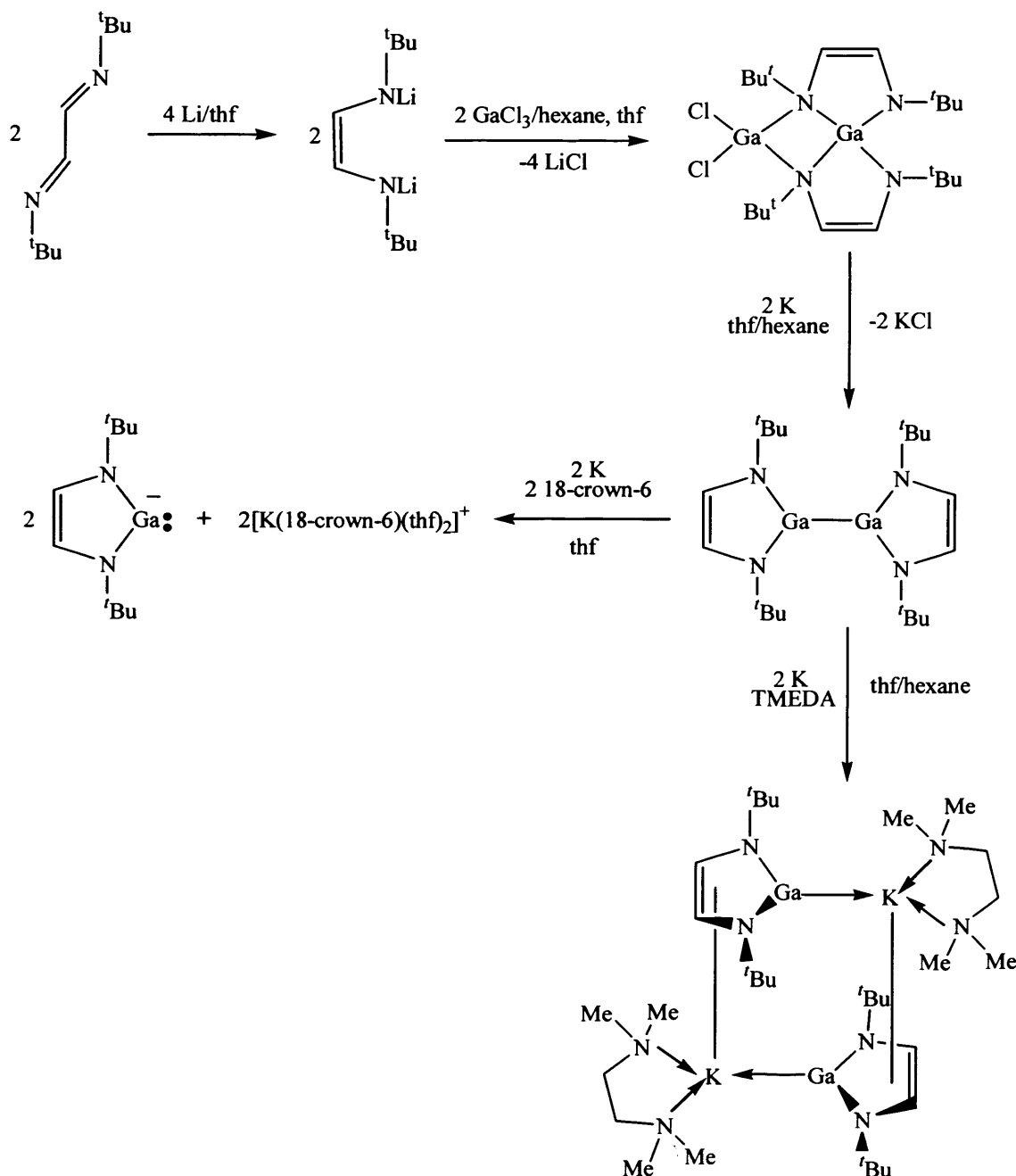


Scheme 17

1.5.1 Synthesis of Anionic 5-Membered Group 13(I) Heterocycles

In 1999, Schmidbaur *et al.* reported the synthesis of the first anionic gallium carbene analogue.⁵⁷ It was demonstrated that reaction of the dilithiated diazabutadiene ligand with $GaCl_3$ yielded the corresponding chlorogallaimidazole, which was further reduced stepwise over a period of 5 days with potassium and crown

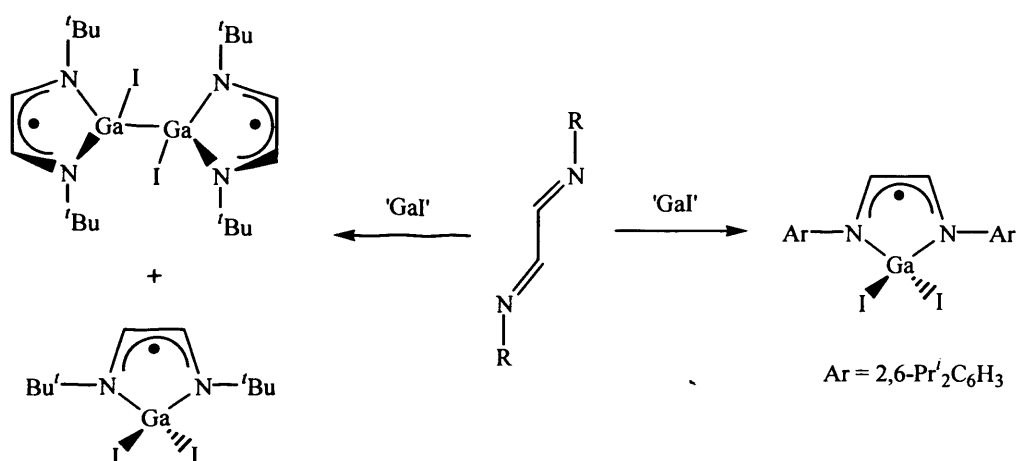
ether to yield the anionic heterocycle in low yield (3 %) (Scheme 18). Further investigations revealed that if the reduction was carried out over 14 days in the presence of TMEDA as the chelating agent the complex was isolated in a higher yield (18 %).



Scheme 18

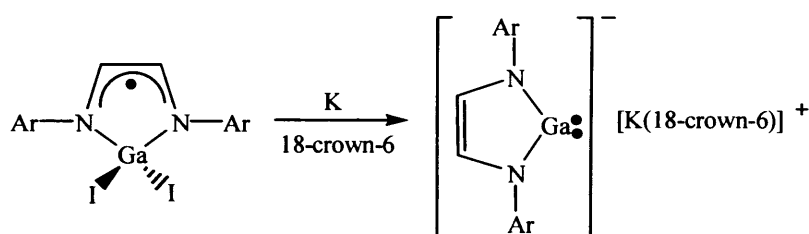
Both compounds $[[K(TMEDA)][Ga\{N('Bu)C_2H_2N('Bu)\}]]_2$ and $[K(18-crown-6)(thf)_2][:Ga\{N('Bu)C_2H_2N('Bu)\}]$ were structurally characterised which revealed that the anionic complex showed no short cation-anion contacts *i.e.* it contains a discrete three-coordinate gallium centre where the oxidation state of the metal is +1. $[[K(TMEDA)][Ga\{N('Bu)C_2H_2N('Bu)\}]]_2$ was shown to be dimeric in the solid state and thus could be considered as consisting of monomeric units comprising a gallium 'carbene' heterocycle η^5 -coordinated to a $[K(TMEDA)]^+$ fragment. It was found that an intermolecular interaction of the gallium lone pairs with two potassium atoms aggregates the monomeric units into centrosymmetric dimers.

Subsequent related work carried out by Jones *et al.* examined the reaction of diazabutadiene ligands with 'Gal' (Scheme 19).⁵⁸ It was found that the nature of the product obtained was largely dependent on the nature of the diazabutadiene N-substituent in terms of whether Ga(II) or Ga(III) complexes were obtained. It was proposed that the mechanism of formation involved a combination of one electron diazabutadiene reduction and disproportionation reactions.



Scheme 19

Further reduction of $I_2Ga(Ar-DAB)$, with potassium metal yielded the Ga(I) heterocycle $[(18-crown-6)KGa(Ar-DAB)]$ (Scheme 20), which is closely related to the earlier tBu substituted compound $[:Ga\{N(tBu)C_2H_2N(tBu)\}][K(18-crown-6)(thf)_2]$ reported by Schmidbauer. It was reported that the anion possesses a singlet lone pair at the gallium centre. As a result of this, the coordination chemistry of $[(18-crown-6)KGa(Ar-DAB)]$ has been extensively studied, revealing close analogies with N-heterocyclic carbenes, particularly in relation to its strong nucleophilic nature and stabilising properties with respect to low coordinate systems.⁵⁹

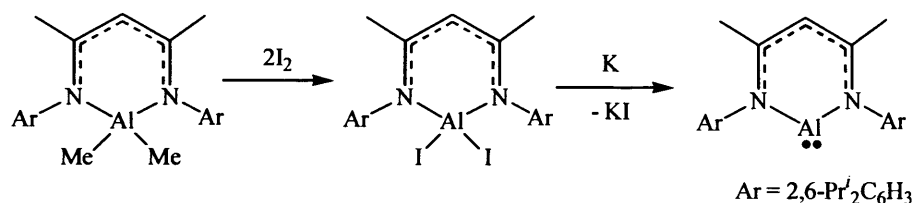


Scheme 20

1.5.2 Synthesis of Neutral 6-Membered Group 13(I) Heterocycles

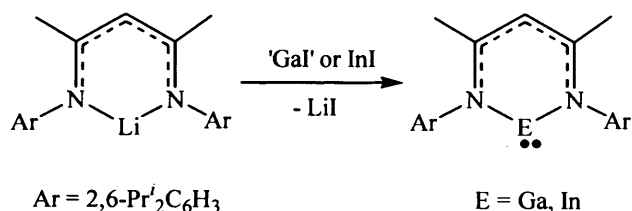
The synthesis of related neutral 6-membered aluminium(I),^{55a} gallium(I),^{55b} indium(I) and thallium(I)⁶⁰ heterocycles derived from the β -diketiminate class of ligand $HC(CMeNAr)_2^-$ ($Ar = 2,6$ -diisopropylphenyl) has also been investigated. It was reported by Roesky *et al.* that reaction of $[HC(CMeNAr)_2]AlMe_2$ with I_2 yielded the corresponding diiodide complex $[HC(CMeNAr)_2]AlI_2$; further reduction of this species with potassium over 3 days yielded the 6-membered neutral aluminium heterocycle $[HC(CMeNAr)_2]Al$ (Scheme 21).^{55a} Crystallographic data revealed well separated monomeric units featuring the first example of a two-coordinate aluminium centre. Further analysis of the Laplacian of electronic density in the plane of the ligand revealed the presence of a lone pair localised on the metal centre and outside the heterocycle in a quasi-trigonal-planar geometry. It was argued that the electrons

originating from an sp^2 configuration of the Al(I) centre are stereochemically active, occupying an sp -like hybrid orbital. It was further proposed that the aluminium atom can be considered as acting as both a Lewis acid in its interaction with the nitrogen atoms of the ligand and potentially as a Lewis base with its lone pair of electrons.



Scheme 21

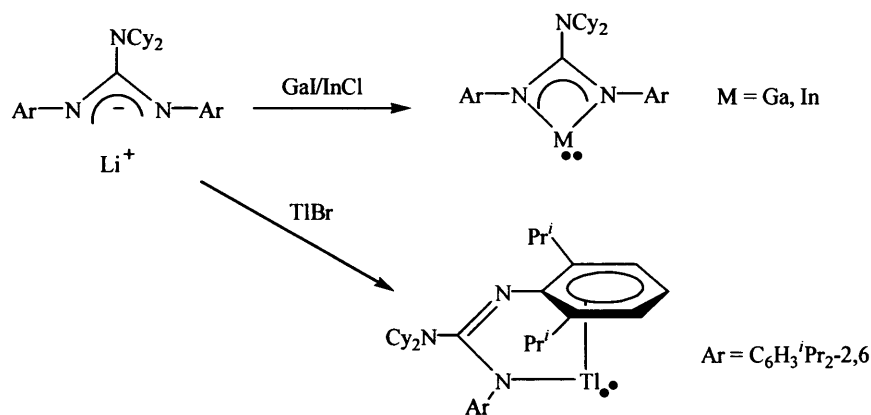
The synthesis of analogous gallium(I), indium(I) and thallium(I) heterocyclic ring systems has also been investigated.^{55b, 60} It was reported that reaction of the β -diketiminate anion and the corresponding metal(I) iodide species yielded the gallium and indium 6-membered heterocyclic complexes *via* salt elimination (Scheme 22). Interestingly, it was found that previous attempts to synthesise the indium species by this method were unsuccessful when InCl was used as the source of In(I).⁶¹ Furthermore, it was reported that the bonding within $[\text{Ga}(\text{NArCMe})_2\text{CH}]$ was best described as a Ga^+ ion chelated by a monoanionic $[(\text{NArCMe})_2\text{CH}]^-$ ligand.



Scheme 22

1.5.3 Synthesis of 4-Membered Group 13(I) Heterocycles

In 2005 Jones *et al.* studied the synthesis of monomeric four-membered group 13 metal(I) heterocycles $[:M\{\eta^2-N,N'-N(R)C(R')N(R)\}]$.⁵⁶ These species represent a synthetically challenging class of compounds as the reactive metal centres of these rings would be less sterically shielded by their N-substituents than the metal centres in five- or six membered heterocycles. In addition, their constrained NCN backbones should lead to significantly more acute NMN angles than seen for the larger rings. Initial studies revealed that reaction of a bulky amidinate salt with metal(I) halides afforded either five membered isomers *i.e.* $[M(\eta^1-N:\eta^3-Ar-Piso)]$ $M = In$ or Tl , $Piso^- = [N(Ar)C(Bu^t)N(Ar)]^-$ or the gallium (II) dimer, $[\{GaI(\eta^2-N,N'-Piso)_2\}]$ the latter *via* disproportion processes. It was found that four-membered heterocycles could be accessed by employing a more N-electron rich ligand with a bulkier backbone substituent to favour N,N-chelation of the electron deficient metal centre. Jones utilised a bulky guanidinate ligand in the synthesis of the first four-membered group 13 metal(I) heterocycle (Scheme 23). Treatment of the respective group 13 metal(I) halide with the lithium guanidinate, $Li[Giso]$, $Giso^- = [(Ar)NC(NCy_2)N(Ar)]^-$ in toluene led to the formation of the guanidinate complexes $[:Ga\{(Ar)NC(NCy_2)N(Ar)\}]$. It was reported that in the cases of the gallium and indium species, N,N-chelation is preferred over N,arene-chelation, which is the observed structural motif for the thallium complex (*cf.* $[M(\eta^1-N:\eta^3-Ar-Piso)]$). This difference was attributed to the increasing ionic radius in the series, $Ga^+ - Tl^+$, which disfavors N,N-chelation of the heavier ion.

**Scheme 23**

1.6 Transition Metal Complexes of Group 13 Diyl Ligands

1.6.1 Introduction to Transition Metal Complexes of Group 13 Diyl Ligands

Group 13 ligands of the type ER featuring coordinatively and electronically unsaturated group 13 elements are rare but have become more common in recent years. The ER ligand can generally adopt two modes of coordination – bridging between two metal fragments with a coordination number of three (or more), or terminally bound to a metal centre, thereby adopting a coordination number of two. Diyl species are versatile starting materials as a result of their ability to function as Lewis bases towards a variety of transition metals. The coordination chemistry of organo ER fragments has only been established in the last few decades, but numerous examples have now been reported.

1.6.2 Synthesis of Transition Metal Complexes of Group 13 Diyl Complexes

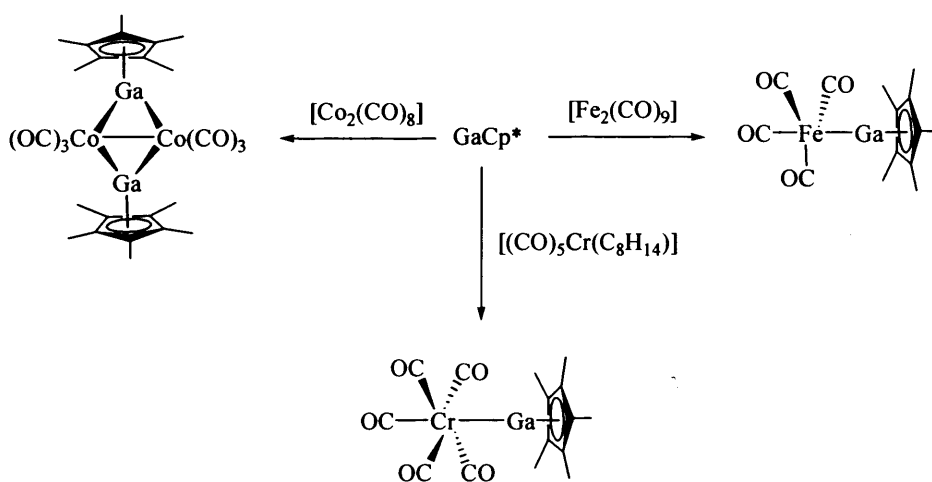
1.6.2.1 Neutral Systems

Typically the synthetic strategies used for the preparation of diyl complexes include: (i) salt elimination between a dianionic metal carbonylate $[\text{M}(\text{CO})_n]^{2-}$ and a

group 13 dihalide, (ii) substitution of labile ligands by ER, and (iii) insertion chemistry.

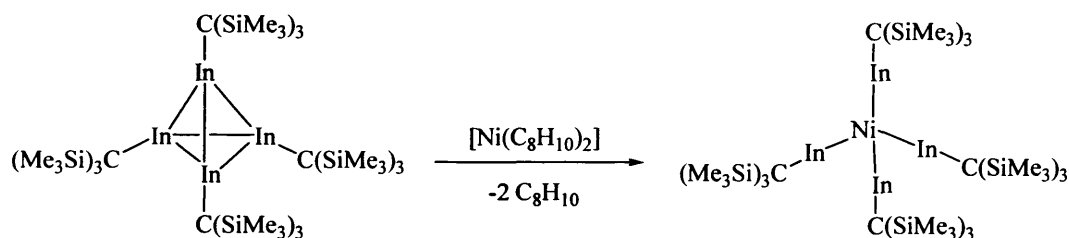
1.6.2.1.1 Substitution of Labile Ligands

It has been demonstrated that, as a result of the isolobal relationship between ER and CO, ER fragments can readily substitute CO ligands, generating transition metal complexes featuring either bridging or terminal ER ligands. In particular, the reaction of ER ligands with homoleptic transition metal carbonyls has been extensively studied. For example, the complexes $\text{Mn}_2(\text{CO})_8[\mu_2\text{-InC}(\text{SiMe}_3)_3]_2$, $\text{Mn}_2(\text{CO})_6[\mu_2\text{-InC}(\text{SiMe}_3)_3]_2$ ⁶² and $\text{Co}(\text{CO})_6[\mu_2\text{-InC}(\text{SiMe}_3)_3]$, were isolated from the reaction of the parent carbonyl dimers with the corresponding $[\text{InC}(\text{SiMe}_3)_3]_4$. The substitution of labile ligands (e.g. nitriles, olefins) in transition metal carbonyl species has been implicated in the syntheses of a number of Cp^*Ga containing complexes e.g. $(\text{Cp}^*\text{Ga})\text{Cr}(\text{CO})_5$ and $(\text{Cp}^*\text{Ga})_2\text{Mo}(\text{CO})_4$. This methodology was employed by Jutzi *et al.*, in the synthesis of a similar series of first row transition metal carbonyl species with coordinated GaCp^* groups in both terminal and bridging positions.⁴¹



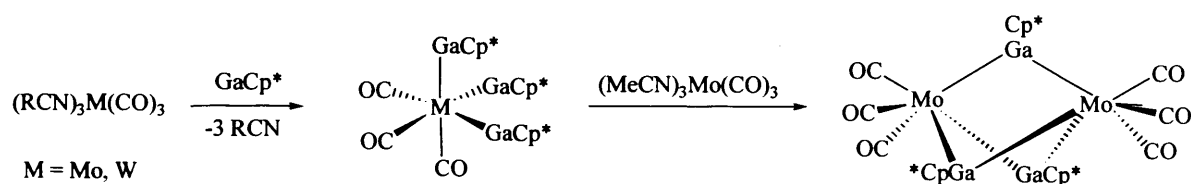
Scheme 24

The substitution of other labile ligands has also been reported. For example, it has been demonstrated that olefin ligands such as norbornadiene,⁶³ cyclooctatetraene,⁶⁴ cycloheptatriene,⁴¹ and cyclooctene⁶⁵ can also be displaced. In 1998, Uhl *et al.* reported the synthesis of an unusual homoleptic Ni(0) complex Ni[InC(SiMe₃)₃]₄, by the reaction of Ni(COD)₂ with [InC(SiMe₃)₃]₄ (Scheme 25). This example illustrates the applicability of synthesising complexes with an ‘inverted’ ratio of group 13:transition metal atoms (E/M > 1) *via* ligand substitution chemistry.⁶⁶ Following this the gallium analogue was later reported.⁶⁷



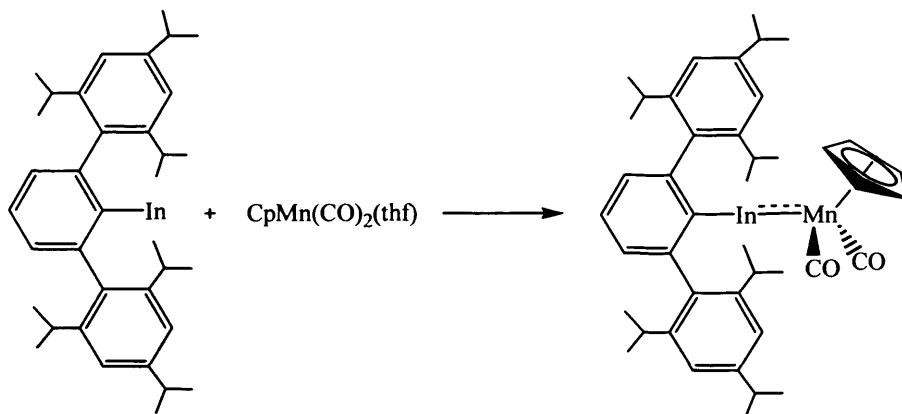
Scheme 25

The substitution of heteroatom donor ligands such as thf and MeCN has also been reported. It was reported that the reaction of GaCp* with *fac*-(MeCN)₃M(CO)₃ yielded monomeric compounds of the type *fac*-(GaCp*)₃M(CO)₃ (M = Mo or W). It was further demonstrated that such species can act as building blocks for dinuclear complexes, in which the GaCp* ligand adopts a bridging mode of coordination (Scheme 26).⁶⁸



Scheme 26

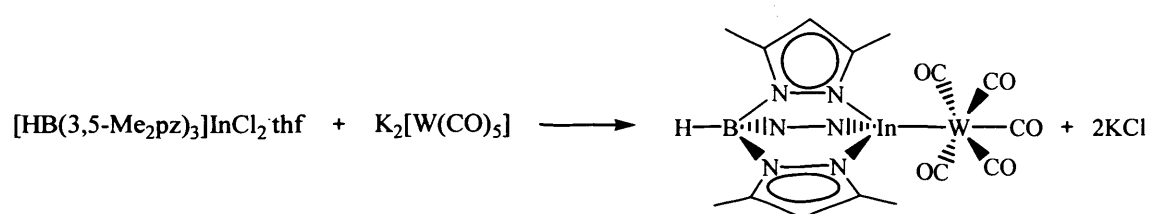
In 1998, Power *et al.* also reported the synthesis of the species $\text{CpMn(CO)}_2\text{InAr}^*$ by reaction of the monomeric indium complex InAr^* with $\text{CpMn(CO)}_2(\text{thf})$ (Scheme 27).^{48a} X-ray diffraction measurements revealed that the InAr^* fragment is bound in a terminal monodentate fashion to the 16-electron CpMn(CO)_2 moiety with an almost linear geometry at the indium centre.



Scheme 27

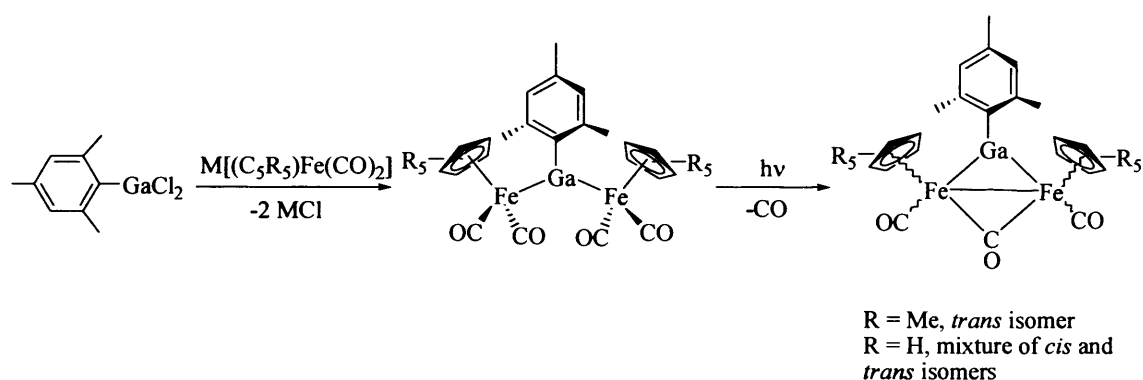
1.6.2.1.2 Salt Elimination

Salt elimination chemistry has proven to be an effective synthetic route in the formation of transition metal group 13 diyl complexes. Reger *et al.* reported the synthesis of the complexes $[\text{HB}(3,5\text{-Me}_2\text{pz})_3]\text{InFe(CO)}_4$ and $[\text{HB}(3,5\text{-Me}_2\text{pz})_3]\text{InW(CO)}_5$ *via* salt elimination chemistry by reaction of $[\text{HB}(3,5\text{-Me}_2\text{pz})_3]\text{InCl}_2\cdot\text{thf}$ and the corresponding metal carbonyl dianion (Scheme 28). The bonding within both complexes was described as an indium(I) group acting as a Lewis base to W(CO)_5 (*i.e.* $\text{In}\rightarrow\text{W}$).⁶⁹



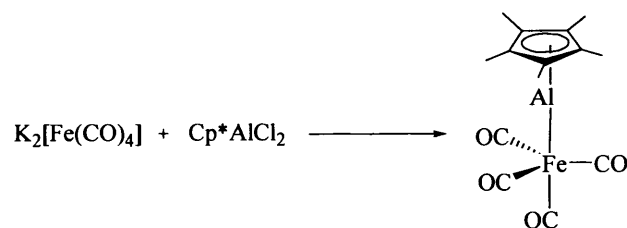
Scheme 28

Ogino *et al.* reported the synthesis of a class of unsupported bridging gallylene species $[(\eta^5\text{-C}_5\text{R}_5)\text{Fe}(\text{CO})_2]_2\text{Ga}(\text{Mes})$ ($\text{R} = \text{H}, \text{Me}$), by reaction of MesGaCl_2 with the corresponding transition metal anion (Scheme 29).⁷⁰ It was found that photolysis of the unsupported complex yielded the supported bridging gallylene species *via* CO loss. Further investigations revealed that the steric bulk of the $\eta^5\text{-C}_5\text{R}_5$ fragment influenced the nature of the complex obtained. For example, it was reported that the bridged species was formed in a mixture of *cis* and *trans* isomers while the *trans* isomer is formed exclusively for the Cp^* analogue, presumably on steric grounds. However this methodology has limited synthetic applicability due to the dependence on the nature of the gallylene precursor.



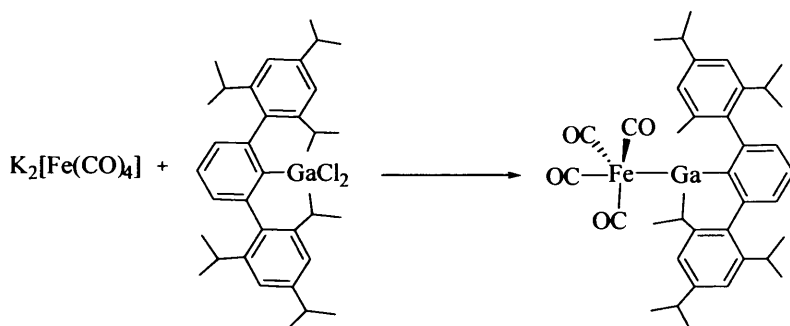
Scheme 29

The metathesis reaction of a carbonylmetallate $[\text{M}(\text{CO})_n]^{2-}$ ($\text{M} = \text{Fe}, n = 4$; $\text{M} = \text{Cr}, n = 5$) and REX_2 in a coordinating solvent generates species of the type $(\text{CO})_n\text{MER}$, such as $(\text{AlCp}^*)\text{Fe}(\text{CO})_4$ ⁷¹ and $(\text{Ar}^*\text{Ga})\text{Fe}(\text{CO})_4$,⁷² although in variable yields (Scheme 30).



Scheme 30

Robinson *et al.* reported the synthesis of the controversial gallium diyl species $(\text{Ar}^*\text{Ga})\text{Fe}(\text{CO})_4$ via salt elimination by reaction of $\text{K}_2[\text{Fe}(\text{CO})_4]$ and Ar^*GaCl_2 (Scheme 31).⁷² The Fe-Ga bonding within $(\text{Ar}^*\text{Ga})\text{Fe}(\text{CO})_4$ was the subject of considerable debate. It was first proposed by Robinson that the Fe-Ga centres were bound *via* a triple bond ($\text{L}_n\text{M}\equiv\text{ER}$), however it was later argued by Cotton and Feng using spectroscopic and computational results that the Fe-Ga bonding was a donor-acceptor interaction ($\text{L}_n\text{M}\leftarrow\text{ER}$).⁸²

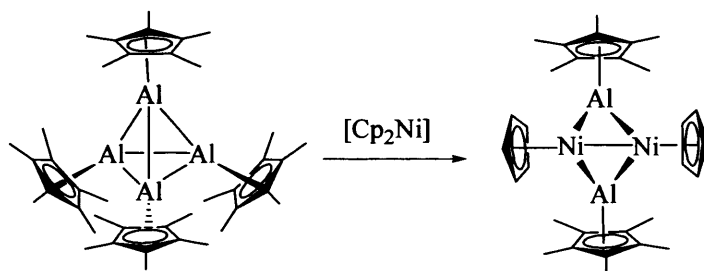


Scheme 31

1.6.2.1.3 ER Insertion

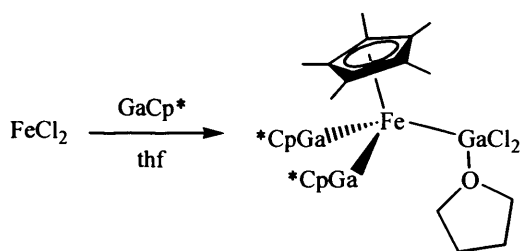
Although insertion reactions of EX (X = halide) have been extensively studied, analogous insertions of organo ER derivatives have received much less attention. Due to the nature of group 13 diyls, insertion chemistry of this type represents a readily accessible route into the formation of M-E bonds, allowing the formation of CO-free systems.

Schnöckel *et al.* reported the synthesis of the first transition metal complex featuring a bridging ER fragment $(\text{CpNi})_2(\mu^2\text{-AlCp}^*)_2$, *via* insertion of AlCp^* into the $\text{Ni-C}(\text{Cp})$ bond of NiCp_2 (Scheme 32).⁷³



Scheme 32

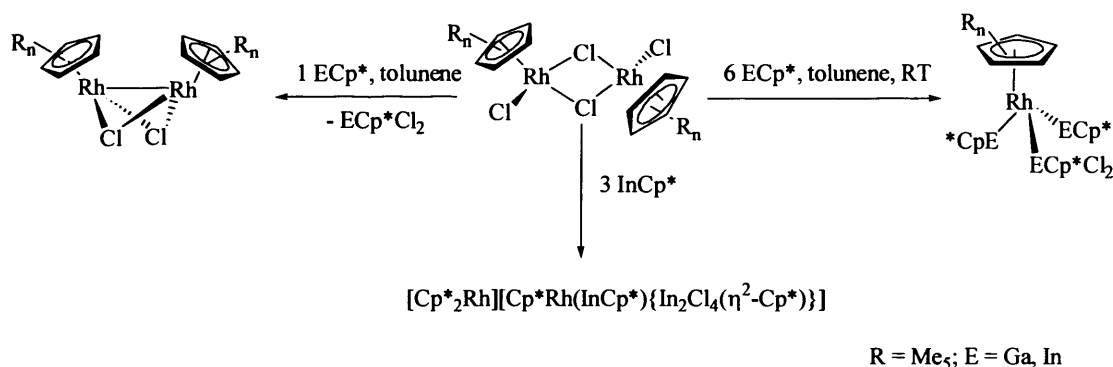
Jutzi *et al.* reported the potential of ER fragments to function as both reducing agents and as Cp^* transfer-reagents; the insertion of GaCp^* into the Fe-Cl bonds of FeCl_2 was reported to yield $\text{Cp}^*\text{Fe}(\text{GaCp}^*)_2(\text{GaCl}_2\cdot\text{thf})$ (Scheme 33).⁷⁴



Scheme 33

It has been demonstrated that typically insertion reactions tend to be highly sensitive to the reaction conditions employed and thus as a result, many different reaction pathways are often possible. This was exemplified by the reaction of $[\text{RhCp}^*\text{Cl}_2]_2$, with ECp^* ($\text{E} = \text{Ga}, \text{In}$). Reaction of $[\text{RhCp}^*\text{Cl}_2]_2$ with six equivalents of ER at room temperature in toluene was shown to yield the monomeric product

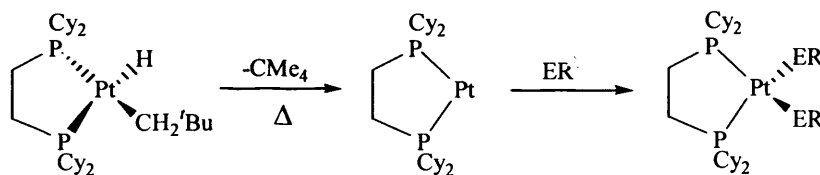
$\text{Cp}^*\text{Rh}(\text{ECp}^*)_3\text{Cl}_2$, whereas reaction with a single equivalent of ECp^* yielded the Rh(II) dimer $[\text{Cp}^*\text{RhCl}]_2$. By contrast, the salt $[\text{Cp}^*_2\text{Rh}][\text{Cp}^*\text{Rh}(\text{InCp}^*)\{\text{In}_2\text{Cl}_4(\eta^2\text{-Cp}^*)\}]$ was prepared by the reaction of $[\text{Cp}^*\text{RhCl}_2]_2$ with three equivalents of InCp^* (Scheme 34).^{6c}



Scheme 34

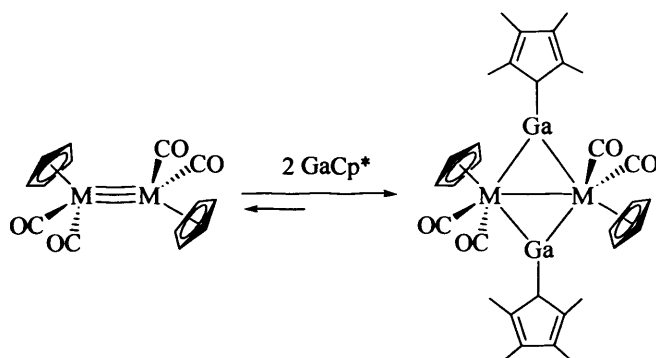
1.6.2.1.4 Addition of ER

Examples of transition metals formed by addition of ECp^* to coordinatively unsaturated centres are relatively few. It has been demonstrated by Fischer *et al.* that it is possible to synthesise *bis*(phosphine)platinum complexes of the type $(\text{dcpe})\text{Pt}(\text{ER})_2$, by trapping the 14 electron intermediate $(\text{dcpe})\text{Pt}$ with a diyl fragment (Scheme 35). The transient intermediate $(\text{dcpe})\text{Pt}$ was produced by reductive C-H elimination from the corresponding platinum hydride $(\text{dcpe})\text{Pt}(\text{H})(\text{CH}_2^t\text{Bu})$.^{9, 68, 75}



Scheme 35

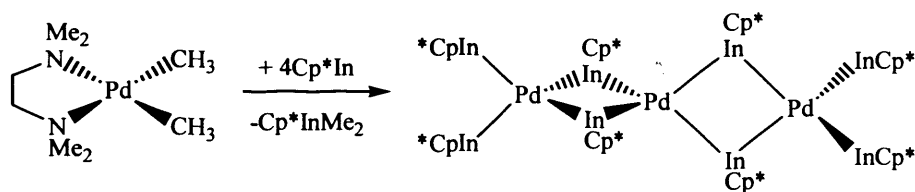
Fischer reported that reaction of GaCp^* with the multiple bonded dimeric complex $[\text{CpM}(\text{CO})_2]_2$ ($\text{M} = \text{Mo}, \text{W}$) yielded the addition products $[\text{CpM}(\text{CO})_2(\mu\text{-GaCp}^*)]_2$. Investigations unexpectedly revealed that the coordination of GaCp^* is weak; species such as those outlined in Scheme 36 display temperature dependent association/dissociation behaviour.^{6c, 68}



Scheme 36

1.6.2.1.5 Oxidation of ER

It has been demonstrated that ER fragments can act as in situ reducing agents towards higher oxidation state transition metal complexes, $[\text{L}_n\text{MX}_n]$, resulting in either insertion products if ER remains coordinated to the transition metal centre (*vide supra*) or low oxidation state complexes, $[\text{M}_a(\text{ER})_b]$, by cleavage of X_2ER (Scheme 37). However, the ease of oxidation of ER provides a less common synthetic pathway to transition metal diyl species.^{6c, 6e}

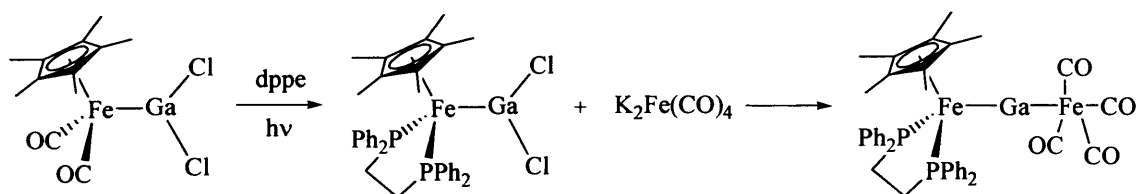


Scheme 37

1.6.3 Group 13 Metalladiyl Complexes

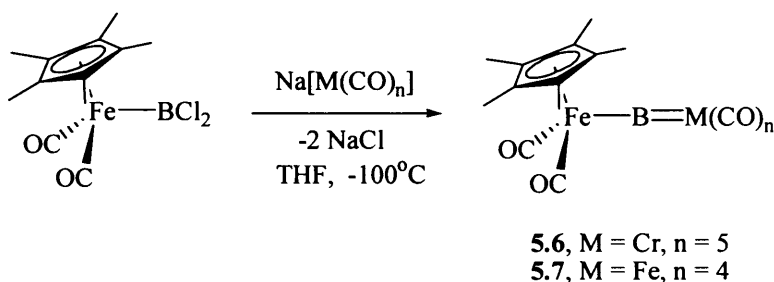
1.6.3.1 Neutral Metalladiyl Complexes

In 2003, Ogino *et al.* reported the synthesis of the first dinuclear complex bridged by a substituent free ‘naked’ gallium centre $\text{Cp}^*\text{Fe}(\text{dppe})(\mu\text{-Ga})\text{Fe}(\text{CO})_4$ (Scheme 38), although the bonding in this system is formally described as a single bond between $\text{Cp}^*\text{Fe}(\text{dppe})$ and Ga, and a double bond between Ga and $\text{Fe}(\text{CO})_4$, the Fe-Ga bond lengths imply appreciable delocalisation of π bonding over the Fe-Ga-Fe framework.²⁴



Scheme 38

Braunschweig *et al.* subsequently reported the synthesis and structural characterisation of analogous neutral boron-containing complexes featuring a boron centre bonded solely to two transition metal fragments (Scheme 39).⁷⁶



Scheme 39

1.6.4 Aspects of Bonding in Transition Metal Complexes of Group 13 Diyls

1.6.4.1 Bonding in Diyl Complexes

ER complexes typically feature the ligand in a singlet ground state and formally possess two empty p orbitals and a lone pair of electrons located at the group 13 centre (Figure 5). As a result of this, the frontier orbitals are similar to those of CO and consequently the ER ligand may be regarded as isolobal with CO, PR_3 , and N_2 , capable of exhibiting both σ donor and π acceptor properties. The relative extents of these bonding components are dependent on the nature of the metal, on E, and on the R substituent. Generally ER fragments are good σ donors with weaker π acceptor properties. In addition theoretical studies suggest that the electrostatic attraction between the group 13 metal and transition metal plays a significant bonding role.^{77, 78}

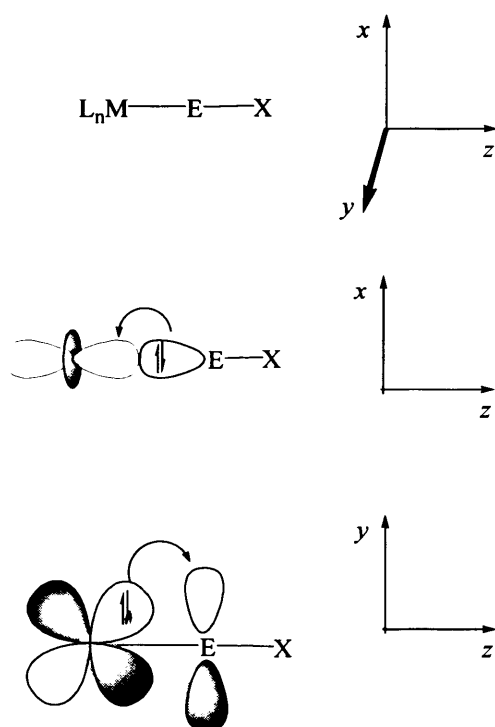


Figure 5

1.6.4.2 Structural and Spectroscopic Aspects of Transition Metal Group 13 Diyl Complexes

A number of structurally authenticated transition metal group 13 diyl complexes have been reported to date and as such only representative examples of structural interest will be discussed herein.

In 1994 Schnöckel *et al.*, reported the synthesis of the first transition metal complex $(\text{CpNi})_2(\mu_2\text{-AlCp}^*)_2$ featuring bridging AlCp^* fragments in which the ER ligand displays a μ_2 mode of coordination with the nickel centre.^{35b} A number of analogous ER bridging ligands have since been reported, for example, $\text{InC}(\text{SiMe}_3)_3$ has been shown to act as a bridging ligand in the transition metal complexes $\text{Mn}_2(\text{CO})_8[\mu_2\text{-InC}(\text{SiMe}_3)_3]_2$ and $\text{Co}_2(\text{CO})_7[\mu_2\text{-InC}(\text{SiMe}_3)_3]_2$.⁶⁴ Conversely, terminal metalladiyls which feature the ER fragment bound to one transition metal centre are relatively fewer in number compared to bridging diyls. $\text{Fe}(\text{CO})_4\text{AlCp}^*$, was the first example of a terminally coordinated Cp^*Al ligand, and this species helped confirm the isolobal relationship between CO and ER.⁷¹ Other reported examples include $(\text{Cp}^*\text{Al})\text{Cr}(\text{CO})_5$,⁶⁵ $(\text{Cp}^*\text{Ga})\text{Fe}(\text{CO})_4$ ⁴¹ and $(\text{Cp}^*\text{Ga})\text{W}(\text{CO})_3$.⁷⁹ Jutzi *et al.*, reported the synthesis of a variety of metal carbonyl clusters containing monomeric GaCp^* groups in which the ligand displays both bridging and terminal modes of coordination.⁴¹ Compounds with more than one terminal ER unit *e.g.* *cis*- $\text{Mo}(\text{CO})_4(\text{Cp}^*\text{Ga})_2$ have also been synthesised.⁶³

Multinuclear homoleptic cluster compounds such as $\text{Pt}_2(\text{GaCp}^*)_5$ and $\text{Pd}_3(\text{InCp}^*)_8$ featuring tetra-coordinated metal clusters, which have no direct carbonyl or phosphine analogues have also been reported. In addition, mononuclear

heteroleptic carbonyl containing complexes of the type $M(\text{CO})_a(\text{ER})_b$ have also been synthesised.^{80, 81} A series of homoleptic complexes of the type $M(\text{ER})_4$ have been reported for the group 10 transition metals (where $M = \text{Ni}, \text{Pd}, \text{Pt}$) where $E = \text{Ga}$ or In and $R = \text{Cp}^*$ or $\text{C}(\text{SiMe}_3)_3$. The homoleptic $\text{Ni}(0)$ complexes $\text{Ni}[\text{InC}(\text{SiMe}_3)_3]_4$ and $\text{Ni}[\text{GaC}(\text{SiMe}_3)_3]_4$ represent the first examples of transition metal complexes in which the metal centre is exclusively coordinated to terminal ER groups in an undistorted tetrahedral coordination sphere.⁶⁷ These species enable direct comparison with $\text{Ni}(\text{CO})_4$ which features isolobal CO ligands. The Ni-In-C moiety in $\text{Ni}[\text{InC}(\text{SiMe}_3)_3]_4$ is linear with Ni-In-C bond angles of 180° . It was reported that the short Ni-In bonds (2.310 Å) are indicative of a degree of π back bonding present. Quantum chemical calculations confirmed the presence of significant π back-bonding from the nickel centre to the empty p orbitals located at indium. Similarly, the Ni-Ga-C moiety in $\text{Ni}[\text{GaC}(\text{SiMe}_3)_3]_4$, is also linear with Ni-Ga-C bond angles of 180° . The comparatively short Ni-Ga bond distances (2.170(14) Å) confirm that back-bonding can be significant for homoleptic systems with competing π acidic ligands.⁶⁷

By contrast the degree of back-bonding within diyl complexes featuring ancillary carbonyl ligands remains a controversial area this in part is due to the lack of systematic spectroscopic, structural and computational data available. The iron gallium diyl complex $(\text{Ar}^*\text{Ga})\text{Fe}(\text{CO})_4$ features one of the shortest Fe-Ga bond lengths (2.2248(7) Å) yet reported. Robinson attributed the linear Fe-Ga-C_(ipso) geometric arrangement and the short Fe-Ga bond length to a triple bond between the iron and gallium centres.⁷² Cotton and Feng⁸² later argued on the basis of spectroscopic and theoretical results that the Fe-Ga bond is a simple donor/acceptor interaction. Theoretical calculations undertaken involved combining the Ar^*Ga unit

with the trigonally symmetric $\text{Fe}(\text{CO})_4$ fragment to build up the molecule with an 18-electron configuration featuring a bond order of 1. It was found that any further increases in this bond order can only occur by back donation of electrons on the iron atom to the empty orbitals on the gallium centre. Therefore to obtain a Ga-Fe triple bond, there would have to be two fully formed $\text{Fe} \rightarrow \text{Ga}$ dative π bonds. Cotton and Feng concluded that this degree of π back bonding was unlikely given the charge separation entailed and comparisons with $\text{Fe}(\text{CO})_4\text{PPh}_3$. For example, the CO stretching frequencies of $(\text{Ar}^*\text{Ga})\text{Fe}(\text{CO})_4$ are actually significantly *lower* than those found in $\text{Fe}(\text{CO})_4\text{PPh}_3$, where only a small amount of π back bonding is thought to occur (2032, 1959, 1941 and 1929 cm^{-1} vs 2052, 1979 and 1947 cm^{-1}). This result implies that there is actually *less* Fe-Ga π back bonding than Fe-P π back bonding. In addition, the Fe-Ga distance 2.2248(7) Å is only slightly shorter than the Fe-P distance 2.2244(1) Å in $\text{Fe}(\text{CO})_4\text{PPh}_3$.

A number of theoretical studies have been carried out on $(\text{GaAr}^*)\text{Fe}(\text{CO})_4$ and related systems from which it was concluded that the degree of iron to gallium back-bonding is minimal due to the relatively high energy of the group 13 metal p-orbitals.⁷⁷ Similar conclusions have been reached for indium diyl complexes. The monomeric organoindium(I) complex InAr^* is thought to act as a two electron donor, displacing a molecule of thf from $\text{Cp}(\text{CO})_2\text{Mn}(\text{thf})$ to yield $\text{Cp}(\text{CO})_2\text{MnInAr}^*$.^{48a} Crystallographic data revealed a near linear Mn-In- C_{ipso} geometric arrangement (175.39(9)°) and a short In-Mn bond (2.4102(9) Å). Carbonyl stretching frequencies (1940 and 1864 cm^{-1}) are comparable to those of $\text{Cp}(\text{CO})_2\text{Mn}(\text{thf})$ (1925 and 1850 cm^{-1}) indicating that InAr^* is a two electron σ donor with weak π acceptor properties. It was reported that the Mn-In distance is *ca.* 0.2 Å shorter than those found in related

bridged complexes such as $[\text{Mn}(\text{CO})_4\{\text{InC}(\text{SiMe}_3)_3\}]_2$,⁶² a factor attributed to the lower coordination number at the indium centre and the terminal nature of the ligand. The measured carbonyl stretching supported the view that the InAr^* fragment is a σ donor with weak π acceptor characteristics. This view also supports the bonding descriptions of $(\text{CO})_4\text{FeIn}\{3,5\text{-Me}_2(\text{pz})\text{BH}\}$ (pz = 3-phenylpyrazolyl, 3,5-di-tert-butylpyrazolyl or 3-tert-butylpyrazolyl),⁶⁹ in which the M-M bonding was described as a dative bond arising from the donation of a lone pair of electrons on indium to the metal carbonyl group, and also confirms that the In-Mn bond (and the analogous Ga-Fe bond in Robinson's compound⁷²) owe their deceptive shortness to the lower coordination number of the group 13 metal atom.

1.6.4.3 Theory of Bonding in Transition Metal Group 13 Diyl Complexes

Investigation of the synthesis of low coordinate diyl complexes (L_nMEX) of the group 13 elements is a relatively recent development and as such the nature of transition metal group 13 M-E bonds has resulted in a number of research groups examining these species from a theoretical viewpoint. As such a number of computational studies have been reported.^{77, 78} The two fundamental questions that have been extensively debated are (i) the degree of covalent and ionic character of the transition metal to ER bonds and (ii) the extent of the metal to ER π back bonding character of the metal-ligand interaction. Neutral complexes such as $(\text{CO})_4\text{FeEX}$, $\text{Fe}(\text{EX})_5$ and $\text{Ni}(\text{EX})_4$ have been studied and the effect of E, X and ancillary π acidic carbonyl ligands on the nature of the M-E bond have been examined.⁷⁸ Macdonald and Cowley investigated the nature of the bonding in diyl complexes of the type $(\text{CO})_4\text{FeER}$ (R = Cp, Me, or $\text{N}(\text{SiH}_3)_2$) by DFT analyses.⁸³ The uncoordinated ER ligands were also examined to establish their ground states, frontier orbitals, and

singlet/triplet separations with a view to understanding the coordination behaviour of ER ligands. Four bonding models were considered for the covalent interaction between group 13 (ER) and transition metal (ML_n) fragments.

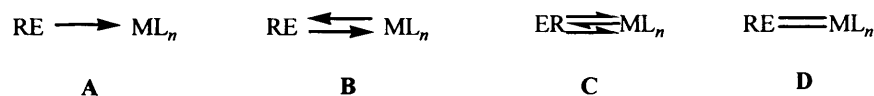


Figure 6

One of the main differences between the bonding situations relates to the electronic state of the group 13 fragment ER. Structures **A**, **B**, and **C** imply that the ER fragment coordinates in a singlet state. As such **A** results from a donor-acceptor interaction between E and M, whilst **B** and **C** result from one and two additional back-bonding interactions from the transition metal to the group 13 centre giving rise to double and triple bonds respectively, between E and M. Conversely the conventional double bonded structure **D**, implies that the ER fragment bonds in a triplet state.

It was found that the HOMO for almost every ER ligand exhibits distinct lone pair (σ -type) character in which the magnitude of the ‘lone pair’ contribution to the wavefunctions decreases with atomic number of the group 13 centre. The nature of the π -type LUMOs and the highest occupied π -type orbitals are dependent upon the conjugative ability of the R substituent. It was reported that in the case of MeE ligands, the p_x and p_y orbitals at the group 13 centre are essentially vacant, while the ($\eta^5\text{-C}_5\text{R}_5$) and (H_3Si)₂N ligands feature donation from either the $\eta^5\text{-C}_5\text{R}_5$ π -orbitals or the nitrogen lone pair into the p_x and/or p_y orbitals on E. These interactions are more important for boron than for the heavier analogues due to the greater electronegativity

and more effective π -bonding capacity of the boron centre. In addition, boron has a smaller atomic radius and its acceptor orbitals are significantly lower in energy. DFT calculations have also revealed that regardless of the substituent R (R = Cp, Cp*, Me, (H₃Si)₂N) each ER fragment essentially adopts a singlet ground state, with the singlet-triplet energy gap, ΔE_{S-T} , increasing with atomic number of the group 13 centre which eliminates the double-bonded model **D**, in which the ER fragment adopts a triplet ground state. Singlet-triplet gaps are larger with π -donating substituents. Thus, in principal, the ER ligands with non- π -donating R substituents could possess some π -acceptor capability (bonding models **B** and **C**). However, it was found that evidence of such metal-ligand back-bonding was only exhibited in the case of the alkyl substituted boranediyl complex MeBFe(CO)₄ and not for the heavier group 13 analogues. Thus it was therefore proposed that ER fragments effectively behave as simple two electron donor ligands (*i.e.* bonding model **A**).⁸³

Frenking and Uddin subsequently investigated the energy of the metal-ligand interactions in the transition metal complexes (CO)₄Fe(ER), Fe(EMe)₅, and Ni(EMe)₄ (E = B-Tl, R = Cp, N(SiH₃)₂, Ph and Me).⁷⁸ It was found that the attractive orbital interaction between (OC)₄Fe and ER components within (CO)₄Fe(ER) arises mainly as a result from σ donation of Fe←ER. A significant Fe→ER π back donating contribution was only found when E is boron, but even here the Fe←ER σ donation remained the dominant orbital interaction term. It was reported that when the R substituent, within (CO)₄Fe(ER), is a poor π donor, the species feature only slightly stronger Fe→ER π back-donation in comparison with stronger π donor substituents. It was also found that the resulting electrostatic and covalent interactions are similar in strength when E is Al-Tl and when the R substituent is a good π donor. The Fe-B

bonds of the boron diyl complexes have a significantly higher ionic character than the heavier group 13 analogues; in addition weaker π donor substituents enhance the ionic character of the $(\text{CO})_4\text{Fe}(\text{ER})$ bond. The electrostatic interactions arise as a result from the attraction between the negative charge concentration at the overall positively charged donor atom E of the Lewis base ER and the positive charge at the iron centre.

By contrast, it was found that the M-E bonds in $\text{Fe}(\text{EMe})_5$ and $\text{Ni}(\text{EMe})_4$ feature greater ionic character than in $(\text{CO})_4\text{Fe}(\text{ER})$. Thus the contribution of $\text{M} \rightarrow \text{E}$ π back-donation to the ΔE_{orb} term is higher in homoleptic complexes where no other π acceptor ligands are present. Surprisingly, it was found that although CO is a stronger π acceptor than BMe when the two ligands compete with each other, the relative contribution of the $\text{Fe} \rightarrow \text{BMe}$ π back donation to the ΔE_{orb} term in $\text{Fe}(\text{BMe})_5$ is almost as high as the $\text{Fe} \rightarrow \text{CO}$ π donation in $\text{Fe}(\text{CO})_5$. It was concluded that the M-E bonds of the homoleptic complexes $\text{Fe}(\text{ER})_5$ and $\text{Ni}(\text{ER})_4$, feature a stronger ionic character than that present in $(\text{CO})_4\text{FeER}$. In addition the contribution of the $\text{M} \rightarrow \text{ER}$ π back donation to the ΔE_{orb} term is higher in homoleptic complexes where no other competing π acceptor ligands, such as CO, are present.

Following these analyses Aldridge *et al.* have sought to characterise the nature of the M-E interaction in cationic diyl complexes of the type $[\text{Cp}^*\text{Fe}(\text{CO})_2\text{E}(\text{Mes})]^+$ (E = B, Al, Ga) and examine a proposed bonding model for such species comprising a $\text{E} \rightarrow \text{Fe}$ σ donation supplemented by $\text{Fe} \rightarrow \text{E}$ π back donation.⁸⁴ On the basis of molecular orbital compositions, bond dissociation energies, ΔE_{orb} values and σ/π covalent ratios, it was found that the bonding within $[\text{Cp}^*\text{Fe}(\text{CO})_2\text{B}(\text{Mes})]^+$, is best described as a double bond between the iron and boron centres. For the heavier group

13 analogues (E = Al, Ga), it was found that π back bonding may become significant as a result of the lowering of the energy of the E-based acceptor orbital for cationic species.

1.6.4.4 Reactivity of Transition Metal Complexes of Group 13 Diyls

1.6.4.4.1 Substitution/Addition Reactions of Transition Metal Complexes of Group 13 Diyls

Transition metal complexes of group 13 diyls feature relatively polar M-E bonds and the large steric demands of ER ligands means that dissociative or associative reactions, at the metal centre are unlikely. It has been demonstrated that sterically saturated monomeric complexes $M(\text{ECp}^*)_4$ are kinetically inert. Conversely, it has been shown that related cluster complexes $M_a(\text{ER})_b$ react with a variety of ligands such as CO and phosphines, to yield di- and trinuclear substitution products. For example, reaction of $M_2(\text{GaCp}^*)_2(\mu_2\text{-GaCp}^*)_3$ with PPh_3 yields the mono- or disubstituted complexes $\text{MPt}(\text{GaCp}^*)(\text{PPh}_3)(\mu_2\text{-GaCp}^*)_3$ (M = Pd, Pt) or $\text{Pd}_2(\text{PPh}_3)_2(\mu_2\text{-GaCp}^*)_3$, respectively. Heteroleptic complexes, $M(\text{GaCp}^*)_{4-x}(\text{L})_x$ (x = 1-4) are not usually accessible by substitution, however Fischer *et al.* demonstrated that the addition of a chelating diphosphine ligand, such as dppe, to $M_2(\text{GaCp}^*)_2(\mu_2\text{-GaCp}^*)_3$ leads to the complete substitution of the GaCp^* units yielding $M(\text{dppe})_2$ (M = Pd, Pt) quantitatively.^{6c}

1.6.4.4.2 Bond Activation Reactions of Transition Metal Complexes of Group 13 Diyls

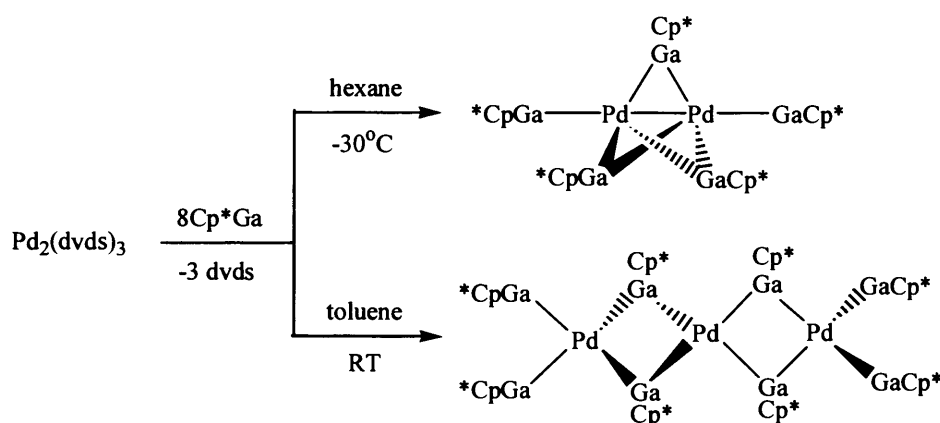
Transition metal complexes of group 13 diyls of the type $L_nM \leftarrow \text{ECp}^*$ feature strong polar donor/acceptor bonds, which has an effect of increasing the electron

density at the transition metal centre on coordination. This feature is of particular interest from a bond activation viewpoint as it might be implicated in facilitating oxidative addition reactions. This type of donor/acceptor bonding results in the metal centre becoming more electron rich and thus more susceptible to oxidation. It has been demonstrated that reaction of $\text{Ni}(\text{cod})_2$ with four equivalents of AlCp^* in benzene unexpectedly yields the complex $\text{NiH}(\text{AlCp}^*)_3(\text{AlCp}^*\text{Ph})$, and not $\text{Ni}(\text{AlCp}^*)_4$. It was proposed that the method of activation involves the formation of the reactive intermediate $(\text{AlCp}^*)_n\text{Ni}(\text{H})(\text{C}_6\text{H}_5)$ with migration of the phenyl group, followed by oxidation of aluminium, in the formation of a strong Al-C bond and coordination of a fourth equivalent of AlCp^* .⁶⁵ Further examples of C-H bond activation involve the reaction of $(\eta^6\text{-C}_6\text{H}_5\text{CH}_3)\text{Fe}(\eta^4\text{-C}_4\text{H}_8)$ with AlCp^* which yielded the chelating species $\text{Cp}^*\text{Al-CH}_2(\text{C}_5\text{Me}_4)\text{Al-CH}_2(\text{C}_5\text{Me}_4)\text{Al}$.^{6c} GaCp^* has also been involved in bond activation reactions. In addition, reaction of $\text{Cp}^*\text{Rh}(\text{CH}_3)_2\text{L}$ (L = dimethyl sulfoxide, pyridine) with GaCp^* gives the zwitterionic rhodium species $\text{Cp}^*\text{Rh}(\eta^5\text{-C}_5\text{Me}_4)\text{Ga}(\text{CH}_3)_3$, the driving force for which was proposed to involve the migration of the phenyl group to ECp^* (E = Al, Ga), with oxidation of the group 13 metal and the formation of a strong E-C bond.⁸⁵

1.6.4.4.3 Formation of Cluster Complexes by Transition Metal Complexes of Group 13 diyls

Group 13 diyls of the type ER (R = Cp^*) have been shown to act as stabilising ligands in metal cluster compounds. Neutral homoleptic cluster complexes such as $\text{M}_a(\text{ECp}^*)_b$ (M = Pd, Pt; $b > a > 1$) represent a relatively new class in the coordination chemistry of ER fragments.

Monomeric compounds of the type $M(\text{GaCp}^*)_4$ ($M = \text{Pt}, \text{Pd}$), can serve as building blocks for the synthesis of dinuclear cluster complexes $\text{MPt}(\text{GaCp}^*)_5$ featuring terminal and bridging GaCp^* ligands. For example, it has been demonstrated that the 1:1 reaction of $\text{Pt}(\text{cod})_2$ and $M(\text{GaCp}^*)_4$ followed by addition of GaCp^* yielded the species $\text{Pt}_2(\text{GaCp}^*)_2(\mu_2\text{-GaCp}^*)_3$ and $\text{PtPd}(\text{GaCp}^*)_2(\mu_2\text{-GaCp}^*)_3$.^{6c} It has also been shown that homoleptic cluster complexes can also be prepared by direct substitution reactions between group 13 diyl ER fragments and transition metal complexes featuring labile ligands. The kinetic control of cluster formation has also been investigated for example, the reaction of $\text{Pd}_2(\text{dvds})_3$ and GaCp^* has been shown to yield two different homoleptic cluster complexes depending on the conditions employed (Scheme 40).^{6c}



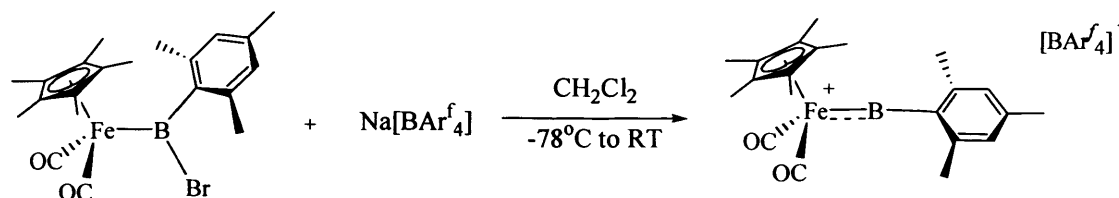
Scheme 40

1.6.5 Cationic Transition Metal Group 13 Diyl Complexes

1.6.5.1 Cationic M-ER Systems

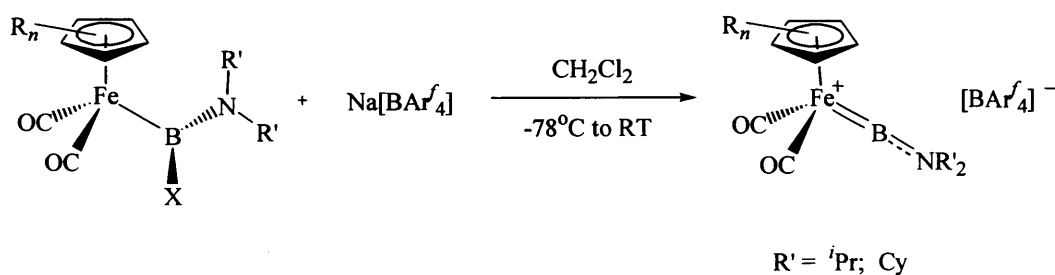
Tilley *et al.* utilised the method of halide abstraction in the synthesis of the first base free silylene complexes of the type $[\text{Cp}^*\text{Fe}(\text{PMe}_3)_2\text{Ru}=\text{SiR}_2]^+$ ($\text{R} = \text{Me}, \text{Ph}$) containing a ruthenium silicon double bond, by the reaction of $\text{Cp}^*(\text{PMe}_3)_2\text{RuSiR}_2(\text{OTf})$ with $\text{LiB}(\text{C}_6\text{F}_5)_4$ in dichloromethane.⁸⁶ In 2003, Aldridge *et*

al. extended this methodology in the synthesis of the first cationic terminal borylene complex $[\text{Cp}^*\text{Fe}(\text{CO})_2\text{B}(\text{Mes})]^+[\text{BAr}^f_4]^-$ (Scheme 41), by reaction of the boryl species $\text{Cp}^*\text{Fe}(\text{CO})_2\text{B}(\text{Mes})\text{Br}$ with $\text{Na}[\text{BAr}^f_4]$.⁸⁷ It was found that the Fe-B distance (1.792(8) Å) is significantly shorter than any other M-B bond reported and *ca.* 9% shorter than the Fe-B single bond in the boryl precursor. This bond distance is consistent with the presence of an Fe=B double bond, which features a significant Fe→B π back-bonding component (*i.e.* analogous to a Fischer carbene⁸⁸). DFT calculations confirmed the presence of multiple bond character within the Fe-B bond revealing an overall 62 % σ and 38 % π bonding character.⁸⁴



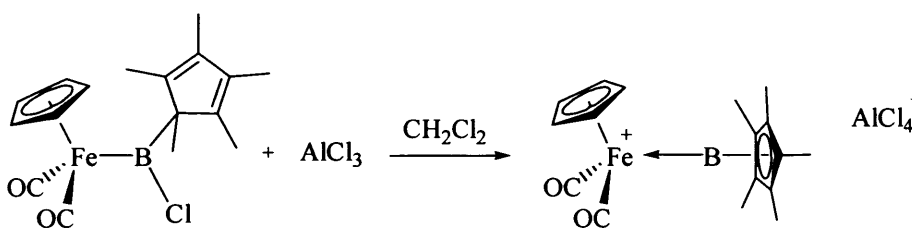
Scheme 41

Subsequent related work involved the synthesis of a range of cationic aminoborylene complexes $[\text{Cp}'\text{Fe}(\text{CO})_2\text{BN}^i\text{Pr}_2]^+$ and $[\text{Cp}\text{Fe}(\text{CO})_2\text{BNCy}_2]^+$ (Scheme 42).⁸⁹ Comparison of the Fe-B bond distances of $[\text{Cp}^*\text{Fe}(\text{CO})_2\text{B}(\text{Mes})]^+$ (1.792(8) Å), $[\text{Cp}'\text{Fe}(\text{CO})_2\text{BN}^i\text{Pr}_2]^+$ (1.835(3) Å) and $[\text{Cp}\text{Fe}(\text{CO})_2\text{BNCy}_2]^+$ (1.859(6) Å), revealed that the Fe-B bond lengths are longer when the boron centre is bound to an amino fragment rather than an aryl group. This trend presumably arises as a result of the boron centre being less electron deficient when bounded to the π -donor amino group (*cf.* mesityl).



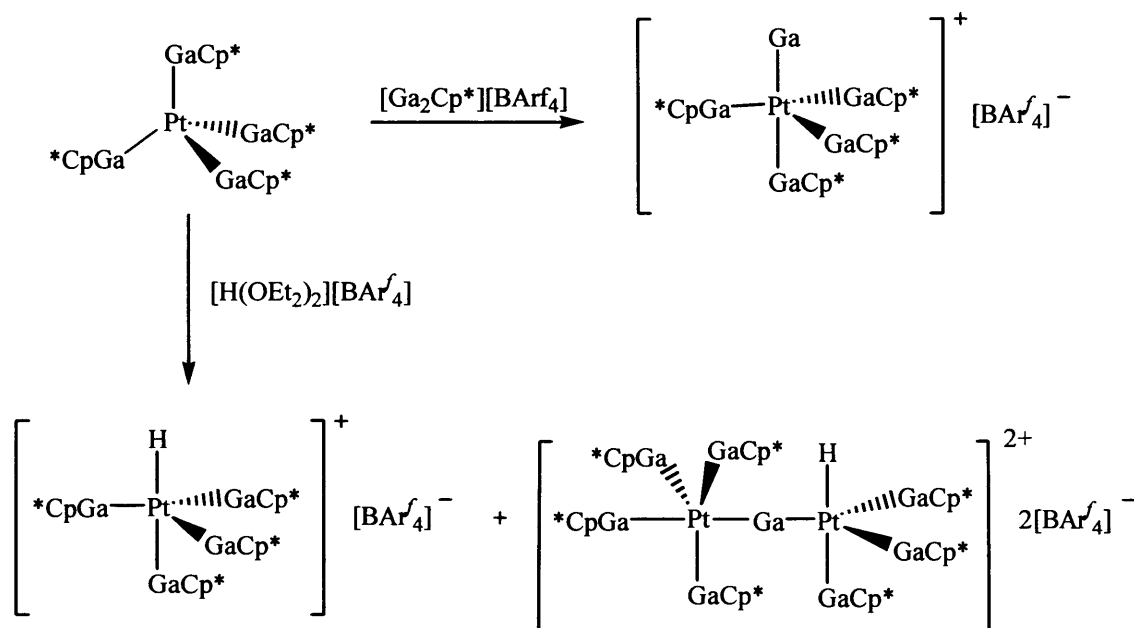
Scheme 42

In 2006, Cowley *et al.* also investigated the effects of varying the boron substituent on the bond order of the M-B bond.⁹⁰ The species $[CpFe(CO)_2(BCp^*)][AlCl_4]$ was synthesised *via* halide abstraction chemistry (Scheme 43) in which DFT calculations revealed the Fe-B bond order as one (*cf.* $[Cp^*Fe(CO)_2B(Mes)]^+$ Fe-B bond order of two). From these results it was concluded that the bond order within such systems is highly sensitive to the electronic properties of the boron substituent.



Scheme 43

In 2006, Fischer exploited the use of Ga^+ - and In^+ -transfer reagents $[E_2Cp^*][BAr'_4]$ in probing the bonding properties of E^+ ligands to electron-rich $[L_nPt]$ fragments. Fischer reported the synthesis of $[GaPt(GaCp^*)_4][BAr'_4]$ by reaction of $Pt(GaCp^*)_4$ with one equimolar amount of $[Ga_2Cp^*][BAr'_4]$ in fluorobenzene (Scheme 44).⁹¹



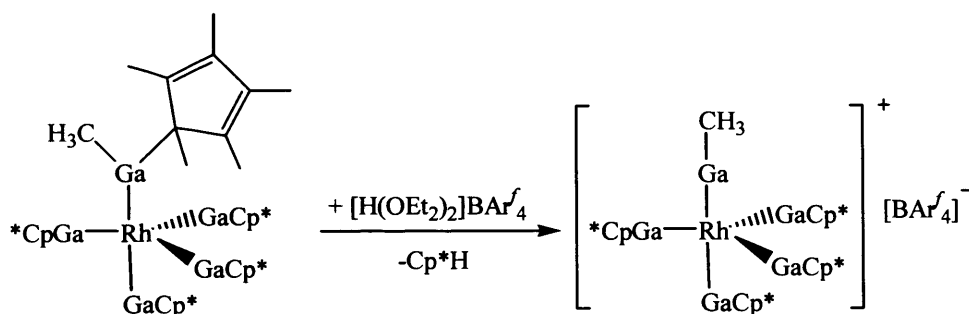
Scheme 44

X-ray diffraction studies revealed that the $[\text{GaPt}(\text{GaCp}^*)_4]^+$ ion exhibited a slightly distorted trigonal-bipyramidal structure with the Ga^+ ligand in an axial position. The equatorial GaCp^* ligands are bent towards the terminal Ga^+ ligand, and the $\text{Ga}(1)\text{-Pt-Ga}_x$ angles ($x = 2, 3, 4$) are closer to 80° than 90° . This property was similar to the umbrella effect of classical carbonyl metal hydride complexes $[(\text{CO})_n\text{M-H}]$.⁹² It was reported that the equatorial Pt-Ga bond lengths average 2.352 \AA and are comparable to those of the parent complex $\text{Pt}(\text{GaCp}^*)_4$ (2.335 \AA). Interestingly it was found that the $\text{Ga}(1)\text{-Pt}$ bond length ($2.459(1) \text{ \AA}$) is close to the value for the axial $\text{Cp}^*\text{Ga}(5)\text{-Pt}$ bond ($2.444(1) \text{ \AA}$), in which both bonds are slightly elongated with respect to the equatorial ones. It was reported that the bonding of the Ga^+ ligand to the closed shell 18-electron complex $\text{Pt}(\text{GaCp}^*)_4$ was as a result of the (soft) Lewis acidic properties of the Ga^+ ligand in contrast to the Lewis basic GaCp^* ligand. It was found that reaction of $\text{Pt}(\text{GaCp}^*)_4$ with $[\text{H}(\text{OEt}_2)_2]^+[\text{BARf}_4]^-$ resulted in the formation of two products $[\text{HPt}(\text{GaCp}^*)_4]^+$ and $[(\text{Cp}^*\text{Ga})_4\text{Pt}(\mu\text{-Ga})\text{Pt}(\text{GaCp}^*)_3\text{H}]^{2+}$.

It was found that the ratio of the two products changed in favour of $[(\text{Cp}^*\text{Ga})_4\text{Pt}(\mu\text{-Ga})\text{Pt}(\text{GaCp}^*)_3\text{H}]^{2+}$ when excess $[\text{H}(\text{OEt}_2)_2]^+[\text{BAR}^f_4]^-$ was used. It was reported that $[\text{HPt}(\text{GaCp}^*)_4]^+$ is an intermediate product in the formation of $[(\text{Cp}^*\text{Ga})_4\text{Pt}(\mu\text{-Ga})\text{Pt}(\text{GaCp}^*)_3\text{H}]^{2+}$. It was also postulated that the species $[\text{GaPt}(\text{GaCp}^*)_3]^+$ may be formed as a result of the release of Cp^*H upon protonation. It was found that monitoring the reactions by NMR spectroscopy revealed a complex spectra with a number of very broad, overlapping peaks indicating H^+ -dependent equilibria. In order to further probe this Fischer further reacted PtL_4 ($\text{L} = \text{PPh}_3, \text{GaCp}^*$) with $\text{Tl}[\text{BAR}^f_4]$ and $\text{In}[\text{BAR}^f_4]$ as sources of Tl^+ and In^+ . Several products were formed including $[\text{InPt}(\text{PPh}_3)_3][\text{BAR}^f_4]$, in which the Pt centre has a trigonal-pyramidal geometry as a result of elimination of the PPh_3 ligand, and the In^+ ligand is located in the axial position. It was concluded that the metal fragments $[\text{PtL}_n]$ within $[\text{GaPt}(\text{GaCp}^*)_4][\text{BAR}^f_4]$ and $[\text{InPt}(\text{PPh}_3)_3][\text{BAR}^f_4]$ are therefore σ donors for E^+ in which neither the variation of L (GaCp^* vs PMe_3 , GaCp^* vs PPh_3) nor variation of the coordination number in $[\text{PtL}_n]$ ($n = 3, 4$) substantially influences the donor properties.

Fischer recently reported the synthesis of $[(\text{Cp}^*\text{Ga})_4\text{Rh}(\text{GaCH}_3)]^+[\text{BAR}^f_4]^-$ in which the methylgallium moiety is bound in a terminal fashion.⁹³ It was reported that reaction of $[\text{Rh}(\text{CH}_3)(\text{cod})(\text{py})]$ with an excess of GaCp^* in hexane at room temperature leads to the substitution of the labile ligands pyridine and 1,5-cyclooctadiene, as well as to the insertion of the carbenoid GaCp^* into the Rh-CH_3 σ -bond to yield the all-Ga-coordinated neutral complex $(\text{Cp}^*\text{Ga})_4\text{Rh}(\eta^1\text{-Cp}^*\text{GaCH}_3)$. Protolysis of $(\text{Cp}^*\text{Ga})_4\text{Rh}(\eta^1\text{-Cp}^*\text{GaCH}_3)$ with a stoichiometric amount of $[\text{H}(\text{OEt}_2)_2]^+[\text{BAR}^f_4]^-$ at -30°C in fluorobenzene lead to the formation of

$[(\text{Cp}^*\text{Ga})_4\text{Rh}(\text{GaCH}_3)]^+[\text{BARf}_4]^-$ (Scheme 45) as pale yellow crystals on slow diffusion of hexanes at 25°C.



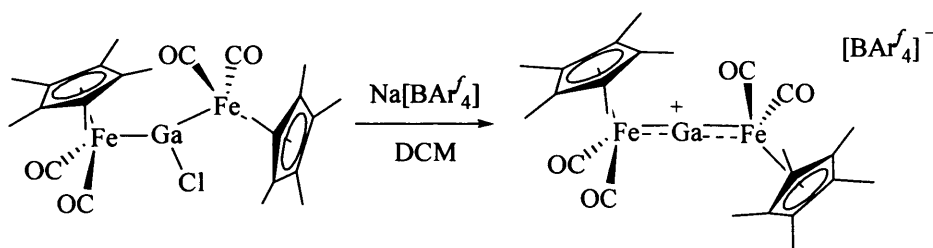
Scheme 45

X-ray diffraction studies revealed a distorted trigonal bipyramidal structure in which the GaCH_3 group occupies an axial position. Surprisingly it was reported that the striking feature of $[(\text{Cp}^*\text{Ga})_4\text{Rh}(\text{GaCH}_3)]^+$ is the counterintuitive fact that the Rh-GaCH_3 bond (247.11(10) pm) is by far the longest Rh-Ga bond within the complex. This Rh-Ga1 bond is about 8 % longer than the axial Rh-Ga and the equatorial Rh-Ga bonds, which differ from each other by only 1 % (2.2815(6)-2.3099(7) Å). In addition these Rh-GaCp^* bonds in the cation $[(\text{Cp}^*\text{Ga})_4\text{Rh}(\text{GaCH}_3)]^+$ are shorter than those in the neutral compound $(\text{Cp}^*\text{Ga})_4\text{Rh}(\eta^1\text{-Cp}^*\text{GaCH}_3)$ (2.3941(13)-2.3476(8) Å). Interestingly, it was found that the Rh-Ga bond becomes shorter when pyridine is coordinated to the gallium centre. This presumably arises due to gallium being a better σ donor (and poorer π acceptor) on coordination of pyridine. As σ bonding is more important than π bonding the bond becomes shorter.

1.6.5.2 Cationic M-E-M Complexes

In 2004, Aldridge *et al.* investigated the synthesis of the cationic bridging metalladiyl systems. It was reported that reaction of $[\text{Cp}^*\text{Fe}(\text{CO})_2]_2\text{GaCl}$ with the

halide abstracting agent $\text{Na}[\text{BAr}^f_4]$ yielded the cationic species $[\{\text{Cp}^*\text{Fe}(\text{CO})_2\}_2(\mu\text{-Ga})]^+$ featuring a ‘naked’ bridging gallium centre. The bonding was described as a partial double bond delocalised over the Fe-Ga-Fe centres.⁹⁴



Scheme 46

Crystallographic evidence reported a linear Fe-Ga-Fe unit [$\angle\text{Fe}(1)\text{-Ga}(1)\text{-Fe}(1') = 178.99(2)^\circ$], which is consistent with a ‘naked’ bridging gallium atom engaging in no significant secondary interactions (*e.g.* with the atom). Computational analysis also revealed a 61 % σ and 38 % π bonding contribution to the covalent Fe-Ga bonds indicating multiple bond character within the species.

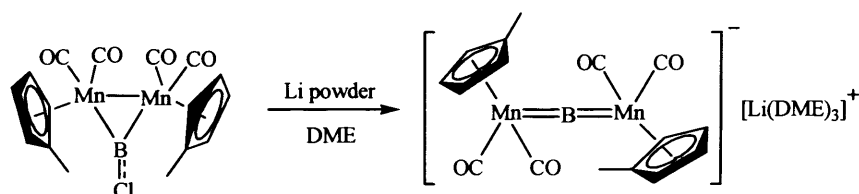
Recently, Braunschweig *et al.* reported the isolation of the first metalloborylene complexes $[\{\text{Mn}(\text{CO})_5\}_2(\mu\text{-B})]^+[\text{BAr}^f_4]^-$ and $[\{\{\eta^5\text{-C}_5\text{H}_4\text{R}\}\text{Fe}(\text{CO})_2\}_2(\mu\text{-B})]^+[\text{BAr}^f_4]^-$ ($\text{R} = \text{H}, \text{Me}$), in which the boron centre is in the coordination sphere of two transition metals, *via* halide abstraction from the corresponding bridged haloborylene complexes.⁹⁵ It was found that reaction of $[\text{Mn}(\text{CO})_5]_2(\mu\text{-BBr})$ with one equivalent of $\text{Na}[\text{BAr}^f_4]$ in dichloromethane yielded the cationic metalloborylene complex $[\{\text{Mn}(\text{CO})_5\}_2(\mu\text{-B})]^+[\text{BAr}^f_4]^-$. X-ray diffraction studies revealed a linear Mn-B-Mn arrangement in which the Mn-B bond length (1.9096(5) Å) is significantly shorter than those in $[\text{Mn}(\text{CO})_5]_2(\mu\text{-BBr})$ (2.149(3) and 2.163(5) Å) or in the dichloroboryl complex $(\text{OC})_5\text{MnBCl}_2$. It was found that the CO

ligands *cis* to the boron atom showed a noticeable umbrella effect as indicated by the average C_{cis} -Mn-B (86.04°) and Mn- C_{cis} -O bond angles (176.6°). Furthermore the Mn- C_{trans} distance ($1.932(4)$ Å) is significantly longer than the corresponding Mn- C_{cis} distances ($1.864(4)$ - $1.884(4)$ Å), which is in agreement with the enhanced *trans*-influence of the boron ligand with respect to the CO ligand. However, it was found that $[\{\text{Mn}(\text{CO})_5\}_2(\mu\text{-B})]^+[\text{BAr}^f_4]^-$ is extremely sensitive and readily decomposes within a few days in the solid state at -35°C under an atmosphere of argon. Monitoring the decay of a sample of $[\{\text{Mn}(\text{CO})_5\}_2(\mu\text{-B})]^+[\text{BAr}^f_4]^-$ in CD_2Cl_2 by ^{11}B NMR spectroscopy revealed (within 2 h) the formation of a compound displaying a doublet at δ 123.9, which was attributed to the formation of $[\text{Mn}(\text{CO})_5]_2(\mu\text{-BF})$ by fluoride abstraction from the $[\text{BAr}^f_4]^-$ ion. Analogous behaviour has also been reported by Aldridge *et al.* for the reaction of $\text{Cp}^*\text{Fe}(\text{CO})_2\text{B}(\text{Cl})\text{OMes}$ with $\text{Na}[\text{BAr}^f_4]$.⁹⁶

Following this, Braunschweig *et al.* investigated the synthesis of potentially more stable cationic metallocarbonylene complexes. It was found that reaction of $[\text{CpFe}(\text{CO})_2]_2(\mu\text{-BCl})$ with $\text{Na}[\text{BAr}^f_4]$ yielded $[\{\text{CpFe}(\text{CO})_2\}_2(\mu\text{-B})]^+[\text{BAr}^f_4]^-$, which showed no propensity to decompose neither in the solid state nor in dichloromethane solution over a period of 2 weeks, and thus it was concluded that its thermal stability is substantially higher than that of $[\{\text{Mn}(\text{CO})_5\}_2(\mu\text{-B})]^+[\text{BAr}^f_4]^-$. Braunschweig subsequently synthesised the Cp'-substituted derivatives including $[\text{Cp}'\text{Fe}(\text{CO})_2]_2(\mu\text{-BCl})$ and $[\{\text{Cp}'\text{Fe}(\text{CO})_2\}_2(\mu\text{-B})]^+[\text{BAr}^f_4]^-$ by an analogous procedure.⁹⁵

1.6.5.3 Anionic M-E-M Complexes

Braunschweig recently reported the synthesis of the anionic dimetalloborylene complex $[\text{Li}(\text{DME})_3]^+[\{\text{Cp}^*\text{Mn}(\text{CO})_2\}_2\text{B}]^-$, by stirring a mixture of large excess of lithium sand and $[\text{Cp}^*\text{Mn}(\text{CO})_2]_2\text{BCl}$ in DME at -10°C and subsequent warming to room temperature, followed by workup of the reaction mixture (Scheme 47). X-ray crystallographic analysis confirmed the anionic nature of the Mn_2B fragment, which is separate from its counter cation $[\text{Li}(\text{DME})_3]^+$.⁹⁷ This anion is isoelectronic with the $[\{\text{Cp}^*\text{Fe}(\text{CO})_2\}_2\text{B}]^+$ cation.



Scheme 47

1.7 Aims of this Research

The chemistry of low coordinate or multiply bonded group 13 ligand systems continues to attract significant research interest and in some cases considerable controversy. Compared to carbenes and silylenes, the structural and reaction chemistry of analogous group 13 diyl species $\text{L}_n\text{M}(\text{EX})$ has been less widely explored, in part due to the limited number of structurally authenticated complexes reported. Diyl species have largely been generated *via* salt elimination or ligand substitution methodologies. With a view to exploring the possible synthetic routes for the preparation of unsaturated group 13 systems, a novel synthetic approach to two-coordinate diyl complexes has been developed within our research group, using halide abstraction chemistry to generate the species $[\text{Cp}^*\text{Fe}(\text{CO})_2\text{B}(\text{Mes})]^+[\text{BAr}_4]^-$ ⁸⁷ and $[\{\text{Cp}^*\text{Fe}(\text{CO})_2\}_2(\mu\text{-Ga})]^+[\text{BAr}_4]^-$.⁹⁴ Preliminary computational studies suggested that

the positive charge in cationic terminal diyl species, $[L_nM(EX)]^+$, is located primarily at the group 13 centre (*e.g.* Mulliken charges +0.438, +0.680, and +0.309 for $[Cp^*Fe(CO)_2B(Mes)]^+$ E = B, Al, Ga), and consequently that M→E back bonding may contribute appreciably to the overall metal ligand interaction (*e.g.* a 38 % π contribution to the FeB bonding density in $[Cp^*Fe(CO)_2B(Mes)]^+$). Hence the Fe=B double bond in $[Cp^*Fe(CO)_2B(Mes)]^+$ can be described as comprising of B→Fe σ donor and Fe→B π acceptor components. Therefore it is our intention to extend this synthetic approach in the synthesis of other heavier group 13 systems and investigate the use of halide abstraction chemistry to generate cationic gallium and indium derivatives. Due to the small number of neutral three coordinate systems of the type $L_nM-E(X)(E'R')$ (E = Ga, In; X = halide) the preparation of these halogallyl precursor complexes suitable for halide abstraction will be firstly explored. The generation of these three coordinate gallium systems has two synthetic approaches *via* (i) direct substitution of a gallium-based halide by an organometallic anion; and (ii) a two step strategy involving insertion of a gallium(I) halide into a metal-halogen (or metal-metal) bond, followed by substitution at the group 13 centre by a suitably sterically hindered anionic nucleophile.

The nature of the M-E bond in cationic systems will then be analysed by comparative spectroscopic, structural and computational studies as a function of the element E, thereby examining the controversial subject of multiple bonding involving the heavier group 13 elements. In addition reactivity studies of these novel cationic systems will also be investigated.

1.8 References for Chapter One

1. (a) Brothers, P. J.; Power, P. P. *Adv. Organomet. Chem.* **1996**, *39*, 1. (b) Fischer, R. A.; Weiß, J. *Angew. Chem. Int. Ed.* **1999**, *38*, 2830. (c) Compton, N. A.; Errington, J. R.; Norman, N. C. *Adv. Organomet. Chem.* **1990**, *31*, 91.
2. Fischer, R. A.; Weiß, J. *Angew. Chem. Int. Ed. Engl.* **1999**, *38*, 2830.
3. (a) Baker, R. T.; Ovenall, D. W.; Calabrese, J. C.; Westcott, S. A.; Taylor, N. J.; Williams, I. D.; Marder, T. D. *J. Am. Chem. Soc.* **1990**, *112*, 9399. (b) Knorr, J. R.; Merola, J. S. *Organometallics* **1990**, *112*, 3008 (c) Irvine, G. J.; Lesley, M. J. G.; Marder, T. B.; Norman, N. C.; Rice, C. R.; Robbins, E. G.; Roper, W. R.; Whittell, G. R.; Wright, L. *J. Chem. Rev.* **1998**, *98*, 2685. (d) Braunschweig, H. *Angew. Chem. Int. Ed. Engl.* **1998**, *37*, 1786. (e) Smith III, M. R. *Prog. Inorg. Chem.* **1999**, *48*, 505. (f) Braunschweig, H.; Colling, M. *J. Organomet. Chem.* **2000**, *614*, 18. (g) Braunschweig, H.; Colling, M. *Coord. Chem. Rev.* **2001**, *223*, 1. (h) Braunschweig, H.; Colling, M. *Eur. J. Inorg. Chem.* **2003**, 393.
4. Downs, A. J. *Coord. Chem. Rev.* **1999**, *189*, 59.
5. Braunschweig, H. *Adv. Organomet. Chem.* **2004**, *51*, 163.
6. (a) Linti, G.; Schnöckel, H. *Coord. Chem. Rev.* **2000**, *206-207*, 285. (b) Schebaum, L. O.; Jutzi, P. *ACS Sym. Ser.* **2002**, 822, 16. (c) Gemel, C.; Steinke, T.; Cokoja, M.; Kempter, A.; Fischer, R. A. *Eur. J. Inorg. Chem.* **2004**, 4161. (d) Cowley, A. H. *J. Organomet. Chem.* **2004**, *689*, 3866. (e) Steinke, T.; Gemel, C.; Winter, M.; Fischer, R. A. *Angew. Chem. Int. Ed.* **2002**, *41*, 4761.
7. (a) Hardman, N. J.; Wright, R. J.; Phillips, A. D.; Power, P. P. *J. Am. Chem. Soc.* **2003**, *125*, 2667. (b) Yang, X. -J.; Quillian, B.; Wang, Y.; Wei, P.; Robinson, G. H. *Organometallics* **2004**, *23*, 5119. (c) Uhl, W.; El-Hamden, A.; Petz, W.; Geiseler, G.;

- Harms, K. *Z. Naturforschungs B* **2004**, *59*, 789. (d) Braunschweig, H.; Radacki, K.; Rais, D.; Seeler, F.; Uttinger, K. *J. Am. Chem. Soc.* **2005**, *127*, 1386.
8. (a) Wadepohl, H. *Angew. Chem. Int. Ed. Engl.* **1997**, *36*, 2441. (b) Braunschweig, H. *Angew. Chem. Int. Ed.* **1998**, *37*, 1787. (c) Schmid, G. *Angew. Chem. Int. Ed. Engl.* **1970**, *9*, 819.
9. St. Denis, J. N.; Butler, W.; Glick, M. D.; Oliver, J. P. *J. Organomet. Chem.* **1977**, *129*, 1.
10. Thorn, D. L.; Harlow, R. L. *J. Am. Chem. Soc.* **1989**, *111*, 2575
11. (a) Eaborn, C.; Pidcock, A.; Steele, B. R. *J. Am. Chem. Soc., Dalton Trans.* **1976**, 767. (b) Eaborn, C.; Kundu, K.; Pidcock, A. *Ibid.* **1981**, 1223. (c) Al-Allaf, T. A. K.; Eaborn, C.; Kundu, K.; Pidcock, A. *J. Chem., Soc. Chem. Commun.* **1981**, 55. (d) Al-Allaf, T. A. K.; Butler, G.; Eaborn, C.; Pidcock, A. *J. Organomet. Chem.* **1980**, *188*, 335.
12. (a) Hsieh, A. T. T.; Mays, M. J. *J. Nucl. Chem. Lett.* **1971**, *7*, 223. (b) Hsieh, A. T. T.; Mays, M. J. *J. Organomet. Chem.* **1972**, *37*, 9.
13. Clarkson, L. M.; Norman, N. C. *Organometallics*, **1991**, *10*, 1286.
14. Green, M. L. H.; Mountford, P.; Smout, G. J.; Speel, S. R. *Polyhedron*, **1990**, *9*, 2763.
15. Corbett, J. D.; McMullen, R. K. *J. Chem. Soc.* **1955**, *77*, 4217.
16. Chadwick, J. R.; Atkinson, A. W.; Huckstepp, B. G. *J. Inorg. Nucl. Chem.* **1966**, *28*, 1021.
17. Gerlach, C.; Hönle, W.; Simon, A. *Z. Anorg. Allg. Chem.* **1982**, *21*, 1876.
18. Wilkinson, M.; Worrall, I. J. *J. Organomet. Chem.* **1979**, *166*, 293.
19. (a) Baker, R. J.; Bettentrup, H.; Jones, C. *Eur. J. Inorg. Chem.* **2003**, 2446. (b) Baker, R. J.; Bettentrup, H.; Jones, C. *Inorg. Chem. Commun.* **2004**, *7*, 1289.

20. See for example (a) Doriat, C. U.; Friesen, M.; Baum, E.; Ecker, A.; Schnöckel, H. *Angew. Chem. Int. Ed. Engl.* **1997**, *36*, 1969. (b) Beagley, B.; Godfrey, S. M.; Kelly, K. J.; Kungwankunakorn, S.; McAuliffe, C. A.; Prichard, R. G. *Chem. Commun.* **1996**, 2179.
21. He, X.; Bartlett, R. A.; Power, P. P. *Organometallics* **1994**, *13*, 548.
22. Cowley, A. H.; Decken, A.; Olazábal, C. A.; Norman, N. C. *Inorg. Chem.* **1994**, *33*, 3435.
23. Borovik, A. S.; Bott, S. G.; Barron, A. R. *Organometallics* **1999**, *18*, 2668.
24. Ueno, K.; Wanatabe, T.; Tobita, H.; Ogino, H. *Organometallics* **2003**, *22*, 4375.
25. Anand, B. N.; Krossing, I.; Nöth, H. *Inorg. Chem.* **1997**, *36*, 1979.
26. Bunn, N. R.; Aldridge, S.; Kays (née Coombs), D. L.; Coombs, N. D.; Day, J. K.; Ooi, L.-L.; Coles, S. J.; Hursthouse, M. B. *Organometallics* **2005**, *24*, 5879.
27. Linti, G.; Li, H.; Pritzkow, H. *J. Organomet. Chem.* **2001**, *626*, 82.
28. Ueno, K.; Watanabe, T.; Ogino, H. *Applied Organomet. Chem.* **2003**, *17*, 403.
29. Dickinson, A. A.; Willock, D. J. Calder, R. J.; Aldridge, S. *Organometallics* **2002**, *21*, 1146.
30. Rickard, C. E. F.; Roper, W. R.; Williamson, A.; Wright, L. J. *Organometallics*, **2002**, *21*, 1714. (b) Schubert, U. *Coord. Chem. Rev.* **1984**, *55*, 261.
31. (a) Frenking, G.; Fröhlich, N. *Chem. Rev.* **2000**, *100*, 717. (b) Giju, K. T.; Bickelhaupt, F. M.; Frenking, G. *Inorg. Chem.* **2000**, *39*, 4776. (c) Sakaki, S.; Biswas, B.; Musashi, Y.; Sugimoto, M. *J. Organomet. Chem.* **2000**, *611*, 288. (d) Lam, W. H.; Lin, Z. *J. Organomet. Chem.* **2001**, *635*, 84. (e) Sivignon, G.; Fleurat-Lessard, P.; Onno, J. M.; Volatron, F. *Inorg. Chem.* **2002**, *41*, 6656.
32. Aldridge, S.; Al-Fawaz, A.; Calder, R. J.; Dickinson, A. A.; Willock, D. J.; Light, M. E.; Hursthouse, M. B. *Chem. Commun.* **2001**, 1846.

33. (a) Tolman, C. A. *J. Am. Chem. Soc.* **1970**, *92*, 2953. (b) Tolman, C. A. *J. Am. Chem. Soc.* **1970**, *92*, 2956. (c) *Infrared and Raman Spectra of Inorganic and Coordination Compounds*, Part B, 5th Edn. Nakamoto, K. Wiley-Interscience, New York, **1997**.
34. Schilling, B. E. R.; Hoffman, R. Lichtenberger, D. L. *J. Am. Chem. Soc.* **1979**, *101*, 585.
35. Dohmeier, C.; Robl, C.; Tacke, M.; Schnöckel, H. *Angew. Chem. Int. Ed. Engl.* **1991**, *30*, 564. (b) Dohmeier, C.; Loos, D.; Schnöckel, H. *Angew. Chem. Int. Ed. Engl.* **1996**, *35*, 129.
36. Loos, D.; Baum, E.; Ecker, A.; Schnöckel, H.; Downs, A. J. *Angew. Chem. Int. Ed. Engl.* **1997**, *36*, 860.
37. Uhl, W.; Hiller, W.; Layh, M.; Schwarz, W. *Angew. Chem. Int. Ed. Engl.* **1992**, *31*, 1364.
38. Uhl, W.; Keimling, S. U. Klinkhammer, K. W.; Schwarz, W. *Angew. Chem. Int. Ed. Engl.* **1997**, *36*, 64.
39. Mennekes, T.; Paetzold, P.; Boese, R.; Blaeser, D. *Angew. Chem. Int. Ed. Engl.* **1991**, *30*, 173.
40. Schulz, S.; Roesky, H. W.; Koch, Sheldrick, G. M.; Stalke, D.; Kuhn, A. *Angew. Chem. Int. Ed. Engl.* **1993**, *32*, 1729.
41. Jutzi, P.; Neumann, B.; Reumann, G.; Stammer, H. G. *Organometallics* **1998**, *17*, 1305.
42. Schnitter, C.; Roesky, H. W.; Roepken, C.; Herbst-Irmær, R.; Schmidt, H. G.; Noltemeyer, M. *Angew. Chem. Int. Ed. Engl.* **1998**, *37*, 1952.
43. Beachley Jr, O. T.; Churchill, M. R.; Fettinger, J. C.; Pazik, J. C. *J. Am. Chem. Soc.* **1986**, *108*, 4666.

44. (a) Schluter, R. D.; Cowley, A. H.; Atwood, D. A.; Jones, R. A.; Atwood, J. L. *J. Coord. Chem.* **1993**, *30*, 35. (b) Uhl, W.; Graupner, R.; Layh, M.; Schütz, J. *Organomet. Chem.* **1995**, *493*, C1.
45. Uhl, W.; Hiller, W.; Layh, M.; Schwarz, W. *Angew. Chem. Int. Ed. Engl.* **1992**, *31*, 1364.
46. Jutzi, P.; Schebaum, L. O. *J. Organomet. Chem.* **2002**, *654*, 176.
47. Schnepf, A; Schnöckel, H. *Angew. Chem. Int. Ed. Engl.* **2002**, *41*, 3533.
48. (a) Haubrich, S. T.; Power, P. P. *J. Am. Chem. Soc.* **1998**, *120*, 2202. (b) Niemeyer, M.; Power, P. P. *Angew. Chem. Int. Ed.* **1998**, *37*, 1277.
49. Wright, R. J.; Brynda, M.; Fettinger, J. C.; Betzer, A. R.; Power, P. P. *J. Am. Chem. Soc.* **2006**, *128*, 12498.
50. Wiberg, N.; Amelunxen, K.; Nöth, H.; Schmidt, M.; Schenk, H. *Angew. Chem. Int. Ed. Engl.* **1996**, *35*, 65.
51. Beachley Jr, O. T.; Blom, R.; Churchill, M. R.; Faegri Jr, K.; Fettinger, J. C.; Pazik, J. C.; Victoriano, L. *Organometallics* **1989**, *8*, 346.
52. Ahlrichs, R.; Ehrig, M.; Horn, H. *Chem. Phys. Lett.* **1991**, *183*, 227.
53. (a) Bourissou, D.; Guerret, O.; Gabbai, F. P.; Bertrand, G. *Chem. Rev.* **2000**, *100*, 39. (b) Carmalt, C. J.; Cowley, A. H. *Adv. Inorg. Chem.* **2000**, *50*, 1. (c) Herrmann, W. A. *Angew. Chem. Int. Ed.* **2002**, *41*, 1290.
54. (a) Haaf, M.; Schmedake, T. A.; West, R. *Acc. Chem. Res.* **2000**, *33*, 704. (b) Köhl, O. *Coord. Chem. Rev.* **2004**, *248*, 411. (c) Carmalt, C. J.; Lomeli, V.; McBurnett, B. G.; Cowley, A. H. *Chem. Commun.* **1997**, 2095. (d) Denk, M. K.; Gupta, S.; Lough, A. J. *Eur J. Inorg. Chem.* **1999**, 41.
55. (a) Cui, C.; Roesky, H. W.; Schmidt, H. -G.; Noltmeyer, M.; Hao, H.; Cimpoesu, F. *Angew. Chem. Int. Ed.* **2000**, *39*, 4274. (b) Hardman, N. J.; Eichler, B. E.; Power.

- P. P. *Chem. Commun.* **2000**, 1991. (c) Hill, M. S.; Hitchcock, P. B.; Pongtavornpinyo, R. *Dalton Trans.* **2005**, 273. (d) Cheng, Y.; Hitchcock, P. B.; Lappert, M. F.; Zhou, M. *Chem. Commun.* **2005**, 752.
56. Jones, C.; Junk, P. C.; Platts, J. A.; Stasch, A. *J. Am. Chem. Soc.* **2006**, *128*, 2206.
57. Schmidt, E. S.; Jockisch, A.; Schmidbaur, H. *J. Am. Chem. Soc.* **1999**, *121*, 9758.
58. Baker, R. J.; Jones, C. *Dalton Trans.* **2005**, *8*, 1341.
59. Baker, R. J.; Farley, R. D.; Jones, C.; Kloth, M.; Murphy, D. M. *J. Chem. Soc. Dalton Trans.* **2002**, 3844.
60. Hill, M. S.; Hitchcock, P. B. *Chem. Commun.* **2004**, 1818. (b) Hill, M. S.; Hitchcock, P. B.; Pongtavornpinyo, R. *Angew. Chem. Int. Ed.* **2005**, *44*, 4231.
61. Stender, M.; Power, P. P. *Polyhedron* **2002**, *21*, 525.
62. Uhl, W.; Keimling, U.; Hiller, W.; Neumeyer, M. *Chem. Ber.* **1996**, *129*, 1137.
63. Jutzi, P.; Neumann, B.; Schebaum, L. O.; Stammler, A.; Stammler, H. G. *Organometallics* **1999**, *18*, 4462.
64. Uhl, W.; Pohlmann, M. *Organometallics* **1997**, *16*, 2478.
65. Yu, Q.; Purath, A.; Donchev, A.; Schnöckel, H. *J. Organomet. Chem.* **1999**, *584*, 94.
66. Uhl, W.; Pohlmann, M.; Warchow, R. *Angew. Chem. Int. Ed.* **1998**, *37*, 961.
67. Uhl, W.; Benter, M.; Melle, S.; Saak, W. *Organometallics* **1999**, *18*, 3778.
68. Cokoja, M.; Gemel, C.; Steinke, T.; Welzl, T.; Winter, M.; Fischer, R. A. *J. Organomet. Chem.* **2003**, 277.
69. Reger, D. L.; Mason, S. S.; Rheingold, A. L.; Haggerty, B. S.; Arnold, F. P. *Organometallics* **1994**, *13*, 5049.
70. Yamaguchi, T.; Ueno, K.; Ogino, H. *Organometallics* **2001**, *20*, 501.

71. Weiss, J.; Stetzkamp, D.; Nuber, B.; Fischer, R. A.; Boehme, C.; Frenking, G. *Angew. Chem. Int. Ed. Engl.* **1997**, *36*, 70.
72. Su, J.; Li, X. -W.; Crittendon, R. C.; Campana, C. F.; Robinson, G. H. *Organometallics* **1997**, *16*, 4511.
73. Dohmeier, C.; Krautscheid, H.; Schnöckel, H. *Angew. Chem. Int. Ed. Engl.* **1994**, *33*, 2482.
74. Jutzi, P.; Neumann, B.; Schebaum, L. O.; Stammler, A.; Stammler, H. G. *Organometallics* **2000**, *19*, 1445.
75. Weiss, D.; Steinke, T.; Winter, M.; Fischer, R. A.; Frölich, N.; Uddin, J.; Frenking, G. *Organometallics* **2000**, *19*, 4583.
76. Braunschweig, H.; Radacki, K.; Scheschkewitz, D.; Whittell, G. R. *Angew. Chem. Int. Ed.* **2005**, *44*, 1658.
77. Boehme, C.; Uddin, J.; Frenking, G. *Coord. Chem. Rev.* **2000**, *197*, 249.
78. Uddin, J.; Frenking, G. *J. Am. Chem. Soc.* **2001**, *123*, 1683.
79. Leiner, E.; Scheer, M. *J. Organomet. Chem.* **2002**, *646*, 247.
80. Weiß, D.; Winter, M.; Fischer, R. A.; Yu, C.; Wichmann, K.; Frenking, G. *Chem. Commun.* **2000**, *24*, 2495.
81. Steinke, T.; Gemel, C.; Winter, M.; Fischer, R. A. *Angew. Chem. Int. Ed. Engl.* **2002**, *41*, 4761.
82. Cotton, F. A.; Feng, X. *Organometallics* **1998**, *17*, 128.
83. (a) Macdonald, C. L. B.; Cowley, A. H. *J. Am. Chem. Soc.* **1999**, *121*, 12113. (b) Cowley, A. H. *J. Organomet. Chem.* **2000**, *600*, 168.
84. Aldridge, S.; Rossin, A.; Coombs, D. L.; Willock, D. J. *Dalton Trans.* **2004**, 2649.
85. Steinke, T.; Gemel, C.; Fischer, R. A. *Angew. Chem. Int. Ed. Engl.* **2004**, *43*, 2299.

86. (a) D. A. Straus, S. D. Grumbine, T. D. Tilley, *J. Am. Chem. Soc.* 1990, **112**, 7801. (b) S. D. Grumbine, T. D. Tilley, *J. Am. Chem. Soc.* **1994**, *116*, 5495.
87. Coombs, D. L.; Aldridge, S.; Jones, C.; Willock, D. J. *J. Am. Chem. Soc.* **2003**, *125*, 6356.
88. (a) Nugent, W. A.; Mayer, J. M. *Metal Ligand Multiple Bonds*, Wiley-Interscience: New York, 1988. (b) Hendon, J. W. *Coord. Chem. Rev.* **2003**, *243*, 3.
89. (a) Kays, D. L.; Day, J. K.; Ooi, L.-L.; Aldridge, S. *Angew. Chem. Int. Ed.* **2005**, *44*, 7457. (b) Aldridge, S.; Jones, C.; Gans-Eichler, T.; Stasch, A.; Kays (née Coombs), D. L.; Coombs, N. D.; Willock, D. J. *Angew. Chem. Int. Ed.* **2006**, *45* 6118.
90. Vidovic, D.; Findlater, M.; Reeske, G.; Cowley, A. H. *Chem. Commun.* **2006**, 3786.
91. Buchin, B.; Gemel, C.; Cadenbach, T.; Fernández, I.; Frenking, G.; Fischer, R. A. *Angew. Chem. Int. Ed.* **2006**, *45*, 5207.
92. Zubieta, J. A.; Zuckerman, J. J. *Prog. Inorg. Chem.* **1978**, *24*, 251.
93. Cadenbach, T.; Gemel, C.; Zacher, D.; Fischer, R. A. *Angew. Chem. Int. Ed.* **2008**, *47*, 3438.
94. Bunn, N. R.; Aldridge, S.; Coombs, D. L.; Rossin, A.; Willock, D. J.; Jones, C.; Ooi, L.-L. *Chem. Commun.* **2004**, 1732. (b) Bunn, N. R.; Aldridge, S.; Kays, D. L.; Coombs, N. D.; Rossin, A.; Willock, D. J.; Day, J. K.; Jones, C.; Ooi, L.-L. *Organometallics* **2005**, *24*, 5891.
95. Braunschweig, H.; Kraft, K.; Kupfer, T.; Radacki, K.; Seeler, F. *Angew. Chem. Int. Ed.* **2008**, *47*, 4931.
96. Kays, D. L.; Rossin, A.; Day, J. K.; Ooi, L. -L.; Aldridge, S. *Dalton Trans.* **2006**, 399.

97. Braunschweig, H.; Burzler, M.; Dewhurst, R. D.; Radacki, K. *Angew. Chem. Int.*

Ed. **2008**, *47*, 1.

Chapter Two

Experimental Techniques

2.1 The Manipulation of Air Sensitive Complexes

Due to the air and moisture sensitivity of many of the complexes investigated in this work, it was essential that their synthesis and manipulation be carried out under the exclusion of air and moisture. The use of standard Schlenk line, high vacuum and glove box techniques were therefore employed throughout this study in the handling of air sensitive compounds. Detailed descriptions of the necessary inert atmosphere techniques can be found in the literature and are reported herein.^{1,2}

2.1.1 Inert Atmosphere Techniques

The handling of air-sensitive compounds requires the manipulation to be carried out under the exclusion of air. Generally this is performed under an atmosphere of argon or nitrogen. Argon is particularly suited to this purpose since it is heavier than air, and thus forms a layer of inert gas directly over the air sensitive compound. The methods utilised throughout this work were (i) Schlenk line techniques, which provide a convenient method of manipulating air sensitive compounds under conditions of inert atmosphere through the use of specifically designed glassware and (ii) glove box techniques, in which air sensitive compounds can be handled and stored under an inert atmosphere.

The Schlenk line utilised throughout this work (Figure 2.1)¹ comprises a Pyrex glass tube connected to an inert gas supply, and a second Pyrex glass tube connected

to a mechanical pump in conjunction with a liquid nitrogen cooled trap to collect and prevent volatiles from contaminating the vacuum pump.

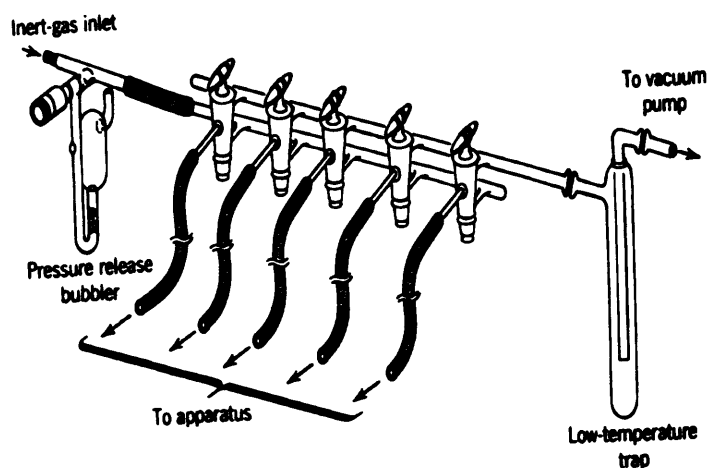


Figure 2.1 Schlenk apparatus

Attached to the inert gas outlet is a mercury bubbler, which prevents excessive pressure build-up within the system. The exposure of the apparatus to either an inert atmosphere or vacuum was performed by the use of two-way stopcock taps, thus allowing the apparatus to be purged or evacuated by means of switching between the inert gas or vacuum lines. To prevent leaks the taps were lubricated with Dow Corning high vacuum grease. Several heavy walled rubber tubes provided a means of attachment of glassware to the Schlenk line, allowing several pieces of apparatus to be purged at the same time. In order to monitor the pressure within the vacuum line, a Pirani gauge with a range of $1\text{-}10^{-3}$ Torr was attached to the end of the line. The Pirani gauge employs thermal conductivity to measure the pressure within the system. Because of its rapid response, it is particularly useful for locating leaks. Furthermore, it responds to water vapour and other condensables such as solvents.

An inert atmosphere was achieved by employing the 'pump and fill' method. This involved evacuation of the apparatus followed by subsequent filling with the inert gas. Several cycles of pumping followed by filling with inert gas were performed to avoid the need to employ high vacuum techniques and to guarantee an atmosphere free of oxygen and moisture. Transferral of liquids and solutions between Schlenk apparatus was achieved *via* cannulae and syringes through rubber septa.

The 'Saffron Scientific Omega' glove box utilised throughout this study provided a convenient means of manipulating and storing air sensitive solids. This consisted of a sealed stainless steel unit featuring a toughened glass viewing panel. Access within the box could be achieved through a pair of neoprene gloves. Equipment was loaded into the box through the side-port employing the 'pump and fill' method. The inert atmosphere maintained within the box was provided by a nitrogen cylinder, which was recirculated internally throughout the box via a catalyst column, a molecular sieve column, and a solvent scrubbing column achieving an atmosphere with oxygen levels at less than 5 ppm and 10 ppm respectively.³

2.1.2 High Vacuum Techniques

Procedures such as vacuum sublimation and removal of trace solvent from compounds were performed on a high vacuum line where a mechanical pump on a Schlenk line did not provide an adequate vacuum to perform these operations. The high vacuum line consisted of a Pyrex glass tube incorporating greaseless Young's taps. A combination of mercury diffusion and mechanical pumps allowed pressures of 10^{-4} Torr to be achieved. The vacuum within the system was monitored by means of a Tesla coil, which produces a discharge at vacuum pressures above 10^{-3} Torr. A

liquid nitrogen cooled trap protected the pumps from contamination by volatile substances.

2.2 Physical Measurements

2.2.1 NMR Spectroscopy

NMR spectra were recorded on either Bruker AM-400 or Jeol Eclipse 300 Plus FT-NMR spectrometers. Residual signals of the solvent were used for ^1H and ^{13}C NMR, a sealed tube containing a solution of $[\text{Bu}_4\text{N}][\text{B}_3\text{H}_8]$ in CDCl_3 was used as an external reference for ^{11}B NMR, CFCl_3 was used as an external reference for ^{19}F NMR and an 85 % solution of H_3PO_4 was used as an external reference for ^{31}P NMR. Samples were prepared for NMR analysis by transferral of the solution *via* cannula into a Young's NMR tube in an NMR Schlenk which had been filled with an inert atmosphere after being prepared using the 'pump and fill' method and flame dried under vacuum.

2.2.2 Infrared Spectroscopy

Infrared spectra were recorded on a Nicolet 500 FT-IR spectrometer, with each compound being measured as either KBr disk or as a solution in dichloromethane. KBr disks were prepared in a glove box by compressing the powdered sample with an approximate 10-fold excess of KBr (which was dried by heating under high vacuum before use).

2.2.3 Mass Spectrometry

Mass spectra were recorded at the EPSRC National Mass Spectrometry Service Centre, University of Wales Swansea. Perfluorotributylamine and

polyethylenamine were used as the standards for high resolution EI and ES mass spectra, respectively.

2.2.4 Chemical Analysis

Elemental analysis was performed by Warwick Analytical Services, University of Warwick. Despite repeated attempts satisfactory elemental microanalyses for many new gallium- and indium-containing species detailed herein was frustrated by their extreme air-, moisture- (and in some cases) thermal instability.

2.2.5 X-ray Crystallography

Data collection was performed on an Enraf Norius Kappa CCD diffractometer. Structure and solution refinement was carried out by Dr L.-L. Ooi, Dr A. Stasch, Prof C. Jones, and Miss J. K. Day (Cardiff University), and by Drs A. R. Cowley and A. L. Thompson (Oxford University). Data collection, structure solution and refinement on small or weakly diffracting crystals was carried out at the EPSRC National Crystallography Service, University of Southampton.

2.2.6 Theoretical Calculations

Details of the computational methodology used in this study are similar to those reported recently, and salient points are outlined here.⁴

Gradient corrected DFT calculations were performed using the ADF2000.01 code,⁵ with functionals for exchange and correlation due to Becke⁶ and Lee, Yang and Parr,⁷ respectively. A basis set constructed from Slater type orbitals at the triple zeta with polarization functions level used for all calculations (ADF IV). The level of

frozen core approximation for B, Al, Ga, C, N, O and F was the 1s orbital and for P, Cl, Br, I, In, Mn and Fe was the 2p orbital. All structures unless otherwise stated, were fully optimised with no symmetry restrictions. Convergence was accepted when the following limits were met: (i) energy change on next step $< 1 \times 10^{-3}$ Ha; (ii) gradient $< 1 \times 10^{-3}$ Ha \AA^{-1} ; and (iii) uncertainty in Cartesian coordinates $< 1 \times 10^{-2}$ \AA . The multiplicity of each structure was determined by using unrestricted calculations with spin states set to reasonable alternatives to determine the lowest energy configuration which conformed to the aufbau principle.

In order to calculate the degree of σ and π bonding contribution between a given bond such as that between the metal and group 13 centre, the optimised structures were re-orientated so that the bond in question was aligned with the z-axis. A bonding analysis was performed following the outline discussed below to give contributions to the bonding density segregated according to the symmetry of the atomic orbitals involved.

The one electron wavefunctions, ψ_i , used to represent the density in these DFT calculations are constructed as a linear combination of atomic basis functions, ϕ :

$$\psi_i = \sum_k^M c_{ik} \phi_k \quad 2.1$$

Where c_{ik} is the coefficient of the k^{th} basis function in the i^{th} molecular orbital and there are a total of M basis functions. The density, ρ , is then given by the summation over the occupied orbitals of the one electron densities.

$$\rho = 2 \sum_i^{N/2} \sum_l^M c_{il} \phi_l \sum_k^M c_{ik} \phi_k = 2 \sum_l^M \sum_k^M \phi_l \phi_k \sum_i^{N/2} c_{il} c_{ik} \quad 2.2$$

Where N is the total number of electrons and only the restricted spin paired situation is considered for simplicity; extension to the spin unrestricted case is straightforward. The rearranged form of the density expression allows the calculation to be performed *via* the definition of two square matrices with the dimension M . The first is usually referred to as the density matrix \mathbf{P} , and its components depend only on the calculated coefficients:

$$P_{lk} = \sum_i^{N/2} c_{il} c_{ik} \quad 2.3$$

The second, the overlap matrix, \mathbf{S} , depends on the basis set and geometry of the molecule:

$$S_{lk} = \phi_l \phi_k \quad 2.4$$

The density can then be represented as a matrix multiplication:

$$\rho = 2 \sum_l^M \sum_k^M S_{lk} P_{kl} \quad 2.5$$

Since the basis set consists of atom centred functions, \mathbf{P} and \mathbf{S} will contain some contributions which are wholly centred on a given atom and some which are due

to the overlap of basis functions on pairs of atoms. The latter contribution is related to the bonding between atoms and therefore the simplest way to address the character of bonding is to examine this portion in isolation. By identifying the basis functions centred on a pair of atoms, A and B for example, we can identify the bonding density, ρ_{AB} , by summing only the relevant contributions in equation 2.5:

$$\rho_{AB} = 2 \sum_{l \in A} \sum_{k \in B} S_{lk} P_{kl} \quad 2.6$$

This is the bonding density as defined by Mulliken.⁸ To differentiate π and σ contributions to the bonding density we simply align the bond of interest with the z-direction and separate the basis functions according to their symmetry, e.g. p_z is of σ type and p_x and p_y are of π type. Equation 2.6 can then be further sub-divided:

$$\rho_{AB} = 2 \sum_{l \in A}^{\sigma} \sum_{k \in B}^{\sigma} S_{lk} P_{kl} + 2 \sum_{l \in A}^{\pi} \sum_{k \in B}^{\pi} S_{lk} P_{kl} + 2 \sum_{l \in A}^{\delta} \sum_{k \in B}^{\delta} S_{lk} P_{kl} + \dots \quad 2.7$$

Where the symmetry labels on the summations indicate the basis function symmetry to be considered. We report the two terms in equation 2.7 separately to judge the degree of π bonding in M-E (E = B, Al, Ga, In) bonds.

This decomposition of the molecular orbital representation of the density to give bonding density is not unique and so to ensure the reliability of our analysis we also consider a bonding density analysis proposed by Mayer.⁹ In the Mayer analysis the product of the density and overlap matrices is first calculated and then the

elements of this product matrix are selected according to the basis functions belonging to the atoms of interest. Again we further partition the matrix in terms of σ and π symmetry:

$$\rho_{AB}^M = 2 \sum_{l \in A}^{\sigma} \sum_{k \in B}^{\sigma} (PS)_{kl} + 2 \sum_{l \in A}^{\pi} \sum_{k \in B}^{\pi} (PS)_{kl} \quad 2.8$$

As part of this work the application of equations 2.7 and 2.8 to the data provided by an ADF output was automated by the development of a dedicated program. The program was tested by calculation of the Mulliken atomic densities which are output by ADF and by analysis of simple test cases such as ethane, ethane, ethyne etc. (these analyses are included in reference 4). The Mayer bond order calculation was tested by comparing the values obtained from our analysis of ADF outputs and those generated at a similar basis set level by the MSI code Dmol.¹⁰ The results of decomposition into σ and π contributions from Mulliken and Mayer approaches consistently showed the same trends and so only the former is reported in the main text.

2.3 Purification and Preparation of Essential Solvents and Reagents

The synthetic routes of precursor complexes prepared during this research from literature sources are described herein. These starting materials were prepared from commercially available reagents and in some cases it was necessary to purify these reagents before use. Table 2.1 lists the sources and procedures for the purification of these reagents.

Table 2.1 Commercial sources and purification procedures of essential reagents and solvents

Compound	Source	Quoted Purity	Procedure
Reagents			
Cyclopentadienyliron-dicarbonyl dimer	Fluorochem	<i>a</i>	Used as supplied
Iron pentacarbonyl	Aldrich	99.999 %	Used as supplied
ⁿ BuLi (1.6 M in hexanes)	Aldrich	<i>a</i>	Used as supplied
Magnesium turnings	Avocado	> 99 %	Activated using iodine in acetone
Hydrochloric acid	Fischer	37 %	Used as supplied
Bromine	Lancaster	> 99 %	Used as supplied
1,2-Dibromoethane	Aldrich	98 %	Used as supplied
Sodium tetrafluoroborate	Aldrich	98 %	Used as supplied
Sodium	Lancaster	99 %	Used as supplied
3,5-Bis(trifluoromethyl)-bromobenzene	Avocado	98 %	Used as supplied
1,3,5-tri-tert-butylbenzene	Fluka	> 97 %	Used as supplied
Mercury	Johnson Matthey Chemicals	99.998 %	Used as supplied
Methyl iodide	Avocado	99 %	Used as supplied
Trimethyl phosphate	Aldrich	97 %	Used as supplied
Iodine (Resublimed)	Acros	99.5 %	Used as supplied
Gallium	Aldrich	99.999 %	Used as supplied
Gallium trichloride	Aldrich	99.999 %	Used as supplied
Indium tribromide	Aldrich	99.999 %	Used as supplied
Indium iodide	Aldrich	99.999 %	Used as supplied
4-Picoline	Alfa Aesar	98 %	Dried over sieves
Molybdenum hexacarbonyl	Alfa Aesar	98 %	Used as supplied
Cycloheptatriene	Aldrich	90 %	Distilled
Trityl tetrafluoroborate	Aldrich	98 %	Used as supplied
Sodium iodide	Alfa Aesar	99+ %	Used as supplied
Trimethylsilyltrifluoromethane sulfonate	Aldrich	99 %	Trap-to-trap distilled and stored

			over sieves
Carbazole	Alfa Aesar	96 %	Used as supplied
N-Bromosuccinimide	Aldrich	99 %	Used as supplied
Pd(PPh ₃) ₄	Alfa Aesar	99 %	Used as supplied
Chlorotrimethylsilane	Aldrich	98 %	Used as supplied
^t BuLi	Aldrich	A	Used as supplied
Triethyl borate	Aldrich	99 %	Used as supplied
Phenyl boronic acid	Alfa Aesar	98 %	Used as supplied
1,2-Bis(diphenylphosphino)ethane	Alfa Aesar	97 %	Used as supplied
Triphenylphosphine	Alfa Aesar	99+ %	Used as supplied
2,2'- ^t Butyl-4,4'-dipyridyl	Aldrich	98 %	Used as supplied
2-Bromomesitylene	Alfa Aesar	99 %	Used as supplied
Solvents			
Toluene	Fisher	> 99 %	Heated under reflux over sodium followed by distillation
Hexane	Fisher	> 99 %	Heated under reflux over potassium followed by distillation
Dichloromethane	Fisher	> 99 %	Heated under reflux over CaH ₂ followed by distillation
Diethyl ether	Fisher	> 99 %	Heated under reflux over sodium followed by distillation
Tetrahydrofuran	Fisher	> 99 %	Heated under reflux over sodium followed by distillation
<i>o</i> -Xylene	Aldrich	> 99 %	Heated under

			reflux over sodium followed by distillation
Benzene	Aldrich	> 99 %	Heated under reflux over sodium followed by distillation
Fluorobenzene		> 99 %	Heated under reflux over CaH ₂ followed by distillation
Octane	Aldrich	98 %	Used as supplied
Deuterated solvents			
Benzene-d ₆	Goss Scientific Instruments Ltd	99.6 atom%	Stored under argon over potassium mirror
Dichloromethane-d ₂	Goss Scientific Instruments Ltd	99.8 atom%	Stored under argon over flamed out molecular sieves
Chloroform-d	Aldrich	99.8 atom%	Stored under argon over flamed out molecular sieves
Fluorobenzene-d ₅	Goss	99.8 atom%	Stored under argon over flamed out molecular sieves
Acetone-d ₅	Goss	99.8 atom%	Used as supplied
Gases			
Argon	B.O.C.	<i>a</i>	Used as supplied
Nitrogen	B.O.C.	<i>a</i>	Used as supplied

^aInformation not available

2.3.1 Preparation of Transition Metal Anions

Preparation of C₅Me₅H

C₅Me₅H was prepared according to the method reported by Fendrick *et al.*¹¹ To a solution of MeMgI (185 mmol) in diethyl ether (160 cm³) [freshly prepared from Mg (7.0 g, 292 mmol) and MeI (26.2 g, 11.5 cm³, 185 mmol)] at 0°C was added dropwise a solution of 2,3,4,5-tetramethylcyclopent-2-enone (21.4 g, 157 mmol) and the reaction mixture stirred at room temperature for 12 h. The remaining MeMgI was quenched with MeOH and water and the mixture was washed with a solution prepared from ammonium chloride (30.0 g, 561 mmol), conc. HCl (30 cm³) and water (150 cm³) until the aqueous layer became acidic. The aqueous layer was extracted with ether and combined with the previous ether phase. The volume of the solution was reduced to 100 cm³ and stirred for 1 h with 2 cm³ of 6 M HCl to ensure that water elimination from the intermediate alcohol was complete. The mixture was then washed with NaHCO₃ and dried over K₂CO₃. After removal of the solvent the brown oil was distilled at 60-65°C at 15 Torr to give > 95 % pure product. Characterisation and purity was determined by comparison of the ¹H and ¹³C NMR data with quoted literature values.

*Preparation of [Cp*Fe(CO)₂]₂*

C₅Me₅H (10 g, 74 mmol) and Fe(CO)₅ (18.5 cm³, 27.5 g, 140 mmol) were heated at reflux in xylenes (40 cm³) for 48 h. An additional 9.5 cm³ of Fe(CO)₅ was added after the first 24 h. After cooling to room temperature the product was filtered, washed with hexane and recrystallised from dichloromethane to yield [Cp*Fe(CO)₂]₂ (approx. 75 % yield). Characterisation was achieved by comparison of the ¹H, ¹³C NMR and IR data with quoted literature values.¹²

*Preparation of Na[Cp*Fe(CO)₂]*

A solution of [Cp*Fe(CO)₂]₂ (3.31 g, 7.55 mmol) dissolved in thf (120 cm³) was stirred over a sodium amalgam (2.60 g, 113 mmol, 16 equivalents of Na) at room temperature for 168 h. Filtration and removal of the volatiles *in vacuo* yielded the sodium salt Na[Cp*Fe(CO)₂]. Since the presence of coordinating solvent such as thf leads to decomposition of the complexes synthesised in this work, it was necessary to remove all traces of this solvent. This was achieved by washing the product with hot toluene (3 × 50 cm³) and hexanes (50 cm³), before being dried under continuous high vacuum to give Na[Cp*Fe(CO)₂] (approx. 40 % yield). The clean product was stored in a glove box prior to use, and used without further characterisation.¹³

Preparation of Na[CpFe(CO)₂]

Na[CpFe(CO)₂] was prepared in an analogous fashion to Na[Cp*Fe(CO)₂]. A solution of [CpFe(CO)₂]₂ (7.01 g, 19.8 mmol) dissolved in thf (80 cm³) was stirred over a sodium amalgam (1.5 g, 65 mmol, 3 equivalents of Na) at room temperature for 48 h. Filtration and removal of the volatiles *in vacuo* yielded the sodium salt Na[CpFe(CO)₂]. The salt was subsequently washed with hot toluene (3 × 50 cm³) and hexanes (1 × 50 cm³) before being dried under continuous high vacuum to give Na[CpFe(CO)₂] (approx. 50 % yield). The clean product was stored in a glove box prior to use, and used without further characterisation.¹⁴

2.3.2 Preparation of Transition Metal Halides*Synthesis of Cp*Fe(CO)₂I*

A round-bottomed flask equipped with a reflux condenser was charged with [Cp*Fe(CO)₂]₂ (1.002 g, 2.286 mmol), I₂ (0.739 g, 2.912 mmol), and CHCl₃ (50 cm³)

and the reaction mixture heated at reflux for 2 h. After cooling to room temperature the mixture was washed with a solution of sodium thiosulphate (10 g) dissolved in water (40 cm³). The dark brown organic layer was separated from the aqueous layer and filtered. The solvent was removed *in vacuo* yielding the product as a dark brown solid, which was dried *in vacuo*. (0.802 g, 53 %). Characterisation was achieved by comparison of ¹H, ¹³C NMR and IR data with quoted literature values.¹⁵

Synthesis of C₇H₈Mo(CO)₃

A solution of molybdenum hexacarbonyl (10.01 g, 37.87 mmol), cycloheptatriene (22.0 cm³, 121 mmol), octane (80 cm³) and thf (2 cm³) was refluxed for 16 h under an inert atmosphere. The resulting dark red solution was cooled to -30°C, whereupon dark red crystals of C₇H₈Mo(CO)₃ were obtained. The crystals were isolated by filtration, washed with petroleum ether (40-60), and dried *in vacuo* (7.863 g, 76 %). Characterisation was achieved by comparison of the ¹H NMR and IR data with that reported in the literature.¹⁶

Synthesis of [(η⁷-C₇H₇)Mo(CO)₃][BF₄]

A solution of trityl tetrafluoroborate (9.54 g, 28.9 mmol) in dichloromethane (100 cm³) was added to a solution of C₇H₈Mo(CO)₃ (7.86 g, 28.9 mmol) in dichloromethane (40 cm³), and the reaction mixture stirred at room temperature for 30 min, with the formation of an orange precipitate. The precipitate was isolated by filtration, washed with dichloromethane (2 × 20 cm³), and dried *in vacuo* yielding [(η⁷-C₇H₇)Mo(CO)₃][BF₄] as an orange powder (9.62 g, 93 %). Characterisation was achieved by comparison of the ¹H NMR and IR data with that reported in the literature.¹⁶

Synthesis of $(\eta^7\text{-C}_7\text{H}_7)\text{Mo}(\text{CO})_2\text{I}$

A solution of NaI (18.82 g, 125.6 mmol) in acetone (90 cm³) was added to a suspension of $[(\eta^7\text{-C}_7\text{H}_7)\text{Mo}(\text{CO})_3][\text{BF}_4]$ (9.58 g, 26.8 mmol) in acetone (100 cm³) with the immediate formation of a dark green solution. The reaction mixture was stirred at room temperature for 16 h, after which the solvent was removed *in vacuo* yielding a dark green precipitate. The precipitate was extracted into dichloromethane (500 cm³), filtered, and volatiles removed *in vacuo*, yielding dark green crystals which were washed with hexanes (3 × 40 cm³), and dried yielding $(\eta^7\text{-C}_7\text{H}_7)\text{Mo}(\text{CO})_2\text{I}$ as dark green crystals (9.03 g, 85 %). Characterisation was achieved by comparison of the ¹H NMR and IR data with that reported in the literature.¹⁶

Synthesis of $(\eta^7\text{-C}_7\text{H}_7)\text{Mo}(\text{dppe})\text{I}$

A solution of dppe (2.01 g, 5.04 mmol) in benzene (150 cm³) was added to a solution of $(\eta^7\text{-C}_7\text{H}_7)\text{Mo}(\text{CO})_2\text{I}$ (2.02 g, 5.09 mmol) in benzene (150 cm³) and the reaction mixture heated to 80°C under an atmosphere of argon for 20 h. The solution was filtered and the volatiles removed *in vacuo*. The green solid was extracted into dichloromethane and filtered, to this hexane (100 cm³) was added. A dark green solid was obtained at -30°C, the precipitate was isolated by filtration and dried *in vacuo* (1.36 g, 38 %). Characterisation was achieved by comparison of the ¹H and ³¹P NMR data with quoted literature values.¹⁷

Synthesis of $\text{CpRu}(\text{PPh}_3)_2\text{Cl}$

Triphenylphosphine (21.0 g, 0.08 mol) was dissolved in degassed ethanol (1000 cm³) by gentle heating in a round-bottomed flask equipped with a reflux condenser and dropping funnel. Ruthenium trichloride trihydrate (5.02 g, 0.02 mol) was dissolved in

degassed ethanol (100 cm³), heated to reflux, and allowed to cool slowly to room temperature. Freshly distilled cyclopentadiene (10.0 cm³, 0.12 mol) was then added to the ruthenium trichloride solution and the mixture so formed added to the triphenylphosphine solution over a period of 10 min. under reflux. The resulting reaction mixture was refluxed for an additional 2 h during which time a dark orange solution formed. The solution was filtered and cooled to -30°C, the resulting orange crystals isolated by filtration, washed with cold ethanol (5 × 20 cm³) and 40-60 petroleum ether (5 × 20 cm³), and dried *in vacuo* to yield CpRu(PPh₃)₂Cl as an orange crystalline solid (72 % yield). Characterisation was achieved by comparison of the ¹H and ³¹P NMR data with that reported in the literature.¹⁹

Synthesis of CpRu(dppe)Cl

A solution of dppe (0.788 g, 1.980 mmol) in toluene (50 cm³) was added to a solution of CpRu(PPh₃)₂Cl (1.437 g, 1.979 mmol) in toluene (80 cm³), and the reaction mixture refluxed for 6 h with the formation of a light orange solution and yellow precipitate. The solution was filtered and concentrated *in vacuo*. A yellow solid was obtained at -30°C, the precipitate was isolated by filtration and dried *in vacuo* (0.868 g, 73 %). Characterisation was achieved by comparison of the ¹H and ³¹P NMR data with quoted literature values.¹⁸

2.3.3 Preparation of Aryl Anions

Synthesis of MesLi

ⁿBuLi (8.20 cm³ of a 1.6M solution in hexanes, 13.1 mmol) was added to a solution of 2-bromomesitylene (1.51 cm³, 10.0 mmol) in diethyl ether (70 cm³) at room temperature with stirring. The pale yellow solution was heated at reflux for 3 h

during which copious amounts of white solid precipitated. The white solid was isolated and dried *in vacuo* (0.584 g, 46 %). The crude product was used without further characterisation.²⁰

*Synthesis of Mes*Br*

A two-necked round-bottomed flask equipped with a reflux condenser was charged with 1,3,5-tri-*tert*-butylbenzene (10.00 g, 40.65 mmol) and trimethyl phosphate (110 cm³). The reaction was heated to 85°C to dissolve the hydrocarbon and then cooled to 70°C whereupon bromine (2.7 cm³) was added and the reaction mixture stirred at this temperature for 30 h. The resulting orange solution was cooled to room temperature and quenched with ice cold water (350 cm³), the aqueous layer washed with petroleum ether (5 × 75 cm³), and the combined organic layers washed with saturated sodium metabisulphite solution (2 × 150 cm³) and dried over magnesium sulphate. The resulting colourless solution was filtered and volatiles removed *in vacuo* yielding impure Mes*Br as a cream coloured solid; recrystallisation from the minimum amount of hot ethanol yielded pure Mes*Br as a white crystalline solid (6.391 g, 48 %). Characterisation was achieved by comparison of ¹H and ¹³C NMR data with quoted literature values.²¹

*Synthesis of Mes*Li(thf)₂*

ⁿBuLi (5.80 cm³ of a 1.6M solution in hexanes, 9.28 mmol) was added to a solution of Mes*Br (3.00 g, 9.22 mmol) dissolved in a mixture of hexane (60 cm³) and thf (15 cm³) at -78°C. The reaction was stirred at this temperature for 3 h and then at 0°C for 1 h. The solution was filtered and concentrated *in vacuo*. Mes*Li(thf)₂ was obtained

as a white solid upon cooling to -30°C (2.56 g, 70 %). Characterisation was achieved by comparison of ^1H and ^{13}C NMR data with quoted literature values.²²

2.3.4 Preparation of [1,8-diphenyl-3,6-dimethylcarbazol-9-yl]Li

Synthesis of 3,6-dibromocarbazole

To a solution of carbazole (5.01 g, 29.9 mmol) dissolved in dichloromethane (300 cm^3), was added silica gel (49.89 g), the mixture cooled to 0°C , and a suspension of N-bromosuccinimide (10.65 g, 280.3 mmol) in dichloromethane (250 cm^3) added at 0°C over a period of 2 h under the exclusion of light. The reaction mixture was then allowed to warm to room temperature and stirred for an additional 4.5 h. The solution was filtered and the filtrate was washed with 1M aqueous NaOH ($3 \times 50 \text{ cm}^3$), 3M aqueous NaCl ($1 \times 50 \text{ cm}^3$) and dried over MgSO_4 . The solution was then filtered and concentrated *in vacuo*, and the resulting off white precipitate isolated and dried *in vacuo* (6.79 g, 70 %). Characterisation was achieved by comparison of ^1H and ^{13}C NMR data with quoted literature values.²³

Synthesis of 3,6-dimethylcarbazole

$n\text{BuLi}$ (13.04 cm^3 of a 1.6M solution, 20.86 mmol) was added dropwise at 0°C to a solution of 3,6-dibromocarbazole (6.30 g, 19.4 mmol) in diethyl ether (200 cm^3). The reaction mixture was stirred at 0°C for 1 h after which chlorotrimethylsilane (2.62 cm^3) was added. After subsequent warming to room temperature and stirring for 1 h, a white precipitate was formed. The suspension was then cooled to -78°C and $t\text{BuLi}$ was added. The suspension was stirred for 3 h at 0°C , after which the reaction mixture was cooled to -78°C and methyl iodide (5.96 cm^3 , 95.7 mmol) added. After warming to room temperature and stirring for a further 12 h, 1M HCl (50 cm^3) was

then added dropwise at room temperature; the layers were separated and the organic phase was washed with 1M HCl ($2 \times 50 \text{ cm}^3$) and H_2O (50 cm^3). The resulting yellow solution was dried over MgSO_4 and filtered. The volatiles were concentrated *in vacuo* and the resulting white solid was isolated and dried *in vacuo* (2.31 g, 61 %). Characterisation was achieved by comparison of ^1H and ^{13}C NMR data with quoted literature values.²⁴

Synthesis of 1,8-dibromo-3,6-dimethyl carbazole

To a solution of 3,6-dimethyl carbazole (4.40 g, 22.5 mmol), dissolved in dichloromethane (400 cm^3) was added silica gel (49.89 g), the mixture cooled to 0°C , and a suspension of N-bromosuccinimide (8.03 g, 45.1 mmol) in dichloromethane (250 cm^3) was then added at 0°C over a period of 2 h. The reaction mixture was then allowed to warm to room temperature and stirred for an additional 30 min. The solution was then filtered and the filtrate washed with 1M aqueous NaOH ($3 \times 50 \text{ cm}^3$) and 3M aqueous NaCl (50 cm^3). The organic phase was dried over MgSO_4 , filtered and the volatiles removed *in vacuo* yielding an off-white solid, which was dried *in vacuo* (6.72 g, 84 %). Characterisation was achieved by comparison of ^1H and ^{13}C NMR data with quoted literature values.²⁴

Synthesis of 1,8-diphenyl-3,6-dimethylcarbazole

1,8-diphenyl-3,6-dimethylcarbazole was prepared by the method of Gibson.²⁵ 1,8-dibromo-3,6-dimethylcarbazole (1.51 g, 4.28 mmol) and $\text{Pd}(\text{PPh}_3)_4$ (0.48 g, 0.04 mmol) were dissolved in toluene (150 cm^3) and a solution of phenylboronic acid (7.34 g, 60.2 mmol) in ethanol (140 cm^3) added, followed by an aqueous solution of 1M Na_2CO_3 (43.45 cm^3). The resulting yellow suspension was degassed in a stream of

argon for 30 min, after which the reaction mixture was heated to 80°C for 16 h. The resulting solution was filtered while hot and the filtrate washed with 1M NaOH (2 × 120 cm³) and water (2 × 120 cm³). The dark brown solution was dried over MgSO₄ and filtered; volatiles were removed *in vacuo* yielding a dark yellow solid which was recrystallised from hot ethanol/hexanes yielding a beige solid which was isolated at -30°C and dried *in vacuo* (yield: 0.923 g, 62 %). Characterisation was achieved by comparison of ¹H and ¹³C NMR data with quoted literature values.

Synthesis of 1,8-diphenyl-3,6-dimethylcarbazol-9-yl lithium

1,8-diphenyl-3,6-dimethylcarbazol-9-yl lithium was prepared by the method of Gibson.²⁵ ⁿBuLi (2.80 cm³, 4.48 mmol) was added to a solution of 1,8-diphenyl-3,6-dimethyl carbazole (1.21 g, 3.48 mmol) in hexane (150 cm³) at room temperature, and the mixture was stirred for 3 h with the formation of a bright yellow precipitate. After concentration *in vacuo* (to *ca.* 20 cm³) the yellow solid was isolated, washed with hexanes (2 × 20 cm³) and dried *in vacuo* (0.54 g, 44 %). The crude product was used without further characterisation.²⁵

2.3.5 Preparation of [2,4,6-^tBu₃C₆H₂EX₂] (E = Ga, In, X = Cl, Br)

Synthesis of 2,4,6-^tBu₃C₆H₂InBr₂

2,4,6-^tBu₃C₆H₂InBr₂ was prepared by the method of Roesky *et al.*²⁶ To a solution of InBr₃ (1.40 g, 3.95 mmol) in diethyl ether (70 cm³) at -78°C was added dropwise an ethereal solution of Mes*Li(thf)₂ (1.54 g, 3.95 mmol). The resulting mixture was stirred for 2 h before being allowed to warm slowly to room temperature, yielding a cloudy solution. After the reaction mixture was stirred for a further 20 h, the solvent was removed *in vacuo*. The product was extracted into hexane, concentrated and

cooled to -30°C , yielding $\text{Mes}^*\text{InBr}_2$ as a fine white powder which was isolated and dried *in vacuo* (0.935 g, 46 %). Characterisation was achieved by comparison of ^1H and ^{13}C NMR data with quoted literature values.

*Synthesis of Mes*GaCl₂*

$\text{Mes}^*\text{GaCl}_2$ was prepared by the method of Roesky *et al.*²⁶ A solution of $\text{Mes}^*\text{Li}(\text{thf})_2$ (1.604 g, 4.044 mmol) in diethyl ether (50 cm^3) was added dropwise to a solution of GaCl_3 (0.714 g, 4.055 mmol) in diethyl ether (15 cm^3) at -78°C . The resulting mixture was stirred at -78°C for 2 h and then allowed to warm slowly to room temperature. After stirring for 20 h, the volatiles were removed *in vacuo*, and the white solid extracted into hexane ($3 \times 50\text{ cm}^3$), concentrated *in vacuo*, and cooled to -30°C yielding $\text{Mes}^*\text{GaCl}_2$ as a white precipitate (0.315 g, 20 %). Characterisation was achieved by comparison of ^1H and ^{13}C NMR data with quoted literature values.

2.3.6 Preparation of Ga(N(SiMe₃)₂)Cl₂·thf

A solution of $\text{LiN}(\text{SiMe}_3)_2$ (0.953 g, 5.695 mmol) dissolved in hexanes (60 cm^3) and thf (2 cm^3) was added dropwise to a solution of GaCl_3 (1.002 g, 5.691 mmol) dissolved in hexanes (50 cm^3) over a period of 1 h at room temperature. The reaction was stirred at room temperature for 22 h after which the resulting pale yellow solution was filtered and the volatiles removed *in vacuo*, yielding a pale yellow oil. After drying the oil *in vacuo* a crystalline solid $\text{GaN}(\text{SiMe}_3)_2\text{Cl}_2\cdot\text{thf}$ formed (1.507 g, 61 %). Characterisation was achieved by comparison of ^1H and ^{13}C NMR data with quoted literature values.²⁷

2.3.7 Preparation of Transition Metal-Group 13 complexes

*Synthesis of Cp*Fe(CO)₂Ga(Mes*)Cl*

Cp*Fe(CO)₂Ga(Mes*)Cl was prepared by the method of Aldridge *et al.*²⁸ A solution of Mes*GaCl₂ (0.317 g, 0.821 mmol) dissolved in diethyl ether (45 cm³) was added to a suspension of Na[Cp*Fe(CO)₂] (0.248 g, 0.918 mmol) in diethyl ether (15 cm³), and the resulting mixture stirred at room temperature for 12 h yielding a dark solution and off-white precipitate. The solution was filtered and concentrated *in vacuo*; a dark yellow precipitate formed upon cooling to -25°C. The precipitate was isolated and washed with hexanes (2 × 10 cm³) yielding a dark yellow solid. The yellow precipitate was dried *in vacuo* (45 mg, 9 %). Characterisation was achieved by comparison of ¹H, ¹³C NMR and IR data with quoted literature values.

*Synthesis of [Cp*Fe(CO)₂]₂GaCl*

[Cp*Fe(CO)₂]₂GaCl was prepared by the method of Aldridge *et al.*²⁸ A solution of GaCl₃ (0.16 g, 0.93 mmol) in diethyl ether (20 cm³) was added to a slurry of Na[Cp*Fe(CO)₂] (0.50 g, 1.86 mmol) in diethyl ether (30 cm³). The resulting mixture was stirred for 12 h with the formation of a yellow precipitate, which was isolated by filtration and extracted into dichloromethane (100 cm³). The solution was concentrated *in vacuo* and hexanes (20 cm³) was added; upon cooling of the mixture to -20°C a yellow powder was formed (0.22 g, 45 %). Characterisation was achieved by comparison of ¹H, ¹³C NMR and IR data with quoted literature values.

*Synthesis of [(Cp*Fe(CO)₂)GaI₂]₂*

[(Cp*Fe(CO)₂)GaI₂]₂ was prepared by the method of Aldridge *et al.*²⁸ A mixture of Ga (0.89 g, 12.8 mmol), I₂ (1.61 g, 6.34 mmol) and toluene (80 cm³) was sonicated in

a 30°C sonic bath for 18 h, after which a solution of $[\text{Cp}^*\text{Fe}(\text{CO})_2]_2$ (1.56 g, 3.16 mmol) in toluene (70 cm³) was added. The reaction mixture was stirred at room temperature for 168 h with the formation of a yellow precipitate, which was isolated by filtration and extracted into dichloromethane. The resulting orange solution was concentrated *in vacuo* with the formation of a yellow precipitate, which was isolated by filtration and dried *in vacuo* (1.78 g, 55 %). Characterisation was achieved by comparison of ¹H, ¹³C NMR and IR data with quoted literature values.

Synthesis of $[\text{Cp}^\text{Fe}(\text{CO})_2]_2\text{InI}$*

$[\text{Cp}^*\text{Fe}(\text{CO})_2]_2\text{InI}$ was prepared by the method of Norman *et al.*²⁹ A solution of $[\text{Cp}^*\text{Fe}(\text{CO})_2]_2$ (0.503 g, 1.018 mmol) in toluene (90 cm³) was added to a suspension of InI (0.248 g, 1.026 mmol) in toluene (10 cm³), and the resulting solution heated at reflux for 21 d yielding a dark brown-yellow solution. The solution was filtered, concentrated *in vacuo* and a yellow precipitate was obtained by cooling the concentrated solution to -30°C. The precipitate was isolated and dried *in vacuo* yielding the product as an orange solid (0.223 g, 30 %). Characterisation was achieved by comparison of ¹H, ¹³C NMR and IR data with quoted literature values.

2.3.8 Preparation of Halide Abstracting Agents

Preparation of $\text{Na}[\text{B}\{3,5-(\text{CF}_3)_2\text{C}_6\text{H}_3\}_4]$

$\text{Na}[\text{B}\{3,5-(\text{CF}_3)_2\text{C}_6\text{H}_3\}_4]$ was prepared by the method of Reger *et al.*³⁰ A round-bottomed flask equipped with a dry ice condenser and a dropping funnel was charged with activated magnesium turnings (1.11 g, 41.7 mmol), NaBF₄ (0.7 g, 6.1 mmol) and diethyl ether (150 cm³). Dibromoethane (0.5 cm³, 5.7 mmol) was added and the slurry was heated for several minutes to initiate the reaction. A solution of 3,5-

bis(trifluoromethyl)bromobenzene (10.1 g, 34.1 mmol) in diethyl ether (100 cm³) was added over a period of 30 min., the reaction mixture was then heated at reflux for 30 min., and stirred at room temperature for a further 12 h. The reaction mixture was added to a solution of Na₂CO₃ (16.0 g, 151 mmol) in water and stirred for 30 min. and the resulting solution filtered. The organic layer was and the aqueous layer was washed several times with diethyl ether (5 × 50 cm³). The combined organic layers were dried over sodium sulphate and treated with decolourising charcoal. Filtration of the solution and removal of the volatiles gave rise to an oily solid, which was then dissolved in benzene (200 cm³) and the water removed by azeotropic distillation. The solvent volume was reduced to approx. 40 cm³ and the solution filtered from the solid product. The solid was washed with hexanes and dried under continuous high vacuum for 12 h affording Na[B{3,5-(CF₃)C₆H₃}₄] (32 % yield). Characterisation was achieved by comparison of ¹H, ¹¹B, ¹³C and ¹⁹F NMR data with quoted literature values.

Preparation of [Et₃Si][B(C₆F₅)₄]

[Et₃Si][B(C₆F₅)₄] was prepared by the method of Heinekey.³¹ A mixture of Ph₃CB(C₆F₅)₄ (0.051 g, 0.055 mmol) and Et₃SiH (3 cm³) was sonicated for 12 h. After which excess Et₃SiH was removed in vacuo yielding [Et₃Si][B(C₆F₅)₄] as a pale yellow solid. The crude product was used without further characterisation.

2.3.9 Synthesis of aryl boronic acids

Synthesis of mesitylboronic acid

Mesitylboronic acid was prepared by the method of Wipf.³² Activated magnesium turnings (3.890 g, 160.1 mmol), thf (160 cm³), bromomesitylene (18.09 cm³, 120.1

mmol) and a crystal of iodine were heated at reflux for 14 h; the resulting grey solution/suspension was cooled to -78°C and triethyl borate (40.80 cm^3 , 239.7 mmol) added. The reaction mixture was warmed to room temperature and stirred for 5 h, then cooled to 0°C and 1M HCl (200 cm^3) added. The mixture was then stirred at room temperature for a further 2 h. The product was extracted with diethyl ether and the combined organic layers were washed with brine, dried over Na_2SO_4 and filtered. The volatiles were removed *in vacuo* yielding an off-white solid, which was recrystallised from hot benzene (6.89 g, 35 %). Characterisation was achieved by comparison of ^1H , ^{13}C and ^{11}B NMR data with quoted literature values.

Synthesis of mesitylboronic acid

$n\text{BuLi}$ (68 cm^3 of a 1.6 M solution in hexanes, 11 mmol) was added to a solution of bromomesitylene (15 cm^3 , 99 mmol) in thf (150 cm^3) at -78°C over 5 min. The reaction mixture was stirred at -78°C for a further 1 h after which triethyl borate (20 cm^3 , 118 mmol) was added dropwise, and the solution stirred for an additional 1.5 h at -78°C . A saturated solution of NH_4Cl (100 cm^3) was then added and the reaction mixture warmed to room temperature. Water (400 cm^3) was added and the aqueous phase was washed with diethyl ether ($2 \times 300\text{ cm}^3$). The organic phase was washed with saturated NaHCO_3 (400 cm^3), saturated NaCl (400 cm^3), dried over MgSO_4 , filtered and the volatiles removed *in vacuo* yielding an off white solid. The product was recrystallised from hot water yielding $\text{MesB}(\text{OH})_2$ as a white crystalline solid (approx. 15 g, 91 %). Characterisation was achieved by comparison of ^1H , ^{13}C and ^{11}B NMR data with quoted literature values.³³

Synthesis of 2,4,6-triisopropylphenylboronic acid

ⁿBuLi (31.5 cm³ of a 1.6M solution in hexanes, 50.4 mmol) was added to a solution of 2,4,6-triisopropylbromobenzene (12.01 g, 42.39 mmol) in diethyl ether (80 cm³) at –5°C. The reaction mixture was stirred at this temperature for 4 h, after which it was cooled to –78°C and thf (60 cm³) and, triethyl borate (14.3 cm³, 84.03 mmol) then added. After stirring at this temperature for 1 h, the reaction mixture was warmed to room temperature and stirred for an additional 15 h; the volatiles were then removed *in vacuo* and the resulting cloudy oil poured onto a mixture of ice and water 1:1 (50 g). The mixture was acidified with 2M HCl to pH 5-6, the aqueous solution extracted with chloroform (3 × 200 cm³), and the combined extracts were dried over MgSO₄. Volatiles were then removed *in vacuo* yielding a yellow oil. Water (100 cm³) was added to the oil and the mixture was heated to reflux for 3 h with the formation of a white solid. The white solid was isolated by filtration and dried *in vacuo* (9.35 g, 89 %). Characterisation was achieved by comparison of ¹H, ¹³C and ¹¹B NMR data with quoted literature values.³⁴

2.4 References for Chapter Two

1. Shriver, D. F.; Drezdson, M. A. *The Manipulation of Air-Sensitive Compounds*, 2nd edn., Wiley-Interscience, New York, 1986.
2. Dodd, R. E.; Robinson, P. L. *Experimental Inorganic Chemistry*, Elsevier, 1954.
3. Saffron Scientific Equipment Ltd., glove box operation manual.
4. Dickinson, A. A.; Willock, D. J.; Calder, R. J.; Aldridge, S. *Organometallics*, 2002, 21, 1146.
5. (a) Baerends, E. J.; Ellis, D. E.; Ros, P. *Chem. Phys.*, 1973, 2, 41. (b) Versluis, L.; Ziegler, T. *Chem. Phys.*, 1988, 88, 322. (c) te Velde, G.; Baerends, E. J. *J. Comput. Phys.*, 1992, 99, 84. (d) Fonseca Guerra, C.; Snijders, J. G.; te Velde, G.; Baerends, E. *J. Theor. Chem. Acc.*, 1998, 99, 391.
6. Becke, A. D. *Phys. Rev. A*, 1988, 38, 3098.
7. Lee, C.; Wang, W.; Parr, R. G. *Phys. Chem. B*, 1988, 37, 785.
8. Mulliken, R. S. *J. Chem. Phys.*, 1955, 23, 1833.
9. Mayer, I. *Int. Quantum Chem.*, 1986, 29, 477.
10. DMOL⁶, Biosym/MSI, San Diego, CA, 1996.
11. Fendrick, C. M.; Schertz, L. D.; Mintz, E. A.; Marks, T. J. *Inorg. Synth.*, 1992, 29, 193.
12. Catheline, D.; Astruc, D. *Organometallics*, 1984, 3, 1094.
13. Clegg, W.; Compton, N. A.; Errington, R. J.; Norman, N. C. *J. Chem. Soc. Dalton Trans.* 1988, 1671.
14. King, R. B.; Pannell, K. H. *Inorg. Chem.*, 1968, 7, 1510.
15. King, R. B.; Stone, F. G. A. *Inorg. Synth.*, 1969, 7, 110.
16. King, R. B. *Organometallic Syntheses*, Vol 1, 1965.
17. Beall, T. W.; Houk, L. W. *Inorg. Chem.*, 1973, 12, 1979.



18. Gutiérrez Alonso, A.; Ballester Reventós, L. *J. Organomet. Chem.*, **1988**, *338*, 249.
19. Bruce, M. I.; Hameister, C.; Swincer, A. G.; Wallis, R. C. *Inorg. Synth.*, **1982**, *21*, 78.
20. Lappert, M. F.; Smith, S. J. *J. Organomet. Chem.*, **1986**, *310*, 21.
21. Cowley, A. H.; Norman, N. C.; Pakulski, M. *Inorg. Synth.*, **1990**, *27*, 236.
22. Wehmschulte, R. J.; Power, P. P. *Inorg. Chem.*, **1996**, *35*, 3262.
23. Smith, K.; James, D. M.; Mistry, A. G.; Bye, M. R.; Faulkner, D. J. *Tetrahedron*, **1992**, *48*, 7479.
24. Britovsek, G. J. P.; Gibson, V. C.; Hoarau, O. D.; Spitzmesser, S. K.; White, A. J. P.; Williams, D. J. *Inorg. Chem.*, **2003**, *42*, 3454.
25. Spitzmesser, S. K.; Gibson, V. C. *J. Organomet. Chem.*, **2003**, *673*, 95.
26. Schulz, S.; Pusch, S.; Pohl, E.; Dielkus, S.; Hernst-Irmer, R.; Meller, A.; Roesky, H. W. *Inorg. Chem.* **1993**, *32*, 3343.
27. Barry, S. T.; Richeson, D. S. *Chem. Mat.* **1994**, *6*, 2220.
28. (a) Bunn, N. R.; Aldridge, S.; Kays (née Coombs) D. L.; Coombs, N. D.; Day, J. K.; Ooi, L. –L.; Coles, S. J.; Hursthouse, M. B. *Organometallics*, **2005**, *24*, 5879. (b) Bunn, N. R.; Coombs, D. L.; Rossin, A.; Willock, D. J.; Jones, C.; Ooi, L. –L. *Chem. Commun.*, **2004**, 1732.
29. Clarkson, L. M.; Norman, N. C.; Farrugia, L. J. *J. Organomet. Chem.*, **1990**, *390*, C10.
30. Reger, D. L.; Wright, T. D.; Little, C. A.; Lamba, J. J. S.; Smith, M. D. *Inorg. Chem.*, **2001**, *40*, 3810.
31. Vogt, M.; Pons, V.; Heinekey, D. M. *Organometallics*, **2005**, *24*, 1832.
32. Wipf, P.; Jung, J.–K. *J. Organomet. Chem.*, **2000**, *65*, 6319.

33. Morgan, J.; Pinhey, T. P. *J. Chem. Soc., Perkin Trans.* **1990**, *1*, 715.

34. Chaumeil, H.; Signorella, S.; Le Drian, C. *Tetrahedron*, **2000**, *56*, 9655.

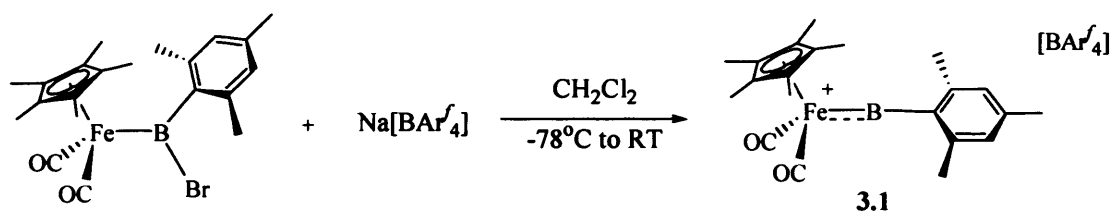
Chapter Three

Asymmetric Indyl and Gallyl Complexes: Synthesis and Reactivity

3.1 Introduction

The synthesis and chemistry of low-coordinate multiply bonded group 13 ligand systems continues to attract significant research interest, with a view to better understanding the fundamental nature of structure and bonding within such species. Whereas the synthesis of transition metal borylene complexes of the type $L_nM(BR)^{1,2}$ has been the subject of extensive recent research effort, the synthesis and characterisation of analogous terminal gallylene complexes, in particular, has been accompanied by significant debate concerning the nature of the metal ligand bond.^{3,4}

It has been demonstrated that transition metal complexes featuring ligands containing three-coordinate, halide-functionalised boron donors represent key precursors to low coordinate unsaturated cationic species of the type $[L_nM(BR)]^+$ via halide abstraction chemistry. This methodology was utilised in 2003, by Aldridge *et al.*,^{2a} in the synthesis of the first cationic terminal borylene complex $[Cp^*Fe(CO)_2(BMes)]^+[BARf_4]^-$ 3.1, by reaction of the corresponding bromoboryl precursor with a suitable halide abstracting agent ($Na[BARf_4]$ or $Ag[CB_{11}H_6Br_6]$); (Scheme 3.1). Initial DFT calculations revealed that the positive charge within such systems is largely located at the group 13 centre, this offers the potential of increasing the $M \rightarrow E$ backbonding component, compared to analogous charge neutral systems, conceivably resulting in higher $M=E$ multiple bond character.^{2b}

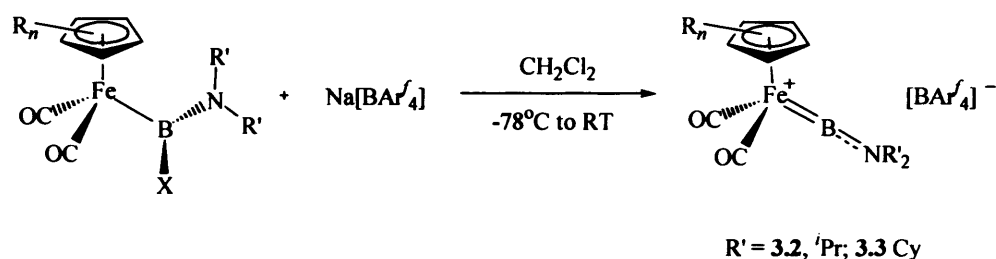


Scheme 3.1

Structural investigations revealed a near linear Fe-B-C unit [$\angle\text{Fe}(1)\text{-B}(1)\text{-C}(1) = 178.3(6)^\circ$], which is consistent with the boron centre engaging in no secondary interactions (*e.g.* with the anion or solvent). In addition the Fe-B distance of [1.792(8) Å] was (and indeed still is) significantly shorter than any other transition metal to boron bond reported in the literature.¹ It was concluded that the short Fe-B distance is consistent with the presence of an Fe=B double bond, which features a significant Fe→B π back bonding component (*i.e.* analogous to a Fischer carbene⁵). The orientation of the mesityl fragment [torsion, $\angle\text{Cp}^*\text{centroid-Fe}(1)\text{-C}(1)\text{-C}(2) = 91.3(6)^\circ$] is optimal for an Fe→B π interaction as this allows interaction of the HOMO of the $[\text{Cp}^*\text{Fe}(\text{CO})_2]^+$ fragment with one of the two formally vacant p orbitals at the boron centre, with the other being stabilised by π interaction with the mesityl ring. This feature is consistent with the measured B(1)-C(1) bond distance of 1.491(10) Å being significantly shorter than that found in the precursor complex of [1.569(3) Å]. Furthermore DFT calculations revealed a breakdown of 62 % σ / 38 % π contributions to the covalent metal boron interaction confirming the presence of significant multiple bonding character within the Fe-B bond.^{2b}

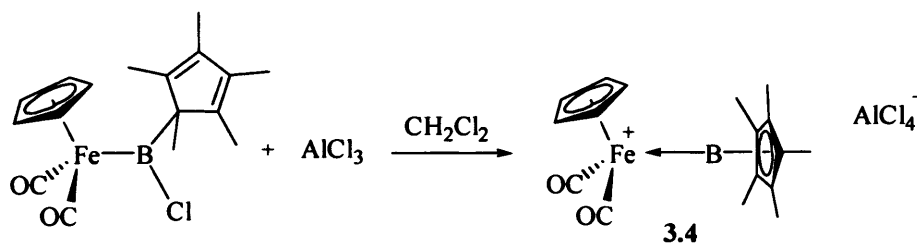
Subsequently in 2005, Aldridge *et al.*,⁶ reported the synthesis of a range of aminoborylene complexes of the type $[\text{L}_n\text{M}(\text{BNR}_2)]^+$ {*e.g.* $[\text{Cp}^*\text{Fe}(\text{CO})_2(\text{BN}^i\text{Pr}_2)]^+$ **3.2** and $[\text{Cp}^*\text{Fe}(\text{CO})_2(\text{BNCy}_2)]^+$ **3.3**} also *via* halide abstraction chemistry, with the aim of

varying the steric and electronic properties of the diyl substituent (Scheme 3.2). It was found that reaction of halide functionalized aminoboryl precursors with $\text{Na}[\text{BAR}'_4]$ yielded the corresponding cationic terminal aminoborylene complex in similar fashion to mesitylborylene species **3.1**. Furthermore it was found that the Fe-B bond distances [1.835(3) and 1.859(6) Å, for **3.2** and **3.3**, respectively] are longer than that found for **3.1** [1.792(8) Å], due the boron centre being less electron deficient when bonded to the π -donor amino group (*cf.* mesityl).



Scheme 3.2

Subsequent related work was reported by Cowley *et al.*⁷ in 2006 and it has thus been demonstrated that the metal-boron bond order could be varied from 1 to 2 depending on the nature of the boron substituent. Thus, reaction of $[\text{CpFe}(\text{CO})_2\{\text{B}(\eta^1\text{-C}_5\text{Me}_5)\text{Cl}\}]$ with AlCl_3 yielded the structurally characterised terminal cationic borylene complex $[\text{CpFe}(\text{CO})_2\{\text{B}(\eta^5\text{-C}_5\text{Me}_5)\}]^+[\text{AlCl}_4]^-$ **3.4** via halide abstraction chemistry (Scheme 3.3). DFT calculations revealed that the B→Fe bond order is one (*cf.* $[\text{Cp}^*\text{Fe}(\text{CO})_2\text{B}(\text{Mes}^*)][\text{BAR}'_4]$: bond order of two). It was concluded that the bond order within such systems is highly sensitive to the electronic properties of the boron substituent.



Scheme 3.3

From these results it was concluded that halide abstraction from complexes containing metal-group 13 element single bonds is a viable synthetic route to the formation of cationic diyl complexes, which with appropriate choice of pendant substituent, can feature an increased metal-ligand bond order.

3.1.1 Aims of Research

Chemical transformations (*e.g.* substitution or abstraction) occurring at an existing group 13 ligand, which proceed with retention of the M-E linkage are relatively rare, reflecting the lability of the metal-ligand bond under the required synthetic conditions.^{8,9}

Salt elimination chemistry has been previously utilised by Aldridge *et al.* in the synthesis of asymmetric halogallyl complexes.⁹ Reaction of $\text{Na}[(\eta^5\text{-C}_5\text{R}_5)\text{Fe}(\text{CO})_2]$ ($\text{R} = \text{H}, \text{Me}$) with $\text{Mes}^*\text{GaCl}_2$, for example, has been shown to generate asymmetric halogallyl complexes of the type $(\eta^5\text{-C}_5\text{R}_5)\text{Fe}(\text{CO})_2\text{Ga}(\text{Mes}^*)\text{Cl}$ ($\text{R} = \mathbf{3.5}, \text{H}; \mathbf{3.6}, \text{Me}$). We have sought to extend this methodology in the synthesis of other heavier group 13 donor ligands, [*e.g.* $(\eta^5\text{-C}_5\text{R}_5)\text{Fe}(\text{CO})_2\text{E}(\text{X})\text{Br}$ ($\text{E} = \text{Ga}, \text{In}; \text{R} = \text{H}, \text{Me}; \text{X} = \text{aryl}, \text{amido etc.}$)] with a view to exploring their potential as precursors to cationic diyl complexes featuring indium and gallium donors. Two possible synthetic

routes to these precursor species will be examined involving salt elimination and insertion/substitution chemistries. The halide abstraction chemistry of these complexes will then be examined with the aim of synthesising low-coordinate cationic species of the type $[(\eta^5\text{-C}_5\text{R}_5)\text{Fe}(\text{CO})_2(\text{ER})]^+$ and investigating the structural and reaction chemistry of such systems.

3.2 Synthesis of Asymmetric Haloindyl and Halogallyl Species

3.2.1 Experimental

Synthesis of CpFe(CO)₂In(Br)Mes (3.7)*

To a slurry of Na[CpFe(CO)₂] (0.183 g, 0.902 mmol) in diethyl ether (5 cm³), was added a solution of Mes*InBr₂ (0.499 g, 0.961 mmol) also in diethyl ether (10 cm³), yielding a dark yellow solution and pale precipitate. The reaction mixture was stirred for 16 h then filtered yielding a dark yellow solution. The solvent was removed *in vacuo* yielding a dark yellow solid, which was washed with hexanes (3 × 10 cm³) and dried *in vacuo* yielding CpFe(CO)₂In(Br)Mes* (3.7) as a yellow powder (0.135 g, 22 %). ¹H NMR (300 MHz, CD₂Cl₂) : δ_H 1.25 (s, 9H, *para*-^tBu of Mes*), 1.50 (s, 18H, *ortho*-^tBu of Mes*), 4.89 (s, 5H, CH of Cp), 7.34 (s, 2H, aromatic CH of Mes*). ¹³C NMR (76 MHz, CD₂Cl₂) : δ_C 31.1 (*para*-^tBu CH₃ of Mes*), 33.5 (*ortho*-^tBu CH₃ of Mes*), 34.8 (*para*-^tBu quaternary C of Mes*), 37.9 (*ortho*-^tBu quaternary C of Mes*), 82.7 (CH of Cp), 122.0 (aromatic CH of Mes*), 150.3 (quaternary aromatic C of Mes*), 155.4 (quaternary aromatic C of Mes*), 213.9 (CO), *ipso* quaternary aromatic not observed. IR (thin film CD₂Cl₂, cm⁻¹) : ν(CO) 1945 st, 1995 st. EI-MS : *m/z* 616.1 {1 %, [M]⁺}, 588.1 {7 %, [M-CO]⁺}, 560.1 {5 %, [M-2CO]⁺}, 537.1 {6 %, [M-Br]⁺}. Exact mass, meas. 588.0163 [M-CO]⁺. Calc. 588.0176 [M-CO]⁺.

Synthesis of Cp*Fe(CO)₂In(Br)Mes* (3.8)

To a slurry of Na[Cp*Fe(CO)₂] (0.195 g, 0.711 mmol) in diethyl ether (5 cm³), was added a solution of Mes*InBr₂ (0.376g, 0.720 mmol) also in diethyl ether (10 cm³), yielding an orange solution and pale precipitate. The reaction was stirred for a further 72 h at 20°C then filtered yielding an orange solution. The solvent was removed *in vacuo* yielding a yellow solid, which was washed with hexanes (3 × 10 cm³) and dried *in vacuo* yielding Cp*Fe(CO)₂In(Br)Mes* (3.8) as a beige powder. Isolated yield 0.124 g, 25 %. ¹H NMR (300 MHz, CD₂Cl₂) : δ_H 1.26 (s, 9H, *para*-^tBu of Mes*), 1.48 (s, 18H, *ortho*-^tBu of Mes*), 1.87 (s, 15H, CH₃ of Cp*), 7.28 (s, 2H, aromatic CH of Mes*). ¹³C NMR (76 MHz, CD₂Cl₂) : δ_C 9.56 (CH₃ of Cp*), 30.3 (*para*-^tBu CH₃ of Mes*), 32.8 (*ortho*-^tBu CH₃ of Mes*), 33.9 (*para*-^tBu quaternary C of Mes*), 37.3 (*ortho*-^tBu quaternary C of Mes*), 94.3 (quaternary C of Cp*), 121.2 (CH aromatic of Mes*), 150.7 (quaternary aromatic C of Mes*), 154.9 (quaternary aromatic C of Mes*), 215.4 (CO), *ipso* quaternary aromatic not observed. IR (thin film CD₂Cl₂, cm⁻¹) : ν(CO) 1928 st, 1977 st. EI-MS : *m/z* 686.1 {1 %, [M]⁺}, 658.1 {2 %, [M-CO]⁺}, 630.1 {1 %, [M-2CO]⁺}, 607.2 {1 %, [M-Br]⁺}. Exact mass, meas. 686.0889 [M]⁺. Calc. 686.0907 [M]⁺.

Synthesis of Cp*Fe(CO)₂Ga(Mes)I (3.10)

To a solution of [Cp*Fe(CO)₂GaI₂]₂ 3.9 (0.303 g, 0.299 mmol) in toluene (50 cm³) was added a solution/suspension of MesLi (0.075 g, 0.595 mmol) also in toluene (40 cm³), and the reaction mixture stirred at room temperature for 12 h. After filtration and removal of volatiles *in vacuo*, the resulting orange oil was extracted into diethyl ether (40 cm³), concentrated (to *ca.* 15 cm³), and cooled to -30°C yielding Cp*Fe(CO)₂Ga(Mes)I (3.10) as a pale yellow crystalline solid. Isolated yield 0.078 g,

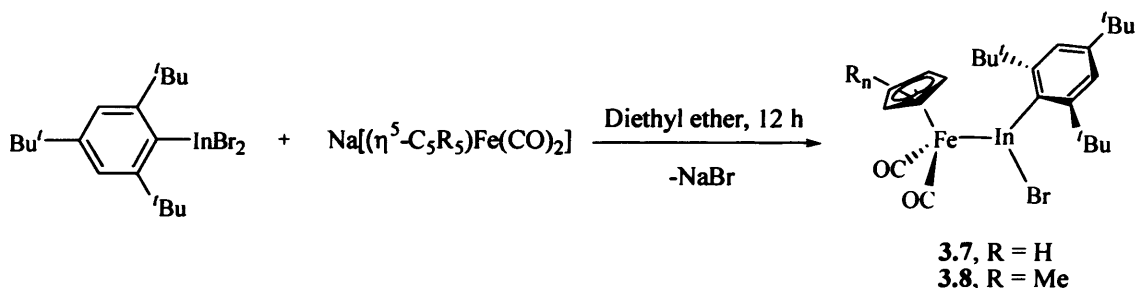
23 %. Crystals suitable for X-ray diffraction were obtained from a concentrated diethyl ether solution at -30°C . ^1H NMR (CD_2Cl_2 , 300 MHz): δ_{H} 1.13 (s, 15H, CH_3 of Cp^*), 1.88 (s, 3H, *para*-Me of Mes), 2.09 (s, 6H, *ortho*-Me of Mes), 6.39 (s, 2H, CH of Mes). ^{13}C NMR (CD_2Cl_2 , 76 MHz): δ_{C} 10.0 (CH_3 of Cp^*), 21.5 (*para*- CH_3 of Mes), 22.7 (*ortho*- CH_3 of Mes), 95.2 (quaternary carbon of Cp^*), 138.6 (*ortho*-quaternary carbon of Mes), 139.8 (*meta*-CH of Mes), 155.6 (*para*-quaternary carbon of Mes), 215.9 (CO), *ipso*-quaternary carbon of Mes not observed. IR (CD_2Cl_2 , cm^{-1}): $\nu(\text{CO})$ 1984 st, 1936 st. EI-MS, m/z : 562.0 {weak, $[\text{Cp}^*\text{Fe}(\text{CO})_2\text{Ga}(\text{Mes})\text{I}]^+$ }, 534.0 {69 %, $[\text{Cp}^*\text{Fe}(\text{CO})\text{Ga}(\text{Mes})\text{I}]^+$ }, 506.0 {14 %, $[\text{Cp}^*\text{FeGa}(\text{Mes})\text{I}]^+$ }, 435.1 {9 %, $[\text{Cp}^*\text{Fe}(\text{CO})_2\text{Ga}(\text{Mes})]^+$ }, 310.1 {100 %, $[(\text{OC})_2\text{FeGaI}]^+$ }. Exact mass: calc. for $[\text{Cp}^*\text{Fe}(\text{CO})_2\text{Ga}(\text{Mes})\text{I}]^+$ (*i.e.* $[\text{M}]^+$) 561.9577, meas. 561.9581; calc. for $[\text{Cp}^*\text{Fe}(\text{CO})\text{Ga}(\text{Mes})\text{I}]^+$ (*i.e.* $[\text{M}-\text{CO}]^+$) 533.9628, meas. 533.9630

3.2.2 Results and Discussion

3.2.2.1 Asymmetric Haloindyl Species

In the case of gallium it has been previously demonstrated that the use of sterically demanding metal fragments of the type $\text{Cp}^*\text{Fe}(\text{CO})_2$ and/or the use of bulky gallyl substituents such as Mes or Mes^* , has allowed the synthesis of three-coordinate asymmetric (halo) gallyl species by preventing aggregation of the complex through bridging halides and thereby promoting a trigonal planar geometry at the group 13 centre.⁹ With this in mind, Mes^* -substituted bromoindyl complexes of the type $(\eta^5\text{-C}_5\text{R}_5)\text{Fe}(\text{CO})_2\text{In}(\text{Mes}^*)\text{Br}$ (**3.7**, R = H, **3.8**, R = Me) were synthesised by the addition of $\text{Mes}^*\text{InBr}_2$ to a suspension of $\text{Na}[(\eta^5\text{-C}_5\text{R}_5)\text{Fe}(\text{CO})_2]$ (R = H, Me) in diethyl ether (Scheme 3.4), a reaction which proceeds with selective substitution of a single bromide for the Mes^* substituent.⁹ The pale yellow microcrystalline compounds were

isolated in moderate yields (*ca.* **3.7**, 22%, **3.8**, 25%). This reaction chemistry is analogous to that reported by Aldridge *et al.* for the corresponding aryl(halo)gallyl systems of the type $[(\eta^5\text{-C}_5\text{R}_5)\text{Fe}(\text{CO})_2\text{Ga}(\text{Mes})\text{Cl}]$ (**3.5**, R = H, **3.6**, R = Me) which are readily synthesised in similarly moderate yields *via* salt elimination chemistry.⁹ Conversely, this chemistry contrasts markedly with the corresponding aryl(halo)boryl species of the type $[(\eta^5\text{-C}_5\text{R}_5)\text{Fe}(\text{CO})_2\text{B}(\text{Aryl})\text{X}]$ (R = H, Me; Aryl = Ph, Mes, 2,6-(2,4,6-*i*-Pr₃C₆H₃)₂C₆H₃; X = F, Cl, Br, I) which have been shown to decompose rapidly in the presence of coordinating solvents such as diethyl ether.^{8b, 10}



Scheme 3.4 Synthetic route to complexes **3.7** and **3.8**.

¹H and ¹³C NMR data support the proposed formulations of **3.7** and **3.8**. The ¹H NMR spectra of **3.7** and **3.8** display peaks with relative intensities of 18:9 corresponding to the *ortho*-^{*i*}Bu, and *para*-^{*i*}Bu moieties of the Mes* fragment within both species. The ¹H and ¹³C NMR of **3.7** also feature singlets corresponding to the Cp fragment with a relative intensity in the ¹H NMR of 5; similarly, **3.8** reveals peaks in the ¹H and ¹³C NMR corresponding to the Cp* fragment with a relative intensity in the ¹H NMR of 15. The ¹³C NMR for **3.7** and **3.8** show the presence of a carbonyl containing species, and the measured carbonyl stretching frequencies ($\nu(\text{CO})$ **3.7**, 1945, 1995 cm⁻¹ and **3.8**, 1928, 1977 cm⁻¹) are also consistent with the formation of a complex featuring a single $[\eta^5\text{-C}_5\text{R}_5\text{Fe}(\text{CO})_2]$ fragment. In addition, EI mass spectra

of **3.7** and **3.8** display weak peaks for the parent $[M]^+$ ions, with strong fragment peaks $[M-CO]^+$ and $[M-2CO]^+$ also being evident. The isotope distributions observed for **3.7** and **3.8** are consistent with species containing one iron, one indium and one bromine atom, thus supporting the proposed substitution of a single bromide with the Mes* ligand.

Single crystals of **3.8** suitable for X-ray diffraction were obtained by cooling a concentrated solution of the compound in diethyl ether to -30°C . The spectroscopic data for **3.8** were confirmed by single crystal X-ray diffraction studies and the structure is illustrated in Figure 3.1. Selected bond lengths and angles for **3.8** are listed in Table 3.1. **3.8** consists of monomeric units with the formulation $\text{Cp}^*\text{Fe}(\text{CO})_2\text{In}(\text{Mes}^*)\text{Br}$ in which the $\text{Cp}^*\text{Fe}(\text{CO})_2$ fragment is bound to the indium through the iron centre. **3.8** represents the first simple neutral haloindyl complex to be structurally characterised.

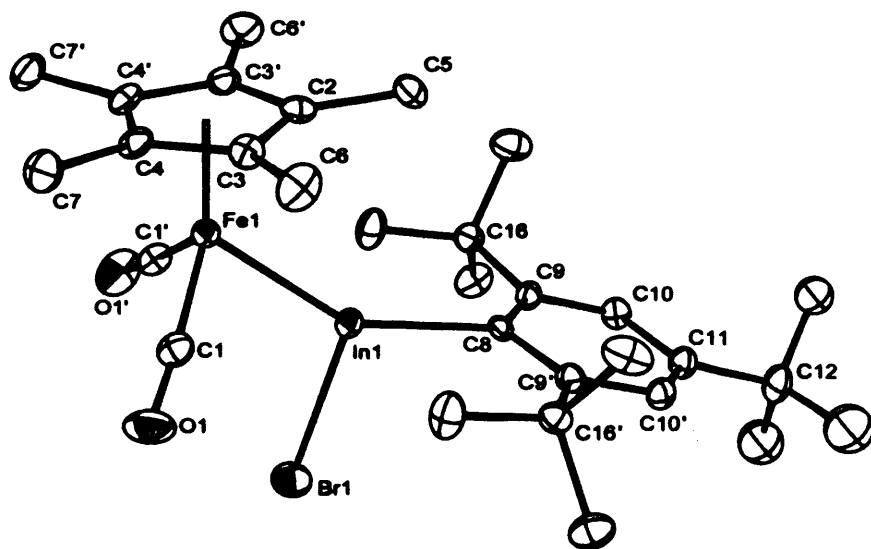


Figure 3.1 The molecular structure of $[\text{Cp}^*\text{Fe}(\text{CO})_2\text{In}(\text{Mes}^*)\text{Br}]$ **3.8**.

Table 3.1 Selected bond lengths [Å] and angles [°] for **3.8**.

Fe(1)-In(1)	2.5087(11)	Fe(1)-Cp* centroid	1.719(5)
Br(1)-In(1)	2.6098(10)	Fe(1)-C(1)	1.747(6)
C(8)-In(1)	2.178(7)		
Fe(1)-In(1)-Br(1)	111.4(1)	Cp* centroid-Fe(1)-In(1)-C(8)	0.0(1)
Fe(1)-In(1)-C(8)	148.92(18)	Fe(1)-In(1)-C(8)-C(9)	94.2(2)
Br(1)-In(1)-C(8)	100.73(18)		

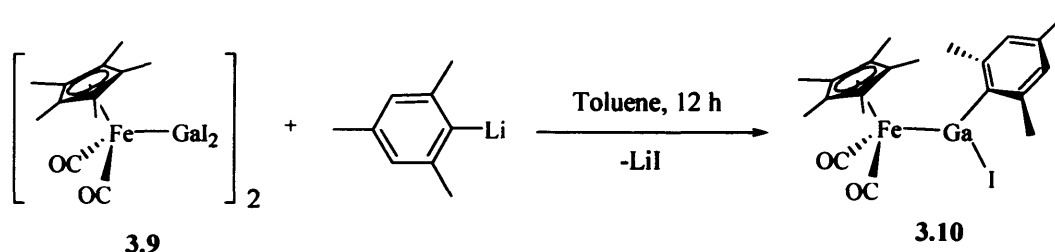
The coordination geometry about the indium centre is trigonal planar, with angles of Fe-In-Br, 110.35(4)°; Fe-In-C, 148.92(18)°; Br-In-C, 100.73(18)° [sum of angles at In(1) = 360.0°]. The iron-indium bond distance of 2.5087(11) Å is comparable to related complexes (*e.g.* 2.513(1) Å [Cp*Fe(CO)₂]₂InI)⁹. The orientation of the indyl ligand is such that it lies co planar with Cp* centroid-Fe-In plane (\angle Cp* centroid-Fe-In-C_{ipso} = 0.0(1)°), a geometry which is enforced by a crystallographic mirror plane. This ligand orientation and the near perpendicular alignment of the indyl and Mes* planes (\angle Fe-In-C_{ipso}-C_{ortho} = 94.2(2)°) minimizes steric interactions between the bulky Cp* and aryl substituents. Furthermore, this geometry mirrors that observed for gallyl and boryl complexes of the type (η^5 -C₅R₅)Fe(CO)₂Ga(Mes*)X⁹ and (η^5 -C₅R₅)Fe(CO)₂B(Mes)X^{8b, 10}. Consequently, due to the orthogonal alignment of the relevant p orbitals in the Fe-In-C_{ipso}-C_{ortho} unit there is no π interaction between the indium centre and Mes* fragment.

Unfortunately, attempts to grow single crystals of **3.7** suitable for X-ray diffraction studies were unsuccessful and the formulation of this complex is therefore

proposed on the basis of NMR, IR and mass spectrometric results, and comparison with the data obtained for structurally authenticated **3.8**.

3.2.2.2 Asymmetric Halogallyl Species

An alternative two-step approach to the generation of asymmetric halogallyl complexes was examined, involving initial insertion of 'Gal' into a M-M bond (with subsequent redistribution chemistry to give a diiodogallyl species), followed by substitution at the group 13 centre by an appropriately bulky anionic nucleophile. Gallium centred iodide substitution in $[\text{Cp}^*\text{Fe}(\text{CO})_2\text{GaI}_2]_2$ **3.9**, with strongly nucleophilic aryl anions was shown to afford asymmetric halogallyl species of the type $\text{Cp}^*\text{Fe}(\text{CO})_2\text{Ga}(\text{Ar})\text{I}$, with retention of the Fe-Ga bond. Thus, addition of MesLi to a solution of **3.9** in toluene proceeds with selective substitution of a single iodide to yield $\text{Cp}^*\text{Fe}(\text{CO})_2\text{Ga}(\text{Mes})\text{I}$ **3.10** (Scheme 3.5) in moderate yield (23%) as a yellow microcrystalline solid.¹¹



Scheme 3.5 Synthetic route to complex **3.10**.

^1H and ^{13}C NMR data support the proposed formulation of **3.10**. The ^1H NMR spectrum displays peaks with relative intensities of 15:6:3 corresponding to the Cp^* , *ortho*- $t\text{Bu}$, and *para*- $t\text{Bu}$ moieties respectively. The ^{13}C NMR spectrum reveals peaks corresponding to the Cp^* and CO moieties, and the measured carbonyl stretching frequencies ($\nu(\text{CO}) = 1936, 1984 \text{ cm}^{-1}$) also support the formation of a

[Cp*Fe(CO)₂] containing species. The EI mass spectrum displays weak peaks for the parent [M]⁺ ion, with fragment peaks [M-CO]⁺ and [M-2CO]⁺ also being evident. Furthermore, the isotope distribution observed for **3.10** is consistent with a complex containing one iron, one gallium, and one iodine atom, thus confirming the substitution of a single iodide for the Mes ligand.

Single crystals suitable for X-ray diffraction were obtained from a concentrated diethyl ether solution at -30°C, and the spectroscopic data for **3.10** was confirmed by single crystal X-ray diffraction studies (Figure 3.2). Relevant bond lengths and angles for **3.10** are listed in Table 3.2.

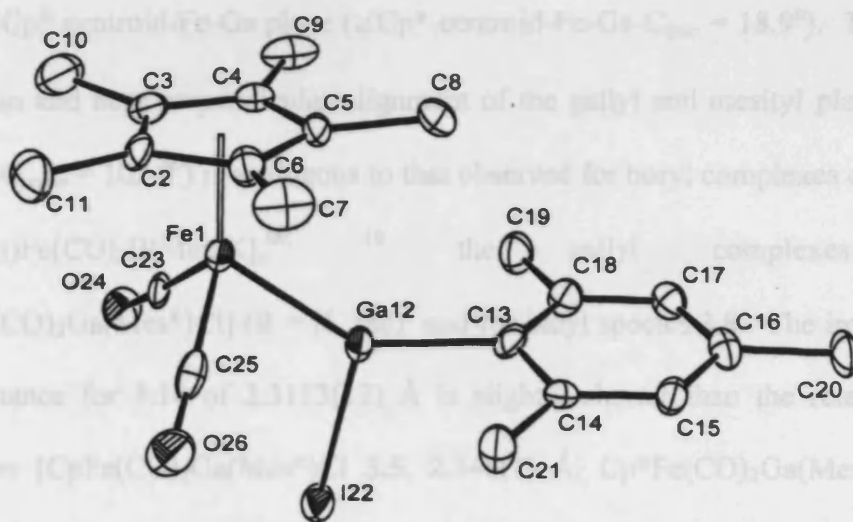


Figure 3.2 The molecular structure of [Cp*Fe(CO)₂Ga(Mes)I] **3.10**.

Table 3.2 Selected bond lengths [Å] and angles [°] for **3.10**.

Fe(1)-Ga(12)	2.3113(12)	Ga(12)-I(22)	2.6073(9)
Fe(1)-C(23)	1.787(8)	C(23)-O(24)	1.116(8)
Ga(12)-C(13)	1.989(6)	C(18)-C(19)	1.488(11)
C(23)-Fe(1)-Ga(12)	86.7(2)	Fe(1)-Ga(12)-I(22)	116.86(4)
I(22)-Ga(12)-C(13)	105.16(8)	Ga(12)-C(13)-C(18)	122.7(6)
Ga(12)-C(13)-C(14)	117.1(6)	C(13)-C(18)-C(19)	121.1(7)
C(23)-Fe(1)-C(25)	94.9(4)	C(13)-Ga(12)-Fe(1)	137.20(19)
Fe(1)-C(23)-O(24)	177.9(7)		

The orientation of the gallyl ligand is such that it lies essentially co-planar with the Cp* centroid-Fe-Ga plane ($\angle \text{Cp}^* \text{ centroid-Fe-Ga-C}_{ipso} = 18.9^\circ$). This ligand orientation and near perpendicular alignment of the gallyl and mesityl planes ($\angle \text{Fe-Ga-C}_{ipso}\text{-C}_{ortho} = 102.9^\circ$) is analogous to that observed for boryl complexes of the type $[(\eta^5\text{-C}_5\text{R}_5)\text{Fe}(\text{CO})_2\text{B}(\text{Mes})\text{X}]$,^{8b, 10} the gallyl complexes $[(\eta^5\text{-C}_5\text{R}_5)\text{Fe}(\text{CO})_2\text{Ga}(\text{Mes}^*)\text{Cl}]$ (R = H, Me)⁹ and for indyl species **3.8**. The iron-gallium bond distance for **3.10** of 2.3113(12) Å is slightly shorter than the related gallyl complexes [CpFe(CO)₂Ga(Mes*)Cl **3.5**, 2.346(1) Å, Cp*Fe(CO)₂Ga(Mes*)Cl **3.6**, 2.372(2) Å] (presumably on steric grounds) and is shorter than that found for the corresponding Fe-In bond length of 2.5087(11) Å for **3.8**, reflecting the smaller covalent radius of the gallium atom compared to indium (1.26 vs. 1.44 Å, respectively).

3.3 Synthesis of Symmetric Bridging Amido Gallyl complexes – Attempted Synthesis of Asymmetric Amino Halogallyl Species

3.3.1 Experimental

Synthesis of [CpFe(CO)₂]₂(μ-GaN(SiMe₃)₂) (3.11)

To a slurry of Na[CpFe(CO)₂] (0.402 g, 2.021 mmol) in diethyl ether was added a solution of (Me₃Si)₂NGaCl₂.thf (0.377 g, 1.010 mmol) also in diethyl ether (30 cm³). The reaction mixture stirred at room temperature for 2 h, after which volatiles were removed *in vacuo*. The resulting yellow oil was dissolved in hexane, filtered, concentrated (to *ca.* 20 cm³) and cooled to –30°C, yielding [CpFe(CO)₂]₂(μ-GaN(SiMe₃)₂) (3.11) as a pale yellow microcrystalline solid. Isolated yield 0.421 g, 38 %. ¹H NMR (300 MHz, C₆D₆): δ_H 0.33 (s, 18H, CH₃ of SiMe₃), 4.21 (s, 10H, CH of Cp). ¹³C NMR (76 MHz, C₆D₆): δ_C 4.2 (CH₃ of SiMe₃), 82.6 (Cp), 215.9 (CO). IR (thin film CD₂Cl₂, cm⁻¹): ν(CO) 1993 st, 1972 st, 1926 st. EI-MS, *m/z*: 555.0 {1 %, [{CpFe(CO)}{CpFe(CO)₂}GaN(SiMe₃)₂]⁺}, 527.0 {4 %, [{CpFe(CO)}₂GaN(SiMe₃)₂]⁺}, 471.0 {17 %, [(CpFe)₂GaN(SiMe₃)₂]⁺}, 406.0 {100 %, [CpFe(CO)₂GaN(SiMe₃)₂]⁺}. Exact mass: calc. for [{CpFe(CO)}{CpFe(CO)₂}GaN(SiMe₃)₂]⁺ {*i.e.* [M-CO]⁺} 554.9557, meas. 554.9554.

*Synthesis of [Cp*Fe(CO)₂]₂(μ-GaN(SiMe₃)₂) (3.12)*

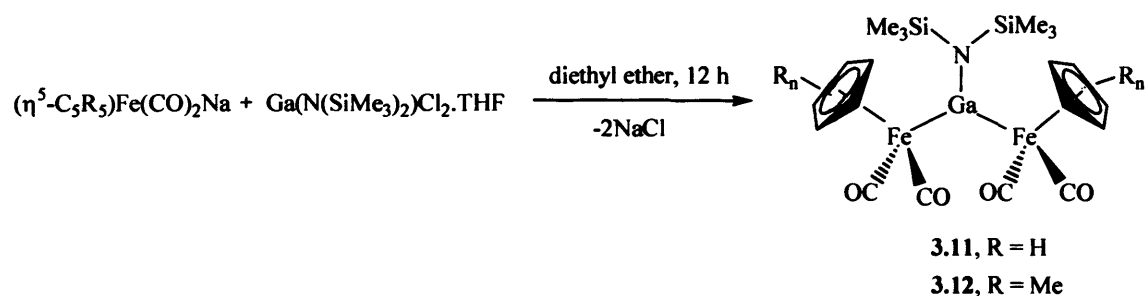
A slurry of Cp*Fe(CO)₂Na (0.482 g, 1.785 mmol) in diethyl ether (15 cm³) was added dropwise to a solution of (Me₃Si)₂NGaCl₂.thf (0.666 g, 1.785 mmol) in diethyl ether (50 cm³) at room temperature. The reaction was stirred at room temperature for 2 h, after which the dark yellow solution was filtered and concentrated (to *ca.* 15 cm³) *in vacuo* yielding [Cp*Fe(CO)₂]₂(μ-GaN(SiMe₃)₂) (3.12) as a yellow microcrystalline solid on cooling to –30°C (0.543 g, 44 %). Crystals suitable for X-ray diffraction

obtained from a concentrated diethyl ether solution at -30°C . Isolated yield 0.543 g, 44 %. ^1H NMR (300 MHz, C_6D_6): δ_{H} 0.52 (s, 18H, CH_3 of SiMe_3), 1.57 (s, 30H, CH_3 of Cp^*). ^{13}C NMR (76 MHz, C_6D_6): δ_{C} 3.9 (CH_3 of SiMe_3), 9.2 (CH_3 of Cp^*), 93.0 (quaternary carbon of Cp^*), CO carbon not observed. IR (thin film CD_2Cl_2 , cm^{-1}): $\nu(\text{CO})$ 1973 st, 1955 st, 1908 st. EI-MS, m/z : 695.1 {2 %, $[\{\text{Cp}^*\text{Fe}(\text{CO})\}\{\text{Cp}^*\text{Fe}(\text{CO})_2\}\text{GaN}(\text{SiMe}_3)_2\}^+]$, 476.1 {41 %, $[\text{Cp}^*\text{Fe}(\text{CO})_2\text{GaN}(\text{SiMe}_3)_2]^+$, 420.1 {24 %, $[\text{Cp}^*\text{FeGaN}(\text{SiMe}_3)_2]^+$, 317.9 {31 %, $[\text{Cp}^*\text{Fe}(\text{CO})_2\text{Ga}]^+$. Exact mass: calc. for $[\{\text{Cp}^*\text{Fe}(\text{CO})\}\{\text{Cp}^*\text{Fe}(\text{CO})_2\}\text{GaN}(\text{SiMe}_3)_2]^+$ *i.e.* $[\text{M}-\text{CO}]^+$ 695.1122, meas. 695.1124.

3.3.2 Results and Discussion

With the aim of varying the steric and electronic properties of gallyl species the synthesis of asymmetric amino halogallyl complexes was investigated. In particular we sought to determine the feasibility of salt elimination chemistry in the generation of gallyl systems of the type $(\eta^5\text{-C}_5\text{R}_5)\text{Fe}(\text{CO})_2\text{Ga}(\text{NR}_2)\text{Cl}$.

Unexpectedly, substitution of *both* gallium bound chloride atoms was observed in the case of $(\text{Me}_3\text{Si})_2\text{NGaCl}_2\text{thf}$, yielding the corresponding bridging gallylene complexes. Further experiments revealed that the disubstituted species formed irrespective of the stoichiometry of reactants used and synthetic conditions employed. Thus the bridging amidogallyl complexes $[\{(\eta^5\text{-C}_5\text{R}_5)\text{Fe}(\text{CO})_2\}_2\{\mu\text{-GaN}(\text{SiMe}_3)_2\}]$ (**3.11**, $\text{R} = \text{H}$, and **3.12**, $\text{R} = \text{Me}$) were synthesised as pale yellow microcrystalline compounds in moderate yields (*ca.* **3.11**, 38 %, and **3.12**, 44 %) (Scheme 3.6).¹¹



Scheme 3.6 Synthetic route to complexes **3.11** and **3.12**.

^1H and ^{13}C NMR data support the proposed formulation. The ^1H NMR spectra for **3.11** and **3.12** both feature just two peaks corresponding to the $\text{N}(\text{SiMe}_3)_2$ and $\eta^5\text{-C}_5\text{R}_5$ moieties [**3.11**, relative intensity 18:10 $\text{N}(\text{SiMe}_3)_2$:Cp; **3.12**, relative intensity 18:30 $\text{N}(\text{SiMe}_3)_2$:Cp*]. The carbonyl stretching frequencies (1926, 1972, 1993, and 1908, 1955, 1973 cm^{-1} , for **3.11** and **3.12** respectively) support the formation of a carbonyl containing species, and EI mass spectra for both **3.11** and **3.12** display peaks for the $[\text{M-CO}]^+$ ions, with fragment peaks due to the $[\text{M-2CO}]^+$ and $[\text{M-4CO}]^+$ ions also being evident. In addition, the isotope distributions observed for both **3.11** and **3.12** correspond to complexes containing two iron, one gallium, and one nitrogen atom (and *no* chlorines) thus confirming the substitution of both chloride moieties.

Single crystals suitable for X-ray diffraction of **3.12** were accessible by cooling a concentrated solution of the complex in diethyl ether to -30°C . The spectroscopic data for **3.12** was thus confirmed by single crystal X-ray diffraction studies and the structure of which is illustrated in Figure 3.3. Relevant bond lengths and angles for **3.12** are listed in Table 3.3.

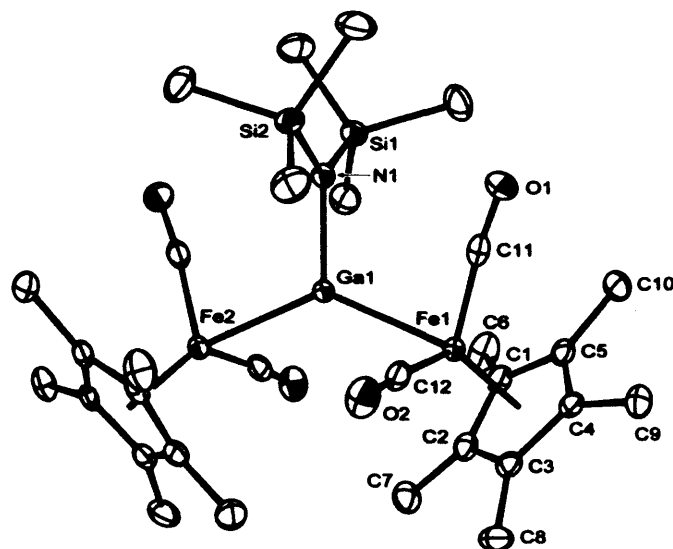


Figure 3.3 The molecular structure of $[\{Cp^*Fe(CO)_2\}_2\{\mu-GaN(SiMe_3)_2\}]$ **3.12**.

Table 3.3 Selected bond lengths [Å] and angles [$^\circ$] for **3.12**.

Fe(1)-Ga(1)	2.4527(4)	Ga(1)-N(1)	1.956(2)
Fe(2)-Ga(1)	2.4559(4)	Si(1)-N(1)	1.721(2)
Si(2)-N(1)-Ga(1)	117.74(11)	Fe(1)-Ga(1)-Fe(2)	133.712(15)
N(1)-Ga(1)-Fe(1)	113.62(6)	Si(2)-N(1)-Si(1)	123.09(12)
N(1)-Ga(1)-Fe(2)	112.67(6)		

The coordination geometry about the gallium centre is approximately trigonal planar, with angles of Fe-Ga-Fe $133.721(15)^\circ$, N-Ga-Fe(1) $113.62(6)^\circ$, N-Ga-Fe(2) $112.67(6)^\circ$ [sum of angles at Ga(1) = 360.0°]. The average iron-gallium bond distance for **3.12** [$2.4543(4)$ Å] is significantly longer than that observed for $[Cp^*Fe(CO)_2]_2(\mu-GaCl)^{12}$ **3.13** [$2.3524(4)$ Å] and $[Cp^*Fe(CO)]_2(\mu-CO)(\mu-GaMes)^{13}$ **3.14** [$2.4315(15)$ Å]; presumably this difference is a reflection of the enhanced steric bulk provided by the $N(SiMe_3)_2$ group at the gallium centre. Moreover, the synthesis of **3.12** mirrors that reported by Braunschweig *et al.*, in which analogous anionic

reagents were shown to react with the sterically encumbered dihaloborane species $(\text{Me}_3\text{Si})_2\text{NBCl}_2$ to generate the aminoborylene complex $[\{\text{Cp}'\text{Fe}(\text{CO})\}_2\{\mu\text{-BN}(\text{SiMe}_3)_2\}(\mu\text{-CO})]^{14}$ **3.15** irrespective of the reaction conditions. For these boron analogues it was concluded that the nature of the aminoborylene complex formed is dependent on electronic rather than steric factors since the analogous reaction with Me_2NBCl_2 results in substitution of one chloride atom.

Unfortunately, attempts to grow single crystals of **3.11** suitable for X-ray diffraction studies were unsuccessful and the formulation of this complex is therefore proposed on the basis of NMR, IR and mass spectrometric results, and comparison of data with structurally authenticated **3.12**.

3.4 Substitution Chemistry of Asymmetric Haloindyl Complexes

3.4.1 Experimental

Synthesis of $\text{Cp}^\text{Fe}(\text{CO})_2\text{In}(\text{OC}_6\text{H}_4^i\text{Bu-4})\text{Mes}^*$ (3.16)*

A solution of **3.8** (0.300 g, 0.437 mmol) in toluene (60 cm³) was added to a suspension of $\text{Na}[\text{OC}_6\text{H}_4^i\text{Bu-4}]$ (0.094 g, 0.546 mmol) also in toluene (5 cm³), and the resulting mixture stirred at room temperature for 48 h, yielding an orange solution. The solution was filtered and the solvent removed *in vacuo* yielding an orange oil which was extracted into hexanes (2 × 10 cm³) thereby generating $\text{Cp}^*\text{Fe}(\text{CO})_2\text{In}(\text{OC}_6\text{H}_4^i\text{Bu-4})\text{Mes}^*$ (**3.16**) as a pale orange crystalline solid at -30°C. Crystals suitable for X-ray diffraction were obtained by cooling the hexane solution to -30°C (0.076 g, 23 %). ¹H NMR (300 MHz, CD₂Cl₂) : δ_{H} 1.11 (s, 9H, *para*-^{*i*}Bu of $\text{OC}_6\text{H}_4^i\text{Bu-4}$), 1.26 (s, 9H, *para*-^{*i*}Bu of Mes^*), 1.44 (s, 18H, *ortho*-^{*i*}Bu of Mes^*), 1.82 (s, 15H, CH₃ of Cp^*), 6.28 (d, *J* = 8.0 Hz, 2H, aromatic CH of $\text{OC}_6\text{H}_4^i\text{Bu-4}$), 6.88 (d,

$J = 8.0$ Hz, 2H, aromatic CH of OC₆H₄^tBu-4), 7.36 (s, 2H, aromatic CH of Mes*^{*}).
¹³C NMR (76 MHz, CD₂Cl₂) : δ_c 10.4 (CH₃ of Cp*^{*}), 31.1 (*para*-^tBu CH₃ of Mes*^{*}), 31.4 (*ortho*-^tBu CH₃ of Mes*^{*}), 33.5 (*para*-^tBu CH₃ of OC₆H₄^tBu-4), 33.7 (quaternary C of OC₆H₄^tBu-4 ^tBu), 34.7 (quaternary C of Mes*^{*} *para*-^tBu), 37.6 (*ortho*-^tBu quaternary C of Mes*^{*}), 94.8 (quaternary C of Cp*^{*}), 119.0 (aromatic CH of OC₆H₄^tBu-4), 121.6 (aromatic CH of Mes*^{*}), 125.5 (aromatic CH of OC₆H₄^tBu-4), 147.7 (quaternary aromatic C of OC₆H₄^tBu-4), 149.4 (quaternary aromatic C of Mes*^{*}), 156.0 (quaternary aromatic C of Mes*^{*}), 216.8 (CO), *ipso* quaternary aromatic not observed. IR (thin film CD₂Cl₂, cm⁻¹) : ν (CO) 1922 st, 1971 st. MS/EI: m/z 756.3 {1 %, [M]⁺}, 700.3 {1 %, [M - 2CO]⁺}. Exact mass: calc. 756.2697 [M]⁺, meas. 756.2690.

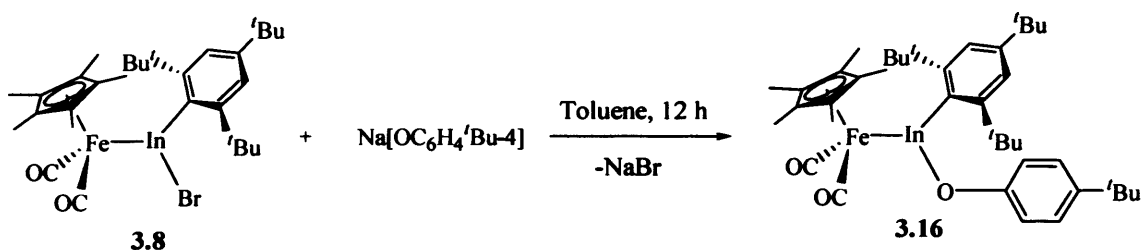
Synthesis of Cp*Fe(CO)₂In(SPh)Mes* (3.17)

A solution of **3.8** (0.153 g, 0.223 mmol) in toluene (40 cm³) was added to a suspension of Na[SPh] (0.063 g, 0.477 mmol) also in toluene (5 cm³), and the reaction mixture was stirred at room temperature for 48 h, yielding a yellow-green solution. The solution was filtered and the solvent was removed *in vacuo* yielding Cp*Fe(CO)₂In(Mes*)SPh (**3.17**) as a yellow-green oil. ¹H NMR (300 MHz, CD₂Cl₂) : δ_H 1.25 (s, 9H, *para*-^tBu of Mes*^{*}), 1.35 (s, 18H, *ortho*-^tBu of Mes*^{*}), 1.83 (15H, CH₃ of Cp*^{*}), 6.89 (m, 3H, aromatic CH of SPh), 6.69 (m, 2H, aromatic CH of SPh), 7.46 (s, 2H, aromatic CH of Mes*^{*}). ¹³C NMR (76 MHz, CD₂Cl₂) : δ_c 10.5 (CH₃ of Cp*^{*}), 31.2 (*para*-^tBu CH₃ of Mes*^{*}), 31.3 (*ortho*-^tBu CH₃ of Mes*^{*}), 34.6 (*para*-^tBu quaternary C of Mes*^{*}), 37.9 (*ortho*-^tBu quaternary C of Mes*^{*}), 94.7 (quaternary C of Cp*^{*}), 121.9 (aromatic CH of Mes*^{*}), 128.2 (aromatic CH of SPh), 129.0 (aromatic CH of SPh), 133.4 (aromatic CH of SPh), 150.1 (quaternary aromatic C of Mes*^{*}), 155.0

(quaternary aromatic C of Mes*), 217.1 (CO), *ipso* quaternary aromatic not observed. IR (thin film CD₂Cl₂, cm⁻¹): ν(CO) 1918 st, 1968 st. Due to the extreme oily nature of **3.17** there was difficulty in fully characterising the complex.

3.4.2 Results and Discussion

The phenoxide-substituted iron indyl complex Cp*Fe(CO)₂In(OC₆H₄^{*t*}Bu-4)Mes* **3.16** was prepared by addition of Na[OC₆H₄^{*t*}Bu-4] to a solution of Cp*Fe(CO)₂In(Mes*)Br **3.8** in toluene (Scheme 3.7). It was found that the reaction proceeds cleanly *via* replacement of the remaining bromide atom with [OC₆H₄^{*t*}Bu-4]. The pale yellow microcrystalline product was isolated in 23% yield.¹⁵



Scheme 3.7 Synthetic route to complex **3.16**.

¹H and ¹³C NMR data support the proposed formulation. The ¹H NMR spectrum of **3.16** reveals peaks with relative intensities of 15:18:9:9 corresponding to the Cp*, *ortho*-^{*t*}Bu, *para*-^{*t*}Bu, and phenoxide-^{*t*}Bu moieties respectively, and ¹³C NMR data reveals the presence of a Cp*Fe(CO)₂ fragment with peaks due to the Cp* and CO ligands. The carbonyl stretching frequencies (1922, 1971 cm⁻¹) imply the presence of a single carbonyl containing moiety. The EI mass spectrum displays a weak peak for the parent [M]⁺ ion with the fragment peak corresponding to [M-2CO]⁺ also being evident. The isotope distribution observed for **3.16** is consistent with a complex containing one iron, one indium and three oxygen atoms, thus supporting the

proposed indium-centred substitution chemistry proceeding with retention of the metal-ligand bond.

Single crystals suitable for X-ray diffraction were accessible by cooling a concentrated solution of the complex in hexanes to -30°C . The spectroscopic data for **3.16** was thus confirmed by single crystal X-ray diffraction studies and the structure is illustrated in Figure 3.4. Relevant bond lengths and angles for **3.16** are listed in Table 3.4. The crystal structure shows that the complex exists as isolated monomeric units with the formulation $\text{Cp}^*\text{Fe}(\text{CO})_2\text{In}(\text{OC}_6\text{H}_4'\text{Bu-4})\text{Mes}^*$ **3.16** in which the bromide atom of the precursor **3.8** has been substituted by the $\text{OC}_6\text{H}_4'\text{Bu-4}$ fragment. The molecular structure of **3.16** not only demonstrates the viability of the substitution methodology proceeding with retention of the M-E bond, but also confirms the expected trigonal planar geometry at the indium centre [sum of angles at $\text{In}(1) = 360.0(2)^{\circ}$] and the near perpendicular alignment of the super-mesityl and indyl planes [torsion $\text{Fe-In-C}_{ipso}\text{-C}_{ortho} = 87.8(2)^{\circ}$] presumably enforced to minimise the steric interactions between the bulky Cp^* and Mes^* substituents. In addition, there is a slight narrowing of the Fe-In-C_{ipso} angle compared to that found in the bromo-substituted precursor **3.8** [143.8(1) vs 148.9(2)], presumably due to the greater bulk of the $\text{OC}_6\text{H}_4'\text{Bu-4}$ substituent (vs bromide).

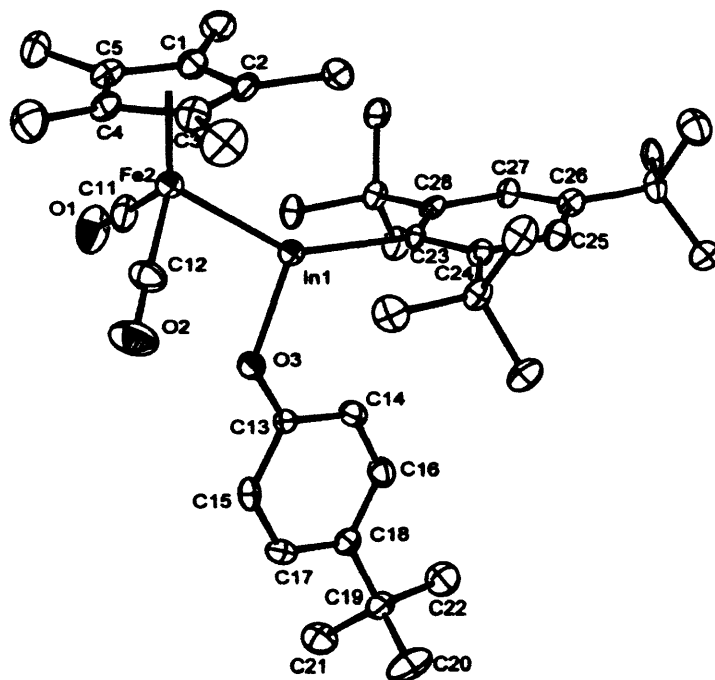


Figure 3.4 The molecular structure of $[\text{Cp}^*\text{Fe}(\text{CO})_2\text{In}(\text{OC}_6\text{H}_4^t\text{Bu-4})\text{Mes}^*]$ **3.16**.

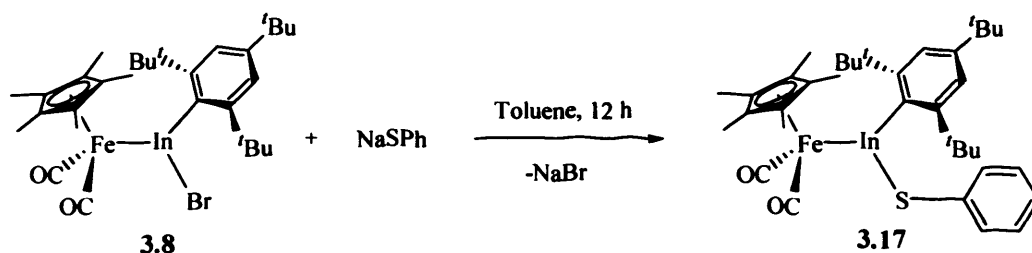
Table 3.4 Selected bond lengths [\AA] and angles [$^\circ$] for **3.16**.

In(1)-O(3)	2.088(5)	O(3)-C(13)	1.305(9)
In(1)-C(23)	2.185(7)	Fe(2)-C(12)	1.745(9)
In(1)-Fe(2)	2.5094(13)	C(12)-O(2)	1.164(10)
O(2)-C(12)-Fe(2)	177.6(9)	O(3)-In(1)-C(23)	111.7(2)
C(11)-Fe(2)-C(12)	94.5(5)	C(23)-In(1)-Fe(2)	143.78(18)
C(11)-Fe(2)-In(1)	84.4(3)	C(13)-O(3)-In(1)	131.7(5)

The Fe-In bond length in **3.16** [2.509(2) \AA] is identical to that found in **3.8** [2.509(1) \AA] and the carbonyl stretching frequencies for the two compounds are also very similar (1977, 1928 and 1971, 1922 cm^{-1} , for **3.8** and **3.16**, respectively). These observations contrast markedly with similar measurements made for the closely related pair of boryl species $\text{CpFe}(\text{CO})_2\text{B}(\text{Br})\text{Mes}$ and $\text{CpFe}(\text{CO})_2\text{B}(\text{OC}_6\text{H}_4^t\text{Bu-4})\text{Mes}$.

4)Mes.^{8b} For example, in the case of the boryl complexes, the aryloxo derivative has a significantly longer Fe-B bond [2.040(2) vs 1.964(5) Å] and lower carbonyl stretching frequencies (1997, 1933 vs 2016, 1962 cm⁻¹) than the bromide. Presumably, the much shorter Fe-B bond (*cf.* Fe-In) is decidedly more sensitive to changes in steric properties and π donor capabilities of pendant substituents, π bonding being significantly more important for boron compared to indium.

The substitution chemistry of Cp*Fe(CO)₂In(Br)Mes* **3.8** was further investigated with the thiophenolate reagent Na[SPh]. The available data suggest that reaction of **3.8** with NaSPh in toluene proceeds as expected with substitution of the indium bound-bromide substituent to yield Cp*Fe(CO)₂In(SPh)Mes* **3.17** (Scheme 3.8). However the product in this case is a pale green oil; thus there was difficulty in fully characterising complex **3.17**.



Scheme 3.8 Synthetic route to complex **3.17**.

The proposed formulation is consistent with the multinuclear NMR and IR data obtained; the ¹H NMR spectrum reveals signals with relative intensities of 15:18:9:2:3 corresponding to the Cp*, *ortho*-^tBu, *para*-^tBu, *ortho*-H and overlapping *meta*-H and *para*-H signals. ¹³C NMR data reveals the presence of a [Cp*Fe(CO)₂] fragment with peaks relating to Cp* and CO fragments. The measured carbonyl

stretching frequencies (1968, 1918 cm^{-1}) also imply the presence of a single carbonyl containing moiety. Unfortunately, attempts to grow single crystals of **3.17** suitable for X-ray diffraction studies were unsuccessful and the formulation of this complex is therefore proposed on the basis of NMR and IR measurements only.

3.5 Halide Abstraction Chemistry of Asymmetric Haloindyl and Halogallyl Complexes

3.5.1 Experimental

Synthesis of $[\{\text{CpFe}(\text{CO})_2\text{InMes}^\}_2(\mu\text{-Br})]^\dagger[\text{BAr}^f_4]^-$ (3.18)*

A solution of **3.7** (0.021 g, 0.034 mmol) in CD_2Cl_2 (2 cm^3) was added to a suspension of $\text{Na}[\text{BAr}^f_4]$ (0.031 g, 0.035 mmol) in CD_2Cl_2 (2 cm^3) at -78°C . The reaction mixture was allowed to warm slowly to room temperature and was sonicated for 30 minutes yielding a yellow solution. ^1H NMR (300 MHz, CD_2Cl_2): δ_{H} 1.18 (s, 18H, *para*-^tBu of Mes*), 1.32 (s, 36H, *ortho*-^tBu of Mes*) 4.81 (s, 10H, CH of Cp) 7.29 (s, 4H, aromatic CH of Mes*), 7.37 (s, *para*-H of $\text{BAr}^f_4^-$), 7.57 (s, *ortho*-H of $\text{BAr}^f_4^-$). ^{13}C NMR (76 MHz, CD_2Cl_2): δ_{C} 31.0 (*para*-^tBu CH_3 of Mes*), 33.6 (*ortho*-^tBu CH_3 of Mes*), 34.9 (*para*-^tBu quaternary C of Mes*), 37.7 (*ortho*-^tBu quaternary C of Mes*), 82.5 (CH of Cp), 117.4 (*para*-CH of $\text{BAr}^f_4^-$), 122.2 (aromatic CH of Mes*), 123.5 (q, $^1J_{\text{CF}} = 273$ Hz, CF_3 of $\text{BAr}^f_4^-$), 128.7 (q, $^2J_{\text{CF}} = 29$ Hz, *meta*-C of $\text{BAr}^f_4^-$), 134.8 (*ortho*-CH of $\text{BAr}^f_4^-$), 151.2 (quaternary aromatic C of Mes*), 155.3 (quaternary aromatic C of Mes*), 161.5 (q, $^1J_{\text{CB}} = 49$ Hz, *ipso*-C of $\text{BAr}^f_4^-$), 212.4 (CO), *ipso* quaternary aromatic not observed. ^{11}B NMR (96 MHz, CD_2Cl_2): δ_{B} -7.6 ($\text{BAr}^f_4^-$). ^{19}F NMR (283 MHz, CD_2Cl_2): δ_{F} -62.7 (CF_3). IR (thin film CD_2Cl_2 , cm^{-1}): $\nu(\text{CO})$ 1968 st, 1977 sh, 2011 st.

Synthesis of $[\text{Cp}^*\text{Fe}(\text{CO})_2\text{InMes}^*\text{f}]^+[\text{BARf}_4^-]$ (3.19)

A solution of **3.8** (0.08 g, 0.117 mmol) in CD_2Cl_2 (15 cm^3) was added dropwise with vigorous stirring to a suspension of $\text{Na}[\text{BARf}_4^-]$ (0.113 g, 0.128 mmol) in CD_2Cl_2 (2 cm^3) at -78°C . The resulting mixture was allowed to warm slowly to room temperature and stirred for 1 h yielding a yellow solution. ^1H NMR (300 MHz, CD_2Cl_2) : δ_{H} 1.16 (s, 9H, *para*-^tBu of Mes*), 1.40 (s, 18H, *ortho*-^tBu of Mes*), 1.81 (15H, s, CH_3 of Cp*), 7.32 (s, 2H, aromatic CH of Mes*), 7.38 (s, *para*-H of BARf_4^-), 7.56 (s, *ortho*-H of BARf_4^-). ^{13}C NMR (76 MHz, CD_2Cl_2) : δ_{C} 10.6 (CH_3 of Cp*), 30.9 (*para*-^tBu CH_3 of Mes*), 31.3 (*ortho*-^tBu CH_3 of Mes*), 34.7 (*para*-^tBu quaternary C of Mes*), 37.8 (*ortho*-^tBu quaternary C of Mes*), 96.8 (quaternary C of Cp*), 117.5 (*para*-CH of BARf_4^-), 122.7 (aromatic CH of Mes*), 123.7 (q, $^1J_{\text{CF}} = 270$ Hz, CF_3 of BARf_4^-), 128.5 (q, $^2J_{\text{CF}} = 24$ Hz, *meta*-C of BARf_4^-), 134.8 (*ortho*-CH of BARf_4^-), 150.1 (quaternary aromatic C of Mes*), 155.9 (quaternary aromatic C of Mes*), 161.5 (q, $^1J_{\text{CB}} = 53$ Hz, *ipso*-C of BARf_4^-), 212.5 (CO), *ipso* quaternary aromatic not observed. ^{11}B NMR (96 MHz, CD_2Cl_2) : δ_{B} -7.6 (BARf_4^-). ^{19}F NMR (283 MHz, CD_2Cl_2) : δ_{F} -62.7 (CF_3). IR (thin film CD_2Cl_2 , cm^{-1}) : $\nu(\text{CO})$ 1965 st, 2006 st.

Synthesis of $[\{\text{Cp}^*\text{Fe}(\text{CO})_2\text{InMes}^*\}_2(\mu\text{-Br})]^+[\text{BARf}_4^-]$ (3.20)

A solution of **3.8** (0.022 g, 0.031 mmol) in CD_2Cl_2 (2 cm^3) was added to a suspension of $\text{Na}[\text{BARf}_4^-]$ (0.035 g, 0.039 mmol) in CD_2Cl_2 (0.5 cm^3) at -78°C . The resulting mixture was allowed to warm slowly to room temperature and was sonicated for 30 minutes yielding a yellow-orange solution. ^1H NMR (300 MHz, CD_2Cl_2) : δ_{H} 1.24 (s, 9H, *para*-^tBu of Mes*), 1.30 (s, 18H, *ortho*-^tBu of Mes*), 1.79 (15H, CH_3 of Cp*), 7.35 (s, 4H, aromatic CH of Mes*), 7.49 (s, 4H, *para*-H of BARf_4^-), 7.64 (s, 8H, *ortho*-H of BARf_4^-). ^{13}C NMR (76 MHz, CD_2Cl_2) : δ_{C} 9.6 (CH_3 of Cp*), 30.5 (*para*-^tBu CH_3

of Mes*), 32.0 (*ortho*-^tBu CH₃ of Mes*), 34.1 (*para*-^tBu quaternary C of Mes*), 37.1 (*ortho*-^tBu quaternary C of Mes*), 94.9 (quaternary C of Cp*), 118.6 (*para*-CH of BARf₄⁻), 122.8 (CH aromatic of Mes*), 124.9 (q, ¹J_{CF} = 270 Hz, CF₃ of BARf₄⁻), 128.3 (q, ²J_{CF} = 24 Hz, *meta*-C of BARf₄⁻), 134.1 (*ortho*-CH of BARf₄⁻), 150.4 (quaternary aromatic C of Mes*), 154.7 (quaternary aromatic C of Mes*), 161.2 (q, ¹J_{CB} = 53 Hz, *ipso*-C of BARf₄⁻), 213.3 (CO), *ipso* quaternary aromatic not observed. ¹¹B NMR (96 MHz, CD₂Cl₂) : δ_B -6.6 (BARf₄⁻). ¹⁹F NMR (283 MHz, CD₂Cl₂) : δ_F -62.8 (CF₃). IR (thin film CD₂Cl₂, cm⁻¹) : ν(CO) 1964 st, 1982 sh, 2004 st.

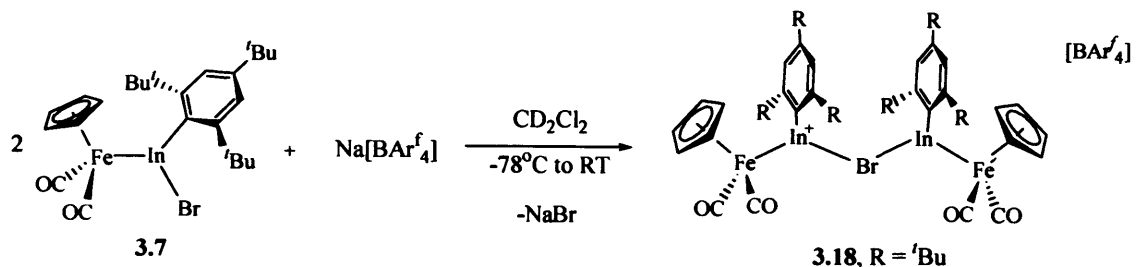
Reaction of Cp*Fe(CO)₂Ga(Mes*)Cl with Na[BARf₄]

A solution of Cp*Fe(CO)₂Ga(Mes*)Cl (0.019 g, 0.032 mmol) dissolved in CD₂Cl₂ (12 cm³) was added to slurry of Na[BARf₄] (0.032 g, 0.035 mmol) in CD₂Cl₂ (2 cm³) dropwise at room temperature over a period of 25 min. The resulting orange solution was stirred for a further 20 min, filtered, and layered with hexanes. A small number of crystals suitable for X-ray diffraction were obtained from a layering of a CD₂Cl₂ solution with hexanes at -30°C. The compound revealed a cluster species [{Cp*Fe(CO)₂Ga}₄F₆][Cp*Fe(CO)₂][BARf₄]₃ (**3.24**).

3.5.2 Results and Discussion

We have sought to utilise halide abstraction chemistry on a range of three-coordinate asymmetric halo-indium and halo-gallium substrates, with a view to exploiting this methodology in the synthesis of two-coordinate heavier group 13 diyl species. Addition of the asymmetric bromoindyl complex CpFe(CO)₂In(Mes*)Br **3.7** to a suspension of Na[BARf₄] in dichloromethane at -78°C generates the bromo-bridged dinuclear species [{CpFe(CO)₂In(Mes*)}₂(μ-Br)]⁺[BARf₄]⁻ **3.18**. Further

investigations revealed that **3.18** is formed irrespective of the reaction stoichiometry, timescale or order of reagent addition (Scheme 3.9) used in the synthesis.

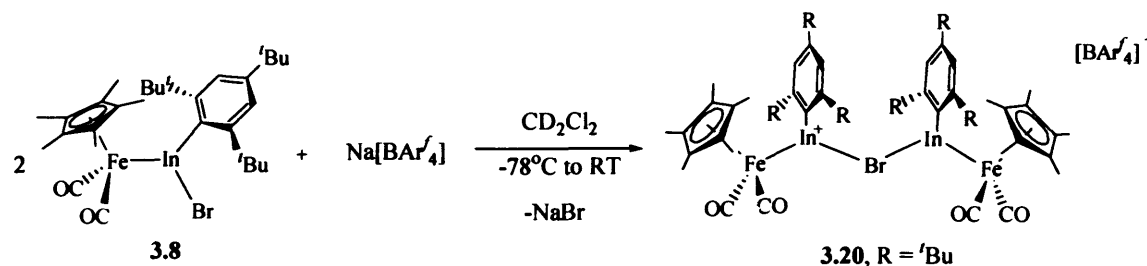


Scheme 3.9 Synthetic route to complex **3.18**.

Analogous reactivity behaviour has been demonstrated by Aldridge *et al.* in the synthesis of the chloride-bridged complex $[\{\text{CpFe(CO)}_2\text{Ga}(\text{Mes}^*)\}_2(\mu\text{-Cl})]^+[\text{BArf}_4]^-$ **3.21** from the analogous reaction of $\text{CpFe(CO)}_2\text{Ga}(\text{Mes}^*)\text{Cl}$ with $\text{Na}[\text{BArf}_4]$.¹⁶ **3.18** presumably results from the trapping of the highly electrophilic first-formed intermediate species $[\text{CpFe(CO)}_2\text{In}(\text{Mes}^*)]^+$ by a second equivalent of the bromoindyl starting material. The formulation of **3.18**, is implied by ¹H NMR monitoring of the reaction in dichloromethane-*d*₂, which reveals a 2:1 ratio of the Cp and $[\text{BArf}_4]^-$ moieties. In addition, IR measured carbonyl stretching frequencies are consistent with the expected shifts to higher wavenumbers on formation of the cationic CpFe(CO)_2 containing product (2011, 1977, 1968 vs 1995, 1945 cm^{-1} for **3.18** and **3.7** respectively). Unfortunately, attempts to grow single crystals of **3.18** suitable for X-ray diffraction studies were unsuccessful and the formulation of this complex is therefore proposed on the basis of NMR, IR spectroscopic results and comparison of data with the structurally authenticated gallium analogue. Given that the molecular structure of $[\{\text{CpFe(CO)}_2\text{Ga}(\text{Mes}^*)\}_2(\mu\text{-Cl})]^+[\text{BArf}_4]^-$ **3.21** was confirmed

crystallographically, the spectroscopic similarities between **3.18** and **3.21** imply a similar In-Br-In bridged structure for **3.18**.

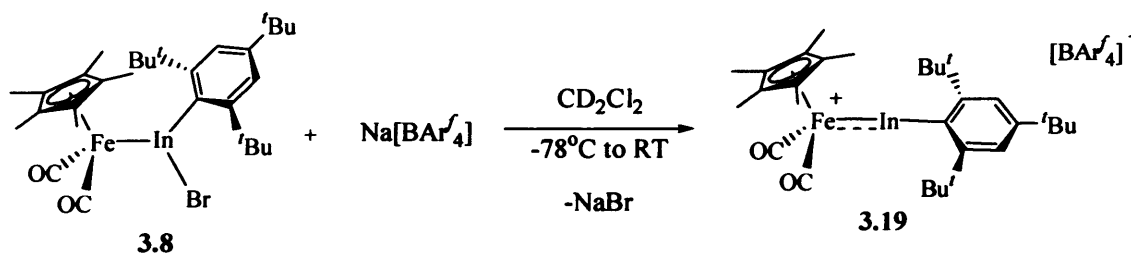
Reaction of the pentamethylcyclopentadienyl complex $\text{Cp}^*\text{Fe}(\text{CO})_2\text{In}(\text{Mes}^*)\text{Br}$ **3.8** with $\text{Na}[\text{BARf}_4]$ in dichloromethane was also investigated with the view that the greater steric bulk provided by the Cp^* moiety would prevent the formation of the bridging species. It was found that varying the reaction conditions led to the formation of different products, *i.e.* depending on conditions products formulated spectroscopically as either the bridged $[\{\text{Cp}^*\text{Fe}(\text{CO})_2\text{In}(\text{Mes}^*)\}_2(\mu\text{-Br})]^+[\text{BARf}_4]^-$ **3.20** or (tentatively) as the terminal indylene $[\text{Cp}^*\text{Fe}(\text{CO})_2\text{In}(\text{Mes}^*)]^+[\text{BARf}_4]^-$ **3.19** could be detected. When insufficient mixing of reactants was employed (*i.e.* when performing the reaction in a Young's NMR tube, with no stirring on addition of reactants) the bridged complex $[\{\text{Cp}^*\text{Fe}(\text{CO})_2\text{In}(\text{Mes}^*)\}_2(\mu\text{-Br})]^+[\text{BARf}_4]^-$ **3.20** was generated in a similar fashion to the corresponding Cp complex **3.18** (Scheme 3.10). ^1H NMR monitoring of the reaction in dichloromethane- d_2 , reveals a 2:1 ratio of Cp^* and $[\text{BARf}_4]^-$ moieties. Presumably **3.20** forms in an analogous fashion to that proposed for **3.18** and **3.21**, by trapping of cationic $[\text{Cp}^*\text{Fe}(\text{CO})_2\text{In}(\text{Mes}^*)]^+$ by $\text{Cp}^*\text{Fe}(\text{CO})_2\text{In}(\text{Mes}^*)\text{Br}$.



Scheme 3.10 Synthetic route to complex **3.20**.

Unfortunately, attempts to grow single crystals of **3.20** suitable for X-ray diffraction studies were unsuccessful and the formulation of this complex is therefore proposed on the basis of NMR, IR spectroscopic results and comparison with $[\{\text{CpFe}(\text{CO})_2\text{Ga}(\text{Mes}^*)\}_2(\mu\text{-Cl})]^+[\text{BARf}_4]^-$ **3.21** and **3.18**.

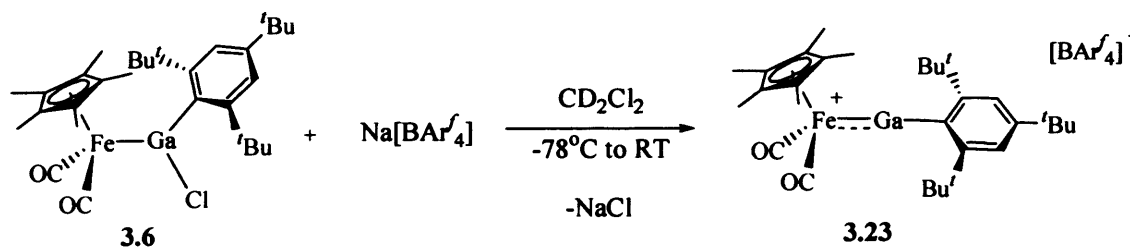
Conversely, when more efficient mixing methods (*i.e.* with vigorous stirring of reactants on addition) and dilute reactant concentrations were employed an indium complex of apparent stoichiometry $[\text{Cp}^*\text{Fe}(\text{CO})_2\text{In}(\text{Mes}^*)]^+[\text{BARf}_4]^-$ **3.19** was formed (Scheme 3.11).



Scheme 3.11 Synthetic route to complex **3.19**.

The formulation of **3.19** is implied by ^1H NMR monitoring of the reaction in dichloromethane- d_2 , which reveals a 1:1 ratio of Cp^* and $[\text{BARf}_4]^-$ moieties. In addition, carbonyl stretching frequencies measured by IR are consistent with the formation of a cationic complex with shifts to higher wavenumbers (**3.19**, 1965 and 2006 cm^{-1} , **3.8**, 1928 and 1977 cm^{-1}). Unfortunately, attempts to grow single crystals of **3.19** suitable for X-ray diffraction studies were unsuccessful and the formulation of this complex is therefore tentatively proposed on the basis of NMR spectroscopic results.

The halide abstraction chemistry of $\text{Cp}^*\text{Fe}(\text{CO})_2\text{Ga}(\text{Mes}^*)\text{Cl}$ **3.6** has been previously investigated by Aldridge *et al.*¹⁶ It was demonstrated that depending on the reaction conditions the products formulated as either $[\{\text{Cp}^*\text{Fe}(\text{CO})_2\text{Ga}(\text{Mes}^*)\}_2(\mu\text{-Cl})]^+[\text{BARf}_4]^-$ (**3.22**) or $[\text{Cp}^*\text{Fe}(\text{CO})_2\text{GaMes}^*]^+[\text{BARf}_4]^-$ (**3.23**) could be formed, with **3.22** having been structurally characterised. We sought to further examine this chemistry by varying the reaction and crystallisation conditions employed with the aim of structurally characterising the cationic complex $[\text{Cp}^*\text{Fe}(\text{CO})_2\text{GaMes}^*]^+$. Addition of the asymmetric (halo)gallyl species $\text{Cp}^*\text{Fe}(\text{CO})_2\text{Ga}(\text{Mes}^*)\text{Cl}$ **3.6** to a suspension of $\text{Na}[\text{BARf}_4]$ in dichloromethane- d_2 at -78°C yielded a gallium complex of the apparent stoichiometry $[\text{Cp}^*\text{Fe}(\text{CO})_2\text{Ga}(\text{Mes}^*)]^+[\text{BARf}_4]^-$ **3.23**, as evident by ^1H NMR monitoring of the reaction revealing a 1:1 ratio of the Cp^* and $[\text{BARf}_4]^-$ moieties (Scheme 3.12). In addition the IR-measured carbonyl stretching frequencies are consistent with the proposed formulation of a cationic complex featuring increased metal-ligand bond order with shifts to higher wavenumbers ($[\text{Cp}^*\text{Fe}(\text{CO})_2\text{Ga}(\text{Mes}^*)]^+[\text{BARf}_4]^-$ **3.23**, 2019 and 1998 cm^{-1} compared to $\text{Cp}^*\text{Fe}(\text{CO})_2\text{Ga}(\text{Mes}^*)\text{Cl}$ **3.6**, 1983, 1931 cm^{-1} and $[\{\text{Cp}^*\text{Fe}(\text{CO})_2\text{Ga}(\text{Mes}^*)\}_2(\mu\text{-Cl})]^+[\text{BARf}_4]^-$ **3.22** 1996, 1986, 1954 and 1932 cm^{-1}).



Scheme 3.12 Synthetic route to complex **3.23**.

A small quantity of single crystals suitable for X-ray diffraction were obtained by layering a concentrated solution of **3.23** with hexanes at -30°C . However, the compound so obtained was not **3.23**, but a cluster species (**3.24**) featuring the $[\{\text{Cp}^*\text{Fe}(\text{CO})_2\text{Ga}\}_4\text{F}_6]^{2+}$ cation, which presumably results from fluoride abstraction from the $[\text{BAr}^f_4]^-$ anion. Similar reactivity towards this anion, giving rise to mono- and difluoroboryl ligands, has been reported for similar, highly reactive putative borylene complexes of the type $[(\eta^5\text{-C}_5\text{R}_5)\text{Fe}(\text{CO})_2(\text{BOAr})]^+$.¹⁷ The structure of the dicationic component of **3.24** is illustrated in Figure 3.5.

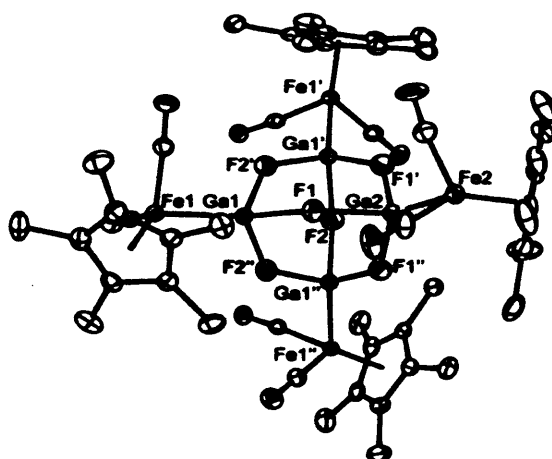


Figure 3.5 The molecular structure of the dicationic component of **3.24**.

3.6 Trapping Reactions

3.6.1 Experimental

Synthesis of $[\{\text{Cp}^\text{Fe}(\text{CO})_2\text{In}(\text{Mes}^*)\}_2(\mu\text{-F})]^+[\text{BF}_4]^-$ (**3.25**)*

A mixture of **3.8** (0.050 g, 0.073 mmol) and 4-picoline (0.010 cm^3 , 0.103 mmol) in CD_2Cl_2 (3 cm^3) was added to a slurry of $\text{Ag}[\text{BF}_4]$ (0.014 g, 0.072 mmol) in CD_2Cl_2 (0.5 cm^3) at -78°C under the exclusion of light. The reaction mixture was allowed to warm to room temperature and sonicated for 1 h. The resulting yellow solution was decanted, concentrated (to *ca.* 1 cm^3) and layered with hexanes. Crystals of

$[\{\text{Cp}^*\text{Fe}(\text{CO})_2\text{In}(\text{Mes}^*)\}_2(\mu\text{-F})]^+[\text{BF}_4]^-$ **3.25** were obtained from the layered solution at -30°C . Isolated yield 0.010 g, 35 %. ^1H (300 MHz, CD_2Cl_2): δ_{H} 1.24 (s, 36H, *ortho*-^tBu of Mes*), 1.84 (s, 18H, *para*-^tBu of Mes*), 1.90 (s, 30H, CH_3 of Cp*), 7.16 (s, 2H, CH of Mes*). ^{13}C (76 MHz, CD_2Cl_2): δ_{C} 11.2 (CH_3 of Cp*), 31.4 (*para*-^tBu quaternary carbon of Mes*), 31.7 (*para*-^tBu CH_3 of Mes*), 34.1 (*ortho*-^tBu quaternary carbon of Mes*), 35.2 (*ortho*-^tBu CH_3 of Mes*), 94.9 (quaternary carbon of Cp*), 119.8 (*meta*-CH of Mes*), 150.5 (*para*-quaternary carbon of Mes*), 157.2 (*ortho*-quaternary carbon of Mes*), 218.1 (CO). ^{19}F (283 MHz, CD_2Cl_2): δ_{F} -57.5 (b, $\mu\text{-F}$), -154.1 (BF_4^-). ^{11}B (96 MHz, CD_2Cl_2): δ_{B} 2.2 (BF_4^-). IR (thin film CD_2Cl_2 , cm^{-1}): $\nu(\text{CO})$ 1937 st, 1988 st.

Synthesis of $[\text{Cp}^*\text{Fe}(\text{CO})_2\text{In}(\text{Mes}^*)(4\text{-pic})]^+[\text{BAr}^f_4]^-$ (3.26)

To a solution of **3.8** (0.051 g, 0.07 mmol) in CD_2Cl_2 (3 cm^3) was added 4-picoline (0.010 cm^3 , 0.1 mmol), the reaction mixture was then added to a slurry of $\text{Na}[\text{BAr}^f_4]$ (0.071 g, 0.08 mmol) in CD_2Cl_2 (0.5 cm^3) at -78°C , warmed to room temperature and sonicated for 30 mins. ^1H (300 MHz, CD_2Cl_2): δ_{H} 1.28 (s, 9H, *para*-^tBu of Mes*), 1.37 (s, 18H, *ortho*-^tBu of Mes*), 1.83 (s, 15H, CH_3 of Cp*), 2.35 (s (b), 3H, CH_3 of 4-pic), 7.40 (s, 2H, aromatic CH of 4-pic), 7.46 (s, 4H, $\text{BAr}^f_4^-$), 7.50 (s, 2H, aromatic CH of 4-pic), 7.63 (s, 8H, $\text{BAr}^f_4^-$). ^{19}F (283 MHz, CD_2Cl_2): δ_{F} -62.9 . ^{11}B (96 MHz, CD_2Cl_2): δ_{B} -8.4 . IR (thin film CD_2Cl_2 , cm^{-1}): $\nu(\text{CO})$ 1937 st, 1984 st.

Reaction of $\text{Cp}^*\text{Fe}(\text{CO})_2\text{Ga}(\text{Mes})\text{I}$ with 4-picoline and $\text{Na}[\text{BAr}^f_4]$: Synthesis of $[\text{Cp}^*\text{Fe}(\text{CO})_2\text{Ga}(\text{Mes})(4\text{-pic})_2]^+[\text{BAr}^f_4]^-$ (3.27)

To a solution of **3.10** (0.050 g, 0.09 mmol) in CD_2Cl_2 (3 cm^3) was added 4-picoline (0.08 cm^3 , 0.09 mmol), the reaction mixture was then added to a slurry of $\text{Na}[\text{BAr}^f_4]$

(0.078 g, 0.09 mmol) in CD_2Cl_2 (0.5 cm^3) at -78°C , warmed to room temperature and sonicated for 30 min. ^1H (300 MHz, CD_2Cl_2): δ_{H} 1.72 (s, 15H, CH_3 of Cp^*), 1.90 (s, 6H, CH_3 of 4-pic), 2.15 (s, 3H, *para*- CH_3 of Mes), 2.21 (s, 6H, *ortho*- CH_3 of Mes), 7.28 (s, 4H, *meta*-aromatic CH of 4-pic), 7.42 (s, 4H, CH of BAr_4^-), 7.59 (s, 8H, CH of BAr_4^-), 8.07 (s, 4H, *ortho*-aromatic CH of 4-pic). ^{19}F (283 MHz, CD_2Cl_2): δ_{F} -62.9. ^{11}B (96 MHz, CD_2Cl_2): δ_{B} -8.4. IR (thin film CD_2Cl_2 , cm^{-1}): $\nu(\text{CO})$ 1919 st, 1928 sh, 1973 st, 1982 sh.

Synthesis of $[\text{Cp}^\text{Fe}(\text{CO})_2\text{Ga}(\text{dtbpy})(\text{Mes})][\text{BAr}_4^-]$ (3.28)*

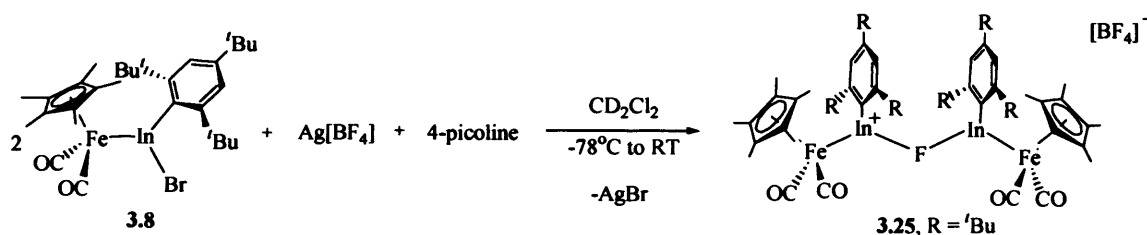
A solution of **3.10** (0.094 g, 0.167 mmol) and dtbpy (0.045 g, 0.168 mmol) in CD_2Cl_2 (3 cm^3) was added to a slurry of $\text{Na}[\text{BAr}_4^-]$ (0.147 g, 0.166 mmol) in CD_2Cl_2 (1 cm^3) at -78°C , and the reaction mixture warmed to room temperature. After sonication for 30 min., the resulting orange solution was layered with hexanes yielding single crystals suitable for X-ray diffraction. Isolated yield 0.080 g, 31 %. ^1H (300 MHz, CD_2Cl_2): δ_{H} 1.34 (s, 18H, ^tBu of dtbpy), 1.76 (s, 15H, CH_3 of Cp^*), 2.07 (s, 3H, *para*- CH_3 of Mes), 2.30 (s, 6H, *ortho*- CH_3 of Mes), 6.66 (s, 2H, CH of Mes), 7.46 (s, 4H, *para*-CH of BAr_4^-), 7.62 (s, 8H, *ortho*-CH of BAr_4^-), 7.72, 8.16, 8.75 (m, each 2H, CH of dtbpy). ^{13}C (76 MHz, CD_2Cl_2): δ_{C} 10.2 (Me of Cp^*), 20.3 (*para*- CH_3 of Mes), 26.2 (*ortho*- CH_3 of Mes), 29.8 (^tBu CH_3 of dtbpy), 36.1 (^tBu quaternary carbon of dtbpy), 95.5 (quaternary carbon of Cp^*), 117.3 (CH of dtbpy), 117.4 (*para*-CH of BAr_4^-), 119.5 (CH of dtbpy), 122.7 (q, $^1J_{\text{CF}} = 273 \text{ Hz}$, CF_3 of BAr_4^-), 124.7 (CH of dtbpy), 126.7 (quaternary carbon of dtbpy), 128.6 (q, $^2J_{\text{CF}} = 29 \text{ Hz}$, *meta*-carbon of BAr_4^-), 134.8 (*ortho*-CH of BAr_4^-), 138.5 (*ortho*-quaternary carbon of Mes), 142.8 (*meta*-CH of Mes), 154.3 (*para*-quaternary carbon of Mes), 147.8 (quaternary carbon of dtbpy), 161.2 (q, $^1J_{\text{CB}} = 49 \text{ Hz}$, *ipso*-carbon of BAr_4^-), 168.2 (*ipso*-carbon of Mes),

217.2 (CO). ^{19}F (283 MHz, CD_2Cl_2): δ_{F} -62.9. ^{11}B (96 MHz, CD_2Cl_2): δ_{B} -8.4. IR (thin film CD_2Cl_2 , cm^{-1}): $\nu(\text{CO})$ 1919 st, 1938 sh, 1971 st, 1999 sh. ES-MS, m/z : (10 V cone voltage) 703.2 {100 %, $[\text{Cp}^*\text{Fe}(\text{CO})_2\text{Ga}(\text{Mes})(\text{dtbpy})]^+$ }; (50 V cone voltage) 703.2 {35 %, $[\text{Cp}^*\text{Fe}(\text{CO})_2\text{Ga}(\text{Mes})(\text{dtbpy})]^+$ }, 435.0 {100 %, $[\text{Cp}^*\text{Fe}(\text{CO})_2\text{Ga}(\text{Mes})]^+$ }. Exact mass: calc. for $[\text{Cp}^*\text{Fe}(\text{CO})_2\text{Ga}(\text{Mes})(\text{dtbpy})]^+$ 701.2519, meas. 701.2518.

3.6.2 Results and Discussion

Ogino *et al.* have previously demonstrated the use of base stabilisation in the isolation/trapping of highly reactive systems. It was reported that abstraction of chloride within $\text{K}[\{\text{Cp}^*\text{Fe}(\text{CO})_2\}(\mu\text{-GaCl})\{\text{Fe}(\text{CO})_4\}]$ was only possible in the presence of bpy yielding the base stabilised species $[\{\text{Cp}^*\text{Fe}(\text{CO})_2\}(\mu\text{-Ga'bpy})\{\text{Fe}(\text{CO})_4\}]$ **3.29**.¹⁸ Previous halide abstraction attempts in the absence of base stabilisation led only to decomposition. Thus, due to the highly reactive nature of the low coordinate indium and gallium complexes targeted, and the lack of success in isolating such compounds in base-free form (as discussed in Section 3.5.2) a series of trapping reactions were investigated with the aim of stabilising the cationic species as nitrogen base adducts.

Addition of a mixture of **3.8** and 4-picoline to a suspension of $\text{Ag}[\text{BF}_4]$ in dichloromethane- d_2 at -78°C yielded the fluoride bridged complex $[\{\text{Cp}^*\text{Fe}(\text{CO})_2\text{In}(\text{Mes}^*)_2(\mu\text{-F})\}][\text{BF}_4]$ **3.25** (Scheme 3.13). Presumably **3.25** was formed by abstraction of fluoride from $[\text{BF}_4]^-$ anion by the highly reactive indium species $[\text{Cp}^*\text{Fe}(\text{CO})_2\text{In}(\text{Mes}^*)]^+$ or by exchange of F^- with 4-picoline in the base-stabilised species.



Scheme 3.13 Synthetic route to complex **3.25**.

^1H and ^{13}C NMR data and carbonyl stretching frequencies (1988, 1937 and 1977, 1928 cm^{-1} , for **3.25** and **3.8** respectively) are consistent with the formation of a cationic species. ^1H NMR monitoring of the reaction in dichloromethane- d_2 reveals a 6:3:5 ratio of the *ortho*- $t\text{Bu}$, *para*- $t\text{Bu}$, and Cp* moieties respectively and ^{13}C NMR data reveals signals corresponding to the CO and Cp* fragments. Single crystals of **3.25** suitable for X-ray diffraction were obtained by cooling a concentrated solution of the complex in hexanes to -30°C . The fluoride-bridged structure of **3.25** is illustrated in Figure 3.6; relevant bond lengths and angles for are listed in Table 3.5.

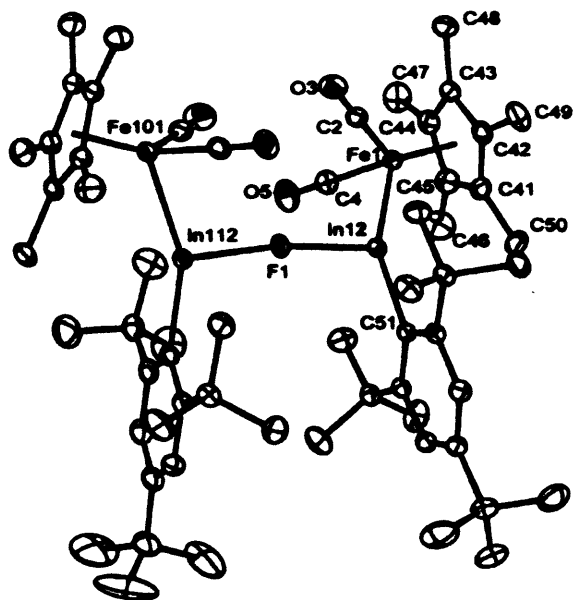


Figure 3.6 The molecular structure of the cationic component of

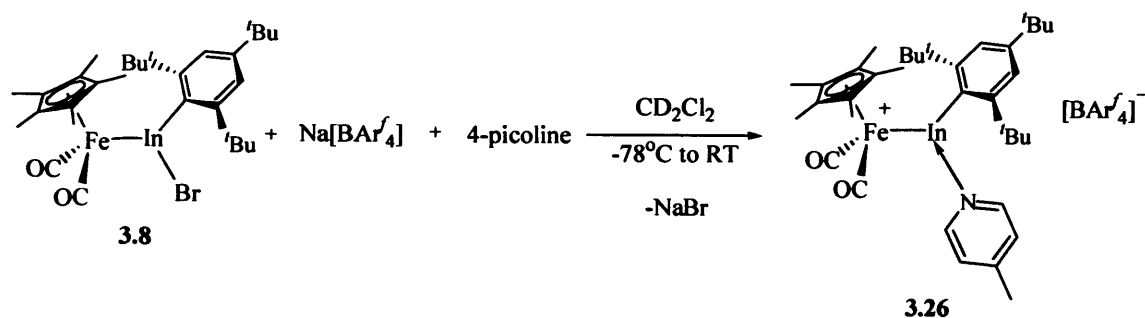


Table 3.5 Selected bond lengths [Å] and angles [°] for **3.25**.

F(1)-In(12)	2.1674(18)	Fe(1)-In(112)	2.4740(5)
C(2)-O(3)	1.148(4)	C(2)-Fe(1)	1.755(3)
In(12)-C(51)	2.154(3)	In(112)-F(1)	2.1637(18)
In(112)-F(1)-In(12)	171.28(11)	Fe(1)-In(12)-F(1)	106.41(6)
C(2)-Fe(1)-C(4)	96.31(17)	Fe(1)-In(12)-C(51)	153.75(8)
O(3)-C(2)-Fe(1)	178.0(3)	C(51)-In(12)-F(1)	99.81(10)
In(12)-C(51)-C(52)	120.8(2)	Fe(101)-In(112)-F(1)	103.74(5)

This confirms the highly reactive nature of the $[\text{BF}_4]^-$ anion, as the putative two-coordinate species $[\text{Cp}^*\text{Fe}(\text{CO})_2\text{In}(\text{Mes}^*)]^+$ appears to more readily abstract a fluoride ion from $[\text{BF}_4]^-$ even in the presence of a coordinating nucleophile such as picoline. Conceivably such a result is reflective of the unusually strong B-F bond.¹⁹ It was thus concluded that $\text{Ag}[\text{BF}_4]$ is not a suitable abstracting agent, as the $[\text{BF}_4]^-$ anion is simply too reactive; a more weakly coordinating counter-ion such as $[\text{BAr}^f_4]^-$ is therefore required.

Trapping reactions of $\text{Cp}^*\text{Fe}(\text{CO})_2\text{In}(\text{Mes}^*)\text{Br}$ **3.8** and $\text{Cp}^*\text{Fe}(\text{CO})_2\text{Ga}(\text{Mes})\text{I}$ **3.10** were investigated with a range of nucleophiles using $\text{Na}[\text{BAr}^f_4]$ as the halide abstracting agent. The 4-picoline coordinated complex $[\text{Cp}^*\text{Fe}(\text{CO})_2\text{In}(\text{Mes}^*)(4\text{-pic})]^+[\text{BAr}^f_4]^-$ **3.26** was prepared by addition of a mixture of **3.8** and excess 4-picoline to a suspension of $\text{Na}[\text{BAr}^f_4]$ in dichloromethane- d_2 at -78°C followed by warming to 20°C (Scheme 3.14).



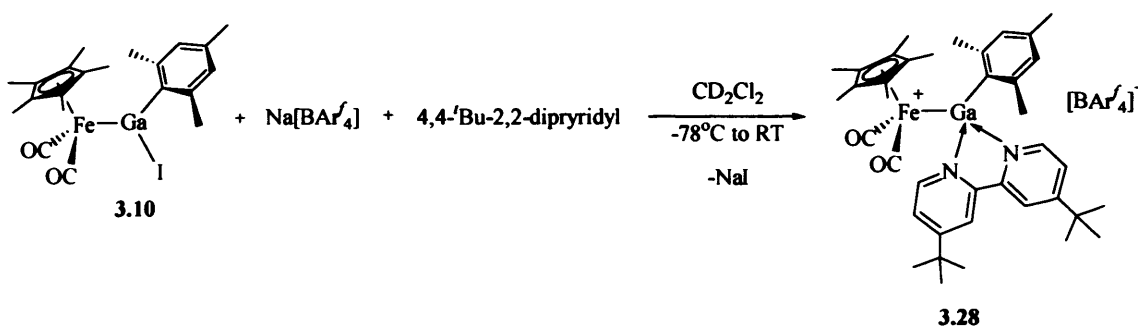
Scheme 3.14 Synthetic route to complexes **3.26**.

The formation of **3.26** was evident by ^1H NMR monitoring of the reaction in dichloromethane- d_2 . Unfortunately, attempts to grow single crystals of **3.26** suitable for X-ray diffraction were unsuccessful and the formulation of this complex is therefore proposed on the basis of NMR and IR spectroscopic results. The 1:1 stoichiometry of **3.26** is implied by integration of the ^1H NMR signals due to the 4-picoline, Cp*, and Mes* moieties. The measured carbonyl stretching frequencies (1937 and 1984 cm^{-1}) are intermediate between those found for the two-coordinate **3.19** [1965 and 2006 cm^{-1}] and *neutral* three coordinate **3.8** [1928 and 1977 cm^{-1}]; coordination of the nitrogen donor at the group 13 centre is consistent with shifts to lower wavenumbers of **3.26** compared to **3.19**.

Interestingly, reaction of Cp*Fe(CO) $_2$ Ga(Mes)I **3.10** with excess 4-picoline to a suspension of Na[BAr' $_4$] in dichloromethane- d_2 at -78°C warmed to 20°C yielded the species [Cp*Fe(CO) $_2$ Ga(Mes)(4-pic) $_2$] $^+$ [BAr' $_4$] $^-$ **3.27**. The formation of **3.27** was also evident by ^1H NMR monitoring of the reaction in dichloromethane- d_2 . Unfortunately, attempts to grow single crystals of **3.27** suitable for X-ray diffraction were unsuccessful and the formulation of this complex is again proposed on the basis of NMR and IR spectroscopic results. The 1:2 stoichiometry of **3.27** is implied by integration of the ^1H NMR signals due to the Cp*, and Mes moieties compared to 4-

picoline. The measured carbonyl stretching frequencies of **3.27** (1919, 1928, 1973, 1982 cm^{-1}) are also consistent with those found for **3.28** (1919, 1938, 1971, 1999 cm^{-1}) which has been additionally characterized by electrospray mass spectrometry (*vide infra*). The coordination of two 4-picoline fragments in **3.27** is presumably due to the smaller degree of steric protection afforded to the gallium centre by the Mes moiety compared to Mes* fragment in **3.26**.

Trapping investigations using 4,4'-*t*-Bu₂-2,2'-dipyridyl as the Lewis base were examined with the aim of better characterizing the resulting base-stabilised cationic complex. Treatment of Cp*Fe(CO)₂Ga(Mes)I **3.10** with an excess of 4,4'-*t*-Bu₂-2,2'-dipyridyl and Na[BAr^f₄] in dichloromethane yielded [Cp*Fe(CO)₂Ga(Mes)(dtbpy)]⁺[BAr^f₄]⁻ **3.28** (Scheme 3.15),¹¹ in which the nitrogen donors of the *t*-Bu-dipyridyl fragment are presumably coordinated to the gallium centre in a chelating fashion; this reactivity is analogous to that observed by Ogino *et al.* for the cationic gallium species [{Cp*Fe(CO)₂ }₂(μ-Ga'bpy)]⁺[BPh₄]⁻ **3.30**.²⁰



Scheme 3.15 Synthetic route to complex **3.28**.

¹H and ¹³C NMR data and carbonyl stretching frequencies (1919, 1938, 1971, 1999 cm^{-1} **3.28** and, 1931, 1984 cm^{-1} , **3.10** respectively) support the proposed formulation, in which the 1:1 stoichiometry of **3.28** is implied by integration of the ¹H

NMR signals due to the dtbpy, Cp*, and Mes moieties (relative intensities of 18:15:3:6:2:4:8 corresponding to the 'Bu of dtbpy, Cp*, *para*-CH₃ of Mes, *ortho*-CH₃ of Mes, CH of Mes, *para*-CH of BAr^f₄, *ortho*-CH of BAr^f₄ fragments respectively). ¹³C NMR data reveals the presence of a [Cp*Fe(CO)₂] fragment with peaks relating to Cp* and CO. Particularly informative for cationic complexes of this type is electrospray mass spectrometry. Interestingly, at a low ionisation voltage (10 V) a flagpole mass spectrum was obtained in which only the molecular ion was observed, however on increasing the ionisation voltage (50 V) a mixture of the dtbpy compound and free terminal gallylene complex was observed (Figure 3.7).

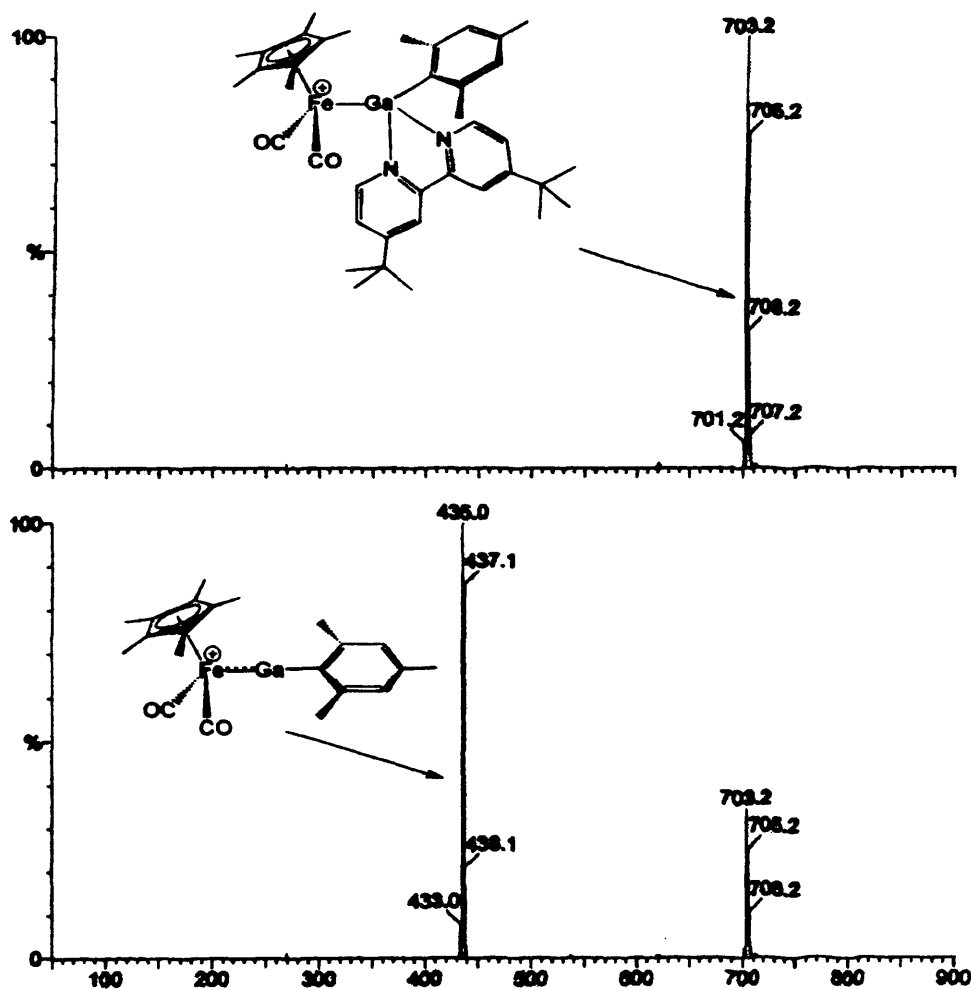


Figure 3.7 electrospray mass spectrometry of $[\{\text{Cp}^*\text{Fe}(\text{CO})_2\}_2(\mu\text{-Ga}^i\text{bpy})]^+[\text{BPh}_4]^-$

Single crystals of **3.28** were obtained from a concentrated solution of the complex layered with hexanes at -30°C , unfortunately this structure could not be solved and the formulation of this complex is therefore proposed on the basis of NMR, IR and mass spectrometric results.

3.7 Conclusions and Suggestions for Further Research

Transition metal species featuring three coordinate asymmetric haloindyl and –gallyl centres represent an important class of precursor complexes which have been implicated in the synthesis of low coordinate cationic group 13 systems.

It has been demonstrated that salt elimination chemistry is a viable synthetic route to the formation of asymmetric haloindyl and –gallyl complexes featuring transition metal fragments. The preparation of $(\eta^5\text{-C}_5\text{R}_5)\text{In}(\text{Mes}^*)\text{Br}$ (**3.7**, $\text{R} = \text{H}$ and **3.8**, $\text{R} = \text{Me}$) can be accomplished in moderate yields *via* salt elimination between the $\text{Mes}^*\text{InBr}_2$ species and $\text{Na}[(\eta^5\text{-C}_5\text{R}_5)\text{Fe}(\text{CO})_2]$ ($\text{R} = \text{H}, \text{Me}$). Furthermore, it has been shown that a two-step insertion/substitution pathway to asymmetric halogallyl species is also viable and $\text{Cp}^*\text{Fe}(\text{CO})_2\text{Ga}(\text{Mes})\text{I}$ **3.10** is readily synthesised by such an approach. Thus, reaction of $[\text{Cp}^*\text{Fe}(\text{CO})_2\text{GaI}_2]_2$ **3.9** with one equivalent of mesityllithium gives selective substitution of one iodide atom yielding $\text{Cp}^*\text{Fe}(\text{CO})_2\text{Ga}(\text{Mes})\text{I}$ **3.10**.

Substitution, abstraction and addition processes have proven to be viable chemistries for the modification of ligand systems featuring the heavier group 13 donors. Thus, substitution of the bromide substituent in $\text{Cp}^*\text{Fe}(\text{CO})_2\text{In}(\text{Br})\text{Mes}^*$ **3.8** can be achieved with retention of the Fe-In bond by reaction with $[\text{OC}_6\text{H}_4\text{Bu-4}]^-$

yielding $\text{Cp}^*\text{Fe}(\text{CO})_2\text{In}(\text{OC}_6\text{H}_4^t\text{Bu-4})\text{Mes}^*$ **3.16**. Structural and spectroscopic comparisons of **3.8** and **3.16** reveal that variation in the steric and/or π donor properties of the indyl ligand substituents have little effect on the nature of the Fe-In bond. Halide abstraction chemistry has shown spectroscopically to yield cationic complexes of the type $[\text{Cp}^*\text{Fe}(\text{CO})_2\text{InMes}^*]^+$ **3.19** and $[\{\text{Cp}^*\text{Fe}(\text{CO})_2\text{InMes}^*\}_2(\mu\text{-Br})]^+$ **3.18** in which the halide bridged species presumably arises by trapping of the highly electrophilic cationic diyl complex. It has been demonstrated that trapping of the low-coordinate cationic systems with two electron donors is also a viable synthetic approach. The net result is substitution of the gallium bound iodide substituent with, for example, the 4,4'- t Bu₂-2,2'-dipyridyl moiety yielding $[(\text{Cp}^*\text{Fe}(\text{CO})_2\text{Ga}(\text{dtbpy})(\text{Mes}))^+[\text{BAr}_4^-]$ **3.28** via a two-step abstraction/addition process.

Attempts to synthesise analogous asymmetric amino halogallyl species via salt elimination proved to be unsuccessful due to the tendency of both chloride atoms within $\text{Ga}(\text{N}(\text{SiMe}_3)_2)\text{Cl}_2\cdot\text{thf}$ to be substituted by the metal fragment yielding $[\{(\eta^5\text{-C}_5\text{R}_5)\text{Fe}(\text{CO})_2\}_2\{\mu\text{-GaN}(\text{SiMe}_3)_2\}]$ (**3.11**, R = H, and **3.12**, R = Me). From these results it was concluded that a more sterically hindered amino group is required to prevent this substitution problem.

Further investigations involve the synthesis of transition metal gallyl systems featuring increased sterically demanding ligands, such as terphenyl ligands, which offer the potential of stabilising the cationic gallylene species on halide abstraction. Utilising other metal fragments in the synthesis of gallyl systems would offer the potential of varying the nature of the cationic gallylene species on halide abstraction.

3.8 References for Chapter Three

1. (a) Cowley, A. H.; Lomeli, V.; Voight, A. *J. Am. Chem. Soc.* **1998**, *120*, 6401. (b) Braunschweig, H.; Kollann, C.; Englert, U. *Angew. Chem. Int. Ed.* **1998**, *37*, 3179. (c) Braunschweig, H.; Colling, M.; Kollann, C.; Stammler, H. G.; Neumann, B. *Angew. Chem. Int. Ed.* **2001**, *40*, 2299. (d) Braunschweig, H.; Colling, M.; Kollann, C.; Merz, K.; Radacki, K. *Angew. Chem. Int. Ed.* **2001**, *40*, 4198. (e) Braunschweig, H.; Colling, M.; Hu, C.; Radacki, K. *Angew. Chem. Int. Ed.* **2003**, *42*, 205. (f) Braunschweig, H.; Colling, M. *Eur. J. Inorg. Chem.* **2003**, 383. (g) Irvine, G. J.; Rickard, C. E. F.; Roper, W. R.; Williamson, A.; Wright, L. J. *Angew. Chem. Int. Ed.* **2000**, *39*, 948. (h) Rickard, C. E. F.; Roper, W. R.; Williamson, A.; Wright, L. J. *Organometallics* **2002**, *21*, 4862. (i) Braunschweig, H. *Adv. Organomet. Chem.* **2004**, *51*, 163.
2. (a) Coombs, D. L.; Aldridge, S.; Jones, C.; Willock, D. J. *J. Am. Chem. Soc.* **2003**, *125*, 6356. (b) Aldridge, S.; Rossin, A.; Coombs, D. L.; Willock, D. J. *Dalton Trans.* **2004**, 2649.
3. (a) Su, J.; Li, X.-W.; Crittendon, R. C.; Campana, C. F.; Robinson, G. H. *Organometallics* **1997**, *16*, 4511. (b) Cotton, F. A.; Feng, X.; *Organometallics*, **1998**, *17*, 128.
4. (a) Jutzi, P.; Neumann, B.; Reumann, G.; Stammler, H.-G. *Organometallics*, **1998**, *17*, 1305. (b) Fischer, R. A.; Schulte, M. M.; Weiss, J.; Zsolnai, L.; Jacobi, A.; Huttner, G.; Frenking, G.; Boehme, C.; Vyboishchikov, S. F. *J. Am. Chem. Soc.* **1998**, *120*, 1237. (c) Reger, D. L.; Garza, D. G.; Rheingold, A. L.; Yap, G. P. A. *Organometallics* **1998**, *17*, 3624. (d) Linti, G.; Köster, W. *Chem. Eur. J.* **1998**, *4*, 942. (e) Uhl, W.; Benter, M.; Melle, S.; Saak, W.; Frenking, G.; Uddin, J. *Organometallics*, **1999**, *18*, 3778. (f) Fölsing, H.; Segnitz, O.; Merz, K.; Winter, M.; Fischer, R. A. *J. Organomet. Chem.* **2000**, *606*, 132. (g) Weiß, W.; Winter, M.; Merz,

K.; Knüfer, A.; Fischer, R. A.; Fröhlich, N.; Frenking, G. *Polyhedron*, **2002**, *21*, 535.

(h) Harman, N. J.; Wright, R. J.; Phillips, A. D.; Power, P. P. *J. Am. Chem. Soc.* **2003**,

125, 2667. (i) Cokoja, M.; Gemel, C.; Steinke, T.; Schröder, F.; Fischer, R. A. *Dalton*

Trans. **2005**, *44*. (j) Steinke, T.; Gemel, M.; Cokoja, M.; Winter, M.; Fischer, R. A.

Dalton Trans. **2005**, *55*. (k) Haubrich, S. T.; Power, P. P. *J. Am. Chem. Soc.* **1998**,

120, 2202.

5. (a) Nugent, W. A.; Mayer, J. M. *Metal Ligand Multiple Bonds*, Wiley-Interscience:

New York, 1988. (b) Hendon, J. W. *Coord. Chem. Rev.* **2003**, *243*, 3.

6. (a) Kays, D. L.; Day, J. K.; Ooi, L.-L.; Aldridge, S. *Angew. Chem. Int. Ed.* **2005**,

44, 7457. (b) Aldridge, S.; Jones, C.; Gans-Eichler, T.; Stasch, A.; Kays (née

Coombs), D. L.; Coombs, N. D.; Willock, D. J. *Angew. Chem. Int. Ed.* **2006**, *45* 6118.

7. Vidovic, D.; Findlater, M.; Reeske, G.; Cowley, A. H. *Chem. Commun.* **2006**,

3786.

8. (a) Aldridge, S.; Coombs, D. L. *Coord. Chem. Rev.* **2004**, *248*, 535. (b) Coombs, D.

L.; Aldridge, S.; Jones, C. *J. Chem. Soc., Dalton Trans.* **2002**, 3851. (c) Ueno, K.

Watanabe, T.; Ogino, H. *Appl. Organomet. Chem.* **2003**, *17*, 403

9. Bunn, N. R.; Aldridge, S.; Kays (née Coombs), D. L.; Coombs, N. D.; Day, J. K.;

Ooi, L.-L.; Coles, S. J.; Hursthouse, M. B. *Organometallics* **2005**, *24*, 5879.

10. (a) Aldridge, A.; Coombs, D. L.; Jones, C. *Chem. Commun.* **2002**, 856. (b)

Coombs, D. L.; Aldridge, S.; Coles, S. J.; Hursthouse, M. B. *Organometallics* **2003**,

22, 4213. (c) Coombs, D. L.; Aldridge, S.; Jones, C. *Appl. Organomet. Chem.* **2003**,

6-7, 356.

11. Coombs, N. D.; Vidovic, D.; Day, J. K.; Thompson, A. L.; Stasch, A.; Clegg, W.;

Russo, L.; Male, L.; Hursthouse, M.B.; Willock, D. J.; Aldridge, S. *submitted*.

12. Bunn, N. R.; Aldridge, S.; Coombs, D. L.; Rossin, A.; Willock, D. J.; Jones, C.; Ooi, L.-L. *Chem. Commun.* **2004**, 1732.

13. Yamaguchi, T.; Ueno, U.; Ogino, H. *Organometallics* **2001**, *20*, 501.

14. Braunschweig, H.; Kollmann, C.; Klinkhammer, K. W. *Eur. J. Inorg. Chem.* **1999**, 1523.

15. Coombs, N. D.; Bunn, N. R.; Kays (née Coombs), D. L.; Day, J. K.; Ooi, L.-L.; Aldridge, S. *Inorganica Chimica Acta* **2006**, *359*, 3693.

16. Bunn, N. R.; Aldridge, S.; Kays, D. L.; Coombs, N. D.; Rossin, A.; Willock, D. J.; Day, J. K.; Jones, C.; Ooi, L.-L. *Organometallics* **2005**, *24*, 5891.

17. Kays (née Coombs), D. L.; Day, J. K.; Aldridge, S.; Harrington, R. W.; Clegg, W. *Angew. Chem. Int. Ed.* **2006**, *45*, 3513.

18. Ueno, K.; Watanabe, T.; Tobita, H.; Ogino, H. *Organometallics* **2003**, *22*, 4375.

19. Greenwood, N. N.; Earnshaw, A. E.; *The Chemistry of the Elements, Second Edition*, Elsevier Butterworth Heinemann: Oxford 1997

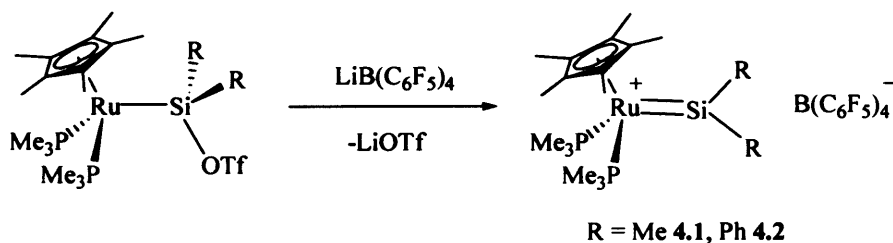
20. Ueno, K.; Watanabe, T.; Ogino, H. *Organometallics* **2000**, *19*, 5679.

Chapter Four

Phosphine Substituted Complexes: Synthesis and Reactivity

4.1 Introduction

In 1990 Tilley *et al.*,¹ reported the synthesis of ruthenium silylene complexes of the type $\text{Cp}^*(\text{PMe}_3)_2\text{Ru}=\text{Si}(\text{SR}_2)^+$ ($\text{R} = \text{Et}, \text{ Tol-}p$), generated *via* abstraction chemistry, in which π -donation from the thiolate substituents stabilises the electrophilic silicon centre. Subsequent work from the same group targeted increased back donation from the metal centre by the use of non π -donor silylene substituents with the aim of increasing the ruthenium to silicon bond order. Thus, abstraction of the silyl-bound triflate group in $\text{Cp}^*(\text{PMe}_3)_2\text{RuSiR}_2(\text{OTf})$ by the use of $\text{LiB}(\text{C}_6\text{F}_5)_4$ resulted in the synthesis of the first base free silylene complexes, $[\text{Cp}^*(\text{PMe}_3)_2\text{Ru}=\text{SiR}_2]^+$ (where $\text{R} = \text{Me}$ 4.1, Ph 4.2), (Scheme 4.1).²



Scheme 4.1 Synthetic route to base-free silylene complexes.

The short Ru-Si bond distance measured for $[\text{Cp}^*(\text{PMe}_3)_2\text{Ru}=\text{SiMe}_2]^+$ (4.1; 2.238(2) Å) was ascribed to a double bond comprised of a $\text{Si} \rightarrow \text{Ru}$ donor/acceptor σ component supplemented by $\text{Ru} \rightarrow \text{Si}$ π back bonding into the vacant Si-based p orbital. It was found that phosphine ancillary ligands at the transition metal

centre were advantageous not only because of the increased electron density at the Ru centre but also because of the increased steric protection. From these results it was concluded that abstraction of a halide or a pseudo-halide (such as triflate) from a complex containing an existing metal-ligand single bond is a viable synthetic route to the formation of cationic complexes featuring increased metal-ligand bond order.

4.1.1 Aims of Research

In view of earlier results reported in this thesis regarding the lability of diyl complexes bearing ancillary carbonyl ligands and with a view, therefore, to maximizing M to E π back-bonding (and hence the degree of multiple bond character) we will target asymmetric precursor complexes of the type $\text{Cp}^*\text{Fe}(\text{PR}_3)_2\text{E}(\text{R})\text{I}$ (where E = Ga, In, R = aryl) in which the transition metal centre features ancillary phosphine ligands. Halide abstraction chemistry will then be investigated with the aim of synthesising cationic two-coordinate complexes of the type $[\text{Cp}^*\text{Fe}(\text{PR}_3)_2\text{ER}]^+$. Asymmetric halogallyl complexes featuring the transition metals molybdenum, iron and ruthenium will also be targeted.

4.2 Phosphine-Iron Containing Systems

4.2.1 Synthesis of Asymmetric Halogallyl Complexes

4.2.1.1 Experimental

Synthesis of $\text{Cp}^\text{Fe}(\text{dppe})\text{GaI}_2$ (4.4)*

To a solution of $[\text{Cp}^*\text{Fe}(\text{CO})_2\text{GaI}_2]_2$ **4.3** (1.414 g, 1.394 mmol) in toluene (100 cm³) was added a solution of dppe (1.110 g, 2.789 mmol) also in toluene (200 cm³), and the reaction mixture photolysed for 86 h. The resulting dark orange solution was filtered, concentrated *in vacuo* and red crystals suitable for X-ray diffraction obtained from a

concentrated toluene solution at -30°C . Isolated yield 0.789 g, 31 %. ^1H NMR (300 MHz, C_6D_6): δ_{H} 1.33 (s, 15H, CH_3 of Cp^*), 2.25 (m, 2H, CH_2), 3.25 (m, 2H, CH_2), 6.95 (m, 8H, CH aromatic), 7.15 (m, 8H, CH aromatic), 7.69 (m, 4H, *para*-CH aromatic). ^{13}C NMR (76 MHz, C_6D_6): δ_{C} 9.4 (CH_3 of Cp^*), 31.6 (dd, $^1J_{\text{PC}} = 15.2$ $^2J_{\text{PC}} = 7.6$ Hz, CH_2 of dppe), 85.2 (quaternary carbon of Cp^*), 127.2 (*meta*-CH of dppe), 127.3 (*meta*-CH of dppe), 127.7 (*para*-CH of dppe), 129.3 (*para*-CH of dppe), 131.6 (*ortho*-CH of dppe), 131.8 (*ortho*-CH of dppe), 141.3 (d, $^1J_{\text{PC}} = 7.60$ Hz, *ipso* carbon of dppe), 141.7 (d, $^1J_{\text{PC}} = 7.60$ Hz, *ipso* carbon of dppe). ^{31}P NMR (122 MHz, C_6D_6): δ_{P} 103.9. EI-MS, m/z : 911.9 {1 %, $[\text{Cp}^*\text{Fe}(\text{dppe})\text{GaI}_2]^+$ }, 716.1 {22 %, $[\text{Cp}^*\text{Fe}(\text{dppe})\text{I}]^+$ }, 589.2 {11 %, $[\text{Cp}^*\text{Fe}(\text{dppe})]^+$ }, 398.2 {100 %, $[\text{dppe}]^+$ }. Exact mass: calc. for $[\text{Cp}^*\text{Fe}(\text{dppe})\text{GaI}_2]^+$ {*i.e.* $[\text{M}]^+$ } 911.9216, meas. 911.9217. Elemental microanalysis: calc for $4.45/4(\text{C}_7\text{H}_8)$ C 52.27, H 4.80; found C 51.91, H 4.35.

Synthesis of $\text{Cp}^*\text{Fe}(\text{CO})(\mu\text{-dppe})\text{GaI}_2$ (4.5), an intermediate in the formation of 4.4

To a solution of 4.3 (1.255 g, 1.237 mmol) in toluene (200 cm^3) was added a solution of dppe (0.986 g, 2.432 mmol) also in toluene (200 cm^3), and the reaction mixture photolysed for 70 h with periodic ^{31}P NMR monitoring (the reaction was determined to be complete when two peaks in the ^{31}P NMR at 65 and -41 were present). The resulting solution was filtered, concentrated *in vacuo* (to *ca.* 15 cm^3), and single crystals suitable for X-ray diffraction obtained by layering a concentrated toluene solution with hexanes. Isolated yield 0.835 g, 35 %. ^1H NMR (300 MHz, CD_2Cl_2): δ_{H} 1.48 (s, 15H, CH_3 of Cp^*), 1.95 (m, 2H, CH_2 of dppe), 2.55 (m, 2H, CH_2 of dppe), 7.10-7.49 (m, 16H, *ortho*- and *meta*-CH of dppe), 7.68, 7.88 (m, each 2H, *para*-CH of dppe). ^{13}C NMR (76 MHz, CD_2Cl_2): δ_{C} 8.7 (CH_3 of Cp^*), 28.1 (dd, $^1J_{\text{PC}} = 15.2$ $^2J_{\text{PC}} = 7.6$ Hz, CH_2 of dppe), 91.0 (quaternary carbon of Cp^*), 124.5 (*meta*-CH of dppe),

127.3 (*meta*-CH of dppe), 128.0 (*para*-CH of dppe), 128.4 (*para*-CH of dppe), 129.5 (*ortho*-CH of dppe), 133.2 (*ortho*-CH of dppe), 134.0 (d, $^1J_{PC} = 7.6$ Hz, *ipso* carbon of dppe), 134.2 (d, $^1J_{PC} = 7.6$ Hz, *ipso* carbon of dppe), CO carbon not observed. ^{31}P NMR (122 MHz, CD_2Cl_2): δ_{P} 65 (Fe-P), -41 (Ga-P). IR (thin film CD_2Cl_2 , cm^{-1}): $\nu(\text{CO})$ 1981 *st.* EI-MS, *m/z*: 939.7 {4 %, $[\text{Cp}^*\text{Fe}(\text{dppe})(\text{CO})\text{GaI}_2]^+$ }, 541.8 {19 %, $[\text{Cp}^*\text{Fe}(\text{CO})\text{GaI}_2]^+$ }, 398.2 {67 %, $[\text{dppe}]^+$ }. Exact mass: calc. for $[\text{Cp}^*\text{Fe}(\text{dppe})(\text{CO})\text{GaI}_2]^+$ {*i.e.* $[\text{M}]^+$ } 939.9165, meas. 939.9169.

*Synthesis of Cp*Fe(dppe)Ga(Mes)I (4.6)*

To a solution/suspension of MesLi (0.036 g, 0.285 mmol) in toluene (25 cm^3) was added a solution of 4.4 (0.150 g, 0.164 mmol) also in toluene (15 cm^3), and the reaction mixture stirred for 16 h at room temperature. The resulting orange solution was filtered, concentrated (to *ca.* 10 cm^3) and 4.6 obtained as an orange microcrystalline material on cooling to -30°C . Crystals suitable for X-ray diffraction were obtained from a concentrated diethyl ether solution at -30°C . Isolated yield 0.114 g, 77 %. ^1H NMR (300 MHz, C_6D_6): δ_{H} 1.42 (s, 15H, CH_3 of Cp*), 2.05 (m, 2H, CH_2 of dppe), 2.10 (s, 6H, *ortho*- CH_3 of Mes), 2.25 (s, 3H, *para*- CH_3 of Mes), 3.95 (m, 2H, CH_2 of dppe), 6.78 (s, 2H, CH of Mes), 7.02 (m, 4H, aromatic CH of dppe), 7.14-7.26 (m, 12H, aromatic CH of dppe), 7.80 (m, 4H, aromatic *para*-CH of dppe). ^{13}C NMR (76 MHz, CD_2Cl_2): δ_{C} 10.3 (CH_3 of Cp*), 20.9 (*ortho*- CH_3 of Mes), 23.5 (*para*- CH_3 of Mes), 30.8 (dd, $^1J_{PC} = 15.2$, $^2J_{PC} = 7.6$ Hz, CH_2 of dppe), 86.4 (quaternary carbon of Cp*), 127.2 (*meta*-CH of dppe), 128.0 (*meta*-CH of dppe), 128.9 (*para*-CH of dppe), 132.5 (*para*-CH of dppe), 133.5 (*ortho*-CH of dppe), 136.3 (*ortho*-CH of dppe), 139.3 (*ortho*-quaternary carbon of Mes), 139.4 (*meta*-CH of Mes), 141.0 (d, $^1J_{PC} = 7.6$ Hz, *ipso* carbon of dppe), 141.5 (d, $^1J_{PC} = 7.6$ Hz, *ipso*

carbon of dppe), 142.5 (*para*-quaternary carbon of Mes). ^{31}P NMR (122 MHz, C_6D_6): δ_{P} 99.0. EI-MS, m/z : 904 {1 %, $\text{M}^+[\text{Cp}^*\text{Fe}(\text{dppe})\text{Ga}(\text{Mes})\text{I}]^+$ }, 777.1 {1 %, $[\text{Cp}^*\text{Fe}(\text{dppe})\text{Ga}(\text{Mes})]^+$ }, 716.0 {4 %, $[\text{Cp}^*\text{Fe}(\text{dppe})\text{I}]^+$ }, 589.2 {9 %, $[\text{Cp}^*\text{Fe}(\text{dppe})]^+$ }, 398.1 {49 %, $[\text{dppe}]^+$ }, 262.1 {42 %, $[\text{Cp}^*\text{FeGa}]^+$ }. Exact mass: calc. for $[\text{Cp}^*\text{Fe}(\text{dppe})\text{Ga}(\text{Mes})\text{I}]^+$ {*i.e.* $[\text{M}]^+$ } 904.1032, meas. 904.1028. Reproducible microanalyses for crystalline samples of **4.4** proved impossible to obtain, possibly due to the presence of diethyl ether within the crystal lattice. **4.6** can also be prepared in an analogous manner using diethyl ether as the reaction solvent. Isolated yield 15 %, 0.34 mmol.

Reaction of $\text{Cp}^\text{Fe}(\text{dppe})\text{GaI}_2$ with $\text{Mes}^*\text{Li}(\text{thf})_2$ attempted synthesis of $(\text{Cp}^*\text{Fe}(\text{dppe}))\text{Ga}(\text{Mes}^*)\text{I}$*

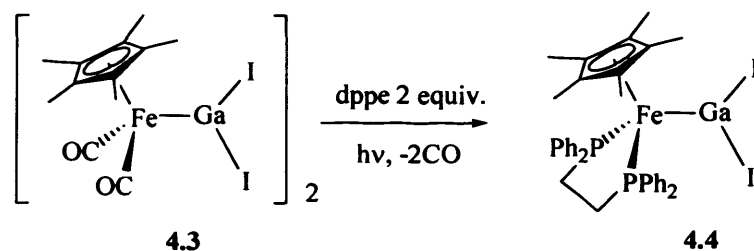
To a solution of $\text{Cp}^*\text{Fe}(\text{dppe})\text{GaI}_2$ (0.151 g) in diethyl ether (50 cm^3) was added a solution/suspension of $\text{Mes}^*\text{Li}(\text{thf})_2$ (0.065 g) in diethyl ether (10 cm^3), the reaction mixture was stirred at room temperature for a further 72 h, ^{31}P NMR monitoring of the solution revealed peaks at δ 104 and 95. Another equivalent of $\text{Mes}^*\text{Li}(\text{thf})_2$ (0.066g) was added and the mixture was stirred at room temperature for a further 12 h; ^{31}P NMR monitoring of the reaction at this point revealed a single peak at δ 95. The solution was filtered and concentrated *in vacuo*, and a portion of the solution was layered with hexanes. The volatiles were removed *in vacuo* from the remaining solution yielding, a brown oil. Unfortunately no tractable phosphine containing compounds were isolated. The analogous reaction of $\text{Cp}^*\text{Fe}(\text{dppe})\text{GaI}_2$ with $\text{Mes}^*\text{Li}(\text{thf})_2$ was also carried using toluene as the reaction solvent, however no tractable phosphine containing compounds were isolated.

4.2.1.2 Results and Discussion

Aldridge *et al.* have previously reported the synthesis of the dimeric species $[\text{Cp}^*\text{Fe}(\text{CO})_2\text{GaI}_2]_2$ **4.3** by a multi-step reaction between $[\text{Cp}^*\text{Fe}(\text{CO})_2]_2$ and 'GaI'.³ Further investigations revealed that **4.3** is not just the simple product of 'GaI' insertion, unlike that reported by Green *et al* for metal halogen bonds.⁴ It was found that at least four equivalents of 'GaI' were required to drive the reaction to completion, and that the reaction mechanism involves initial insertion of 'GaI' into the Fe-Fe bond, yielding $[\text{Cp}^*\text{Fe}(\text{CO})_2]_2\text{GaI}$, followed by halide transfer from a second equivalent of 'GaI' generating half an equivalent each of **4.3** and $[\text{Cp}^*\text{Fe}(\text{CO})_2]_2$ together with one equivalent of gallium metal. Thus half of the original $[\text{Cp}^*\text{Fe}(\text{CO})_2]_2$ is consumed by reaction with two equivalents of 'GaI', and four equivalents of 'GaI' are therefore required to synthesise one equivalent of **4.3**. We have sought to extend this methodology with the aim of substituting the CO ligands at the iron centre within **4.3** for less π acidic ligands such as tertiary phosphines PR_3 , and thereby increase the extent of π back-bonding to the group 13 centre on halide abstraction.

The dppe ligand has previously been shown to offer enhanced electronic and steric protection to the gallium centre in $\text{Cp}^*\text{Fe}(\text{dppe})\text{GaFe}(\text{CO})_4$ **4.7**,⁵ so the synthesis of a halogallyl species featuring an ancillary dppe ligand seemed a logical starting point. The two-step methodology examined during this study involves initial substitution of the CO groups for the chelating phosphine ligand, followed by substitution (at gallium) of a halide by a sterically demanding aryl substituent. Photolysis of the dimer $[\text{Cp}^*\text{Fe}(\text{CO})_2\text{GaI}_2]_2$ **4.3** with two equivalents of dppe proceeds as expected with substitution of both CO groups for the dppe ligand yielding the

complex $[\text{Cp}^*\text{Fe}(\text{dppe})\text{GaI}_2]_n$ (**4.4**) in a moderate yield (31 %) as a dark red microcrystalline solid (Scheme 4.2).⁶



Scheme 4.2 Synthetic route to complex **4.4**.

The ^{31}P NMR chemical shift for **4.4** (δ_{P} 104 ppm) is consistent with a phosphine ligand bound to the iron centre in a chelating fashion. Multinuclear NMR and IR data support the proposed formulation; the ^1H NMR spectrum displays peaks for the Cp^* , methylene and Ph proton signals at chemical shifts of 1.33, 2.25, 3.25, 6.95, 7.15, and 7.69 with relative intensities of 15:2:2:8:8:4 respectively, confirming the formation of a phosphine ligated species. The loss of the CO ligands is revealed in both ^{13}C NMR and IR measurements by the disappearance of features at 213.4 ppm and 2012, 1970 cm^{-1} associated with the dicarbonyl starting material **4.3**. The EI mass spectra display weak peaks for the parent $[\text{M}]^+$ ion, with fragment peaks $[\text{M}-\text{GaI}_2]^+$ also being evident; the isotope distribution is as expected for a complex containing one iron, one gallium, two iodine, and two phosphorus atoms.

As in the case of dimeric $[\text{Cp}^*\text{Fe}(\text{CO})_2\text{GaI}_2]_2$ (**4.3**)³ it is clearly difficult to infer from multinuclear NMR and IR data the state of aggregation of **4.4** in solution or in the solid state. Moreover past experience has shown that even mass spectrometry is not reliable in this regard, due to the ready fragmentation of dimers such as **4.3**

under electron impact ionization conditions. Consequently, definitive assignment of the state of aggregation of **4.4** was dependant on crystallographic data. Single crystals of **4.4** suitable for X-ray diffraction were accessible by cooling a concentrated solution in toluene to -30°C . As a result, the spectroscopic data for **4.4** have been corroborated by single crystal X-ray diffraction studies and the structure illustrated in Figure 4.1. Relevant bond lengths and angles for **4.4** are listed in Table 4.1. The crystal structure confirms that **4.4** exists as monomeric units, $\text{Cp}^*\text{Fe}(\text{dppe})\text{GaI}_2$, in which both phosphorus atoms are bound to the iron centre in a chelating fashion.

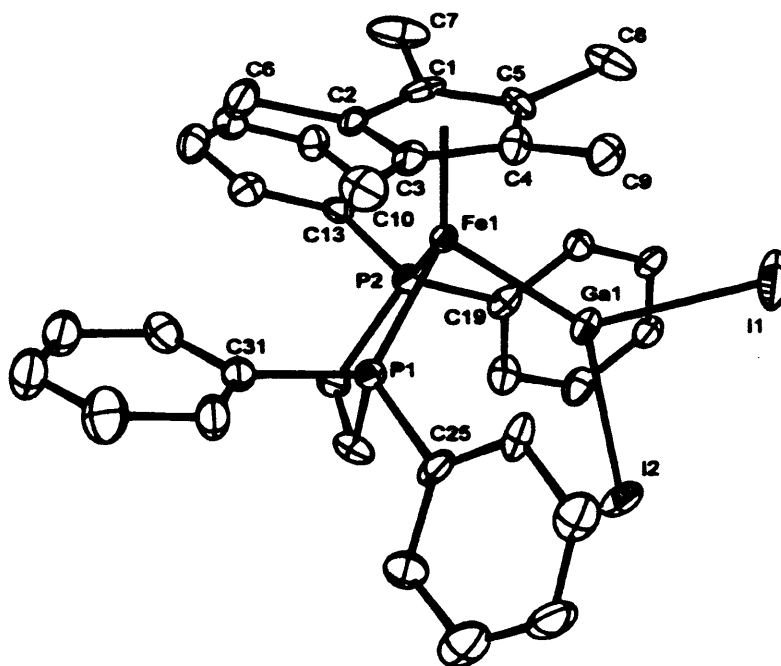


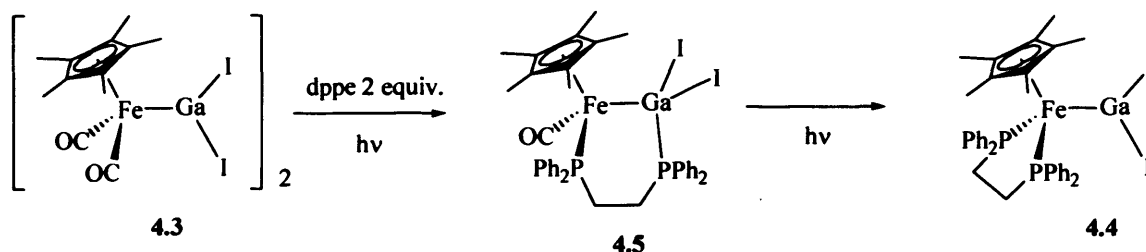
Figure 4.1 The molecular structure of $\text{Cp}^*\text{Fe}(\text{dppe})\text{GaI}_2$ **4.4**.

Table 4.1 Selected bond lengths [Å] and angles [°] for **4.4**.

P(1)-Fe(1)	2.193(2)	Ga(1)-I(2)	2.6323(11)
P(2)-Fe(1)	2.208(2)	C(12)-P(2)	1.848(8)
Fe(1)-Ga(1)	2.3236(14)	C(19)-P(2)	1.851(8)
Ga(1)-I(1)	2.6294(11)	C(11)-C(12)	1.488(12)
C(12)-C(11)-P(1)	109.3(6)	Fe(1)-Ga(1)-I(2)	134.02(5)
P(1)-Fe(1)-P(2)	86.88(9)	I(1)-Ga(1)-I(2)	94.30(4)
Fe(1)-Ga(1)-I(1)	131.67(5)	P(1)-Fe(1)-Ga(1)	88.02(7)

The monomeric nature of $\text{Cp}^*\text{Fe}(\text{dppe})\text{GaI}_2$ **4.4**, contrasts markedly with the dimeric structure of $[\text{Cp}^*\text{Fe}(\text{CO})_2\text{GaI}_2]_2$ **4.3**.³ This failure to aggregate presumably arises as a result of the greater steric bulk of the dppe ligand compared to 2 CO moieties. The coordination geometry about the gallium centre is approximately trigonal planar, with angles of Fe-Ga-I(1), 131.67(5)°; Fe-Ga-I(2), 134.02(5)°; I(1)-Ga-I(2), 94.30(4)° [sum of angles at Ga = 360.0°]. The Fe-Ga bond length [2.3246(11) Å] is comparable to that found for analogous gallyl systems (*e.g.* $[\text{Cp}^*\text{Fe}(\text{CO})_2\text{GaI}_2]_2$, 2.314(1) Å). The molecular structure of **4.4** demonstrates that photolytic substitution of the CO groups for phosphine ligands of the type PR_3 , is a feasible pathway in the generation of gallium containing transition metal phosphine complexes. Interestingly, the Fe-Ga bond distance for **4.4** is marginally longer than that found for **4.3** despite the gallium centre in **4.4** being only three-coordinate (*cf.* four-coordinate for **4.3**). This presumably arises as a result of the steric influence of the dppe ligand in **4.4**.

Investigation into the mechanism of carbonyl substitution, performed by ^{31}P NMR monitoring of the reaction, revealed that the reaction proceeds *via* the intermediate $\text{Cp}^*\text{Fe}(\text{CO})(\mu\text{-dppe})\text{GaI}_2$ (**4.5**). **4.5** was isolated as a red microcrystalline solid in moderate yield 35 %.⁶ ^{31}P NMR data for **4.5** reveals two peaks with chemical shifts of δ_{P} 65 and -41 ppm, indicating that one phosphorus atom is bound to the iron centre (δ_{P} 65) and the other is bound to gallium (δ_{P} -41). The measured ^{31}P NMR shifts are consistent with those reported by Ueno *et al.* in the synthesis of $\text{Cp}^*\text{Fe}(\text{dmpe})\text{GaCl}_2$ **4.8**; in this case the proposed intermediate $\text{Cp}^*\text{Fe}(\text{CO})(\mu\text{-dmpe})\text{GaCl}_2$ (although not structurally authenticated) gives rise to two ^{31}P NMR peaks with chemical shifts of δ_{P} 35 (Fe-P) and -42 (Ga-P).⁷ The mechanism of substitution is thought to involve initial coordination of a single phosphorus donor to the gallium centre followed by photolytic removal of a single CO accompanied by coordination of the pendant phosphorus donor at iron. Finally, loss of a second CO ligand promotes migration of the gallium-bound phosphorus centre to iron, thus yielding $\text{Cp}^*\text{Fe}(\text{dmpe})\text{GaCl}_2$ **4.8**. A similar mechanism for CO substitution can therefore be proposed for the synthesis of **4.4** (albeit with crystallographic confirmation of intermediate identities) in which the reaction proceeds through the intermediate **4.5** (Scheme 4.3).



Scheme 4.3 Synthetic route to complex **4.4** proceeding *via* the intermediate **4.5**.

Multinuclear NMR data obtained for the isolated compound **4.5** are consistent with the formation of a dppe containing species; the ^1H NMR spectrum displays Cp*, methylene and Ph proton signals of the dppe ligand at chemical shifts of 1.48, 1.95, 2.55, 7.10-7.49, 7.68 and 7.88 with relative intensities of 15:2:2:16:2:2, respectively. The single carbonyl stretching frequency ($\nu(\text{CO})$ 1981 cm^{-1}) supports the conclusion that one carbonyl group has been substituted by the phosphine ligand. The EI mass spectrum displays weak peaks for the parent $[\text{M}]^+$ ion with peaks for the fragment ion $[\text{M-dppe}]^+$ also being evident; the isotope distribution is as expected for a complex containing one oxygen, one iron, one gallium, two iodine and two phosphorus atoms.

Confirmation of the mode of coordination of the dppe ligand in **4.5** was obtained by analysis of X-ray crystallographic data. Single crystals of **4.5** suitable for X-ray diffraction were obtained by layering a concentrated solution of **4.5** in toluene with hexanes at -30°C and the structure is illustrated in Figure 4.2. Relevant bond lengths and angles for **4.5** are listed in Table 4.2.

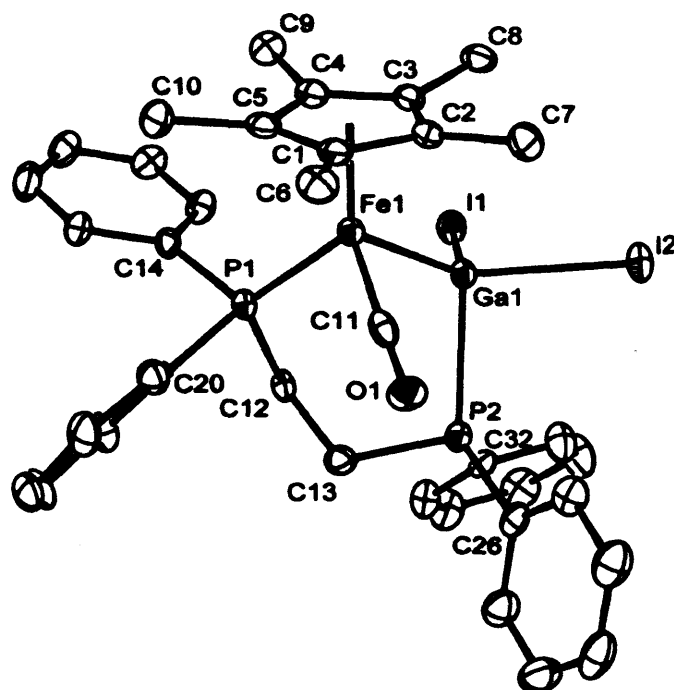


Figure 4.2 The molecular structure of $\text{Cp}^*\text{Fe}(\text{dppe})(\text{CO})\text{GaI}_2$ **4.5**.

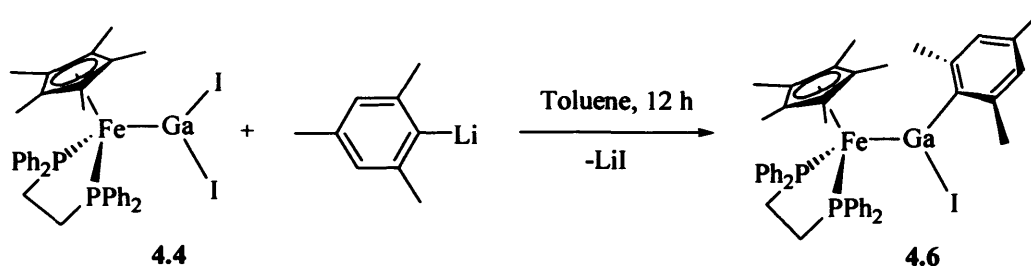
Table 4.2 Selected bond lengths [Å] and angles [°] for **4.5**.

I(1)-Ga(1)	2.6855(7)	Ga(1)-I(2)	2.6416(8)
Ga(1)-Fe(1)	2.3558(10)	Fe(1)-P(1)	2.2107(13)
Ga(1)-P(2)	2.5288(12)	O(1)-C(11)	1.161(5)
P(1)-C(14)	1.835(4)	P(1)-C(12)	1.847(4)
Fe(1)-C(11)	1.726(5)		
Fe(1)-Ga(1)-P(2)	109.79(4)	I(2)-Ga(1)-I(1)	97.80(2)
Fe(1)-Ga(1)-I(2)	126.55(3)	C(14)-P(1)-Fe(1)	119.44(13)
P(2)-Ga(1)-I(2)	96.35(3)	C(12)-P(1)-Fe(1)	117.71(13)
C(13)-P(2)-Ga(1)	101.52(14)	C(11)-Fe(1)-Ga(1)	86.65(13)
C(11)-Fe(1)-P(1)	92.77(14)	P(1)-Fe(1)-Ga(1)	92.59(4)

The crystal structure confirms the presence of monomeric units with the formulation $\text{Cp}^*\text{Fe}(\text{CO})(\mu\text{-dppe})\text{GaI}_2$ **4.5**, in which each unit features a four coordinate gallium centre. The structure of **4.5** therefore supports the proposed substitution mechanism (Scheme 4.3) in which, one phosphorus atom has photolytically substituted a single CO ligand, with the second phosphorus atom coordinated to gallium. The coordination geometry about the gallium centre is approximately tetrahedral, with angles of Fe(1)-Ga(1)-P(2), $109.79(4)^\circ$; Fe(1)-Ga(1)-I(1), $122.35(3)^\circ$; Fe(1)-Ga(1)-I(2), $126.55(3)^\circ$; I(1)-Ga(1)-I(2), $97.80(2)^\circ$. The Fe-Ga bond length [$2.3558(10)$ Å] is somewhat longer than that found for **4.4** [$2.3236(14)$ Å].

In order to complete the two-step methodology shown in Scheme 4.4 the reaction of **4.4** with sources of sterically demanding aryl ligands was investigated, with the aim of synthesising an asymmetric halogallyl species. Addition of MesLi to a solution/suspension of **4.4** in toluene proceeds as expected with selective substitution of an iodide atom for the mesityl ligand yielding $\text{Cp}^*\text{Fe}(\text{dppe})\text{Ga}(\text{Mes})\text{I}$ (**4.6**) as an orange microcrystalline solid in high yield (77%) (Scheme 4.4). The synthesis was initially carried out using diethyl ether as the reaction solvent, however the yield obtained was significantly improved by carrying out the reaction in toluene (*i.e.* a 77 % yield in toluene, 15 % yield in diethyl ether). In addition, a significant amount of a second organometallic species was evident when performing the reaction in diethyl ether, in contrast to the corresponding chemistry in toluene. This impurity was evident in the ^1H NMR spectra, which revealed the presence of two sets of Cp* peaks, two sets of methylene protons and two sets of two methyl peaks corresponding to two mesityl fragments. These signals were found with relative integrated intensities

of 15:2:3:6:2 (corresponding to **4.6**, by comparison with an authentic sample, *vide infra*) and 15:2:6:12:2 (corresponding to the impurity). This integration suggests that the second species has been formed by substitution of both iodide atoms presumably generating $\text{Cp}^*\text{Fe}(\text{dppe})\text{Ga}(\text{Mes})_2$.



Scheme 4.4 Synthetic route to $\text{Cp}^*\text{Fe}(\text{dppe})\text{Ga}(\text{Mes})\text{I}$ **4.6**.

The ^{31}P NMR chemical shift for **4.6** (δ_{P} 99 ppm) is consistent with the retention of the chelating (dppe)Fe unit. The ^1H and ^{13}C NMR spectra reveal the presence of a mesityl containing species; two methyl signals are evident in the ^1H NMR spectrum at 2.10 and 2.25 ppm corresponding to the *ortho* and *para* CH_3 groups of the mesityl ligand. In addition, the presence of the Cp^* ligand and dppe methylene protons further suggests that the substitution proceeds with retention of the metal-ligand bond; the relative intensities (15:2:3:6:2) of signals corresponding to the Cp^* , CH_2 -dppe, *para*- CH_3 , *ortho*- CH_3 and CH_2 -dppe groups respectively, suggests that a single iodide has been substituted by a mesityl fragment. The EI mass spectrum displays weak peaks for the parent $[\text{M}]^+$ ion with peaks corresponding to the fragment ion $[\text{M}-\text{I}]^+$ also being evident; the isotope distribution is as expected for a complex containing one iron, one gallium, one iodine and two phosphorus atoms.

Table 4.3 Selected bond lengths [Å] and angles [°] for **4.6**.

P(1)-Fe(1)	2.191(4)	P(1)-C(20)	1.843(3)
P(2)-Fe(1)	2.187(4)	P(2)-C(21)	1.842(3)
Fe(1)-Ga(1)	2.3548(27)	Ga(1)-C(11)	2.075(4)
Ga(1)-I(1)	2.7237(20)		
P(1)-Fe(1)-P(2)	85.69(14)	Fe(1)-Ga(1)-I(1)	127.57(7)
P(1)-Fe(1)-Ga(1)	90.85(9)	Fe(1)-Ga(1)-C(11)	140.41(11)
P(2)-Fe(1)-Ga(1)	91.21(9)	I(1)-Ga(1)-C(11)	92.02(9)

The crystal structure confirms that **4.6** exists as monomeric units with the formulation Cp*Fe(dppe)Ga(Mes)I, in which one of the iodide substituents on the gallium centre has been substituted for the mesityl ligand. The coordination geometry about the gallium centre is approximately trigonal planar, with angles of Fe-Ga-I, 127.57(7)°; Fe-Ga-C, 140.41(11)°; I-Ga-C, 92.02(9)° [sum of angles at Ga = 360.0°]. The Fe-Ga bond length of 2.3548(27) Å is longer than that found for the related dicarbonyl species Cp*Fe(CO)₂Ga(Mes)I **3.10** (2.3113(12) Å), presumably on steric grounds. The orientation of the gallyl ligand is such that it lies essentially co-planar with the Cp* centroid-Fe-Ga plane (\angle Cp* centroid-Fe-Ga-C_{ipso} = 15.4°). This ligand orientation and near perpendicular alignment of the gallyl and mesityl planes (\angle Fe-Ga-C_{ipso}-C_{ortho} = 81.6°) is analogous to that observed for Cp*Fe(CO)₂Ga(Mes)I. The molecular structure of **4.6** not only demonstrates the viability of the proposed substitution methodology, but also confirms the expected trigonal planar geometry at the gallium centre.

The synthesis of analogous phosphine containing iodogallyl species featuring larger sterically demanding aryl substituents has also been investigated. However,

reaction of **4.4** with one equivalent of $\text{Mes}^*\text{Li}(\text{thf})_2$ did not yield any tractable phosphine containing compounds. This lack of reactivity presumably reflects the enhanced steric bulk around the gallium centre.

4.2.2 Halide Abstraction Chemistry of Asymmetric Halogallyl Complexes

4.2.2.1 Experimental

Attempted reaction of $\text{Cp}^\text{Fe}(\text{dppe})\text{Ga}(\text{Mes})\text{I}$ with $\text{Na}[\text{BAR}^f_4]$*

A solution of $\text{Cp}^*\text{Fe}(\text{dppe})\text{Ga}(\text{Mes})\text{I}$ **4.6** (0.046 g, 0.051 mmol) in dichloromethane (30 cm^3) was added dropwise to a suspension of $\text{Na}[\text{BAR}^f_4]$ (0.052 g, 0.052 mmol) in dichloromethane (10 cm^3) at -40°C . The mixture was stirred at this temperature for 1 h after which the reaction was warmed to room temperature and stirred for a further 1 h. The dark brown solution was filtered, concentrated *in vacuo*. ^{31}P NMR (122 MHz, CD_2Cl_2) : δ_{p} 92. Unfortunately, attempts to crystallize the species by layering the concentrated solution with hexanes and storing at -30°C , did not yield any tractable compounds.

Attempted reaction of $\text{Cp}^\text{Fe}(\text{dppe})\text{Ga}(\text{Mes})\text{I}$ with $[\text{Et}_3\text{Si}]^+[\text{B}(\text{C}_6\text{F}_5)_4]^-$*

A solution of $\text{Cp}^*\text{Fe}(\text{dppe})\text{Ga}(\text{Mes})\text{I}$ **4.6** (0.050 g, 0.055 mmol) in dichloromethane (15 cm^3) was added dropwise to a solution of $[\text{Et}_3\text{Si}]^+[\text{B}(\text{C}_6\text{F}_5)_4]^-$ (0.026 g, 0.051 mmol) in dichloromethane (10 cm^3) at -30°C . The mixture was stirred at this temperature for 1 h. The dark brown solution was concentrated *in vacuo*. ^{31}P NMR (122 MHz, CD_2Cl_2) : δ_{p} 92, 88. Unfortunately, attempts to crystallize the species by layering the concentrated solution with hexanes and storing at -30°C , did not yield any tractable compounds.

**Attempted reaction of $Cp^*Fe(dppe)Ga(Mes)I$ with $Ag^+[OTf]^-$:
 $Ag^+[Cp^*Fe(dppe)Ga(Mes)(OTf)I]^-$ (4.9)**

A solution of $Cp^*Fe(dppe)Ga(Mes)I$ **4.6** (0.071 g, 0.077 mmol) in D_6 -benzene (3 cm^3) was added to $Ag^+[OTf]^-$ (0.020 g, 0.078 mmol) with the immediate formation of a grey precipitate. The mixture was sonicated for 15 min after which the brown solution was isolated. ^{31}P NMR (122 MHz, C_6D_6) : δ_p 13. No tractable compounds were isolated. Unfortunately, attempts to crystallize the species by layering the concentrated solution with hexanes and storing at $-30^\circ C$, did not yield any tractable compounds.

**Reaction of $Cp^*Fe(dppe)Ga(Mes)I$ with Me_3SiOTf then $Na^+[BAR^f_4]^-$: Isolation of
 $[Cp^*Fe(dppe)Cl]^+[BAR^f_4]^-$ (4.10)**

To a solution of $Cp^*Fe(dppe)Ga(Mes)I$ **4.6** (0.102 g, 0.011 mmol) in CD_2Cl_2 (2 cm^3) was added Me_3SiOTf (0.020 cm^3 , 0.011 mmol) at $-30^\circ C$; the reaction mixture was warmed to room temperature and sonicated for 5 min with the immediate formation of a dark red solution. Volatiles were removed *in vacuo* and the residue extracted into dichloromethane (4 cm^3). The solution was added to a suspension of $Na^+[BAR^f_4]^-$ (0.098 g, 0.011 mmol) in dichloromethane at $-78^\circ C$, warmed to $-40^\circ C$ and stirred at that temperature for 25 min, leading to the formation of a purple solution. ^{31}P NMR monitoring of the reaction mixture at this point revealed a broad peak at δ_p 89. 1H NMR (300 MHz, CD_2Cl_2) : δ_H 1.37 (s, 15H, CH_3 of Cp^*), 2.24-2.28 (m, 4H, CH_2 of dppe), 7.19-7.65 (m, 20H, Ar CH of dppe). However, after leaving the reaction mixture at $20^\circ C$ for 24 h, a brown solution resulted and ^{31}P NMR monitoring revealed the disappearance of the ^{31}P NMR resonance at 89 ppm, with no features appearing to grow in; 1H NMR spectrum measured at this point revealed only a number of broad

resonances. Crystals suitable for X-ray diffraction were obtained from a layering of the solution with hexanes at -30°C which subsequently proved to contain the 17-electron $[\text{Cp}^*\text{Fe}(\text{dppe})\text{Cl}]^+$ cation isolated as the $[\text{BAr}^f_4]^-$ salt.

Synthesis of $[\text{Cp}^*\text{Fe}(\text{dppe})(\text{GaI})][\text{BAr}^f_4]$ (4.11)

To a suspension of $\text{Na}[\text{BAr}^f_4]$ (0.053 g, 0.060 mmol) in fluorobenzene (1 cm^3) at -30°C was added an orange-red solution of 4.4 (0.049 g, 0.054 mmol) also in fluorobenzene (2 cm^3) and the reaction mixture warmed to room temperature over a period of 20 min. Monitoring of the reaction by $^{31}\text{P}\{^1\text{H}\}$ NMR spectroscopy revealed quantitative conversion of 4.4 (δ_{P} 103.9) to a single phosphorus containing species giving rise to a broad resonance at δ_{P} 87.0. The resulting deep violet solution was filtered, concentrated *in vacuo* and purple crystals suitable for X-ray diffraction obtained by layering with hexanes and storage at -30°C . Isolated yield 0.018 g, 20 %.

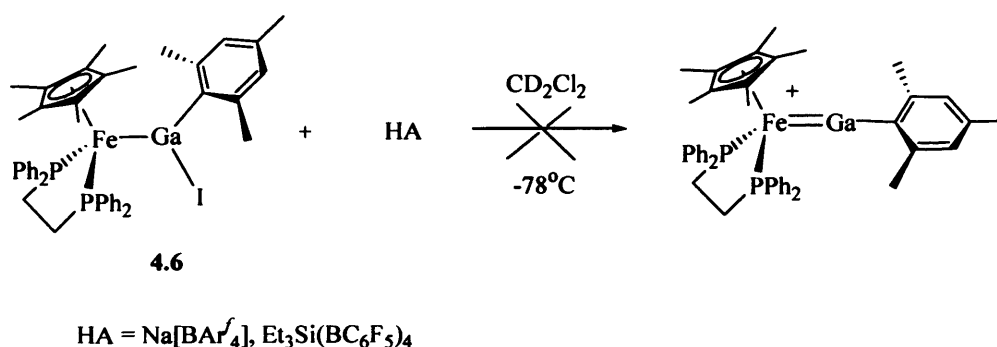
^1H NMR (300 MHz, $\text{C}_6\text{D}_5\text{F}$): δ_{H} 1.18 (s, 15H, CH_3 of Cp^*), 1.88 (m, 2H, CH_2 of dppe), 2.04 (m, 2H, CH_2 of dppe), 7.14-7.37 (overlapping m, 20H, aromatic CH of dppe), 7.54 (s, 4H, *para*-CH of BAr^f_4), 8.27 (s, 8H, *ortho*-CH of BAr^f_4). ^{13}C NMR (76 MHz, $\text{C}_6\text{D}_5\text{F}$): (i) signals due to cation: δ_{C} 9.2 (CH_3 of Cp^*), 31.5 (m, CH_2 of dppe), 86.5 (quaternary carbon of Cp^*), 128.0 (pseudo t, $J = 4.6$ Hz, *meta*-CH of dppe), 130.0 (pseudo t, $J = 4.6$ Hz, *meta*-CH of dppe), 129.1 (pseudo t, $J = 5.1$ Hz, *ortho*-CH of dppe), 131.8 (pseudo t, $J = 5.1$ Hz, *ortho*-CH of dppe), 130.4 (*para*-CH of dppe), 130.8 (*para*-CH of dppe), *ipso*-carbons of dppe not observed; (ii) signals due to anion: 117.0 (sept, $J = 4.1$ Hz, *para*-CH of BAr^f_4), 124.3 (1:3:3:1 q, $J = 272.1$ Hz, CF_3 of BAr^f_4), 128.5 (1:3:3:1 q, $J = 29.8$ Hz, *meta*-carbon of BAr^f_4), 134.4 (*ortho*-CH of BAr^f_4), 161.9 (1:1:1:1 q, $J = 49.8$ Hz, *ipso*-carbon of BAr^f_4). ^{11}B NMR (96 MHz, $\text{C}_6\text{D}_5\text{F}$): δ_{B} 1.9. ^{19}F NMR (282 MHz, $\text{C}_6\text{D}_5\text{F}$): δ_{F} -62.7. ^{31}P NMR (122 MHz,

C_6D_5F): δ_p 87.0 b. ES-MS (positive ion mode), m/z : 785.0 {100 %, $[Cp^*Fe(dppe)(GaI)]^+$ }, correct isotope pattern for $C_{36}H_{39}FeGaIP_2$. Exact mass: calc. for $[Cp^*Fe(dppe)(GaI)]^+$ (*i.e.* M^+) 785.0173, meas. 785.0204. FT-Raman (C_6D_5F solution): 186 cm^{-1} . UV/vis (C_6H_5F solution): $\lambda_{max} = 549\text{ nm}$; $\epsilon = 754\text{ cm}^{-1}\text{ mol}^{-1}\text{ dm}^3$. Reproducible microanalyses for crystalline samples of **4.11** proved impossible to obtain, possibly due to the extreme sensitivity of this compound to air and moisture.

4.2.2.2 Results and Discussion

Investigations have revealed that the usefulness of halide abstraction chemistry in delivering terminal gallylene complexes from halogallyl precursors **4.4** and **4.6** is strongly dependent on the gallium bound substituents, the halide abstraction agent, and the solvent used.

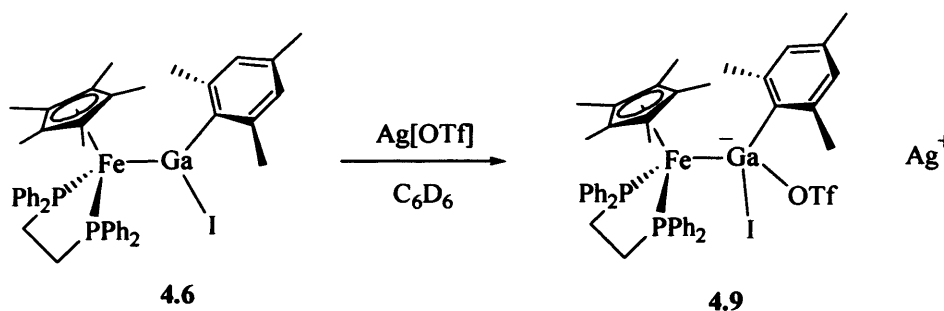
The halide abstraction chemistry of **4.6** has been investigated using a number of abstraction agents. ^{31}P NMR monitoring of the reaction of **4.6** with $Na^+[BAR^f_4]^-$ in dichloromethane at $-78^\circ C$, yielded a sharp peak in the ^{31}P NMR at δ 92 (Scheme 4.5), however no tractable compounds could be isolated.



Scheme 4.5

Similar reaction chemistry of **4.6** with Heinekey's more reactive abstraction reagent $[\text{Et}_3\text{Si}]^+[\text{B}(\text{C}_6\text{F}_5)_4]^-$,⁸ revealed multiple sharp peaks in the ^{31}P NMR (Scheme 4.5). Unfortunately no tractable phosphorus containing compounds could be isolated.

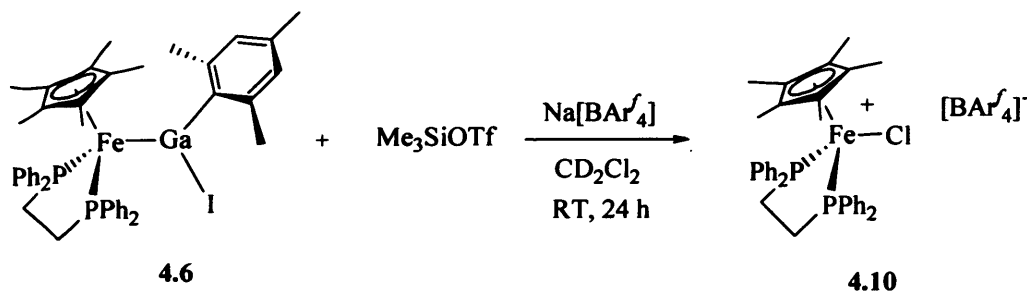
The substitution of the iodide substituent for triflate was also investigated with the aim of generating the corresponding asymmetric halogallyl species with a potentially enhanced leaving group, as demonstrated by Tilley *et al.* in the formation of the silylene complexes $[\text{Cp}^*(\text{PMe}_3)_2\text{Ru}=\text{SiR}_2]^+$ (where R = Me **4.1**, Ph **4.2**).² Reaction of **4.6** with $\text{Ag}[\text{OTf}]$ in C_6D_6 was investigated. ^{31}P NMR monitoring of the reaction revealed a sharp peak at δ_{P} 13. As a result of the large change in the ^{31}P NMR shift from δ_{P} 99 to 13, it was postulated that the OTf moiety had simply coordinated to gallium resulting in the formation of a four coordinate gallium centre (Scheme 4.6). However, as no tractable compounds were isolated the formation of **4.9** is based on ^{31}P NMR data and as such is only speculative.



Scheme 4.6

Reaction of **4.6** with $[\text{PPN}]^+[\text{OTf}]^-$ in fluorobenzene followed by further reaction with $\text{Na}^+[\text{BARf}_4]^-$ was also examined, however ^{31}P NMR monitoring of the reaction revealed multiple sharp peaks and unfortunately no tractable compounds were isolated.

In an attempt to investigate the use of softer sources of the triflate moiety, the reactivity of gallyl species towards Me_3SiOTf was investigated. Addition of Me_3SiOTf to a solution of **4.6** in CD_2Cl_2 followed by reaction with $\text{Na}[\text{BARf}_4^-]$ yielded a phosphorus containing species characterized by a broad peak at δ_{P} 89 after 25 min stirring at -40°C . In addition, ^1H NMR monitoring of the reaction revealed the disappearance of the peaks corresponding to the mesityl fragment after 18 h, with only the Cp^* and dppe resonances being retained. The broad nature of the ^{31}P NMR peak is consistent with the formation of a cationic derivative (*cf.* silylene chemistry reported by Tilley), however the disappearance of the mesityl fragment indicates that the Ga-C bond is labile. Continued ^{31}P NMR monitoring of the reaction mixture revealed the disappearance of the phosphorus signal after 24 h at 20°C , and ^1H NMR monitoring revealed only broad peaks. Thus, determination of the nature of the species generated was therefore heavily dependent on crystallographic data. Crystals suitable for X-ray diffraction were obtained from layering a concentrated solution at -30°C . The structure of **4.10** was thus obtained by single crystal X-ray diffraction studies, and its structure illustrated in Figure 4.4. Relevant bond lengths and angles for **4.10** are listed in Table 4.4. **4.10** is thus identified as the monomeric paramagnetic salt $[\text{Cp}^*\text{Fe}(\text{dppe})\text{Cl}]^+[\text{BARf}_4^-]$ **4.10** (Scheme 4.7), featuring a 17-electron iron-containing cation.



Scheme 4.7 Synthetic route to complex **4.10**.

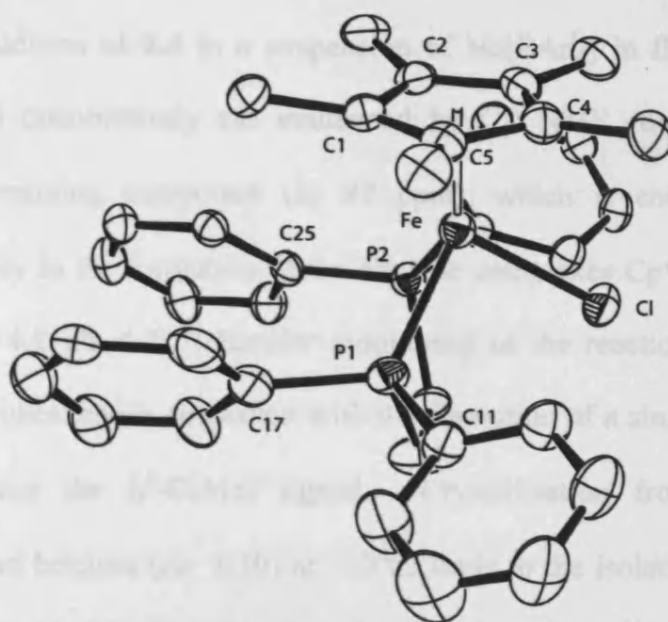


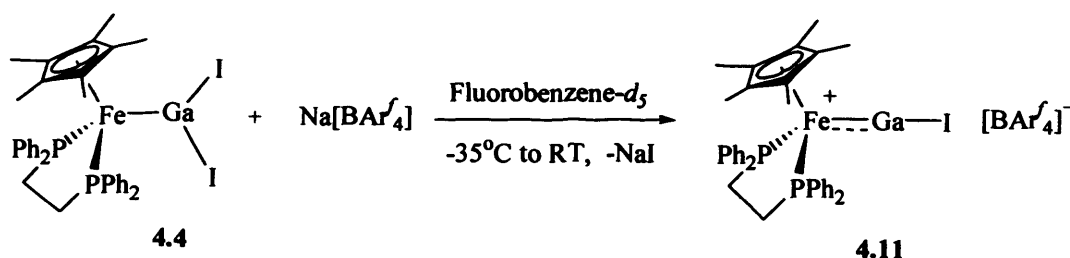
Figure 4.4 The molecular structure of $[\text{Cp}^*\text{Fe}(\text{dppe})\text{Cl}]^+[\text{BAR}_4]^-$ **4.10**.

Table 4.4 Selected bond lengths [\AA] and angles [$^\circ$] for **4.10**.

Fe-Cl	2.2257(18)	Fe-P(2)	2.2837(18)
Fe-P(1)	2.2624(19)		
Cl-Fe-P(1)	89.66(7)	Cl-Fe-P(2)	86.63(6)
P(1)-Fe-P(2)	81.85(6)		

While the formation of **4.10** is unexpected, a precedent of sorts can be established by a combination of multinuclear NMR, UV/vis and FT-Raman spectroscopies. Particularly informative are the positive-ion electrospray mass spectra obtained for **4.11** in dichlorobenzene (including exact mass measurements and isotopic profiling and hybrid fragmentation of the molecular ion $[\text{Cp}^*\text{Fe}(\text{dppe})(\text{Gal})]^+$ peak at $m/z = 785$ (100%) displaying the correct isotope pattern for $\text{C}_{21}\text{H}_{25}\text{FeGaP}_2$). In addition to providing definitive identification of the molecular ion by isotopic therefore be postulated for the formation of $[\text{Cp}^*\text{Fe}(\text{dppe})\text{Cl}]^+[\text{BAR}_4]^-$ **4.10**.

From these results the halide abstraction chemistry of **4.4** was also investigated. Addition of **4.4** to a suspension of Na[BAr^f₄] in fluorobenzene-*d*₅ at -35°C generated quantitatively (as evidenced by ³¹P NMR monitoring) a single phosphorous containing compound (δ_P 87 ppm), which is consistent with that observed by Tilley in the formation of the silylene complexes Cp*(PMe₃)₂Ru=SiR₂⁺ (where R = Me **4.1**, Ph **4.2**).² Similar monitoring of the reaction by ¹H NMR in perdeuterio-fluorobenzene is consistent with the formation of a single organometallic product containing the η⁵-C₅Me₅ ligand. Crystallisation from a mixture of fluorobenzene and hexanes (*ca.* 1:10) at -30°C, leads to the isolation of the cationic gallylene complex [Cp*Fe(dppe)Gal]⁺[BAr^f₄]⁻ **4.11** in 35 % isolated yield, featuring the first reported synthesis of a terminally bound Gal ligand (Scheme 4.8).¹⁰



Scheme 4.8 Synthetic route to [Cp*Fe(dppe)Gal]⁺[BAr^f₄]⁻ **4.11**.

The constitution of [Cp*Fe(dppe)Gal]⁺[BAr^f₄]⁻ **4.11** has been unambiguously established by a combination of multinuclear NMR, UV/Vis and FT-Raman spectroscopies. Particularly informative are the positive-ion electrospray mass spectra obtained for **4.11** in fluorobenzene (including exact mass measurements and isotopic profiling and MS/MS fragmentation of the molecular ion [Cp*Fe(dppe)(Gal)]⁺ peak at *m/z* = 785 (100 %) displaying the correct isotope pattern for C₃₆H₃₉FeGaIP₂). In addition to providing definitive identification of the molecular ion by isotopic

profiling, fragmentation data revealed the presence of the coordinated GaI ligand. Thus MS-MS performed on the molecular ion are consistent with ready fragmentation generating the $[\text{Cp}^*\text{Fe}(\text{dppe})]^+$ cation by loss of GaI. The ^1H NMR revealed signals with relative intensities of 15:2:2:20:4:8, which is consistent with the formation of a Cp^* dppe containing species featuring a $[\text{BAr}'_4]^-$ fragment. The presence of the Cp^* and dppe moieties suggests that the abstraction proceeds with retention of the $\text{Cp}^*\text{Fe}(\text{dppe})$ fragment, and the relative peak intensities imply the formation of a $\text{Cp}^*\text{Fe}(\text{dppe})$ containing cationic species in which the cation:anion ratio is 1:1. ^{13}C NMR data supports the formation of a cationic containing $\text{Cp}^*\text{Fe}(\text{dppe})$ species. In addition the ^{11}B and ^{19}F NMR chemical shifts ($\delta_{\text{B}} -2$, and $\delta_{\text{F}} -62$) are also consistent with a BAr'_4^- containing species.

Definitive identification of a Fe-Ga-I bond was dependent on crystallographic data. Single crystals suitable for X-ray diffraction were obtained by layering a concentrated solution of **4.11** in fluorobenzene with hexanes and storage at -30°C . The spectroscopic data for **4.11** was confirmed by single crystal X-ray diffraction studies and the structure is illustrated in Figure 4.5. Relevant bond lengths and angles for **4.11** are listed in Table 4.5.

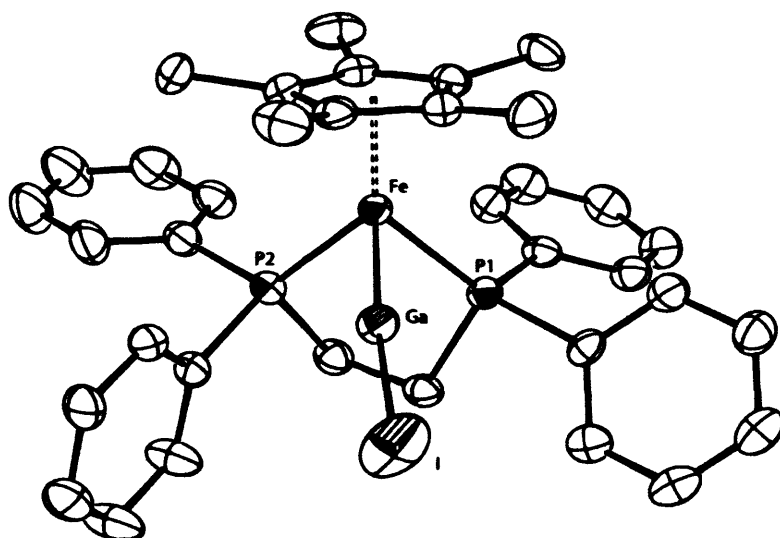


Figure 4.5 The molecular structure of the major component of the cationic part of



Table 4.5 Selected bond lengths [Å] and angles [°] for 4.11.

Fe-Ga	2.2221(6)	Ga-I	2.4436(5)
Fe-P(2)	2.2199(10)		
Ga-Fe-P(1)	86.16(3)	P(1)-Fe-P(2)	86.80(3)
Ga-Fe-P(2)	91.02(3)	Fe-Ga-I	171.37(3)

Disorder within the structure was successfully modelled; the major component (79 %) features discrete $[\text{Cp}^*\text{Fe}(\text{dppe})(\text{GaI})]^+$ and $[\text{BARf}_4]^-$ ions, with no short secondary interactions involving the Fe-Ga-I ligand (within standard van der Waals contacts). Key structural features are the essentially linear arrangement of the iron, gallium and iodine atoms [$\angle(\text{Fe-Ga-I}) = 171.37(3)^\circ$] typical of a terminally bound diatomic ligand (*cf.* $\angle\text{Fe-C-O} = 175.8(5)^\circ$ for $[\text{Cp}^*\text{Fe}(\text{dppe})(\text{CO})]^+[\text{PF}_6]^-$ 4.12)¹¹ and the extremely short Fe-Ga [2.2221(6) Å] and Ga-I [2.4436(5) Å] distances. The metal-gallium distance is among one of the shortest yet reported involving *any*

transition metal (and the shortest involving iron); likewise the Ga-I distance is also the shortest yet reported.¹² Structural evidence also points to a soft bending deformation of the Fe-Ga-I bond, *viz.* large displacement ellipsoid amplitude for the iodine atom perpendicular to the Fe-Ga-I axis. Secondary off-axis electron density has been modelled as a minor (21 %) cationic component featuring a markedly more bent Fe-Ga-I unit ($148.92(5)^\circ$), and contacts between I' and C(55)-C(58) of one of the $[\text{BAr}_4]^-$ aromatic rings which fall within the sum of the van der Waals radii of iodine and carbon. Large librational amplitudes at oxygen in related metal carbonyl complexes are often associated with analogous Fe-C-O bending motions, and the ready deformation of the linear Fe-Ga-I fragment in **4.11** (and a small calculated energy difference between the linear and bent geometries) is consistent with the smaller absolute magnitude of directional covalent contributions to the metal ligand bond (*viva infra*).

A contributory factor to these short bond lengths in **4.11** is the low coordination number at the gallium centre. Thus a short Fe-Ga bond is also observed for two-coordinate $(\text{OC})_4\text{FeGa}[\text{C}_6\text{H}_3(\text{C}_6\text{H}_2\text{Pr}_3)_2-2,6]$ **4.13** [$2.2248(7)$ Å],¹³ while longer bonds are measured for the three-coordinate precursor **4.4** [$d(\text{Fe-Ga}) = 2.322$ Å (mean); $d(\text{Ga-I}) = 2.630$ Å (mean)] and for the four-coordinate system $[\text{Cp}^*\text{Fe}(\text{CO})_2\text{GaCl}(\text{phen})]^+$ **4.14** [$d(\text{Fe-Ga}) = 2.3047(4)$ Å].^{14, 15} Potentially, a second factor underlying these short distances is the presence of off-axis electronic contributions to the bonding, involving gallium-based orbitals of π symmetry. The contraction of the Fe-Ga bond on halide abstraction (*ca.* 4.3 % for **4.11** compared to **4.4**) is markedly less than for analogous boron-containing systems (typically 9-10 %),¹⁶ for which descriptions incorporating Fe=B π bonds have been advanced for the

cationic products. That said, smaller changes in bond length as a function of bond order are typically found for the heavier main group elements,¹⁷ and the Fe-Ga contraction between **4.11** and **4.4** mirrors that found between double and single bonds involving the adjacent group 14 element germanium (*e.g.* 4.7 % between Mn-Ge and Mn=Ge bonds).¹⁸ Thus, the molecular structure of **4.11** confirms that halide abstraction is a viable synthetic route to the formation of cationic gallium complexes featuring increased metal-ligand bond order.

Attempts to isolate **4.11** from the corresponding reaction in dichloromethane led instead to the formation of paramagnetic products. Monitoring of the reaction mixture by ³¹P NMR reveals initial conversion of **4.4** to a single species which gives rise to a broad resonance (δ_P 87.0) very similar to that observed for the analogous reaction in fluorobenzene solution (together with a similar red to violet colour change). In dichloromethane solution this signal has a half-life of *ca.* 30 min at room temperature; after several hours the solution is typically brown in colour and exhibits no discernible ³¹P resonances. While it is difficult to state definitively the ultimate outcome of this apparent decomposition reaction, it has previously been shown that cationic osmium silylene complexes react with chlorocarbons *via* chlorine atom abstraction.⁹ In addition as shown in the formation of **4.10**, isolation of the paramagnetic 17-electron [Cp*Fe(dppe)Cl]⁺ cation (as the [BAR₄]⁻ salt) was successful by reaction of **4.6** with Me₃SiOTf and Na[BAR₄]⁻ in CD₂Cl₂.

In order to examine the bonding in the unprecedented ligand system present in **4.11** and to provide comparison of group 13/17 ligands with group 14/16 and group 15/15 counterparts, computational investigations of the bonding in **4.11** and related

complexes was also undertaken. Density Functional Theory analyses of electronic structure were carried out using the model systems $[\text{CpFe}(\text{dmpe})(\text{EX})]^+$ ($\text{EX} = \text{GaI}$, BF , CO and N_2) shown in Table 4.6. Computational results revealed an essentially linear minimum-energy geometry for $\text{EX} = \text{GaI}$ ($\angle\text{Fe-Ga-I} = 174.4^\circ$) consistent with crystallographic studies. Moreover, a very shallow potential energy surface is found to be associated with the Fe-Ga-I bending deformation ($\Delta E < +35 \text{ kJ mol}^{-1}$ for $159 < \vartheta < 179^\circ$, and $\Delta E = +11 \text{ kJ mol}^{-1}$ for $\vartheta = 149^\circ$).

Table 4.6 Calculated σ and π bonding contributions

Compound	Fe-E		E-X	
	σ	π	σ	π
$[\text{CpFe}(\text{dmpe})\text{GaI}]^+$	66.9 %	32.8 %	47.5 %	52.5 %
$[\text{CpFe}(\text{dmpe})\text{BF}]^+$	57.6 %	42.1 %	55.4 %	44.6 %
$[\text{CpFe}(\text{dmpe})\text{CO}]^+$	60.8 %	39.0 %	39.0 %	61.0 %
$[\text{CpFe}(\text{dmpe})\text{NN}]^+$	61.4 %	38.4 %	39.0 %	61.1 %

E = B, Ga, C, N and X = F, I, O, N

From a bonding perspective, a breakdown of the covalent (orbital) components of the metal-ligand bonds of each of the four model compounds reveals notable similarities. In each case, orbital interactions of π symmetry are significant representing 33 (GaI), 42 (BF), 39 (CO), and 38 % (N_2) of the total covalent bonding density.¹⁹ Moreover, the fragment correlation diagram for $[\text{CpFe}(\text{dmpe})(\text{GaI})]^+$ (Figure 4.6) reveals HOMO-5 ($E = -9.55 \text{ eV}$) and HOMO-2/HOMO-1 ($E = -8.34, -7.95 \text{ eV}$) orbitals consistent with $\text{Ga} \rightarrow \text{Fe}$ σ donor and $\text{Fe} \rightarrow \text{Ga}$ π back-bonding

interactions, respectively. Despite this, the magnitude of the covalent (orbital) bonding component for the GaI complex (-236 kJ mol^{-1}) can be put into context by values of -469 , -397 and -262 kJ mol^{-1} for the corresponding BF, CO and N₂ complexes and by a value of -234 kJ mol^{-1} for the *electrostatic* contribution to the (highly polar) Fe-GaI bond. Presumably, despite the higher energy of the HOMO for GaI (-6.08 eV *c.f.* -9.03 eV for CO) and the greater localisation of the LUMO at the donor atom, the weaker orbital contribution for GaI reflects (at least in part) the more diffuse nature of the 4s/4p derived orbitals at gallium and less effective interaction with the fragment orbitals of [CpFe(dmpe)]⁺.²⁰

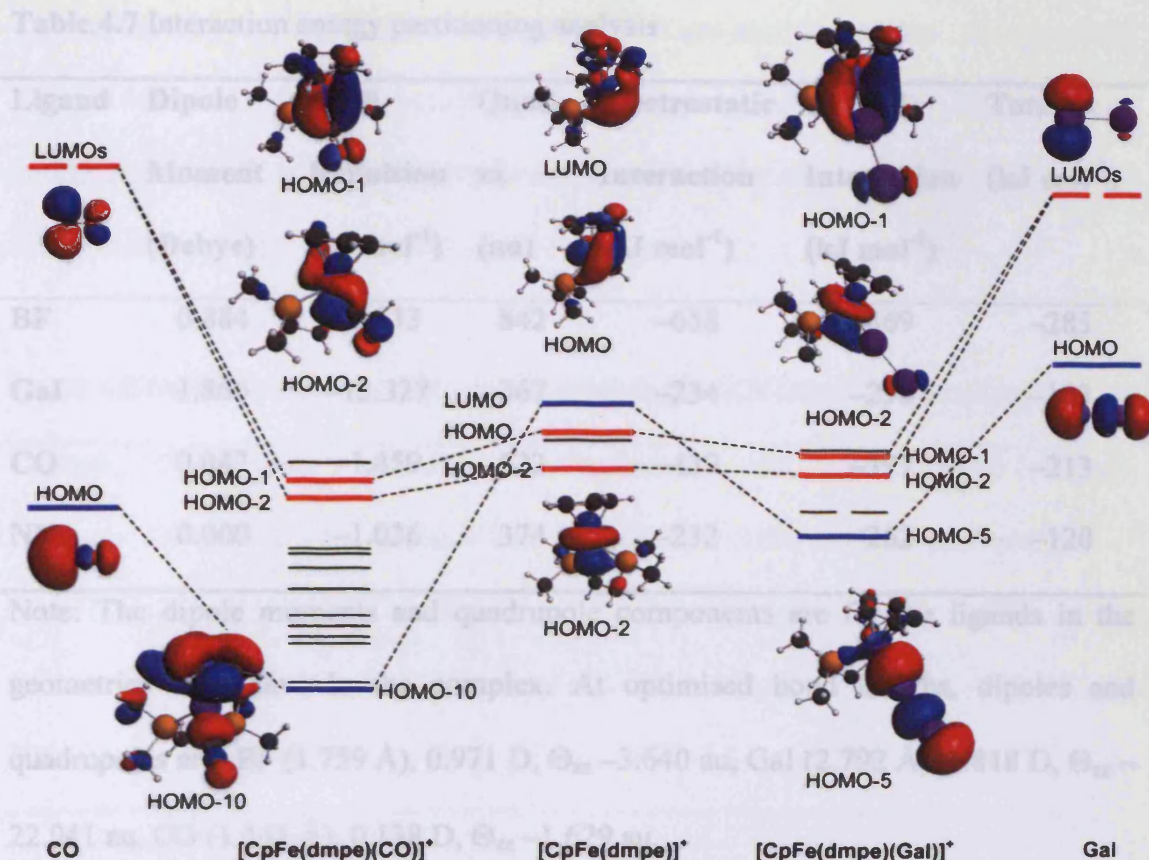


Figure 4.6 Molecular orbital energy level diagram for the model complexes $[\text{CpFe}(\text{dmpe})(\text{CO})]^+$ and $[\text{CpFe}(\text{dmpe})(\text{Gal})]^+$ showing correlation with the $[\text{CpFe}(\text{dmpe})]^+$ and CO/Gal fragments. Local σ symmetry interactions involving the LUMO of $[\text{CpFe}(\text{dmpe})]^+$ and the HOMO of the CO/Gal ligand are shown in blue; π symmetry interactions originating in the HOMO and HOMO-2 of $[\text{CpFe}(\text{dmpe})]^+$ and the degenerate pair of LUMOs of CO/Gal are shown in red.

Table 4.7 Interaction energy partitioning analysis

Ligand	Dipole Moment (Debye)	Pauli Repulsion (kJ mol ⁻¹)	Quad. zz (au)	Electrostatic Interaction (kJ mol ⁻¹)	Orbital Interaction (kJ mol ⁻¹)	Total (kJ mol ⁻¹)
BF	0.884	-3.533	842	-658	-469	-285
GaI	1.866	-13.327	367	-234	-236	-103
CO	0.047	-1.459	623	-439	-397	-213
NN	0.000	-1.036	374	-232	-262	-120

Note: The dipole moments and quadrupole components are for the ligands in the geometries they have in the complex. At optimised bond lengths, dipoles and quadrupoles are: BF (1.759 Å), 0.971 D, Θ_{zz} -3.640 au, GaI (2.792 Å), 3.818 D, Θ_{zz} -22.941 au, CO (1.141 Å), 0.138 D, Θ_{zz} -1.629 au.

Overall metal-ligand bond strengths ($\Delta E_{\text{int}} = -103$ (GaI), -285 (BF), -213 (CO) and -120 kJ mol⁻¹ (N₂)²¹ (Table 4.7)) reveal significantly weaker binding of the GaI ligand,^{19, 22, 23} which can consequently be displaced quantitatively from **4.11** by the addition of CO (at 1 atmosphere pressure) to give [Cp*Fe(dppe)(CO)]⁺[BAR₄]⁻. In the absence of such reagents, **4.11** is stable for weeks in fluorobenzene solution, presumably reflecting (i) effective steric shielding of the gallium centre by the ancillary phosphine and Cp* ligands; (ii) a net cationic charge which retards the tendency towards dimerization found in putative charge neutral systems;²⁴ and (iii) population of the LUMOs of the GaI molecule through π overlap with the HOMO and HOMO-2 of the [Cp*Fe(dppe)]⁺ fragment.

An alternative breakdown of the fragment interaction energy into contributions from the Hamiltonian potentials is given in Table 4.8. The exchange energy for the GaI ligand is notably lower than the other two cases, due to the more diffuse nature of the valence orbitals.

Table 4.8 Interaction energy partitioning according to KS Hamiltonian potentials

Ligand	Electrostatic (kJ mol ⁻¹)	Kinetic (kJ mol ⁻¹)	Coulomb (kJ mol ⁻¹)	XC (kJ mol ⁻¹)	Total (kJ mol ⁻¹)
GaI	-234	-326	536	-79	-103
CO	-439	-306	703	-171	-213
NN	-232	-221	447	-114	-120

4.2.3 Reactions of [Cp*Fe(dppe)GaI]⁺[BAR₄]⁻ 4.11

4.2.3.1 Experimental

*Reaction of [Cp*Fe(dppe)GaI]⁺[BAR₄]⁻ 4.11 with [tⁿBu₄N]⁺I⁻: Synthesis of Cp*Fe(dppe)GaI₂ 4.4*

To a solution of [tⁿBu₄N]I (0.022 g, 0.06 mmol) in fluorobenzene-*d*₅ was added a solution of [Cp*Fe(dppe)GaI]⁺[BAR₄]⁻ 4.11 in fluorobenzene-*d*₅, at 20°C with the immediate formation of an orange solution. ³¹P NMR (122 MHz, C₆D₅F): δ_P 104. ¹H NMR (300 MHz, C₆D₅F): δ_H 1.33 (s, 15H, CH₃ of Cp*), 2.25 (m, 2H, CH₂), 3.25 (m, 2H, CH₂), 6.95 (m, 8H, CH aromatic), 7.15 (m, 8H, CH aromatic), 7.69 (m, 4H, *para*-CH aromatic). ¹³C NMR (76 MHz, C₆D₅F): δ_C 9.4 (CH₃ of Cp*), 31.6 (dd, ¹J_{PC} = 15.2, ²J_{PC} = 7.6 Hz, CH₂ of dppe), 85.2 (quaternary carbon of Cp*), 127.2 (*meta*-CH of dppe), 127.3 (*meta*-CH of dppe), 127.7 (*para*-CH of dppe), 129.3 (*para*-CH of

dppe), 131.6 (*ortho*-CH of dppe), 131.8 (*ortho*-CH of dppe), 141.3 (d, $^1J_{PC} = 7.60$ Hz, *ipso* carbon of dppe), 141.7 (d, $^1J_{PC} = 7.60$ Hz, *ipso* carbon of dppe).

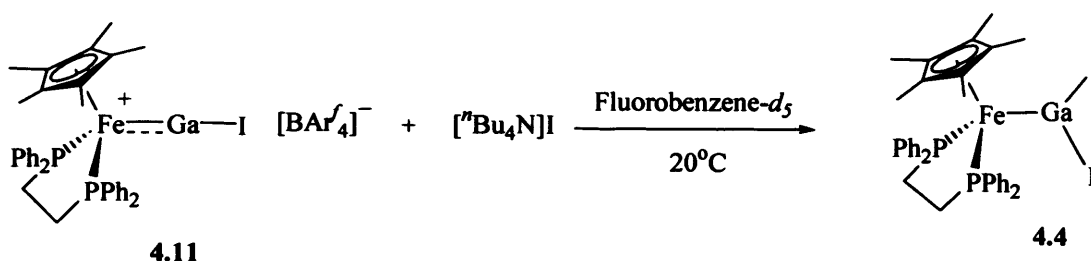
Reaction of $[\text{Cp}^*\text{Fe}(\text{dppe})\text{GaI}]^+[\text{BAr}_4^-]$ 4.11 with CO: Synthesis of $[\text{Cp}^*\text{Fe}(\text{dppe})\text{CO}]^+[\text{BAr}_4^-]$ (4.15)

A solution of $[\text{Cp}^*\text{Fe}(\text{dppe})\text{GaI}]^+[\text{BAr}_4^-]$ 4.11 in fluorobenzene- d_5 , was exposed to an atmosphere of CO for 20 h. at 20°C; resulting in an orange solution. ^{31}P NMR (122 MHz, $\text{C}_6\text{D}_5\text{F}$): δ_{P} 87 (s). ^1H (300 MHz, $\text{C}_6\text{D}_5\text{F}$): δ_{H} 1.48 (s, 15H, CH_3 of Cp^*), 2.38 (m, 4H, CH_2 of dppe), 6.78-7.30 (m, 20H, aromatic CH of dppe), 7.54 (s, 4H, BAr_4^-), 8.21 (s, 8H, BAr_4^-). ^{13}C (76 MHz, $\text{C}_6\text{D}_5\text{F}$): δ_{C} 9.8 (CH_3 of Cp^*), 30.5 (CH_2 of dppe), 95.6 (quaternary C of Cp^*), 117.4 (*para*-CH of BAr_4^-), 123.5 (q, $^1J_{\text{CF}} = 273$ Hz, CF_3 of BAr_4^-), 128.7 (q, $^2J_{\text{CF}} = 29$ Hz, *meta*-C of BAr_4^-), 128.5-135.0 (aromatic CH of dppe), 134.8 (*ortho*-CH of BAr_4^-), 161.5 (q, $^1J_{\text{CB}} = 49$ Hz, *ipso*-C of BAr_4^-), 218.2 (t, $^2J_{\text{CP}} = 25$ Hz, CO). ^{11}B NMR (96 MHz, $\text{C}_6\text{D}_5\text{F}$): δ_{B} 1.9. ^{19}F NMR (282 MHz, $\text{C}_6\text{D}_5\text{F}$): δ_{F} -62.7. IR (thin film $\text{C}_6\text{D}_5\text{F}$, cm^{-1}): $\nu(\text{CO})$ 1950 st.

4.2.3.2 Results and Discussion

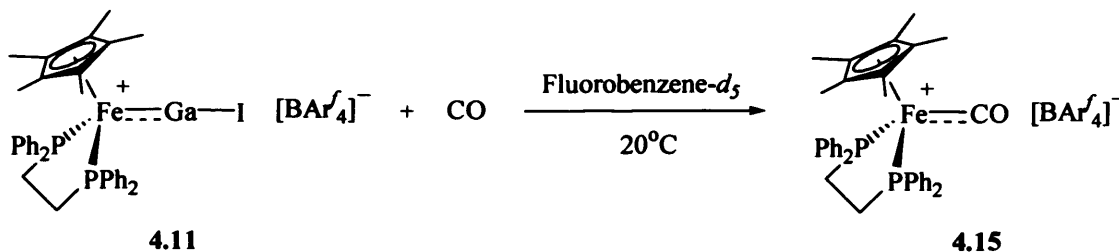
The reaction of $[\text{Cp}^*\text{Fe}(\text{dppe})\text{GaI}]^+[\text{BAr}_4^-]$ 4.11, with iodide was investigated by addition of $[\text{Bu}_4\text{N}]\text{I}$ in Fluorobenzene- d_5 . It has been previously demonstrated by Aldridge *et al.*²⁵ that reaction of $[\text{Cp}^*\text{Fe}(\text{CO})_2\text{B}(\text{Mes})]^+[\text{BAr}_4^-]$ with a suitable anion yields the corresponding three-coordinate boryl species $\text{Cp}^*\text{Fe}(\text{CO})_2\text{B}(\text{Mes})\text{X}$ ($\text{X} = \text{BF}_4^-$, Cl^- , or Br^-) *via* nucleophilic addition to the boron centre. In the case of I^- reaction with $[\text{Cp}^*\text{Fe}(\text{CO})_2\text{B}(\text{Mes})]^+[\text{BAr}_4^-]$ resulted in the formation of two distinct species $\text{Cp}^*\text{Fe}(\text{CO})_2\text{B}(\text{Mes})\text{I}$ and $\text{Cp}^*\text{Fe}(\text{CO})_2\text{I}$. Addition of $[\text{Cp}^*\text{Fe}(\text{dppe})\text{GaI}]^+[\text{BAr}_4^-]$ 4.11 to a solution of $[\text{Bu}_4\text{N}]\text{I}$ led to the formation of

$\text{Cp}^*\text{Fe}(\text{dppe})\text{GaI}_2$ **4.4** as evident by ^{31}P NMR monitoring of the reaction, in which an instantaneous colour change from dark violet to orange was observed and the ^{31}P NMR revealed a change in the chemical shift from a broad peak at δ_{P} 87 to a sharp peak at δ_{P} 104 (*cf.* $\text{Cp}^*\text{Fe}(\text{dppe})\text{GaI}_2$ **4.4**) (Scheme 4.9), thus confirming the formation of $\text{Cp}^*\text{Fe}(\text{dppe})\text{GaI}_2$ **4.4**. ^1H and ^{13}C NMR data obtained is also consistent with the formation of $\text{Cp}^*\text{Fe}(\text{dppe})\text{GaI}_2$ **4.4**.



Scheme 4.9 Synthetic route to complex **4.4**.

Investigations into the substitution of the GaI bound fragment revealed that on exposure of a solution of $[\text{Cp}^*\text{Fe}(\text{dppe})\text{GaI}]^+[\text{BARf}_4]^-$ **4.11** to an atmosphere of CO for 20 h resulted in the selective substitution of GaI yielding $[\text{Cp}^*\text{Fe}(\text{dppe})\text{CO}]^+[\text{BARf}_4]^-$ **4.15** as an orange solution (Scheme 4.10).



Scheme 4.10 Synthetic route to complex **4.15**.

The proposed formulation is supported by multinuclear NMR, in which the ^{13}C NMR revealed a triplet at δ_{C} 218.2 corresponding to the CO bound ligand. ^{31}P NMR monitoring of the reaction revealed a sharp peak growing at δ_{P} 87 corresponding to $[\text{Cp}^*\text{Fe}(\text{dppe})\text{CO}]^+[\text{BARf}_4]^-$ **4.15** which is consistent with that reported by Frédéric *et al.* for the species $[\text{Cp}^*\text{Fe}(\text{dppe})\text{CO}]^+[\text{PF}_6]^-$. The ease of GaI substitution is consistent with the calculated metal-ligand bond strengths, which reveal significantly weaker binding for GaI compared to CO (*cf.* $\Delta E_{\text{int}} = -103$ (GaI), -213 (CO) kJmol^{-1}).

4.3 Attempted Synthesis of Heavier Group 13 Analogues of $\text{Cp}^*\text{Fe}(\text{dppe})\text{EI}_2$

4.3.1 Experimental

Synthesis of $[\text{Cp}^\text{Fe}(\text{CO})_2\text{InI}_3][\text{Cp}^*\text{Fe}(\text{toluene})]$ (4.16) : attempted synthesis of $[\text{Cp}^*\text{Fe}(\text{CO})_2\text{InI}_2]_2$*

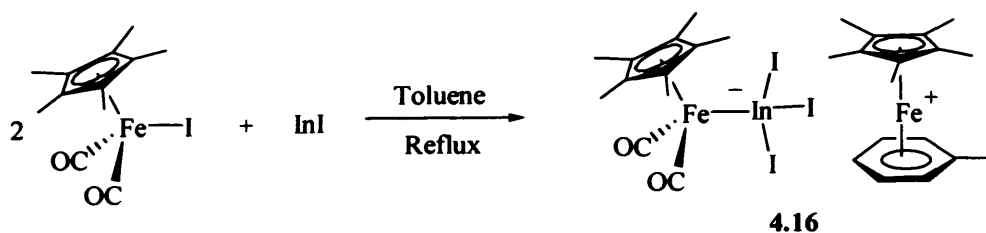
A solution of $\text{Cp}^*\text{Fe}(\text{CO})_2\text{I}$ (0.408 g, 1.091 mmol) in toluene (80 cm^3) was added to a suspension of InI (0.264 g, 1.092 mmol) also in toluene (5 cm^3) and the reaction mixture heated at reflux for 36 h, yielding a clear orange solution. The solution was filtered while hot and cooled to -30°C whereupon an orange crystalline solid precipitated. The solid was isolated and dried *in vacuo* yielding $[\text{Cp}^*\text{Fe}(\text{toluene})]^+[\text{Cp}^*\text{Fe}(\text{CO})_2\text{InI}_3]^-$ (**4.16**) as an orange crystalline solid yield 0.238 g, 27 %. Crystals suitable for X-ray diffraction were obtained from a concentrated toluene solution layered with hexanes at -30°C . ^1H NMR (300 MHz, CD_2Cl_2) : δ_{H} 1.83 (s, 15H, Cp*), 1.88 (s, 15H, Cp*), 2.32 (s, 3H, CH_3 of $\text{C}_6\text{H}_5\text{Me}$), 5.31 (m, 2H, $\text{C}_6\text{H}_5\text{Me}$), 5.57 (m, 1H, $\text{C}_6\text{H}_5\text{Me}$), 5.75 (m, 2H, $\text{C}_6\text{H}_5\text{Me}$). ^{13}C NMR (76 MHz, CD_2Cl_2) : δ_{C} 10.0 (CH_3 of Cp*), 10.3 (CH_3 of Cp*), 18.1 (CH_3 of $\text{C}_6\text{H}_5\text{Me}$), 77.1 (quaternary C of Cp*), 88.7 (quaternary C of Cp*), 89.4 (CH of $\text{C}_6\text{H}_5\text{Me}$), 90.9 (CH

of C₆H₅Me), 94.4 (CH of C₆H₅Me), 216.0 (CO). IR (thin film CH₂Cl₂, cm⁻¹) : ν(CO) 1922 st, 1970 st. MS EI : *m/z* 743.1 {3 %, [Cp*Fe(CO)₂InI₃]⁺}.

4.3.2 Results and Discussion

Aldridge *et al.* have previously demonstrated that insertion of 'Gal' into the M-X bond of CpFe(CO)₂I or into the M-M bond of [Cp*Fe(CO)₂]₂ leads to the formation of the dimeric complexes of the type [(η⁵-C₅R₅)Fe(CO)₂Gal₂]₂.³ We have sought to extend this approach to heavier group 13 systems in an attempt to synthesise analogous complexes of the type [Cp*Fe(CO)₂EX₂]₂ (where E = In), with the aim of investigating the subsequent substitution chemistry of the CO ligands at the metal centre.

The attempted synthesis of [Cp*Fe(CO)₂InI₂]₂ was performed in an analogous fashion to that used for [(η⁵-C₅R₅)Fe(CO)₂Gal₂]₂. However, addition of Cp*Fe(CO)₂I to a suspension of InI in toluene unexpectedly yielded [Cp*Fe(toluene)]⁺[Cp*Fe(CO)₂InI₃]⁻ **4.16** as an orange microcrystalline solid (Scheme 4.11).²⁶



Scheme 4.11 Synthetic route to complex **4.16**.

The proposed formulation is supported by multinuclear NMR and IR data, in which the ¹H NMR displays peaks corresponding to two CH₃ Cp* fragments, and one

CH₃ and three aromatic CH moieties of the toluene fragment at chemical shifts of 1.83, 1.88, 2.32, 5.31, 5.57, and 5.75 with relative intensities of 15:15:3:2:1:2, respectively. ¹³C NMR data is consistent with the presence of two Cp* fragments, CH₃ and CH toluene moieties and a CO fragment. The measured CO stretching frequencies [$\nu(\text{CO}) = 1970$ and 1922 cm^{-1}] are consistent with the formation of a carbonyl containing species, although this region of the spectrum is complicated by bands due to the coordinated toluene molecule.

Determination of the nature of **4.16** was ultimately dependent on crystallographic data; single crystals suitable for X-ray diffraction were obtained by layering a concentrated toluene solution with hexanes and storage at -30°C . The structure of **4.16** is illustrated in Figure 4.7; relevant bond lengths and angles are listed in Table 4.9.

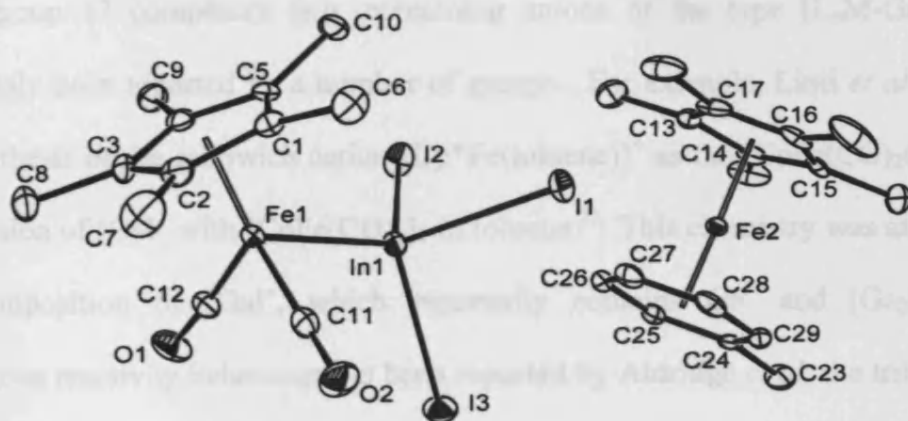


Figure 4.7 The molecular structure of $[\text{Cp}^*\text{Fe}(\text{toluene})]^+ [\text{Cp}^*\text{Fe}(\text{CO})_2\text{InI}_3]^-$ **4.16**.

Table 4.9 Selected bond lengths [Å] and angles [°] for **4.16**.

Fe(1)-In(1)	2.5275(9)	I(3)-In(1)	2.8060(6)
I(1)-In(1)	2.7943(6)	C(11)-O(2)	1.148(8)
I(2)-In(1)	2.8045(6)	C(11)-Fe(1)	1.749(2)
O(2)-C(11)-Fe(1)	176.4(6)	I(1)-In(1)-I(2)	101.091(17)
O(1)-C(12)-Fe(1)	175.8(6)	Fe(1)-In(1)-I(3)	114.56(2)
C(12)-Fe(1)-In(1)	85.2(2)	I(1)-In(1)-I(3)	101.118(19)
Fe(1)-In(1)-I(1)	115.62(3)	I(2)-In(1)-I(3)	101.139(18)
Fe(1)-In(1)-I(2)	120.46(3)	∠ centroid-Fe(1)-In(1)-I(3)	178.9(3)

4.16 adopts a salt-like structure featuring the metallated trihaloindate ion $[\text{Cp}^*\text{Fe}(\text{CO})_2\text{InI}_3]^-$, thereby confirming insertion of an InI unit into the Fe-I bond. The tendency of related systems to yield corresponding salt-like transition metal/group 13 complexes (*e.g.* containing anions of the type $[\text{L}_n\text{M}-\text{GaX}_3]^-$) has previously been reported by a number of groups. For example, Linti *et al.*, reported the synthesis of the sandwich cation $[\text{Cp}^*\text{Fe}(\text{toluene})]^+$ as the $[\text{CpFe}(\text{CO})_2\text{GaI}_3]^-$ salt, by reaction of 'Gal' with $[\text{CpFe}(\text{CO})_2]_2$ in toluene.²⁷ This chemistry was attributed to the composition of 'Gal', which reportedly contains Ga^+ and $[\text{Ga}_2\text{I}_6]^{2-}$ ions. Analogous reactivity behaviour has been reported by Aldridge *et al.*; the trihalogallate ion $[\text{CpFe}(\text{CO})_3]^+[\text{Cp}^*\text{Fe}(\text{CO})_2\text{Ga}(\text{I})\text{Br}_2]^-$ **4.17** has been synthesised by the reaction of 'Gal' with $\text{CpFe}(\text{CO})_2\text{I}$ in a reaction which is strongly dependant on the choice of solvent system.²⁶ In a similar fashion, the analogous trihalogallate salts $[\text{Et}_3\text{NH}]^+[\text{CpFe}(\text{CO})_2\text{GaI}_3]^-$ **4.18**, $[\text{tmpH}_2]^+[\text{CpFe}(\text{CO})_2\text{GaBr}_3]^-$ **4.19**, and $[\text{tmpH}_2]^+[\text{Cp}^*\text{Fe}(\text{CO})_2\text{GaI}_3]^-$ **4.20** have been isolated from the reactions of $[(\eta^5\text{-C}_5\text{R}_5)\text{Fe}(\text{CO})_2\text{GaI}\text{Br}_2]$ with Et_3N or $\text{Li}[\text{tmp}]$. Subsequent related work has shown that

reaction of $[\text{CpFe}(\text{CO})_2\text{InBrI}]_2$ with $\text{Li}[\text{tmp}]$ in toluene generates the corresponding salt $[\text{tmpH}_2]^+[\text{CpFe}(\text{CO})_2\text{InBrI}_2]^-$ **4.21** in an analogous fashion to that found for the gallium systems.²⁸

The geometry of **4.16** features a staggered conformation about the Fe-In bond [$\angle_{\text{centroid-Fe}(1)\text{-In}(1)\text{-I}(3)} = 178.9(3)^\circ$], which is consistent to that found for $[\text{tmpH}_2]^+[\text{CpFe}(\text{CO})_2\text{InBrI}_2]^-$ **4.21** (180° , crystallographically enforced). The Fe-In distance [2.528(1) Å] is also consistent with that found for other examples of $[(\eta^5\text{-C}_5\text{R}_5)\text{Fe}(\text{CO})_2]$ fragments bound to four-coordinate indium based ligands {e.g. 2.553(1) Å for $[\text{CpFe}(\text{CO})_2]_4\text{In}_2(\mu\text{-Cl})_2$ }.²⁹

4.4 Molybdenum Containing Systems

4.4.1 Experimental

*Synthesis of $[(\eta^7\text{-C}_7\text{H}_7)\text{Mo}(\text{CO})_2\text{GaI}_2]_2$ (**4.22**)*

To a suspension of 'Gal' prepared by sonicating gallium (1.057 g, 15.16 mmol) and I_2 (1.925 g, 7.58 mmol) in toluene (50 cm³) for 16 h at 30°C was added a solution of $(\eta^7\text{-C}_7\text{H}_7)\text{Mo}(\text{CO})_2\text{I}$ (2.003 g, 5.41 mmol) also in toluene (100 cm³). The reaction mixture was stirred at room temperature for 72 h leading to the formation of a red solution and dark purple precipitate. The precipitate was isolated, recrystallised from dichloromethane (300 cm³) by cooling to -30°C, isolated by filtration and dried *in vacuo*. Crystals suitable for X-ray diffraction, were obtained at -30°C from a concentrated solution in dichloromethane. Isolated yield, 1.108 g, 36 %. ¹H NMR (300 MHz, CD₂Cl₂) : δ_{H} 5.60 (s, 14H, CH of $(\eta^7\text{-C}_7\text{H}_7)$). ¹³C NMR (76 MHz, CD₂Cl₂) : δ_{C} 93.5 (CH of $(\eta^7\text{-C}_7\text{H}_7)$), carbonyl carbon not observed. IR (thin film CD₂Cl₂, cm⁻¹) : $\nu(\text{CO})$ 2001 st, 1952 st. MS (negative ion CI): m/z 694.6 {3 %, $[(\eta^7\text{-$

$\text{C}_7\text{H}_7\text{Mo}(\text{CO})_2\text{GaI}_3\text{]}^-$ }, 567.2 {2 %, $[(\eta^7\text{-C}_7\text{H}_7)\text{Mo}(\text{CO})_2\text{GaI}_2\text{]}^-$ }; (EI): m/z 567.7 {1 %, $[(\eta^7\text{-C}_7\text{H}_7)\text{Mo}(\text{CO})_2\text{GaI}_2\text{]}^+$ }, 539.7 {1 %, $[(\eta^7\text{-C}_7\text{H}_7)\text{Mo}(\text{CO})\text{GaI}_2\text{]}^+$ }, 511.7 {2 %, $[(\eta^7\text{-C}_7\text{H}_7)\text{MoGaI}_2\text{]}^+$ }. Exact mass (negative ion CI): Calcd. 539.6902 $[(\eta^7\text{-C}_7\text{H}_7)\text{Mo}(\text{CO})\text{GaI}_2\text{]}^-$; measd. 539.6904.

Synthesis of $[(\eta^7\text{-C}_7\text{H}_7)\text{Mo}(\text{CO})_2\text{GaI}_2]_2(\mu\text{-dppe})$ (4.23)

A solution of dppe (0.779 g, 1.96 mmol) in toluene (150 cm³) was added to a solution of $[(\eta^7\text{-C}_7\text{H}_7)\text{Mo}(\text{CO})_2\text{GaI}_2]_2$ 4.22 (1.108 g, 0.98 mmol) in toluene (150 cm³) at 20°C with the immediate formation of a light red precipitate. The sparingly soluble precipitate was extracted into dichloromethane (500 cm³) and filtered; the resulting dark orange solution was concentrated *in vacuo*, and a red solid was obtained at –30°C. Crystals suitable for X-ray diffraction were obtained from the concentrated solution at –30°C. Isolated yield, 0.383 g, 26 %. ¹H NMR (300 MHz, CD₂Cl₂) : δ_{H} 2.55 (m, 2H, CH₂ of dppe), 2.92 (m, 2H, CH₂ of dppe), 5.18 (s, 7H, ($\eta^7\text{-C}_7\text{H}_7$)), 7.23 (m, 8H, aromatic CH of dppe), 7.49 (m, 8H, aromatic CH of dppe), 7.62 (m, 4H, aromatic CH of dppe). ³¹P NMR (122 MHz, CD₂Cl₂) : δ_{P} –28 b. IR (thin film CD₂Cl₂, cm⁻¹) : $\nu(\text{CO})$ 1982 st, 1928 st. MS (EI): m/z 712.0 {5 %, $[(\eta^7\text{-C}_7\text{H}_7)\text{Mo}(\text{CO})_2\text{Ga}(\text{dppe})\text{]}^+$ }. The extremely low solubility of $[(\eta^7\text{-C}_7\text{H}_7)\text{Mo}(\text{CO})_2\text{GaI}_2]_2(\mu\text{-dppe})$ in compatible solvents precluded the measurement of reliable ¹³C NMR spectra.

Reaction of $[(\eta^7\text{-C}_7\text{H}_7)\text{Mo}(\text{CO})_2\text{GaI}_2]_2(\mu\text{-dppe})$ with dppe: attempted synthesis of $(\eta^7\text{-C}_7\text{H}_7)\text{Mo}(\text{dppe})\text{GaI}_2$

A solution of dppe (0.055 g, 0.138 mmol) in toluene (20 cm³) was added to a suspension of $[(\eta^7\text{-C}_7\text{H}_7)\text{Mo}(\text{CO})_2\text{GaI}_2]_2(\mu\text{-dppe})$ **4.23** (0.383 g, 0.276 mmol) in toluene (40 cm³). The reaction mixture was heated to 80°C for 12 h, filtered and the volatiles removed *in vacuo*, yielding a brown oil. Extraction into benzene (20 cm³) and concentration of the resulting orange solution yielded a small quantity of crystals of $[\{(\eta^7\text{-C}_7\text{H}_7)\text{Mo}(\text{CO})_2\text{Ga}\}_2(\mu\text{-OGaI}_3)\{\mu\text{-OGaI}(\text{OH})_2\}]_2$ **4.24** suitable for X-ray diffraction. **4.24** presumably results from the presence of adventitious water in the reaction mixture. Due to the low yield of the reaction and problems associated with replicating the reaction conditions, spectroscopic data was not obtained.

Reaction of $(\eta^7\text{-C}_7\text{H}_7)\text{Mo}(\text{dppe})\text{I}$ with ‘Gal’ isolation of $[(\eta^7\text{-C}_7\text{H}_7)\text{Mo}(\text{dppe})\text{Cl}]^+[\text{GaCl}_4]^-$ (**4.25**)

To a suspension of ‘Gal’ synthesised by sonicating gallium (0.507 g, 7.272 mmol) and I₂ (0.923 g, 3.637 mmol) in toluene (50 cm³) for 16 hrs at 30°C was added a solution of $(\eta^7\text{-C}_7\text{H}_7)\text{Mo}(\text{dppe})\text{I}$ (1.296 g, 1.819 mmol) in toluene (100 cm³), the reaction mixture was stirred at room temperature for 7 d with the formation of a brown solution and purple precipitate. The purple precipitate was extracted into dichloromethane and filtered whereupon the solution turned yellow. Exact mass (negative ion ES): Calcd. 208.8015 [GaCl₄]⁻; measd. 208.8018. Correct isotope distribution one molybdenum, one chloride, and two phosphorus atoms. Exact Mass (ES +ve): Calcd. 616.0652 $[(\eta^7\text{-C}_7\text{H}_7)\text{Mo}(\text{dppe})\text{Cl}]^+$; measd. 616.0652. Correct isotope distribution one gallium and four chloride atoms. Due to the low yield of the

reaction and problems associated with crystallization spectroscopic data was not obtained.

Reaction of $[(\eta^7\text{-C}_7\text{H}_7)\text{Mo}(\text{CO})_2\text{GaI}_2]_2$ with PCy_3 isolation of $[\text{Cy}_3\text{PH}]^+[(\eta^7\text{-C}_7\text{H}_7)\text{Mo}(\text{CO})_2\text{GaI}_3]^-$ (4.26)

A solution of PCy_3 (0.446 g, 1.590 mmol) in toluene (20 cm³) was added to a solution/suspension of $[(\eta^7\text{-C}_7\text{H}_7)\text{Mo}(\text{CO})_2\text{GaI}_2]_2$ **4.22** (0.818 g, 0.722 mmol) in toluene (30 cm³). The reaction mixture was heated to 55°C for 39 h, filtered and concentrated to yield red crystals of **4.26** suitable for X-ray diffraction after storage at -30°C. Isolated yield, 0.134 g, 19 %. ¹H NMR (300 MHz, CD₂Cl₂) : δ_{H} 0.95-2.42 (Cy₃), 4.95 (s, 7H, ($\eta^7\text{-C}_7\text{H}_7$)). ¹³C NMR (76 MHz, CD₂Cl₂) : δ_{C} 24.5 (CH₂ of Cy₃), 26.3 (CH₂ of Cy₃), 28.3 (CH₂ of Cy₃), 28.9 (CH₂ of Cy₃), 32.1 (CH₂ of Cy₃), 32.2 (CH₂ of Cy₃), 92.1 (CH of ($\eta^7\text{-C}_7\text{H}_7$)), carbonyl carbon not observed. ³¹P NMR (122 MHz, CD₂Cl₂) : δ_{P} -30 b. IR (thin film CH₂Cl₂, cm⁻¹) : $\nu(\text{CO})$ 1970 st, 1914 st. MS (ES +ve): m/z 281.3 {100 %, $[\text{Cy}_3\text{PH}]^+$ }. Due to the low yield of the reaction full spectroscopic data was not obtained.

Reaction of MesLi with $[(\eta^7\text{-C}_7\text{H}_7)\text{Mo}(\text{CO})_2\text{GaI}_2]_2$ isolation of $[(\text{thf})_4\text{Li}]^+[(\eta^7\text{-C}_7\text{H}_7)\text{Mo}(\text{CO})_2\text{GaI}_3]^-$ (4.27)

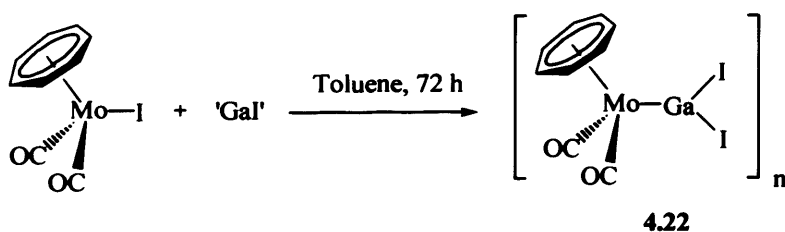
A suspension of MesLi (0.067 g, 0.531 mmol) in toluene (50 cm³) was added to a solution/suspension of $[(\eta^7\text{-C}_7\text{H}_7)\text{Mo}(\text{CO})_2\text{GaI}_2]_2$ **4.22** (0.300 g, 0.265 mmol) also in toluene (50 cm³), and the reaction mixture stirred at room temperature for 96 h. The resulting dark orange precipitate was isolated by filtration and extracted into thf. Crystals suitable for X-ray diffraction were obtained from a layering of a concentrated

thf solution with hexanes at -30°C . Due to the low yield of the reaction and problems associated with crystallization spectroscopic data was not obtained.

4.4.2 Results and Discussion

Green *et al.* have previously reported the synthesis of the complexes $[(\eta^5\text{-C}_5\text{H}_4\text{Me})\text{Mo}(\text{CO})_3\text{GaI}_2\cdot\text{Et}_2\text{O}]$ **4.28**, and $[(\eta^7\text{-C}_7\text{H}_7)\text{Mo}(\text{CO})_2\text{GaI}_2\cdot\text{thf}]$ **4.29** by insertion of 'Gal' into the Mo-I bond of the corresponding molybdenum carbonyl complex.⁴ We sought to extend this methodology by investigating the substitution of the CO groups within related molybdenum gallyl complexes. The synthetic pathway investigated during this study therefore involves a two-step methodology: insertion of 'Gal' into the metal-halogen bond of a metal carbonyl complex followed by substitution of the CO ligands by a chelating phosphine.

Reaction of $(\eta^7\text{-C}_7\text{H}_7)\text{Mo}(\text{CO})_2\text{I}$ with 'Gal' proceeds as expected *via* insertion of 'Gal' into the Mo-I bond yielding the gallium species $[(\eta^7\text{-C}_7\text{H}_7)\text{Mo}(\text{CO})_2\text{GaI}_2]_n$ **4.22** in modest yield (*ca.* 36%) after recrystallisation from dichloromethane (Scheme 4.12).³⁰



Scheme 4.12 Synthetic route to complex **4.22**.

The proposed formulation is supported by ^1H and ^{13}C NMR and IR data, in which the ^1H NMR reveals a single proton environment corresponding to the $\eta^7\text{-C}_7\text{H}_7$

ring. The measured CO stretching frequencies (2001, 1952 cm^{-1}) are consistent with the formation of a carbonyl containing species. Mass spectroscopy provides evidence of a GaI_2 -containing species; EI mass spectra display weak peaks for the parent $[\text{M}]^+$ ion (where $\text{M} = (\eta^7\text{-C}_7\text{H}_7)\text{Mo}(\text{CO})_2\text{GaI}_2$) with fragment peaks corresponding to the $[\text{M-CO}]^+$ and $[\text{M-2CO}]^+$ ions; the isotope distribution is as expected for a complex containing one molybdenum, one gallium, two iodine and two oxygen atoms.

Experience with the corresponding iron-containing systems, such as $[\text{Cp}^*\text{Fe}(\text{CO})_2\text{GaI}_2]_2$, have revealed aggregation of the putative diiodogallyl complex to form a dimer.³ Definitive identification of a metal-gallium bond and of the state of aggregation of the diiodogallyl complex in **4.22** was therefore dependant on crystallographic data. Single crystals of **4.22** suitable for X-ray diffraction were accessible by cooling a concentrated solution in toluene to -30°C . The structure of **4.22** is illustrated in Figure 4.8; relevant bond lengths and angles are listed in Table 4.10. The crystal structure confirms that the complex exists as dimeric units in the solid state with the formulation $[(\eta^7\text{-C}_7\text{H}_7)\text{Mo}(\text{CO})_2\text{GaI}_2]_2$.

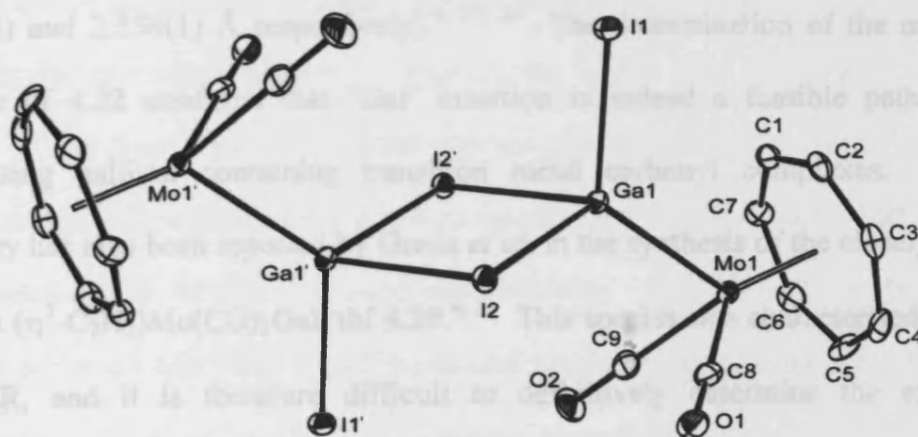


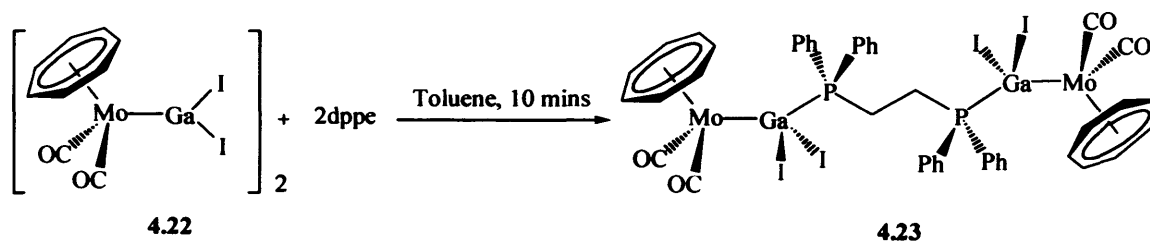
Figure 4.8 The molecular structure of $[(\eta^7\text{-C}_7\text{H}_7)\text{Mo}(\text{CO})_2\text{GaI}_2]_2$ **4.22**.

Table 4.10 Selected bond lengths (Å) and angles (°) for **4.22**.

Mo(1)-Ga(1)	2.577(1)	Mo(1)-C(8)	2.010(6)
Mo(1)-centroid	1.651(6)	Ga(1)-I(1)	2.619(1)
Ga(1)-I(2)	2.764(1)	Ga(1)-I(2')	2.807(1)
Mo(1)-Ga(1)-I(1)	125.9(4)	Mo(1)-Ga(1)-I(2)	120.0(1)
Mo(1)-Ga(1)-I(2')	116.9(1)	I(1)-Ga(1)-I(2)	98.1(1)
I(1)-Ga(1)-I(2')	98.6(1)	I(2)-Ga(1)-I(2')	89.7(1)

The molecular structure of **4.22** features dimeric $[(\eta^7\text{-C}_7\text{H}_7)\text{Mo}(\text{CO})_2\text{GaI}_2]_2$ units in which each $(\eta^7\text{-C}_7\text{H}_7)\text{Mo}(\text{CO})_2\text{GaI}_2$ fragment is linked to the other through the bridging iodine ligands of the $\text{Ga}(\mu\text{-I})_2\text{Ga}$ core. The coordination geometry about each gallium centre is slightly distorted from tetrahedral, featuring Mo-Ga-I angles of 125.9(4), 120.0(3) and 116.9(3)°, and I-Ga-I angles of 98.2(3), 98.6(4) and 89.7(3)°. The narrower I-Ga-I angle of *ca.* 90° associated with the bridging iodine atoms finds precedent in the structures of related systems {*e.g.* 92.01(2)° in $[\text{Cp}^*\text{Fe}(\text{CO})_2\text{GaI}_2]_2$ }. The Mo-Ga bond length of 2.5771(11) Å is similar to those reported within the complexes $[(\eta^5\text{-C}_5\text{H}_4\text{Me})\text{Mo}(\text{CO})_3\text{GaI}_2\cdot\text{Et}_2\text{O}]$ **4.28** and *cis*- $\text{Mo}(\text{Cp}^*\text{Ga})_2(\text{CO})_4$ **4.30** [2.582(2) and 2.554(1) Å respectively].^{4, 31, 32} The determination of the molecular structure of **4.22** confirms that ‘Gal’ insertion is indeed a feasible pathway for synthesising gallium containing transition metal carbonyl complexes. Similar chemistry has also been reported by Green *et al.* in the synthesis of the closely related complex $(\eta^7\text{-C}_7\text{H}_7)\text{Mo}(\text{CO})_2\text{GaI}_2\cdot\text{thf}$ **4.29**.^{4, 31} This species was characterised only by ¹H NMR, and it is therefore difficult to definitively determine the extent of aggregation of this complex and/or the lability of the coordinated thf molecule.

In order to complete the two-step synthesis of $[(\eta^7\text{-C}_7\text{H}_7)\text{M}(\text{PR}_3)_2\text{GaI}_2]_n$, **4.22** was further reacted with the potentially chelating phosphine ligand dppe. Photolytically or thermally initiated substitution reactions of $(\eta^7\text{-C}_7\text{H}_7)\text{M}(\text{CO})_2\text{X}$ with phosphines have been previously reported in the literature.³³ However, on addition of dppe to **4.22** at room temperature an immediate reaction resulted with the formation of copious amounts of a red precipitate, which was subsequently determined crystallographically to contain the dinuclear phosphine bridged species $[(\eta^7\text{-C}_7\text{H}_7)\text{Mo}(\text{CO})_2\text{GaI}_2]_2(\mu\text{-dppe})$ **4.23** (Scheme 4.13).



Scheme 4.13 Synthetic route to complex **4.23**.

Previous work with iron-containing systems is consistent with initial formation of $\text{R}_3\text{P} \rightarrow \text{Ga}(\text{III})$ adducts, but has shown that subsequent photolysis can lead to migration of the phosphine donor from gallium to the transition metal on loss of CO, with the phosphine ultimately coordinating to the iron centre in a chelating fashion. It was found that the dinuclear species **4.23** is only very sparingly soluble in organic solvents, in which it does not decompose. In addition it was found that **4.23** is not amenable to further photo-induced reactivity. The ^1H and ^{31}P NMR data obtained are consistent with a gallium-bound phosphine containing species [broad resonance at $\delta_{\text{P}} -28$, cf. -41 for the analogous phosphorus centre in $\text{Cp}^*\text{Fe}(\text{CO})(\mu\text{-dppe})\text{GaI}_2$]. IR measured carbonyl stretching frequencies (1982 and 1928 cm^{-1})

indicate retention of the $\text{Mo}(\text{CO})_2$ fragment within the complex, and therefore that phosphine substitution has not occurred at the molybdenum centre. Single crystals suitable for X-ray diffraction were accessible by cooling a concentrated solution of **4.23** in toluene to -30°C . The spectroscopic data for **4.23** was confirmed by single crystal X-ray diffraction studies and the structure is illustrated in Figure 4.9. Relevant bond lengths and angles are listed in Table 4.11.

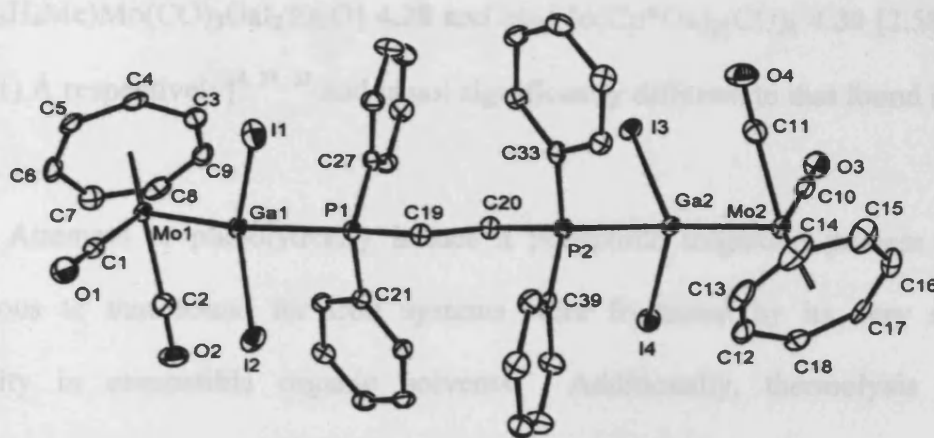


Figure 4.9 The molecular structure of $[(\eta^7\text{-C}_7\text{H}_7)\text{Mo}(\text{CO})_2\text{GaI}_2]_2\mu\text{-dppe}$ **4.23**.

Table 4.11 Selected bond lengths (Å) and angles ($^\circ$) for **4.23**.

Mo(1)-Ga(1)	2.577(1)	Mo(1)-C(1)	1.997(5)
Mo(1)-centroid	1.660(5)	Ga(1)-I(1)	2.632(1)
Ga(1)-I(2)	2.650(1)	Ga(1)-P(1)	2.467(2)
Mo(1)-Ga(1)-I(1)	118.2(1)	Mo(1)-Ga(1)-I(2)	122.4(1)
Mo(1)-Ga(1)-P(1)	119.8(1)	I(1)-Ga(1)-I(2)	100.7(1)
I(1)-Ga(1)-P(1)	97.9(1)	I(2)-Ga(1)-P(1)	92.3(1)

The molecular structure of **4.23** features the dppe ligand acting as a bridging ligand between two $(\eta^7\text{-C}_7\text{H}_7)\text{Mo}(\text{CO})_2\text{GaI}_2$ units; the 1:2 dppe:Mo ratio in the product (*cf.* the 2:1 reaction stoichiometry) is presumably driven by the insolubility of **4.23**. The coordination geometry about the Ga centre is distorted tetrahedral with Mo-Ga-I angles of 118.21(3) and 122.39(3) $^\circ$ and significantly narrower P-Ga-I angles of 92.3(4) and 97.9(5) $^\circ$. This geometry at gallium is similar to that found in **4.22**. The Mo-Ga bond length of 2.5814(9) is within the range reported for the complexes $[(\eta^5\text{-C}_5\text{H}_4\text{Me})\text{Mo}(\text{CO})_3\text{GaI}_2\cdot\text{Et}_2\text{O}]$ **4.28** and *cis*- $\text{Mo}(\text{Cp}^*\text{Ga})_2(\text{CO})_4$ **4.30** [2.582(2) and 2.554(1) Å respectively]^{4, 31, 32} and is not significantly different to that found in **4.22**.

Attempts to photolytically induce a phosphine migration process for **4.23** analogous to that found for iron systems were frustrated by its very sparingly solubility in compatible organic solvents. Additionally, thermolysis of **4.23** invariably resulted in decomposition. It was found that further reaction of $[(\eta^7\text{-C}_7\text{H}_7)\text{Mo}(\text{CO})_2\text{GaI}_2]_2(\mu\text{-dppe})$ **4.23** with dppe at 80 $^\circ\text{C}$ yielded a small quantity of crystals suitable for X-ray diffraction, the molecular structure of which was determined crystallographically as $[\{(\eta^7\text{-C}_7\text{H}_7)\text{Mo}(\text{CO})_2\text{Ga}\}_2(\mu\text{-OGaI}_3)\{\mu\text{-OGaI}(\text{OH})_2\}]_2$ **4.24**. This compound presumably arises from the reaction of $[(\eta^7\text{-C}_7\text{H}_7)\text{Mo}(\text{CO})_2\text{GaI}_2]_2(\mu\text{-dppe})$ **4.23** with adventitious water. However, due to the low yield of the reaction and problems associated with replicating the reaction conditions, spectroscopic data was not obtained. The molecular structure of **4.24** is illustrated in Figure 4.10. Relevant bond lengths and bond angles for **4.24** are listed in Table 4.12.

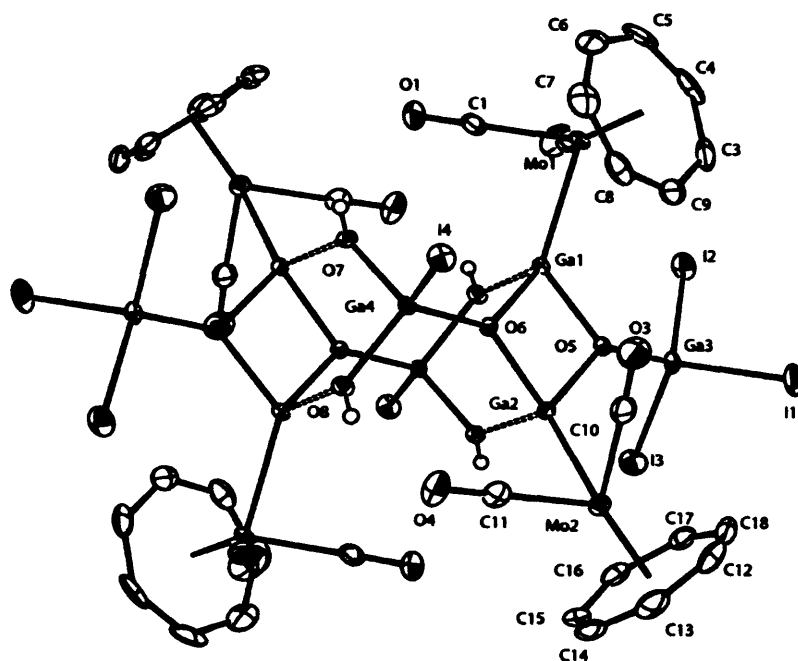


Figure 4.10 The molecular structure of



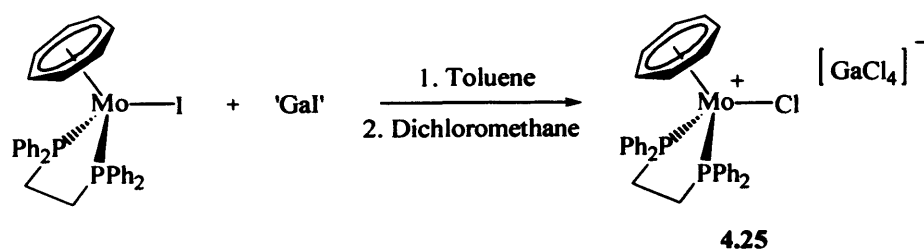
Table 4.12 Selected bond lengths (Å) and angles (°) for **4.24**.

Mo(1)-Ga(1)	2.5478(10)	Mo(2)-Ga(2)	2.5646(8)
Ga(1)-O(5)	1.922(3)	Ga(3)-I(2)	2.5334(9)
Ga(3)-I(1)	2.5367(10)		
O(5)-Ga(1)-O(6)	81.69(11)	Mo(1)-Ga(1)-Ga(2)	147.30(3)
O(5)-Ga(1)-Mo(1)	127.68(8)	O(5)-Ga(3)-I(2)	111.26(8)
O(5)-Ga(1)-Ga(2)	40.83(8)	I(2)-Ga(3)-I(1)	106.79(3)

The molecular structure of **4.24** consists of dinuclear $[\{(\eta^7\text{-C}_7\text{H}_7)\text{Mo}(\text{CO})_2\text{Ga}\}_2(\mu\text{-OGaI}_3)\{\mu\text{-OGaI}(\text{OH})_2\}]_2$ units, which are further aggregated into tetra-molybdenum clusters *via* Ga-O(H)-Ga bridges. The coordination geometry about each molybdenum-bound gallium centre is approximately tetrahedral with Mo-

Ga-O angles of 127.7(1), 127.7(1), and 122.9(1) $^{\circ}$ for Ga(1). The Mo-Ga bond length of 2.541 Å (mean) is similar to those reported for the complexes (η^5 -C₅H₄Me)Mo(CO)₃GaI₂·Et₂O **4.28** and *cis*-Mo(Cp*Ga)₂(CO)₄ **4.30** [2.582(2) and 2.554(1) Å respectively].^{4, 31, 32} On the other hand, the Ga-O bond lengths for **4.24** [1.922(3), 1.941(3) and 1.983(3) Å for Ga(1)] are somewhat shorter than that reported for (η^5 -C₅H₄Me)Mo(CO)₃GaI₂·Et₂O **4.28** [2.04(1) Å], with the Ga-O(H)Ga distance [1.983(3) Å] being significantly longer than those associated with the Ga(μ_3 -O) units [1.922(3), 1.941(3) Å].

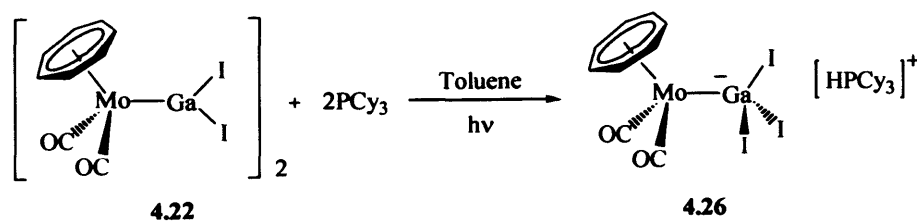
A second synthetic route to the formation of (η^7 -C₇H₇)Mo(dppe)GaI₂ was investigated, which involved insertion of 'Gal' into the Mo-I bond of (η^7 -C₇H₇)Mo(dppe)I. Addition of (η^7 -C₇H₇)Mo(dppe)I to a suspension of 'Gal' in toluene resulted in the formation of purple precipitate after 7 days stirring at 20 $^{\circ}$ C. Due to the lack of solubility, the only solvent into which the compound was sparingly soluble was dichloromethane, however, on addition there was an immediate reaction with the formation of a yellow solution, yielding [(η^7 -C₇H₇)Mo(dppe)Cl]⁺[GaCl₄]⁻ **4.25** as a microcrystalline solid (Scheme 4.14).



Scheme 4.14 Synthetic route to **4.25**.

The ES mass spectrum of **4.25** displays strong peaks for the parent ions; ES⁺ cone 10V [(η⁷-C₇H₇)Mo(dppe)Cl]⁺ and ES⁻ cone 10V [GaCl₄]⁻. The isotope distribution observed is consistent with a positively charged fragment containing one chlorine, one molybdenum and two phosphorus atoms and a negatively charged fragment containing one gallium and four chlorine atoms. Single crystals were obtained from a saturated dichloromethane solution of **4.25** layered with hexanes; unfortunately the structure could not be unequivocally solved, although preliminary solutions were consistent with the mass spectral data.

The reaction of [(η⁷-C₇H₇)Mo(CO)₂GaI₂]₂ **4.22** with non chelating phosphines such as PCy₃ was also examined, with the aim of substituting one or both CO groups on the transition metal centre. In addition the use of PCy₃ was investigated with a view to increasing the solubility (compared to dppe) of any initially formed phosphine/gallane adducts. However, photolysis of [(η⁷-C₇H₇)Mo(CO)₂GaI₂]₂ **4.22** with PCy₃ in toluene yielded instead the salt [Cy₃PH]⁺[(η⁷-C₇H₇)Mo(CO)₂GaI₃]⁻ **4.26** (18 %) in modest yield (Scheme 4.15).



Scheme 4.15 Synthetic route to complex **4.26**.

Multinuclear NMR and IR data support the proposed formulation in which the ¹³C NMR spectrum confirmed the presence of the cyclohexyl and η⁷-C₇H₇ moieties. IR spectroscopy revealed two strong CO stretches at 1970 and 1941 cm⁻¹ confirming

retention of the $\text{Mo}(\text{CO})_2$ fragment. ^{31}P NMR data showed the presence of a phosphorus containing species with a broad peak at δ -30. Determination of the nature of **4.26** was ultimately dependent on crystallographic data. Single crystals suitable for X-ray diffraction were accessible by cooling a concentrated solution of **4.26** in toluene at -30°C . The molecular structure of the anionic component of **4.26** is illustrated in Figure 4.11 and the relevant bond lengths and angles are listed in Table 4.13.

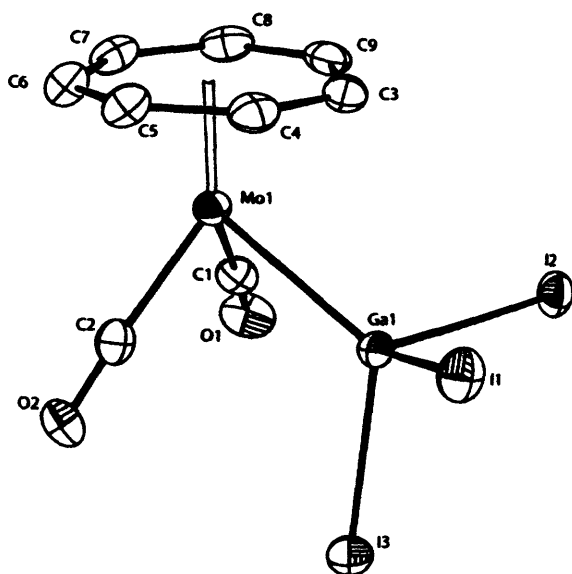


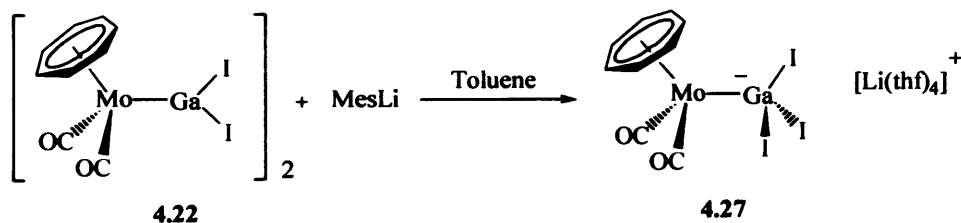
Figure 4.11 The molecular structure of $[\text{Cy}_3\text{PH}]^+[(\eta^7\text{-C}_7\text{H}_7)\text{Mo}(\text{CO})_2\text{GaI}_3]^-$
($[\text{Cy}_3\text{PH}]^+$ omitted) **4.26**.

Table 4.13 Selected bond lengths (Å) and angles ($^\circ$) for **4.26**.

Mo(1)-Ga(1)	2.6015(17)	Ga(1)-I(2)	2.6760(12)
Ga(1)-I(3)	2.6235(16)	Ga(1)-I(1)	2.6817(16)
Mo(1)-Ga(1)-I(3)	124.36(6)	Mo(1)-Ga(1)-I(2)	112.47(6)
I(3)-Ga(1)-I(2)	101.66(6)	Mo(1)-Ga(1)-I(1)	111.72(6)

The anion features an approximately staggered conformation about the Mo-Ga bond [$\angle(\eta^7\text{-C}_7\text{H}_7)\text{centroid-Mo(1)-Ga(1)-I(3)} = 177.8^\circ$] presumably on steric grounds. This geometry is consistent with those observed previously for the related species $[\text{CpFe}(\text{CO})_2\text{GaI}_3]^-$, $[\text{CpFe}(\text{CO})_2\text{GaBr}_2\text{I}]^-$, and $[\text{Cp}^*\text{Fe}(\text{CO})_2\text{InI}_3]^-$.²⁸ The Mo-Ga distance of 2.602(2) Å is slightly longer than those reported previously for related species featuring a four-coordinate iodo-gallium ligand bound to molybdenum (*cf.* Mo-Ga distances of 2.582(2) and 2.577(1) Å for $(\eta^5\text{-C}_5\text{H}_4\text{Me})\text{Mo}(\text{CO})_3\text{GaI}_2\cdot\text{Et}_2\text{O}$ **4.28** and $(\eta^7\text{-C}_7\text{H}_7)\text{Mo}(\text{CO})_2\text{GaI}_2$ **4.22**, respectively), while the Ga-I distances [2.623(2)-2.682(2) Å] are consistent with those previously reported.⁴

Reaction of MesLi with $(\eta^7\text{-C}_7\text{H}_7)\text{Mo}(\text{CO})_2\text{GaI}_2$ **4.22** was investigated with the aim of synthesising an asymmetric mesityl derivatised halogallyl species, however crystallographic data revealed the structure of the product to be $[(\text{thf})_4\text{Li}]^+[(\eta^7\text{-C}_7\text{H}_7)\text{Mo}(\text{CO})_2\text{GaI}_3]^-$ **4.27** (Scheme 4.16).



Scheme 4.16 Synthetic route to complex **4.27**.

The structure of the anionic component of **4.27** (not shown) is very similar to that found for $[\text{Cy}_3\text{PH}]^+[(\eta^7\text{-C}_7\text{H}_7)\text{Mo}(\text{CO})_2\text{GaI}_3]^-$ **4.26** and related systems, featuring an approximately staggered conformation about the Mo-Ga bond [$\angle(\eta^7\text{-C}_7\text{H}_7)\text{centroid-Mo(1)-Ga(1)-I(3)} = 167.8^\circ$]. As with $[\text{Cy}_3\text{PH}]^+[(\eta^7\text{-C}_7\text{H}_7)\text{Mo}(\text{CO})_2\text{GaI}_3]^-$

4.26 the Mo-Ga distance of 2.606(1) Å is slightly longer than those previously reported for related species,²⁸ while the Ga-I distances [2.639(1)-2.675(1) Å] are consistent with those found for $[\text{Cy}_3\text{PH}]^+[(\eta^7\text{-C}_7\text{H}_7)\text{Mo}(\text{CO})_2\text{GaI}_3]^-$ **4.26**. In addition, it was found that secondary contacts (within the sum of van der Waals radii) involving the iodine atoms and hydrogens of adjacent ($\eta^7\text{-C}_7\text{H}_7$) ligands [for I(1) and I(3)] or $[\text{Li}(\text{thf})_4]^+$ counterions for [for I(2)] may be responsible for the disparity in the measured Ga-I distances observed.

It has been demonstrated that insertion of 'Gal' into Mo-I bonds has proven to be effective in the synthesis of the halogallyl molybdenum species $[(\eta^7\text{-C}_7\text{H}_7)\text{Mo}(\text{CO})_2\text{GaI}_2]_2$ **4.22**. Further attempts to substitute the CO ligands by photolysis in the presence of the phosphine ligands dppe or PCy₃ instead yielded the species $[(\eta^7\text{-C}_7\text{H}_7)\text{Mo}(\text{CO})_2\text{GaI}_2](\mu\text{-dppe})$ **4.23**, $[\text{Cy}_3\text{PH}]^+[(\eta^7\text{-C}_7\text{H}_7)\text{Mo}(\text{CO})_2\text{GaI}_3]^-$ **4.26**.

4.5 Ruthenium Containing Systems

4.5.1 Attempted 'Gal' Insertion into Metal-Halogen Bonds

4.5.1.1 Experimental

Synthesis of CpRu(PPh₃)₂(μ-I)GaI₃ (4.30)

To a suspension of 'Gal' synthesised by sonicating gallium (0.272 g, 3.901 mmol) and I₂ (0.499 g, 1.966 mmol) in toluene (60 cm³) for 16 h at 30°C was added a solution of CpRu(PPh₃)₂Cl (0.939 g, 1.292 mmol) in toluene (100 cm³), and the reaction mixture stirred at room temperature for 16 h with the formation of an orange solution and orange precipitate. The solid was isolated by filtration and recrystallised from dichloromethane (150 cm³) by cooling to -30°C. Crystals suitable for X-ray

diffraction, were obtained at -30°C from a concentrated solution in dichloromethane. Isolated yield, 0.682 g, 42%. ^1H NMR (300 MHz, CD_2Cl_2) : δ_{H} 4.61 (s, 5H, CH of Cp), 7.09 (12H, aromatic CH of PPh_3), 7.27 (12H, aromatic CH of PPh_3), 7.39 (6H, aromatic CH of PPh_3). ^{13}C NMR (76 MHz, CD_2Cl_2) : δ_{C} 80.2 (CH of Cp), 128.3 (aromatic CH of PPh_3), 129.9 (aromatic CH of PPh_3), 133.8 (aromatic CH of PPh_3), 137.5 (aromatic *ipso*-C of PPh_3). ^{31}P NMR (122 MHz, CD_2Cl_2) : δ_{P} 35. MS EI : m/z 556.2 {2 %, $[\text{CpRu}(\text{PPh}_3)\text{I}]^+$ }, 449.7 {30 %, $[\text{GaI}_3]^+$ }, 322.8 {35 %, $[\text{GaI}_2]^+$ }.

Reaction of $\text{CpRu}(\text{PPh}_3)_2(\mu\text{-I})\text{GaI}_3$ with excess 'Gal'

To a suspension of 'Gal' synthesised by sonicating gallium (0.790 g, 11.331 mmol) and I_2 (1.437 g, 5.662 mmol) in toluene (80 cm^3) for 16 h at 30°C was added a solution of $\text{CpRu}(\text{PPh}_3)_2(\mu\text{-I})\text{GaI}_3$ (0.682 g, 0.537 mmol) in toluene (100 cm^3), and the reaction mixture stirred at 60°C for 3 days. The yellow solution was filtered and volatiles removed *in vacuo*. The resulting dark yellow oil was washed with hexane ($2 \times 50\text{ cm}^3$) yielding an orange solid. The solid was dried *in vacuo*, however multiple phosphorus peaks (^{31}P NMR δ_{P} 52, 38) were observed which could not be separated.

Reaction of $\text{CpRu}(\text{dppe})\text{Cl}$ with 'Gal' synthesis of $[\text{CpRu}(\text{dppe})]^+[\text{GaI}_4]^-$ (4.31)

To a suspension of 'Gal' prepared by sonicating gallium (0.581 g, 8.333 mmol) and I_2 (1.057 g, 4.165 mmol) in toluene (60 cm^3) for 16 h at 30°C was added a solution of $\text{CpRu}(\text{dppe})\text{Cl}$ (0.499 g, 0.830 mmol) also in toluene (80 cm^3). The reaction mixture was stirred at room temperature for 72 h with the formation of a pale yellow solution and yellow precipitate. The solution was filtered, and concentrated *in vacuo*, a yellow solid was obtained at -30°C . Crystals suitable for X-ray diffraction were obtained by layering a toluene solution with hexanes and cooling to -30°C . Isolated yield, 0.121

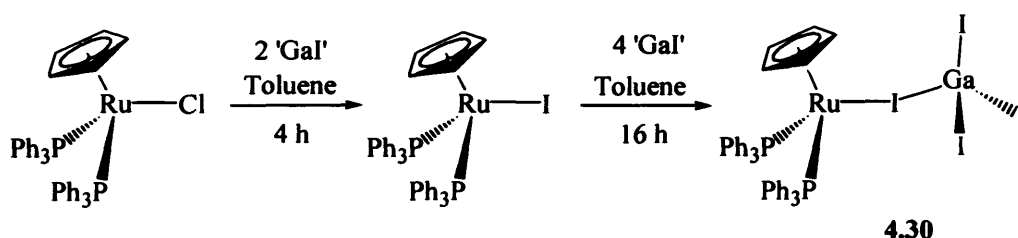
g, 13 %. ^1H NMR (300 MHz, CD_2Cl_2) : δ_{H} 2.51 (m, 2H, CH_2 of dppe), 2.59 (m, 2H, CH_2 of dppe), 4.86 (s, 5H, CH of Cp), 7.16 (8H, aromatic CH of Ph), 7.28 (8H, aromatic CH of Ph), 7.69 (4H, aromatic CH of Ph). ^{13}C NMR (76 MHz, CD_2Cl_2) : δ_{C} 21.2 (CH_2 of dppe), 79.7 (CH of Cp), 128.8 (aromatic CH of Ph), 129.9 (aromatic CH of Ph), 130.7 (aromatic CH of Ph), 134.1 (aromatic *ipso*-C of Ph). ^{31}P NMR (122 MHz, CD_2Cl_2) : δ_{P} 76. MS nanospray: m/z 887.8 {2 %, $[\text{CpRu}(\text{dppe})\text{GaI}_2]^+$ }, 761.0 {2 %, $[\text{CpRu}(\text{dppe})\text{GaI}]^+$ }, 692.1 {64 %, $[\text{CpRu}(\text{dppe})\text{I}]^+$ }, 565.2 {100 %, $[\text{CpRu}(\text{dppe})]^+$ }. Exact mass calcd. 760.9089 $[\text{CpRu}(\text{dppe})]^+$. measd. 760.9089. A small amount of dark orange crystalline material was also obtained from the layering the structure was solved by X-ray diffraction to be the isomeric product $[\text{CpRu}(\text{dppe})(\text{GaI}_4)]_2$ (4.32).

4.5.1.2 Results and Discussion

Direct insertion of 'GaI' into the metal-halogen bond of a phosphine-ligated complex was investigated with respect to the synthesis of systems of the type $[\text{CpRu}(\text{PR}_3)_2\text{GaI}_2]_n$. This route is advantageous in that it involves a single step synthesis from complexes of the type $\text{CpRu}(\text{PR}_3)_2\text{hal}$ which are numerous in the chemical literature.^{3, 4, 31} Relatively forcing conditions were employed (*e.g.* the use of a large excess of 'GaI'), since preliminary studies indicated that the use of equimolar quantities of 'GaI' at room temperature simply yielded the halide substituted species $\text{CpRu}(\text{PPh}_3)_2\text{I}$. Reactions of both $\text{CpRu}(\text{PPh}_3)_2\text{Cl}$ and $\text{CpRu}(\text{dppe})\text{Cl}$ with an excess of 'GaI' appear to follow a similar course and in each case one major product is generated which can be isolated *via* crystallisation from the reaction supernatant, by layering with hexanes and storage at -30°C . In each case ^{31}P NMR data is consistent

with retention of the $\text{Ru}(\text{PR}_3)_2$ fragment, however the mass spectra are consistent with ready fragmentation into GaI_n and $\text{CpRu}(\text{phosphine})_n\text{I}$ moieties

Reaction of $\text{CpRu}(\text{PPh}_3)_2\text{Cl}$ with 'Gal' (four equivalents) yielded the complex $\text{CpRu}(\text{PPh}_3)_2(\mu\text{-I})\text{GaI}_3$ **4.30** (Scheme 4.17), isolated as an orange microcrystalline solid in modest (42%) yield after recrystallisation from dichloromethane. The ^1H and ^{13}C NMR data obtained are consistent with the formation of a species containing Cp and Ph fragments, in which the ^1H NMR data obtained reveals a peak at a chemical shift of 4.61 corresponding to the Cp fragment, multiple peaks with chemical shifts of 7.09, 7.27 and 7.39 corresponding to the phenyl rings of the phosphine moiety were also observed (relative intensities 5:12:12:6). ^{13}C NMR data confirmed the presence of Cp and Ph groups. The ^{31}P NMR revealed a sharp peak at δ_{P} 35 confirming the formation of a phosphine containing species in which the phosphorus atom is bound to the metal centre.



Scheme 4.17 Synthetic route to complex **4.30**.

Identification of the nature of the product was dependent on crystallographic data. Single crystals of **4.30** suitable for X-ray diffraction were accessible by cooling a concentrated solution in dichloromethane at -30°C . The structure of **4.30** is illustrated in Figure 4.12; relevant bond lengths and angles are listed in Table 4.14. The molecular structure reveals a bis(phosphine) half sandwich complex containing a

tetraiodogallate fragment coordinated to the ruthenium centre *via* a single bridging iodine atom. To our knowledge **4.30** represents the first example of transition metal complex containing a coordinated $[\text{GaI}_4]^-$ ligand. Alternatively, **4.30** can be thought of as a Lewis acid/base adduct between $\text{CpRu}(\text{PPh}_3)_2\text{I}$ and GaI_3 .

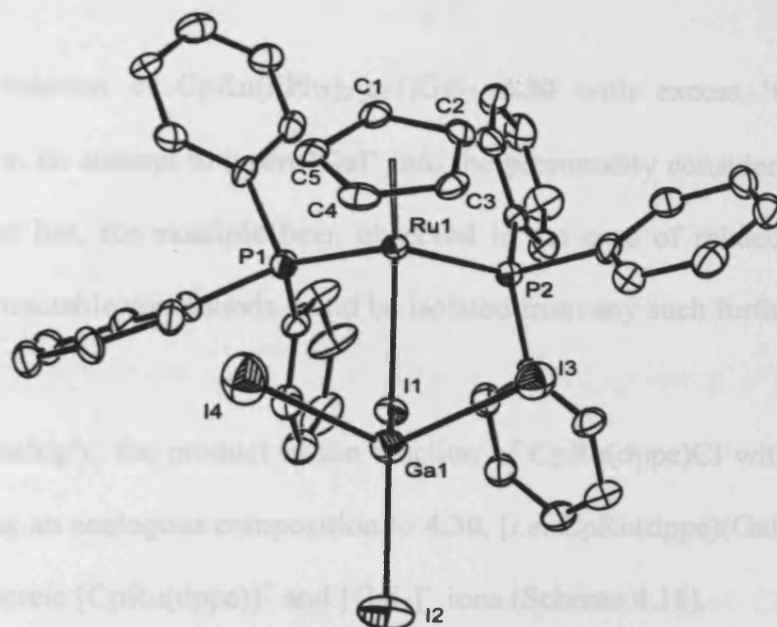


Figure 4.12 The molecular structure of $\text{CpRu}(\text{PPh}_3)_2(\mu\text{-I})\text{GaI}_3$ **4.30**.

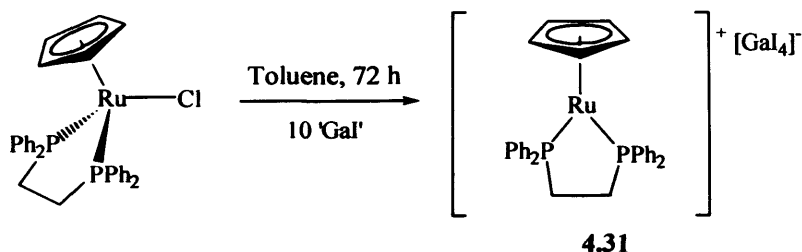
Table 4.14 Selected bond lengths (Å) and angles ($^\circ$) for **4.30**.

Ru(1)-P(1)	2.345(4)	Ru(1)-centroid	1.849(3)
Ru(1)-I(1)	2.742(2)	Ga(1)-I(1)	2.603(2)
Ga(1)-I(2)	2.513(2)	Ga(1)-I(3)	2.533(2)
Ga(1)-I(4)	2.528(2)		
P(1)-Ru(1)-P(2)	102.6(2)	Ru(1)-I(1)-Ga(1)	112.0(1)
I(1)-Ga(1)-I(2)	103.7(1)	I(1)-Ga(1)-I(3)	108.4(1)
I(1)-Ga(1)-I(4)	111.6(1)	I(2)-Ga(1)-I(3)	112.9(1)
I(2)-Ga(1)-I(4)	111.4(1)	I(3)-Ga(1)-I(4)	108.8(1)

The coordination geometry about the gallium centre is approximately tetrahedral with I-Ga-I bond angles of 103.7(1), 111.6(1) and 108.4(1) $^{\circ}$. As expected the Ga-I bond associated with the bridging unit [2.603(2) Å] is considerably longer than the terminal Ga-I linkages [2.513(2), 2.533(2), and 2.528(2) Å].

The reaction of $\text{CpRu}(\text{PPh}_3)_2(\mu\text{-I})\text{GaI}_3$ **4.30** with excess 'Gal' was also investigated in an attempt to insert 'Gal' into the presumably considerably weakened Ru-I bond, as has, for example been observed in the case of related iron systems. However no tractable compounds could be isolated from any such further reaction.

Interestingly, the product of the reaction of $\text{CpRu}(\text{dppe})\text{Cl}$ with 'Gal' (**4.31**), despite having an analogous composition to **4.30**, [*i.e.* $\text{CpRu}(\text{dppe})(\text{GaI}_4)$], is found to consist of discrete $[\text{CpRu}(\text{dppe})]^+$ and $[\text{GaI}_4]^-$ ions (Scheme 4.18).



Scheme 4.18 The Synthetic route to $[\text{CpRu}(\text{dppe})]^+ [\text{GaI}_4]^-$ **4.31**.

The multinuclear NMR data obtained for the reaction mixture is consistent with a phosphine ligand bound to the transition metal centre in a chelating fashion, with a sharp peak in the ^{31}P NMR spectrum at δ_{p} 76. The ^1H NMR data displays peaks for the methylene, Cp and Ph protons at chemical shifts of 2.51, 2.59, 4.86, 7.16, 7.28, 7.69 with relative intensities of 2:2:5:8:8:4 respectively. The nanospray

mass spectra displays strong peaks for the parent $[\text{CpRu}(\text{dppe})\text{Ga}_4]^+$ ions with fragment peaks corresponding to $[\text{M}-\text{I}_2]^+$, $[\text{M}-\text{I}_3]^+$ and $[\text{M}-\text{Ga}_3]^+$ being evident.

Here too determination of the identity of the species formed was dependent on crystallographic data. Single crystals of **4.31** suitable for X-ray diffraction were obtained by layering a concentrated solution with hexanes and storage at -30°C . The structure of **4.31** is illustrated in Figure 4.13; relevant bond lengths and angles for **4.31** are listed in Table 4.15. The shortest Ru-I contact [5.535 Å] is comfortably outside the sum of van der Waals radii,³⁴ and contrasts with the Ru-I distance of 2.742(2) Å found for **4.30**. In common with the related system $[\text{Cp}^*\text{Ru}(\text{PMe}'\text{Pr}_2)_2]^+$ **4.33**,³⁵ the trigonal planar geometry at the metal centre defined by the two phosphorus atoms and the cyclopentadienyl centroid [$\Sigma(\text{angles at ruthenium}) = 358.8^\circ$ for **4.31**] implies negligible secondary interactions (for example with ligand CH bonds) with the 16-electron cationic ruthenium centre. The difference in coordinating ability for the tetraiodogallate ion with respect to the metal centres in **4.30** and **4.31** can conceivably be rationalised on the basis of reduced electrophilicity for the ruthenium centre found in conjunction with the more strongly σ basic dppe ligand (*cf.* PPh_3).

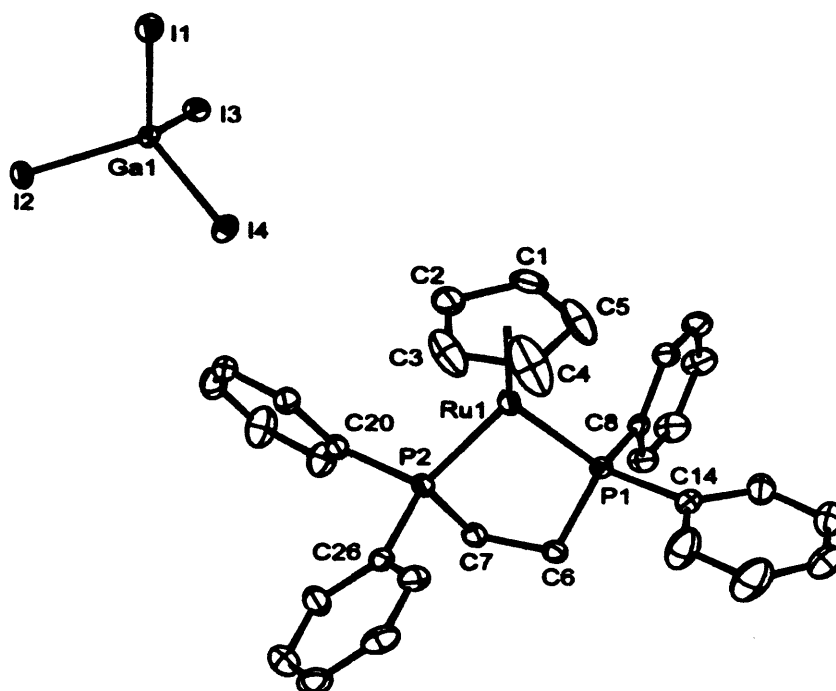


Figure 4.13 The molecular structure of $[\text{CpRu}(\text{dppe})]^+[\text{GaI}_4]^-$ **4.31**.

Table 4.15 Selected bond lengths (Å) and angles (°) for **4.31**.

Ru(1)-P(1)	2.286(1)	Ru(1)-centroid	1.855(6)
Ga(1)-I(1)	2.545(1)	Ga(1)-I(2)	2.543(1)
Ga(1)-I(3)	2.554(1)	Ga(1)-I(4)	2.539(1)
P(1)-Ru(1)-P(2)	86.5(1)	I(1)-Ga(1)-I(2)	108.6(1)
I(1)-Ga(1)-I(3)	109.1(1)	I(1)-Ga(1)-I(4)	109.0(1)
I(2)-Ga(1)-I(3)	109.8(1)	I(2)-Ga(1)-I(4)	110.2(1)
I(3)-Ga(1)-I(4)	110.2(1)		

A second product was also obtained from the $\text{CpRu}(\text{dppe})\text{Cl}/\text{GaI}^+$ system, which was determined from crystallographic studies to be an isomer of **4.31**, namely $[\text{CpRu}(\text{dppe})(\text{GaI}_4)]_2$ **4.32** (see Figure 4.14). The molecular structure of **4.32** reveals not only bridging (rather than chelating) dppe ligands, but also an η^1 -coordinated

$[\text{GaI}_4]^-$ moiety with Ru-I [2.714(10) Å] and GaI [2.612(9) Å] contacts for the bridging unit which are closely reminiscent of those found for 4.30.

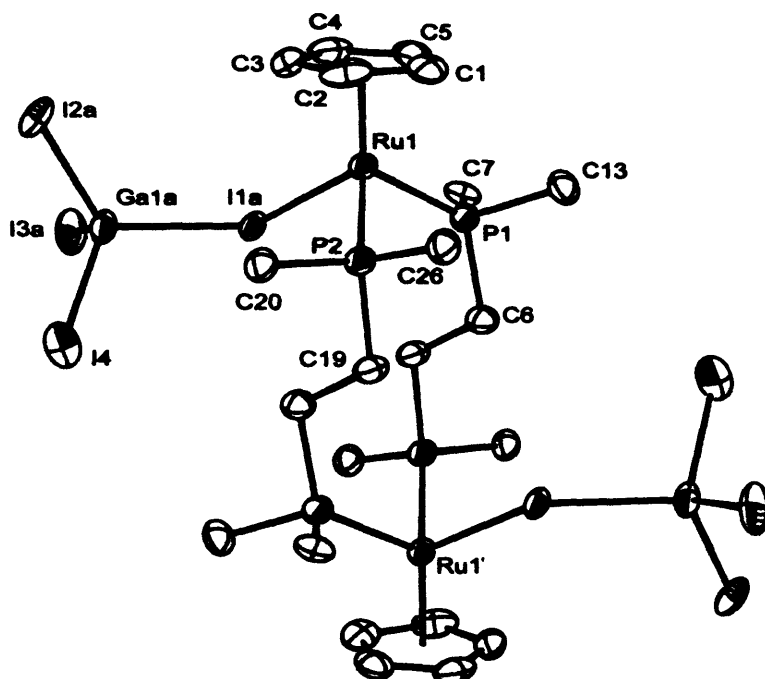


Figure 4.13 The molecular structure of $[\text{CpRu}(\text{GaI}_4)(\mu\text{-dppe})]_2$ 4.32.

Table 4.16 Selected bond lengths (Å) and angles ($^\circ$) for 4.32.

Ru(1)-P(1)	2.338(3)	Ru(1)-centroid	1.850(10)
Ru(1)-I(1a)	2.748(9)	Ga(1a)-I(1a)	2.590(8)
Ga(1a)-I(2a)	2.532(4)	Ga(1a)-I(3a)	2.523(4)
Ga(1a)-I(4)	2.462(4)		
P(1)-Ru(1)-P(2)	98.0(1)	Ru-I(1a)-Ga(1a)	124.9(4)
I(1a)-Ga(1a)-I(2a)	117.3(3)	I(1a)-Ga(1a)-I(3a)	99.0(2)
I(1a)-Ga(1a)-I(4)	109.0(2)	I(2a)-Ga(1a)-I(3a)	114.7(2)
I(2a)-Ga(1a)-I(4)	106.0(1)	I(3a)-Ga(1a)-I(4)	110.8(1)

Possible explanations for the formation of *both* **4.31** and **4.32** in the reaction of CpRu(dppe)Cl with 'Gal' include: (i) parallel reaction pathways originating from the CpRu(dppe)Cl starting material, or (ii) contamination of the starting material CpRu(dppe)Cl with a trace impurity [CpRuCl(μ -dppe)]₂. This dimeric species is known to be minor product formed in the synthesis of CpRu(dppe)Cl from CpRu(PPh₃)₂Cl and dppe (as was employed herein),³⁶ although no trace was detected in the ³¹P NMR spectrum of the starting material. Conceivably however, given the minute amounts of **4.32** which are isolated, the presence of a trace quantity of [CpRuCl(μ -dppe)]₂ impurity cannot be ruled out. Furthermore, the structures determined crystallographically for the isomeric species **4.31** and **4.32** point to relatively small energetic difference between the coordinating and non-coordinating modes of the [GaI₄]⁻ anion.

It is noteworthy that for neither of the ruthenium phosphine precursors examined was any evidence found for insertion of 'Gal' into the Ru-halogen bond. On the contrary a range of products has been isolated containing the tetraiodogallate moiety. From a synthetic viewpoint, phosphine ligands are known to promote disproportionation of 'Gal' to Ga metal and GaI₃.³¹ It is therefore possible that transient dissociation of one of the phosphine donors located at the ruthenium centre might allow for reaction with excess 'Gal' to form GaI₃, which then further reacts with the halide substituted Ru-I complex to form **4.30** and **4.31**.

4.6 Conclusions and Suggestions for Further Research

It has been demonstrated that photolysis of the dimeric species [Cp*Fe(CO)₂GaI₂]₂ **4.3** with dppe proceeds with retention of the iron-gallium bond,

yielding the monomeric complex $\text{Cp}^*\text{Fe}(\text{dppe})\text{GaI}_2$ **4.4**. Further investigations have revealed that the mechanism of substitution proceeds *via* the intermediate $\text{Cp}^*\text{Fe}(\mu\text{-dppe})(\text{CO})\text{GaI}_2$ **4.5** in which the phosphorus atoms are bound to the iron and gallium centres in a bridging fashion. The versatility of $\text{Cp}^*\text{Fe}(\text{dppe})\text{GaI}_2$ **4.4** as a starting material for the formation of asymmetric halogallyl species is illustrated by the synthesis of $\text{Cp}^*\text{Fe}(\text{dppe})\text{Ga}(\text{Mes})\text{I}$ **4.6** which proceeds with selective substitution of a single iodide atom.

Halide abstraction chemistry has proven to be effective in the synthesis of the first cationic gallylene complex $[\text{Cp}^*\text{Fe}(\text{dppe})(\text{Gal})]^+[\text{BAR}'_4]^-$ **4.11** featuring a terminally bound Gal ligand, by reaction of $\text{Cp}^*\text{Fe}(\text{dppe})\text{GaI}_2$ **4.4** with $\text{Na}^+[\text{BAR}'_4]^-$. In addition **4.11** represents the first example of a terminally bound EX ligand (where E = any group 13 element and X = halide), which is valence electronic with CO; this chemistry therefore warrants further investigation for example utilizing other metals (e.g. ruthenium) and more strongly σ -basic phosphines.

Insertion of 'Gal' into Mo-I bonds has proven to be effective in the synthesis of the halogallyl molybdenum species $[(\eta^7\text{-C}_7\text{H}_7)\text{Mo}(\text{CO})_2\text{GaI}_2]_2$ **4.22**. Attempts to substitute the CO ligands by photolysis in the presence of the phosphine ligands dppe and PCy_3 instead yielded the species $[(\eta^7\text{-C}_7\text{H}_7)\text{Mo}(\text{CO})_2\text{GaI}_2]_2(\mu\text{-dppe})$ **4.23**, $[\text{Cy}_3\text{PH}]^+[(\eta^7\text{-C}_7\text{H}_7)\text{Mo}(\text{CO})_2\text{GaI}_3]^-$ **4.26**.

Insertion of 'Gal' into the metal-halogen bond of phosphine-ligated ruthenium complexes has also been examined, although without any evidence being generated for reactivity proceeding *via* 'Gal' insertion. Reaction of $\text{CpRu}(\text{PPh}_3)_2\text{Cl}$ with four

equivalents of 'GaI' yielded $\text{CpRu}(\text{PPh}_3)_2(\mu\text{-I})\text{GaI}_3$ **4.30**. Similarly reaction of $\text{CpRu}(\text{dppe})\text{Cl}$ with ten equivalents of 'GaI' yielded the salt species $[\text{CpRu}(\text{dppe})]^+[\text{GaI}_4]^-$ **4.31**, together with the isomeric species $[\text{CpRu}(\text{dppe})(\text{GaI}_4)]_2$ (**4.32**).

Further investigations involve substituting the CO moieties within cationic borlyene systems for less π acidic phosphine ligands with the aim of increasing the multiple bond character between the metal-boron centre. Recent work carried out within the group has demonstrated that complexes such as $[\text{CpM}(\text{CO})(\text{PR}_3)=\text{BNCy}_2]^+[\text{BAr}^f_4]^-$ (where $\text{M} = \text{Fe}, \text{Ru}$ and $\text{R} = \text{Me}, \text{Ph}, \text{and OMe}$) can be readily synthesised by photolysis with the corresponding phosphine. Further examinations involve the synthesis of analogous $[\text{Cp}^*\text{M}(\text{dppe})\text{GaI}]^+[\text{BAr}^f_4]^-$ species (where $\text{M} = \text{Ru}$). Recent work carried out within the group has demonstrated that the gallyl complex $\text{Cp}^*\text{Ru}(\text{dppe})\text{GaI}_2$ can be readily synthesised by photolytic substitution of the CO moieties within $[\text{Cp}^*\text{Ru}(\text{CO})_2\text{GaI}_2]_2$, which represents a potential precursor complex in the synthesis of $[\text{Cp}^*\text{Ru}(\text{dppe})\text{GaI}]^+[\text{BAr}^f_4]^-$.

4.7 References for Chapter Four

1. D. A. Straus, S. D. Grumbine, T. D. Tilley, *J. Am. Chem. Soc.* 1990, **112**, 7801.
2. S. D. Grumbine, T. D. Tilley, *J. Am. Chem. Soc.* 1994, **116**, 5495.
3. Bunn, N. R.; Aldridge, S.; Kays (née Coombs) D. L.; Coombs, N. D.; Day, J. K.; Ooi, L.-L.; Coles, S. J.; Hursthouse, M. B. *Organometallics* 2005, **24**, 5879.
4. Green, M. L. H.; Mountford, P.; Smout, G. J.; Speel, S. R. *Polyhedron* 1990, **9**, 2763.
5. Ueno, K.; Watanabe, T.; Tobita, H.; Ogino, H. *Organometallics* 2003, **22**, 4375.
6. Coombs, N. D.; Vidovic, D.; Day, J. K.; Thompson, A. L.; Stasch, A.; Clegg, W.; Rosso, L.; Male, L.; Hursthouse, M. B.; Willock, D. J.; Aldridge, S. – paper submitted.
7. Ueno, K.; Hirotsu, M.; Hatori, N. *J. Organomet. Chem.* 2007, **692**, 88.
8. Vogt, M.; Pons, V.; Heinekey, D. M. *Organometallics* 2005, **24**, 1832.
9. (a) Wanandi, P. W.; Glaser, P. B.; Tilley, T. D. *J. Am. Chem. Soc.* 2000, **122**, 972.
(b) Glaser, P. B.; Wanandi, P. W.; Tilley, T. D. *Organometallics* 2004, **23**, 693. (c) Wanandi, P. W.; Tilley, T. D. *Organometallics* 1997, **16**, 4299.
10. Coombs, N.D.; Aldridge, S.; Willock, D. J. *J. Am. Chem. Soc.* 2008, **130**, *in press*.
11. Paul, F.; Toupet, L.; Roisnel, P.; Hamon, P.; Lapinte, C. *R. Chimie* 2005, **8**, 1174.
12. As determined from a survey of the Cambridge Structural Database 12/01/2008.
13. Su, J.; Li, X. –W.; Crittendon, R. C.; Campana, C. F.; Robinson, G. H. *Organometallics* 1997, **16**, 4511.
14. Materials and methods are available as supporting material on *Science* online.
15. Ueno, K.; Watanabe, T.; Ogino, H. *Appl. Organomet. Chem.* 2003, **17**, 403.
16. See, for example, Coombs, D. L. Aldridge, S.; Jones, C.; Willock, D. J. *J. Am. Chem. Soc.* 2003, **125**, 6356.

17. Power, P. P. *Chem. Rev.* **1999**, *99*, 3463.
18. Melzer, D.; Weiss, E. *J. Organomet. Chem.* **1984**, *263*, 67.
19. Frenking, G.; Fröhlich, N. *Chem. Rev.* **2000**, *100*, 717.
20. Schilling, B. E. R.; Hoffmann, R.; Lichtenberger, D. *J. Am. Chem. Soc.* **1979**, *101*, 585.
21. Under the energy decomposition analysis proposed by Morokuma, the interaction energy ΔE_{int} between two fragments is given by the sum of attractive orbital (ΔE_{orb}) and electrostatic ($\Delta E_{\text{electrostat}}$) and repulsive pauli (ΔE_{Pauli}) terms:
$$\Delta E_{\text{int}} = \Delta E_{\text{orb}} + \Delta E_{\text{electrostat}} + \Delta E_{\text{Pauli}}$$
22. Ehlers, A. W.; Baerends, E. J.; Bickelhaupt, F. M.; Radius, U. *Chem. Eur. J.* **1998**, *4*, 210.
23. Radius, U.; Bickelhaupt, F. M.; Ehlers, A. W.; Goldberg, N.; Hoffmann, R. *Inorg. Chem.* **1998**, *37*, 1080.
24. Braunschwig, H.; Colling, M.; Hu, C.; Radacki, K. *Angew. Chem. Int. Ed.* **2002**, *41*, 1359.
25. Coombs, D. L.; Aldridge, S.; Rossin, A.; Jones, C.; Willock, D. J. *Organometallics* **2004**, *23*, 2911.
26. Aldridge, S.; Kays (née Coombs), D. L.; Bunn, N. R.; Coombs, N. D.; Ooi, L. –L. *Main Group Metal Chemistry* **2005**, *28*, 201.
27. Linti, G.; Li, G.; Pritzkow, H. *J. Organomet. Chem.* **2001**, *626*, 82.
28. Dr Natalie R. Bunn, PhD Thesis, Cardiff University.
29. Clarkson, L. M.; Norman, N. C. *Organometallics* **1991**, *10*, 1286.
30. Coombs, N. D.; Stasch, A.; Aldridge, S. *Inorganica Chimica Acta.* **2008**, *361*, 449.
31. Baker, R. J.; Jones, C. *Dalton Trans.* **2005**, 1341 and references therein.

32. Jutzi, P.; Neuman, B.; Schebaum, L. O.; Stammler, A.; Stammler, H. –G. *Organometallics* **1999**, *18*, 4462.
33. Beall, T. W.; Houk, L. W. *Inorg. Chem.* **1973**, *12*, 1979.
34. Emsley, J. *The Elements*, Oxford University Press, Oxford University Press, Oxford, 2nd Edition, **1991**.
35. Jiménez-Tenorio, M, Mereiter, K.; Puerta, M. C.; Valerga, P. *J. Am. Chem. Soc.* **2000**, *122*, 11230. (b) Aneetha, H.; Jiménez-Tenorio, M.; Puerta, M. C.; Valerga, P. *Organometallics* **2002**, *21*, 5334.
36. Moura, E. M. Dickman, M. H.; Siebald, H. G. L.; Gama, G. L. *Polyhedron* **1999**, *18*, 2899.

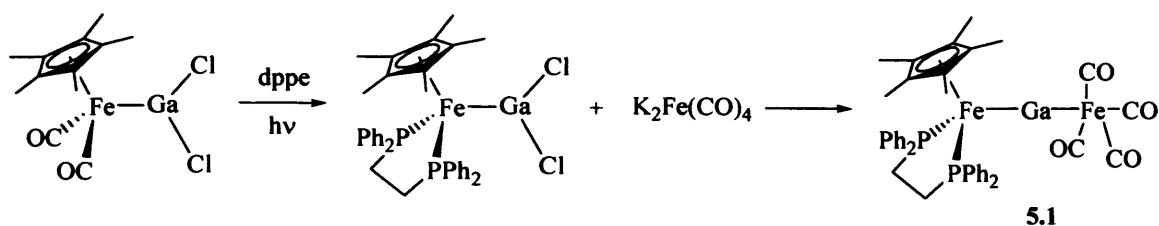
Chapter Five

Trinuclear Complexes Containing a 'Naked' Bridging Group 13 Atom: Synthesis and Reactivity

5.1 Introduction

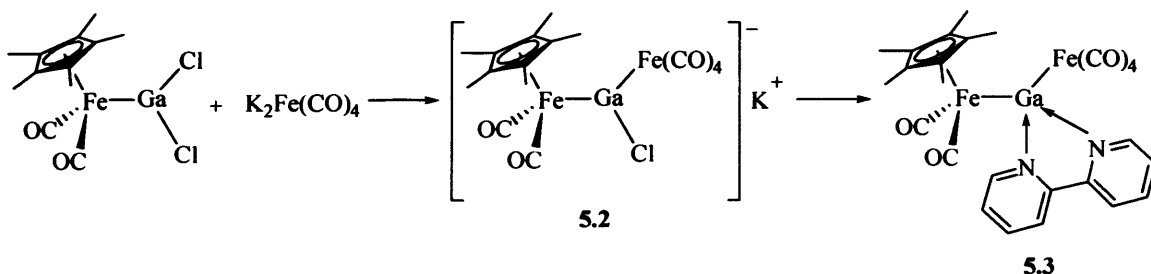
The necessity to electronically stabilise and/or sterically protect the two coordinate group 13 centres present in transition metal complexes containing diyl or related ligands has been demonstrated by a number of groups.¹ This stabilisation can be achieved *via* a number of routes, for example, by utilizing back donation from an electron-rich transition metal centre to the group 13 atom, as utilised by Ogino *et al.* in the synthesis of the first dinuclear complex [Cp*(dppe)Fe-Ga-Fe(CO)₄] **5.1** featuring a substituent free gallium centre.² The two-step synthesis employed involved initial photolysis of Cp*Fe(CO)₂GaCl₂ in the presence of dppe, yielding Cp*Fe(dppe)GaCl₂, followed by further reaction with K₂[Fe(CO)₄], thereby generating the dinuclear complex [Cp*(dppe)Fe-Ga-Fe(CO)₄] **5.1** by salt metathesis (Scheme 5.1).

The structure of **5.1** in the solid state was obtained crystallographically; an interesting feature to note is that the Cp*(dppe)Fe-Ga bond length (2.2479(10) Å) is shorter than that found for the (CO)₄Fe-Ga linkage (2.2931(10) Å) despite the fact that valence bond formalisms would represent these as single and double FeGa bonds, respectively. This apparent contradiction was rationalized by Ogino in terms of the stronger π basic character of the Cp*Fe(dppe) fragment compared to Fe(CO)₄. This reduces the extent of back donation from the Fe(CO)₄ fragment leading to elongation of the Ga-Fe(CO)₄ bond and consequent shortening of the Cp*(dppe)Fe-Ga bond.



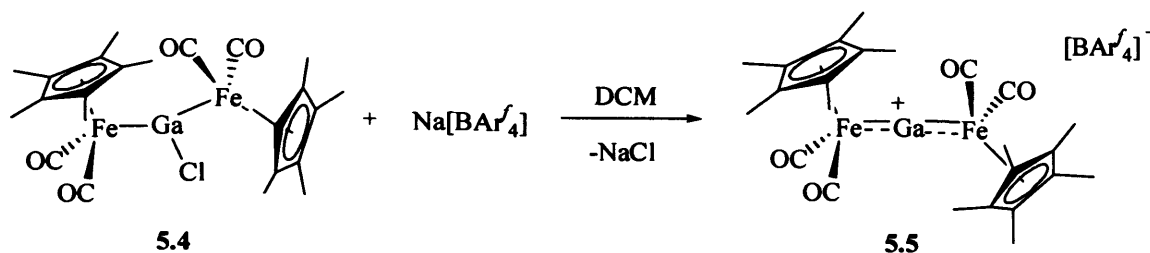
Scheme 5.1

The reaction of $\text{Cp}^*\text{Fe}(\text{CO})_2\text{GaCl}_2$ with $\text{K}_2\text{Fe}(\text{CO})_4$ was also examined; this was shown to yield the complex $\text{K}[\{\text{Cp}^*\text{Fe}(\text{CO})_2\}_2(\mu\text{-GaCl})\{\text{Fe}(\text{CO})_4\}]$ **5.2** (Scheme 5.2). However attempts to abstract a chloride ion from the gallium centre in the absence of a stabilising base led to decomposition. Due to the highly reactive nature of the complex, a halide-free complex could only be isolated as a base stabilised adduct by reaction with bpy (compound **5.3**).



Scheme 5.2

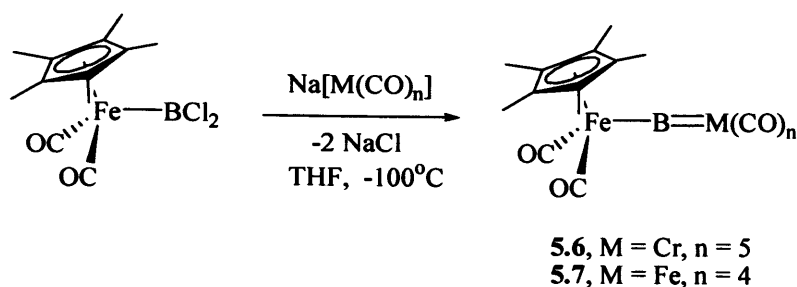
Aldridge *et al.*, have investigated the syntheses of cationic bridging gallium species. It was reported that reaction of $[\text{Cp}^*\text{Fe}(\text{CO})_2]_2\text{GaCl}$ **5.4** with one equivalent of $\text{Na}[\text{BAR}_4^-]$ yielded the cationic trimetallic complex $[\{\text{Cp}^*\text{Fe}(\text{CO})_2\}_2(\mu\text{-Ga})]^+[\text{BAR}_4^-]$ **5.5**, the molecular structure of which also features a 'naked' bridging gallium centre (Scheme 5.3).³



Scheme 5.3

Crystallographic evidence revealed a linear Fe-Ga-Fe unit [$\angle\text{Fe}(1)\text{-Ga}(1)\text{-Fe}(1') = 178.99(2)^\circ$], which is consistent with a 'naked' bridging gallium atom engaging in no significant secondary interactions (*e.g.* with the anion). The measured Fe-Ga bond lengths of [2.266(1) and 2.272(1) Å] are shorter than those found in the precursor complex and are similar to those reported by Ogino for [Cp*Fe(dppe)]Ga[Fe(CO)₄] **5.1** [2.248(1) Å]. In addition the centroid-Fe(1)-Fe(2)-centroid torsion angle of $84.62(3)^\circ$ in **5.5**, allows for optimal Fe-Ga π back bonding involving the pair of mutually perpendicular, formally vacant p orbitals at gallium. Computational analysis revealed a 61 % σ and a 38 % π contribution to the covalent Fe-Ga bonds revealing significant π back-bonding character.

Braunschweig *et al.*⁴ subsequently reported the synthesis and structural characterisation of analogous neutral boron containing complexes featuring a bridging boron centre bonded solely to two transition metal fragments *via* salt metathesis chemistry (Scheme 5.4).



Scheme 5.4

Initial studies revealed that reaction of $\text{CpFe}(\text{CO})_2\text{BCl}_2$ with $\text{Na}[\text{Cr}(\text{CO})_5]$ yielded $\text{Na}[\{\text{CpFe}(\text{CO})_2\}(\mu\text{-BCl})\{\text{Cr}(\text{CO})_5\}]$, the formulation of which could only be determined spectroscopically due to the stability of the complex. In subsequent studies Braunschweig and others have observed that the thermal-stability of half-sandwich iron-boryl complexes of the type $(\eta^5\text{-C}_5\text{R}_5)\text{Fe}(\text{CO})_2\text{BX}_2$, increases markedly ongoing from Cp to Cp*. Thus, it was found that when the same reaction was repeated with $\text{Cp}^*\text{Fe}(\text{CO})_2\text{BCl}_2$, $[\{\text{Cp}^*\text{Fe}(\text{CO})_2\}(\mu\text{-B})\{\text{Cr}(\text{CO})_5\}]$ **5.6** was obtained featuring a substituent free boron centre bridging two transition metal fragments. Very recent work from the same group has seen the synthesis and structural characterization of the isoelectronic pair of complexes $[\{\text{Cp}'\text{Fe}(\text{CO})_2\}(\mu\text{-B})]^+$ and $[\{\text{Cp}'\text{Mn}(\text{CO})_2\}(\mu\text{-B})]^-$.⁴

5.1.1 Aims of Research

Given the success of halide abstraction chemistry in the synthesis of the cationic trimetallic gallium complex $[\{\text{Cp}^*\text{Fe}(\text{CO})_2\}_2(\mu\text{-Ga})]^+[\text{BAR}'_4]^-$ **5.5**,³ we aim to extend this approach to analogous indium systems. The synthesis of precursor complexes of the type $[\text{L}_n\text{M}]_2\text{InX}$ will be investigated and halide abstraction chemistry will be explored. The reactivity of these systems will be examined *e.g.* with two electron donors.

5.2 Synthesis of $[(\eta^5\text{-C}_5\text{R}_5)\text{Fe}(\text{CO})_2]_2\text{InX}$ Systems

5.2.1 Experimental

Synthesis of $[\text{Cp}^\text{Fe}(\text{CO})_2]_2\text{InBr}$ (5.8)*

To a suspension of $\text{Na}[\text{Cp}^*\text{Fe}(\text{CO})_2]$ (0.201 g, 0.74 mmol) in diethyl ether (20 cm³) was added a solution of InBr_3 (0.131 g, 0.37 mmol) also in diethyl ether (10 cm³), and the reaction mixture stirred at 20°C for 16 h. Filtration of the supernatant solution, removal of volatiles *in vacuo*, and recrystallisation from toluene (60 cm³) at -30°C yielded $[\text{Cp}^*\text{Fe}(\text{CO})_2]_2\text{InBr}$ 5.8 as an orange microcrystalline solid (0.121 g, 47%). X-ray quality crystals could be grown by slow diffusion of hexanes into a solution in toluene at -30°C. ¹H NMR (300 MHz, CD₂Cl₂): δ_{H} 1.83 (s, 30H, CH₃ of Cp*). ¹³C NMR (76 MHz, CD₂Cl₂): δ_{C} 10.0 (CH₃ of Cp*), 94.2 (quaternary C of Cp*), 216.1 (CO). IR (thin film CD₂Cl₂, cm⁻¹): $\nu(\text{CO})$ 1979 st, 1946 st, 1925 st. MS EI: m/z 687.9 {5 %, [M]⁺}, correct isotope distribution for 2 iron, 1 indium, and 1 bromine atom, significant fragment ion peaks at m/z 661.9 {100 %, [M-CO]⁺}, 663.9 {20 %, [M-2CO]⁺}; exact mass calc for [M]⁺ 687.9060, measured 687.9066.

Synthesis of $[\text{Cp}^\text{Fe}(\text{CO})_2]_2\text{InI}$ (5.9)*

To a suspension of InI (0.245 g, 1.01 mmol) in toluene (10 cm³) was added a solution of $[\text{Cp}^*\text{Fe}(\text{CO})_2]_2$ (0.501 g, 1.01 mmol) in toluene (50 cm³), and the reaction mixture refluxed for 144 h. Filtration, concentration, and cooling of the solution to -30°C yielded $[\text{Cp}^*\text{Fe}(\text{CO})_2]_2\text{InI}$ 5.9 as a microcrystalline solid (0.396 g, 53%). Single crystals suitable for X-ray diffraction could be obtained by slow diffusion of hexanes into a toluene solution at -30°C. ¹H NMR (400 MHz, CD₂Cl₂): δ_{H} 1.71 (s, 30H, Cp*). ¹³C NMR (76 MHz, CD₂Cl₂): δ_{C} 9.6 (CH₃ of Cp*), 93.7 (quaternary of Cp*), 126.3 (CO). IR (thin film CH₂Cl₂, cm⁻¹): $\nu(\text{CO})$ 1969 st, 1957 st, 1922 st. MS EI: m/z

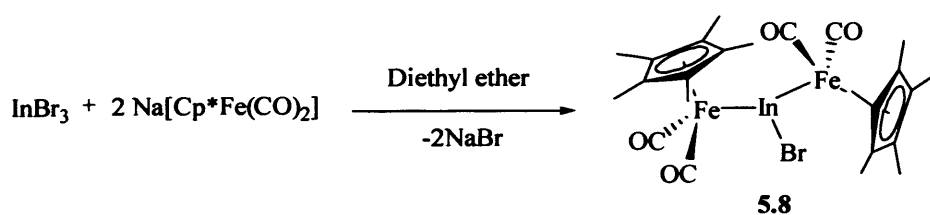
736 {weak, $[M]^+$ }, correct isotope distribution for 2 iron, 1 indium, and 1 iodine atom, significant fragment ions at m/z 708 {100 %, $[M-CO]^+$ }, 680 {8 %, $[M-2CO]^+$ }; exact mass calc for $[M-CO]^+$ 707.8972, measured 707.8961.

5.2.2 Results and Discussion

Two possible synthetic routes have been investigated in the synthesis of bridging indanediyl complexes of the type $[Cp^*Fe(CO)_2]_2InX$, namely (i) salt elimination and, (ii) insertion of InX into an Fe-Fe bond.

5.2.2.1 Salt elimination

The bridging haloindanediyl complex $[Cp^*Fe(CO)_2]_2InBr$ **5.8** was prepared by addition of $InBr_3$ to a suspension of $Na[Cp^*Fe(CO)_2]$ in diethyl ether and isolated as an orange microcrystalline solid in *ca.* 47% yield. Under the conditions used the reaction proceeds with selective substitution of the two bromide atoms (*i.e.* no monosubstituted product was obtained).⁵



Scheme 5.5 Synthetic route to complex **5.8**.

The proposed formulation is implied by 1H and ^{13}C NMR and IR data, which support the formation of a $Cp^*Fe(CO)_2$ containing species. The 1H NMR reveals the presence of a single peak at a chemical shift of δ 1.83, corresponding to Cp^* ligand. Resonances associated with the carbons of the Cp^* and carbonyl moieties were

observed in the ^{13}C NMR with at δ 10.0, 94.2 and 216.1 ppm respectively which are consistent with the proposed formulation, and are similar to those found for the analogous bridging gallyl complex $[\text{Cp}^*\text{Fe}(\text{CO})_2]_2\text{GaCl}$ **5.4** [δ 9.7, 94.4 (Cp^*) and 217.2 (CO)]. IR spectroscopy revealed three strong CO stretches at 1979, 1946 and 1925 cm^{-1} , indicating that the reaction proceeds with retention of the $\text{Cp}^*\text{Fe}(\text{CO})_2$ fragment. The EI mass spectra displays weak peaks for the parent $[\text{M}]^+$ ions with fragment peaks corresponding to the $[\text{M}-\text{CO}]^+$ and $[\text{M}-2\text{CO}]^+$ ions also being evident; the isotope distribution is as expected for a complex containing one indium, one bromine and two iron atoms.

Given the relatively little information available from NMR experiments, definitive identification of a bridging indium-bromide species was dependant on crystallographic data. Single crystals of **5.8** suitable for X-ray diffraction were obtained by a layering of a concentrated toluene solution of **5.8** layered with hexanes at -30°C . The spectroscopic data for **5.8** was confirmed by single crystal X-ray diffraction studies and the structure is illustrated in Figure 5.1. Relevant bond lengths and angles are listed in Table 5.1.

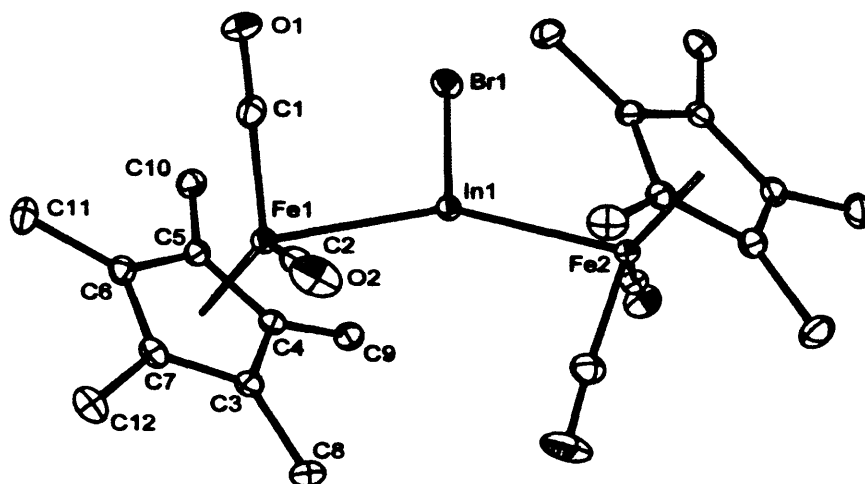


Figure 5.1 The molecular structure of $[\text{Cp}^*\text{Fe}(\text{CO})_2]_2\text{InBr}$ **5.8**.

Table 5.1 Selected bond lengths [\AA] and angles [$^\circ$] for **5.8**.

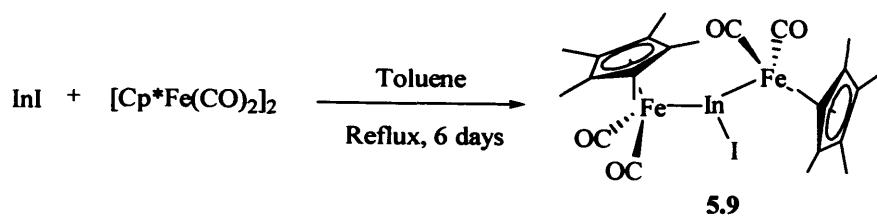
C(1)-O(1)	1.152(3)	Fe(2)-In(1)	2.5086(3)
C(1)-Fe(1)	1.758(3)	Br(1)-In(1)	2.6413(3)
Fe(1)-In(1)	2.5133(3)		
O(1)-C(1)-Fe(1)	178.9(2)	Fe(2)-In(1)-Fe(1)	141.457(11)
O(2)-C(2)-Fe(1)	176.9(2)	Fe(2)-In(1)-Br(1)	110.642(10)
C(2)-Fe(1)-In(1)	89.23(7)	Fe(1)-In(1)-Br(1)	107.768(10)
C(1)-Fe(1)-In(1)	85.28(7)		

The molecular structure of **5.8** displays a monomeric trigonal planar geometry in the solid state [sum of angles at In = 360° within the standard 3σ limit], and shows no hint of oligomerisation *via* In-Br-In bridges. This differs markedly from that found for the related ($\eta^5\text{-C}_5\text{H}_5$) derivative $[\text{CpFe}(\text{CO})_2\text{InI}_2]_2$ **5.10** which is dimeric featuring an In($\mu\text{-I}$)₂In core. The monomeric geometry of **5.8** presumably results from the larger steric demands of the $\text{Cp}^*\text{Fe}(\text{CO})_2$ fragment. Similar chemistry has also been

observed for the analogous $[(\eta^5\text{-C}_5\text{R}_5)\text{Fe}(\text{CO})_2]_2\text{GaCl}$ species ($\text{R} = \text{H}, \text{CH}_3$), viz. $[\text{CpFe}(\text{CO})_2]_2\text{GaCl}$ (**5.11**) is reported to be polymeric featuring bridging Ga-Cl-Ga units,⁶ while $[\text{Cp}^*\text{Fe}(\text{CO})_2]_2\text{GaCl}$ **5.4** is known to be monomeric.⁵ It was found that whereas $[\text{CpFe}(\text{CO})_2]_2\text{GaCl}$ **5.11** readily coordinates bases such as thf, dioxane, or chloride,^{7,8} $[\text{Cp}^*\text{Fe}(\text{CO})_2]_2\text{GaCl}$ **5.4** could be recrystallised from thf without any coordination of solvent molecules at the gallium centre.⁵ The Fe-In distance of 2.5086(3) Å is analogous to that found for the related indyl species $\text{Cp}^*\text{Fe}(\text{CO})_2\text{In}(\text{Mes}^*)\text{Br}$ [2.509(11) Å].⁵

5.2.2.2 Insertion of InI

An alternative approach to the synthesis of three coordinate haloindium systems involves insertion of In(X) into a M-X or M-M bond to yield a dihaloindyl, $[\text{L}_n\text{M-E(I)X}]_n$, or haloindanediyl complex, $(\text{L}_n\text{M})_2\text{EI}$. This approach is advantageous in that unlike organometallic substitution chemistry, as discussed above, it avoids the reliance on anionic precursors. A greater range of complexes is therefore potentially accessible, which offers the possibility of synthesising cationic diyl systems $[\text{L}_n\text{M}(\text{EX})]^+$ without competing ancillary π acidic ligands (*i.e.* carbonyls). Thus, insertion of commercially available InI into metal-metal bonds was exploited to generate three-coordinate halo-indium ligand systems. The iodoindanediyl complex $[\text{Cp}^*\text{Fe}(\text{CO})_2]_2\text{InI}$ **5.9** was prepared by the reaction of InI with $[\text{Cp}^*\text{Fe}(\text{CO})_2]_2$ under reflux conditions in toluene and isolated as an orange microcrystalline solid in *ca.* 53% yield (Scheme 5.6).⁵



Scheme 5.6 Synthetic route to complex **5.9**.

As with the corresponding bromide-substituted species **5.8**, the proposed formulation is supported by ^1H and ^{13}C NMR and IR data, which imply the formation of a $\text{Cp}^*\text{Fe}(\text{CO})_2$ containing species. Multinuclear NMR data is consistent with the presence of Cp^* and CO fragments with peaks at δ 1.71 in the ^1H NMR and at δ 9.6, 93.7 and 126.3 in the ^{13}C NMR spectrum. Similarly the measured IR spectrum features three strong CO stretches at 1969, 1957 and 1922 cm^{-1} . The EI mass spectra displays weak peaks for the parent $[\text{M}]^+$ ions with fragment peaks corresponding to the $[\text{M}-\text{CO}]^+$ and $[\text{M}-2\text{CO}]^+$ ions also being evident; the isotope distribution is as expected for a complex containing one indium, one iodine and two iron atoms.

Definitive identification of a bridging indium-iodide species was again dependant on crystallographic data. Single crystals of **5.9** suitable for X-ray diffraction were obtained by a layering of a concentrated toluene solution of **5.9** layered with hexanes at -30°C . The spectroscopic data for **5.9** was confirmed by single crystal X-ray diffraction studies and the structure is illustrated in Figure 5.2. Relevant bond lengths and angles are listed in Table 5.2.

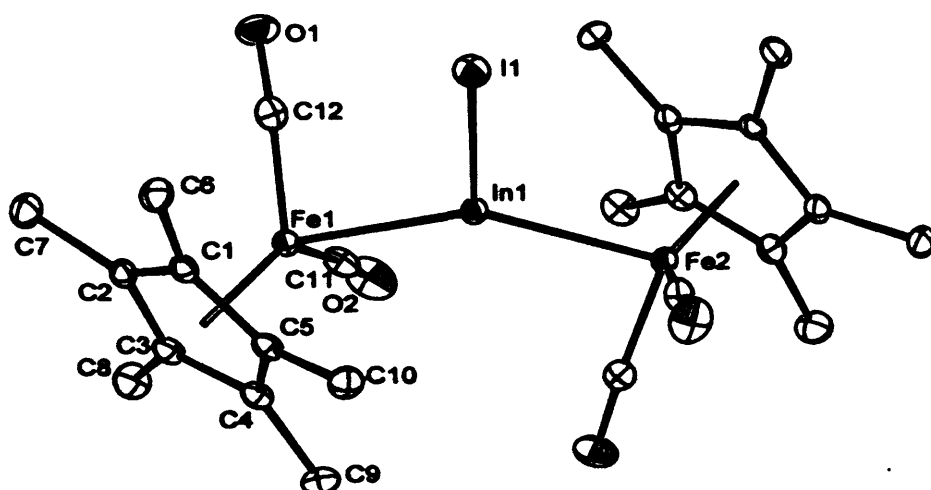


Figure 5.2 The molecular structure of $[\text{Cp}^*\text{Fe}(\text{CO})_2]_2\text{InI}$ **5.9**.

Table 5.2 Selected bond lengths [\AA] and angles [$^\circ$] for **5.9**.

Fe(1)-In(1)	2.513(1)	Fe(1)-Cp* centroid	1.726(5)
Fe(2)-In(1)	2.519(1)	In(1)-I(1)	2.854(4)
Fe(1)-C(11)	1.754(5)		
Fe(1)-In(1)-Fe(2)	141.98(2)	Fe(2)-In(1)-I(1)	107.61(2)
Fe(1)-In(1)-I(1)	110.30(2)		

The molecular structure of **5.9** features a monomeric trigonal planar geometry in the solid state [$\Sigma(\text{angles at In}) = 360^\circ$ within the standard 3σ limit], which is analogous to that found for the related systems $[\text{Cp}^*\text{Fe}(\text{CO})_2]_2\text{InBr}$ **5.8** and $[\text{Cp}^*\text{Fe}(\text{CO})_2]_2\text{GaCl}$ **5.4**.⁵ As with **5.8** the observed reaction chemistry and monomeric geometry differs markedly to that found for the analogous $(\eta^5\text{-C}_5\text{H}_5)\text{Fe}(\text{CO})_2$ derivative and confirms that the steric bulk of the $(\eta^5\text{-C}_5\text{R}_5)\text{Fe}(\text{CO})_2$ fragment has a strong influence on the structural and reaction chemistry of these systems. The Fe-In

distance of 2.519(1) Å, is consistent to that found for [Cp*Fe(CO)₂]₂InBr **5.8** [2.5086(3) Å].

5.3 Halide Abstraction Chemistry

5.3.1 Experimental

Synthesis of [$\{\text{Cp}^*\text{Fe}(\text{CO})_2\}_2(\mu\text{-In})\}[\text{BAr}^f_4]$ (**5.12**)

To a suspension of Na[BAr^f₄] (0.057 g, 0.064 mmol) in dichloromethane (4 cm³) at -78°C was added a solution of [Cp*Fe(CO)₂]₂InBr **5.8** (0.044 g, 0.064 mmol) in dichloromethane (4 cm³), and the reaction mixture was warmed to 20°C over 30 min. Further stirring for 90 min. filtration, and layering with hexanes and storage at -30°C yielded [$\{\text{Cp}^*\text{Fe}(\text{CO})_2\}_2(\mu\text{-In})\}[\text{BAr}^f_4]$ **5.12** as orange crystals suitable for X-ray diffraction (0.060 g, 64%). ¹H NMR (300 MHz, CD₂Cl₂): δ_H 1.85 (s, 30H, Cp*), 7.44 (s, 4H, *para* CH of BAr^f₄), 7.64 (s, 8H, *ortho* CH of BAr^f₄). ¹³C NMR (76 MHz, CD₂Cl₂): δ_C 10.4 (CH₃ of Cp*), 96.5 (quaternary of Cp*), 117.8 (*para* CH of BAr^f₄), 124.6 (q, ¹J_{CF} = 272 Hz, CF₃ of BAr^f₄), 128.9 (q, ²J_{CF} = 35 Hz, *meta* C of BAr^f₄), 134.8 (*ortho* CH of BAr^f₄), 161.8 (q, ¹J_{CB} = 50 Hz, *ipso* C of BAr^f₄), 211.9 (CO). ¹⁹F NMR (283 MHz, CD₂Cl₂): δ_F -62.7 (CF₃). ¹¹B NMR (96 MHz, CD₂Cl₂): δ_B -7.6 (BAr^f₄). IR (thin film CD₂Cl₂, cm⁻¹): ν(CO) 2005, 1983, 1951. MS ES⁻: *m/z* 863 {100 %, [BAr^f₄]⁻}; ES⁺: *m/z* 609 {6 %, [M]⁺}, correct isotope distribution for 2 iron and 1 indium atoms, significant fragment ions at *m/z* 581 {weak, [M-CO]⁺}, 553 {5 %, [M-2CO]⁺}. Exact mass calcd for [M]⁺ 608.9876, found 608.9884.

Reaction of $[\text{Cp}^*\text{Fe}(\text{CO})_2]_2\text{InI}$ 5.9 with $\text{Na}[\text{BAr}^f_4]$ isolation of $[\{\text{Cp}^*\text{Fe}(\text{CO})_2\}_2(\mu\text{-I})][\text{BAr}^f_4]$ (5.13).

To a suspension of $\text{Na}[\text{BAr}^f_4]$ (0.111 g, 0.13 mmol) in dichloromethane (6 cm³) at -78°C was added a solution of $[\text{Cp}^*\text{Fe}(\text{CO})_2]_2\text{InI}$ 5.9 (0.092 g, 0.13 mmol) in dichloromethane (8 cm³), and the reaction mixture warmed to 20°C over 30 min. Further stirring for 3 h, filtration and layering with hexanes yielded orange crystals of $[\{\text{Cp}^*\text{Fe}(\text{CO})_2\}_2(\mu\text{-I})][\text{BAr}^f_4]$ 5.13. Isolated yield (0.028 g, 15%). ¹H NMR (400 MHz, CD₂Cl₂): δ_H 1.84 (s, 30H, Cp*), 7.48 (s, 4H, *para* CH of BAr^f₄⁻), 7.64 (s, 8H, *ortho* CH of BAr^f₄⁻). ¹³C NMR (76 MHz, CD₂Cl₂): δ_C 10.4 (CH₃ of Cp*), 96.1 (quaternary of Cp*), 117.5 (*para* CH of BAr^f₄⁻), 124.6 (q, ¹J_{CF} = 274 Hz, CF₃ of BAr^f₄⁻), 128.9 (q, ²J_{CF} = 31 Hz, *meta* C of BAr^f₄⁻), 134.8 (*ortho* CH of BAr^f₄⁻), 161.8 (q, ¹J_{CB} = 49 Hz, *ipso* C of BAr^f₄⁻), 212.8 (CO). ¹⁹F NMR (283 MHz, CD₂Cl₂): δ_F -62.8 (CF₃). ¹¹B NMR (96 MHz, CD₂Cl₂): δ_B -7.6 (BAr^f₄⁻). IR (thin film CH₂Cl₂, cm⁻¹): ν(CO) 2003 st, 1984 st, 1952 st. MS ES⁻: 863 {100 %, [BAr^f₄]⁻}; ES⁺, 621 {50 %, [M]⁺}, correct isotope distribution for 2 iron and one iodine atoms, significant fragment ions at *m/z* 593 {weak, [M-CO]⁺}, 565 {20 %, [M-2CO]⁺}, 537 {45 %, [M-3CO]⁺}, 509 {5 %, [M-4CO]⁺}. Exact mass: calcd for [M]⁺ 620.9882, measd 620.9872.

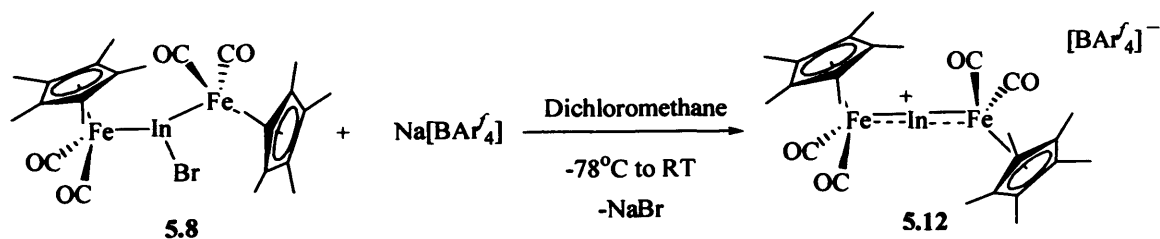
Reaction of $[\text{Cp}^*\text{Fe}(\text{CO})_2]_2\text{InI}$ 5.9 with $\text{Na}[\text{BPh}_4]$

To a suspension of $\text{Na}[\text{BPh}_4]$ (0.074 g, 0.22 mmol) in dichloromethane (10 cm³) at -78°C was added a solution of $[\text{Cp}^*\text{Fe}(\text{CO})_2]_2\text{InI}$ 5.9 (0.080 g, 0.11 mmol) in dichloromethane (10 cm³), and the reaction mixture was warmed slowly to 20°C. Monitoring the reaction mixture by IR spectroscopy over a period of 72 h led to the gradual disappearance of the peaks due to the starting material (1969, 1957, and 1922

cm^{-1}) and the growth of bands at 2016, 1995, 1970, and 1940 cm^{-1} . Monitoring of the reaction by ^{11}B NMR spectroscopy also revealed the growth of a broad signal at δ_{B} 67.0. Filtration of the supernatant solution, removal of the volatiles *in vacuo*, and recrystallisation from hexanes at -30°C led to the formation of crops of colourless and dark red microcrystalline material, which were identified as BPh_3 (δ_{B} 67.0) and a mixture of $\text{Cp}^*\text{Fe}(\text{CO})_2\text{I}$ ($\nu(\text{CO})$ 2016 and 1970 cm^{-1}) and $\text{Cp}^*\text{Fe}(\text{CO})_2\text{Ph}$ ($\nu(\text{CO})$ 1995 and 1940 cm^{-1}), respectively by comparison of multinuclear NMR, IR, and mass spectrometric data with those reported previously.⁹

5.3.2 Results and Discussion

Halide abstraction chemistry has been examined for the three-coordinate bridging haloindanediyl complexes $[\text{Cp}^*\text{Fe}(\text{CO})_2]_2\text{InBr}$ (**5.8**) and $[\text{Cp}^*\text{Fe}(\text{CO})_2]_2\text{InI}$ (**5.9**). Thus, addition of $[\text{Cp}^*\text{Fe}(\text{CO})_2]_2\text{InBr}$ **5.8** to a suspension of $\text{Na}[\text{BAr}'_4]$ in dichloromethane at -78°C , over a period of 2 h, yielded $[\{\text{Cp}^*\text{Fe}(\text{CO})_2\}_2(\mu\text{-In})]^+[\text{BAr}'_4]^-$ **5.12** (Scheme 5.7) in 64 % yield.^{3b}



Scheme 5.7 Synthetic route to complex **5.12**.

The formation of **5.12** is implied by ^1H and IR monitoring of the reaction in dichloromethane- d_2 , in particular by a 2:1 ratio of the Cp^* and $[\text{BAr}'_4]^-$ signals observed in the ^1H NMR spectrum and by characteristic shifts in the IR to higher

wavenumbers on formation of the cationic complex (2005, 1983, 1951 vs 1979, 1946 1925 cm^{-1} for **5.12** and **5.8** respectively). Electrospray mass spectra display weak peaks for the parent $[\text{M}]^+$ ions with fragment peaks corresponding to the $[\text{M-CO}]^+$ and $[\text{M-2CO}]^+$ ions also being evident; the isotope distribution is as expected for a complex containing one indium and two iron atoms.

Single crystals of **5.12** suitable for X-ray diffraction were obtained by layering a concentrated dichloromethane solution of **5.12** with hexanes at -30°C . The spectroscopic data for **5.12** was confirmed by single crystal X-ray diffraction studies and the structure is illustrated in Figure 5.3. Relevant bond lengths and angles are listed in Table 5.3. The solid state structure confirms the presence of a base-free cationic two-coordinate indium centre. The geometry of the cationic component features a near linear trimetallic unit with an $\angle\text{Fe-In-Fe}$ angle of $175.32(6)^\circ$, in which the central indium atom engages in no significant intra- or intermolecular secondary interactions, for example with the $[\text{BAR}_4]^-$ anion.

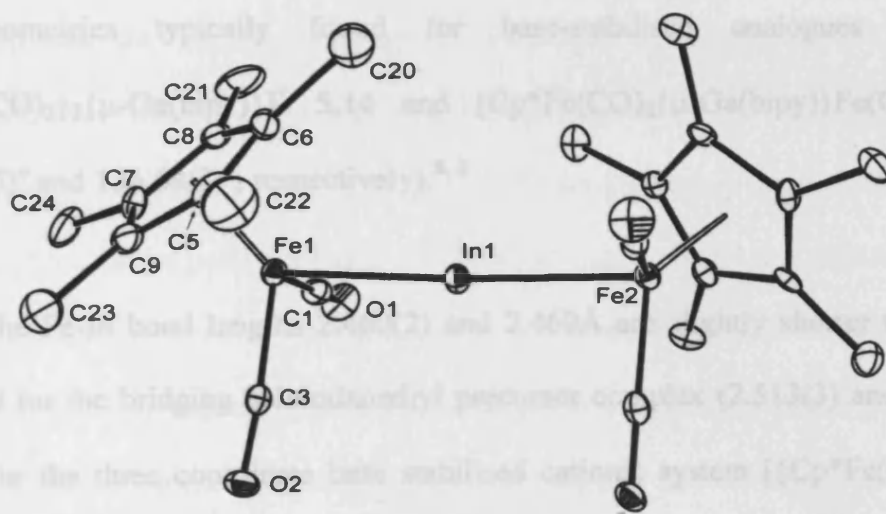


Figure 5.3 The molecular structure of $[\{\text{Cp}^*\text{Fe}(\text{CO})_2\}_2(\mu\text{-In})]^+[\text{BAR}_4]^-$ **5.12**.

Table 5.3 Selected bond lengths [Å] and angles [°] for **5.12**.

Fe(1)-In(1)	2.460(2)	Fe(1)-Cp* centroid	1.725(10)
Fe(2)-In(1)	2.469(2)	Fe(1)-C(1)	1.757(13)
C(1)-O(1)	1.174(13)		
Fe(1)-In(1)-Fe(2)	175.32(6)	O(1)-C(1)-Fe(1)	177.5(10)
C(1)-Fe(1)-In(1)	88.1(4)	Cp* centroid-Fe(1)-Fe(2)-Cp* centroid	86.8(3)

Compound **5.12** represents a rare example of a structurally characterised cationic species featuring a 'naked' two coordinate cationic indium centre in which the group 13 atom is bound to two transition metal centres. The only other examples of isolated transition metal complexes featuring 'naked' bridging gallium or indium centres is the cationic species $[\{\text{Cp}^*\text{Fe}(\text{CO})_2\}_2(\mu\text{-Ga})][\text{BARf}_4]$ **5.5** reported by Aldridge,³ and the neutral species $[\text{Cp}^*\text{Fe}(\text{dppe})](\mu\text{-Ga})[\text{Fe}(\text{CO})_4]$ **5.1** reported by Ogino.² Both complexes feature a near linear geometry at the group 13 centre [$178.99(2)^\circ$ and $176.01(4)^\circ$, respectively]. This feature is in marked contrast to the bent geometries typically found for base-stabilised analogues such as $[\{\text{CpFe}(\text{CO})_2\}_2\{\mu\text{-Ga}(\text{bipy})\}]^+$ **5.14** and $[\text{Cp}^*\text{Fe}(\text{CO})_2\{\mu\text{-Ga}(\text{bipy})\}\text{Fe}(\text{CO})_4]$ **5.3** ($132.81(5)^\circ$ and $136.68(2)^\circ$, respectively).^{8,2}

The Fe-In bond lengths 2.460(2) and 2.469 Å are slightly shorter than those measured for the bridging haloindanediyl precursor complex (2.513(3) and 2.509(3) Å) and for the three coordinate base stabilised cationic system $[\{\text{Cp}^*\text{Fe}(\text{CO})_2\}_2(\mu\text{-In}(\text{thf}))][\text{BARf}_4]^+$ **5.15** (2.494(2) and 2.498(2) Å, *vide infra*).^{3b} The Fe-In bond shortening is consistent with both steric and electronic factors *i.e.* with a reduction in the coordination number at the indium centre and/or with an increase in the extent of

Fe→In back bonding. The extent of bond shortening accompanying the halide abstraction process is significantly less for **5.12** (< 2%) than that measured for $[\{\text{Cp}^*\text{Fe}(\text{CO})_2\}_2(\mu\text{-Ga})]^+[\text{BAR}'_4]^-$ (**5.5**, *ca.* 3.5%),³ as expected due to the larger size of the indium atomic radius compared to gallium. This observation is consistent with both underlying electronic and steric factors *i.e.* both the extent of Fe→E back bonding and the relief of steric strain are likely to be less pronounced within **5.12**, due to the longer Fe-E linkages. A further significant point to note is the relative alignment of the two $[\text{Cp}^*\text{Fe}(\text{CO})_2]$ fragments. The Cp* centroid-Fe(1)-Fe(2)-Cp* centroid torsion angle is close to 90° (86.8(3)°); given the presence of two formally vacant p orbitals at the group 13 centre, this alignment allows for optimal π back bonding from the HOMO of each of the two $[\text{Cp}^*\text{Fe}(\text{CO})_2]^+$ fragments.

The extent of σ and π bonding contributions were investigated, DFT calculations were carried out at the BLYP/TZP level, and salient parameters relating to the fully optimised geometry of $[\{\text{Cp}^*\text{Fe}(\text{CO})_2\}_2\text{In}]^+$ are detailed in Table 5.4. It was found that the minimum energy conformation calculated by DFT actually corresponds to a centroid-Fe-Fe-centroid torsion angle of 161.8°, in contrast to the experimentally determined value of 86.3(3)°. Closer inspection however reveals that there is a very shallow potential energy surface for rotation about this axis and that the energy difference between the minimum energy conformer and that corresponding to the approximately orthogonal alignment found in the solid state is very small (*e.g.* $\Delta E = 1.78 \text{ kcal mol}^{-1}$ between the rotamers corresponding to torsion angles of 161.8 and 82.4). σ and π contributions to the overall Fe-In bonding density were therefore calculated for both of these conformations. The analogous DFT calculations were carried out for the gallium metalladiyl complex $[\{\text{Cp}^*\text{Fe}(\text{CO})_2\}_2\text{Ga}]^+$ (work carried

out by Dr A. Rossin).³ In this case, unlike $[\{\text{Cp}^*\text{Fe}(\text{CO})_2\}_2\text{In}]^+$, it was found that the agreement between the calculated and experimentally derived geometric parameters was good, with the near linear Fe-Ga-Fe trimetallic framework and near orthogonal alignment of the $[\text{Cp}^*\text{Fe}(\text{CO})_2]$ fragments being accurately reproduced computationally.

Table 5.4 Calculated and Crystallographically Determined structural Parameters for the Cationic Components of $[\{\text{Cp}^*\text{Fe}(\text{CO})_2\}_2(\mu\text{-E})]^+[\text{BAR}'_4]^-$ (**5.12**, E = In; **5.5**, E = Ga).

Compound	Fe-E distance (Å)	Fe-E-Fe angle (deg)	Ct-Fe-Fe-Ct torsion angle (deg)	$\sigma:\pi$ break- down	E_{rel} (kcal mol^{-1}) ^a
5.12 (exptl)	2.460(2), 2.469(2)	175.32(6)	86.8(3)		
5.12 (calcd)	2.463, 2.463	179.40	161.8	74:26	0
5.12 (calcd)	2.469, 2.649	179.87	82.8	74:26	+1.78
5.5 (exptl)	2.266(1), 2.272(1)	718.99(2)	84.6(1)		
5.5 (calcd)	2.338, 2.337	177.93	86.5	61:38	0

^aCalculated energy relative to minimum energy conformation

A bond population analysis for $[\{\text{Cp}^*\text{Fe}(\text{CO})_2\}_2\text{In}]^+$ was performed revealing a 74:26 $\sigma:\pi$ breakdown of the covalent Fe-In interaction (as shown in Table 5.4 for both conformations); these values can be compared to an 11% calculated π contribution for the formal Fe-In single bond in the model compound $\text{CpFe}(\text{CO})_2\text{InCl}_2$.¹⁰ A bond population analysis for $[\{\text{Cp}^*\text{Fe}(\text{CO})_2\}_2\text{Ga}]^+$ was also performed (work carried out by Dr A. Rossin) revealing a 61:38 $\sigma:\pi$ breakdown of the

covalent Fe-Ga interaction, which can be put into context by comparison with a ratio of 84:14 for the formal Fe-Ga single bond in the model compound $\text{CpFe}(\text{CO})_2\text{GaCl}_2$.^{10, 11} Further evidence for a significant Fe-Ga π component in $[\{\text{Cp}^*\text{Fe}(\text{CO})_2\}_2\text{Ga}]^+$ is provided by the orbitals HOMO-3 to HOMO-6, each of which features in phase contributions from gallium- and iron-centred π symmetry orbitals (Ga $4p_x$ and $4p_y$; Fe $3d_{xz}$ and $3d_{yz}$) (Figure 5.4).

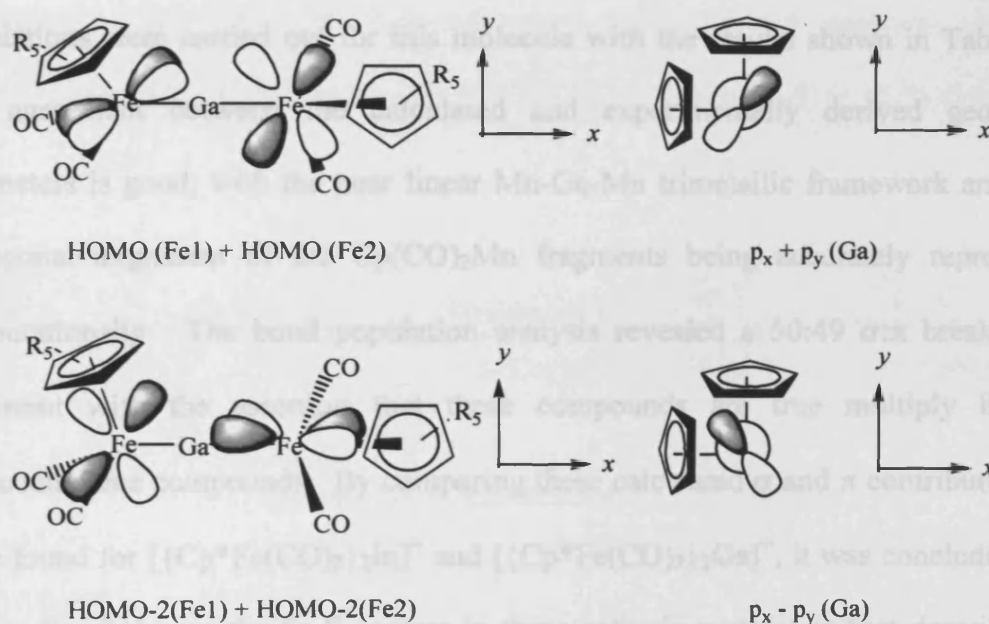


Figure 5.4

Similar analysis for the indium-centred cation $[\{\text{Cp}^*\text{Fe}(\text{CO})_2\}_2\text{In}]^+$ are consistent with a significantly smaller π contribution to the metal-group 13 element bond. Such a finding is as expected on the well- precedented basis of diminished π orbital overlap for the heavier main group elements. In addition, although the barrier to rotation about the Fe-In-Fe axis is not a direct measure of π bond strength (rather the difference in π contributions between 0 and 90° orientations), the relatively flat

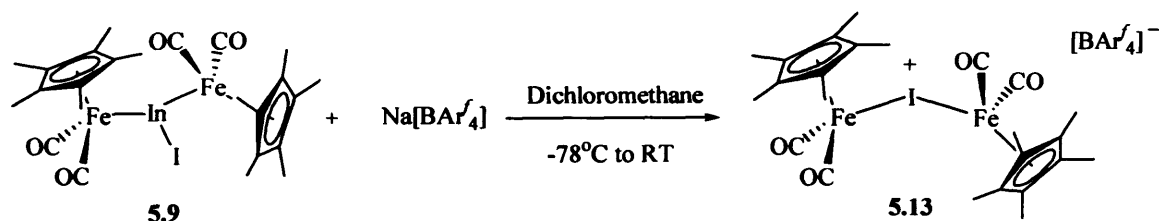
potential function for rotation about this bond is consistent with the smaller (and relatively low) π contributions calculated for both conformations.

Metalloheterocumulene complexes of the type $[\{(\eta^5\text{-C}_5\text{R}_5)\text{Mn}(\text{CO})_2\}_2(\mu\text{-E})]$ (E = Ge, Sn) have been investigated by a number of groups, including those of Hüttner and Herrmann, and are reported in the literature as featuring Mn=E double bonds.¹² The Ge and Sn compounds of this type are formally isoelectronic with the cationic components of 5.12 and $[\{\text{Cp}^*\text{Fe}(\text{CO})_2\}_2(\mu\text{-Ga})][\text{BAR}^f_4]$ 5.5. To investigate the extent of σ and π bonding within $[\{(\eta^5\text{-C}_5\text{R}_5)\text{Mn}(\text{CO})_2\}_2(\mu\text{-Ge})]$ comparative DFT calculations were carried out for this molecule with the results shown in Table 5.5. The agreement between the calculated and experimentally derived geometric parameters is good, with the near linear Mn-Ge-Mn trimetallic framework and near orthogonal alignment of the $\text{Cp}(\text{CO})_2\text{Mn}$ fragments being accurately reproduced computationally. The bond population analysis revealed a 50:49 σ : π breakdown, consistent with the assertion that these compounds are true multiply bonded heterocumulene compounds. By comparing these calculated σ and π contributions to those found for $[\{\text{Cp}^*\text{Fe}(\text{CO})_2\}_2\text{In}]^+$ and $[\{\text{Cp}^*\text{Fe}(\text{CO})_2\}_2\text{Ga}]^+$, it was concluded that the bonding between the Fe-E centres in these cationic systems is best described as being significantly less than a double bond, especially in the case of $[\{\text{Cp}^*\text{Fe}(\text{CO})_2\}_2\text{In}]^+$.

Table 5.5 Calculated and Crystallographically Determined structural Parameters for the Components of $[\{\text{CpMn}(\text{CO})_2\}_2(\mu\text{-Ge})]$ **5.16**.

Compound	Mn-Ge distance (Å)	Mn-Ge-Mn angle (deg)	Ct-Mn-Mn-Ct torsion angle (deg)	$\sigma:\pi$ break -down	E_{rel} (kcal mol^{-1})
5.16 (exptl)	2.18(2)	179(1)	83(3)		
5.16 (calcd)	2.21(2)	178(8)	88(4)	50:49	0

In contrast to the simple bromide abstraction chemistry observed for **5.8**, the corresponding chemistry with iodo-substituted indanediyl **5.9** generates the iodo bridged species $[\{\text{Cp}^*\text{Fe}(\text{CO})_2\}_2(\mu\text{-I})]^+[\text{BAr}_4^-]$ (**5.13**, Scheme 5.8) in 15 % yield.^{3b}



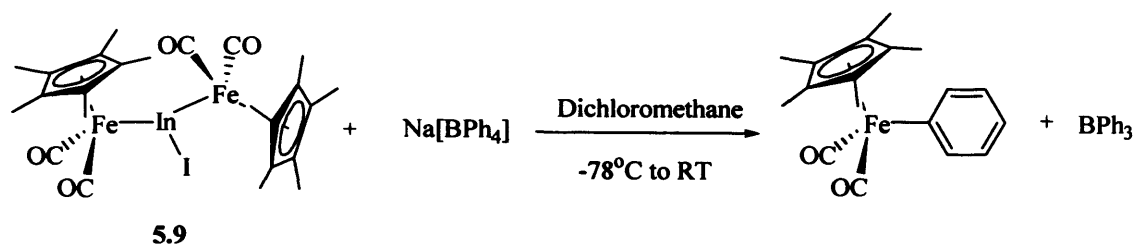
Scheme 5.8 Synthetic route to complex **5.13**.

The proposed formulation of **5.13** is supported by multinuclear NMR data and by the IR measured carbonyl stretching frequencies. The ^1H NMR spectrum implies the presence of two $\text{Cp}^*\text{Fe}(\text{CO})_2$ fragments to one $[\text{BAr}_4]^-$ anion on the basis of a 2:1 ratio of the relevant integrated intensities. Three strong CO stretches were observed in the IR spectrum at 2003, 1984 and 1952 cm^{-1} , which are similar to those found for $[\{\text{Cp}^*\text{Fe}(\text{CO})_2\}_2(\mu\text{-In})]^+$. Electrospray mass spectra display weak peaks for the parent $[\text{M}]^+$ ions with fragment peaks $[\text{M}-\text{CO}]^+$, $[\text{M}-2\text{CO}]^+$, $[\text{M}-3\text{CO}]^+$, $[\text{M}-4\text{CO}]^+$ being evident; the isotope distribution is as expected for a complex containing one iodine and two iron atoms.

Single crystals of **5.13** were obtained by a layering a concentrated dichloromethane solution of **5.13** with hexanes at -30°C . Unfortunately, due to the poor quality of the crystals the structure could not be resolved and thus the structure is proposed on the basis of spectroscopic data. Very recently the structure of this iodide-bridged product has been confirmed crystallographically (work carried out by Dr Drasko Vidovic in the Aldridge group in 2008). Most notably, the structure features a bent geometry at the bridging (iodine) atom and a Fe-I-Fe angle of *ca.* $114.9(1)^{\circ}$, in contrast to the near linear geometries measured for the gallium- and indium-bridged cations.

Although the precise mechanism for the formation of $[\{\text{Cp}^*\text{Fe}(\text{CO})_2\}_2(\mu\text{-I})]^+[\text{BARf}_4]^-$ **5.13** is not clear, IR monitoring reveals that $\text{Cp}^*\text{Fe}(\text{CO})_2\text{I}$ is an intermediate on the overall reaction pathway. In addition, indium metal is deposited during the reaction.

It has therefore been demonstrated that the identity of the halide substituent can affect the subsequent nature of the product generated; in addition further experiments have revealed that the composition of the halide abstracting agent is also vital to the course of the reaction. Thus reaction of $[\text{Cp}^*\text{Fe}(\text{CO})_2]_2\text{InI}$ **5.9** with $\text{Na}[\text{BPh}_4]$ leads to the formation of $\text{Cp}^*\text{Fe}(\text{CO})_2\text{Ph}$ and BPh_3 shown in Scheme 5.9.



Scheme 5.9.

This chemistry is presumably due to the more reactive nature of the $[\text{BPh}_4]^-$ anion compared to $[\text{BARf}_4]^-$. The presence of both BPh_3 and $\text{Cp}^*\text{Fe}(\text{CO})_2\text{Ph}$ products among the reaction products is indicative of abstraction of a phenyl group from the tetraphenylborate counter ion.⁹ Similar reactivity has previously been displayed with highly electrophilic borylene and gallylene complexes of iron. For example, Aldridge *et al.* have previously reported that reaction of $[\text{Cp}^*\text{Fe}(\text{CO})_2]_2\text{GaCl}$ 5.4 with $\text{Na}[\text{BPh}_4]$ similarly yielded $\text{Cp}^*\text{Fe}(\text{CO})\text{Ph}$ and BPh_3 .^{3b} Consequently, $\text{Na}[\text{BARf}_4]$ is generally the preferred halide abstracting agent due to the weaker coordinating ability of the $[\text{BARf}_4]^-$ counter ion.

5.4 Trapping Reactions

5.4.1 Experimental

Synthesis of $[\{\text{Cp}^\text{Fe}(\text{CO})_2\}_2(\mu\text{-In}^{\text{thf}})]^+[\text{BARf}_4]^-$ (5.15)*

To a solution of $[\{\text{Cp}^*\text{Fe}(\text{CO})_2\}_2\{\mu\text{-In}\}][\text{BARf}_4]$ 5.12 in dichloromethane, prepared in situ from $\text{Na}[\text{BARf}_4]$ (0.059 g, 0.067 mmol) and $[\text{Cp}^*\text{Fe}(\text{CO})_2]_2\text{InBr}$ 5.8 (0.041 g, 0.068 mmol) at -78°C , was added thf (2 cm³), and the reaction mixture was warmed to 20°C over 30 min. After the mixture was stirred for a further 1 h at 20°C , the reaction was judged to be complete by IR spectroscopy; filtration and cooling to -30°C led to the isolation of $[\{\text{Cp}^*\text{Fe}(\text{CO})_2\}_2\{\mu\text{-In}^{\text{thf}}\}][\text{BARf}_4]$ 5.15 as a yellow

microcrystalline solid suitable for X-ray diffraction (0.030 g, 41%). ^1H NMR (400 MHz, CD_2Cl_2): δ_{H} 1.69 (b m, 4H, CH_2 of thf), 1.86 (s, 30H, Cp*), 3.63 (b m, 4H, CH_2 of thf), 7.48 (s, 4H, *para* CH of BAr_4^-), 7.64 (s, 8H, *ortho* CH of BAr_4^-). ^{13}C NMR (76 MHz, CD_2Cl_2): δ_{C} 10.5 (CH_3 of Cp*), 27.3 (CH_2 of thf), 59.1 (CH_2 of thf), 96.5 (quaternary of Cp*), 117.4 (*para* CH of BAr_4^-), 124.6 (q, $^1J_{\text{CF}} = 272$ Hz, CF_3 of BAr_4^-), 128.9 (q, $^2J_{\text{CF}} = 34$ Hz, *meta* C of BAr_4^-), 134.8 (*ortho* CH of BAr_4^-), *ipso* C of BAr_4^- and CO signals not observed. IR (thin film thf, cm^{-1}): $\nu(\text{CO})$ 1974, 1958, 1922. MS EI: m/z 609.0 {75 %, $[\text{M} - \text{thf}]^+$ }, correct isotope distribution for 2 iron and 1 indium atoms. Exact mass: calcd for $[\text{M} - \text{thf}]^+$ 608.9876, measd 608.9874.

Synthesis of $[\{\text{Cp}^*\text{Fe}(\text{CO})_2\}_2(\mu\text{-In}4\text{pic})]^+[\text{BAr}_4^-]$ (5.17)

A solution of $[\text{Cp}^*\text{Fe}(\text{CO})_2]_2\text{InBr}$ **5.8** (0.052 g, 0.08 mmol) in dichloromethane (10 cm^3) was added to slurry of $\text{Na}[\text{BAr}_4^-]$ (0.072 g, 0.08 mmol) also in dichloromethane (2 cm^3) at -78°C with vigorous stirring. The reaction was allowed to warm to room temperature and stirred for 2 h; IR sampling at this point revealed bands at 2004, 1983, and 1952 cm^{-1} characteristic of $[\{\text{Cp}^*\text{Fe}(\text{CO})_2\}_2\text{In}]^+[\text{BAr}_4^-]$ (**5.12**). The solution was then filtered and a solution of 4-picoline in dichloromethane (0.90 cm^3 of a 0.1 M solution, 0.08 mmol) was added with an immediate colour change from orange to light yellow. The reaction was stirred for 1 h, concentration, layering with hexanes and storage at -30°C yielded $[\{\text{Cp}^*\text{Fe}(\text{CO})_2\}_2(\mu\text{-In}4\text{pic})]^+[\text{BAr}_4^-]$ (**5.17**) as an orange oil. ^1H NMR (300 MHz, CD_2Cl_2): δ_{H} 1.74 (s, 30H, CH_3 of Cp*), 2.38 (3H, s, CH_3 of picoline), 7.37 (d, $J = 5.44$ Hz, 2H, CH of picoline), 7.48 (s, 4H, *para*-H of BAr_4^-), 7.64 (s, 8H, *ortho*-H of BAr_4^-), 8.27 (d, $J = 6.63$ Hz, 2H, CH of picoline). ^{13}C NMR (76 MHz, CD_2Cl_2): δ_{C} 9.9 (CH_3 of Cp*), 21.4 (CH_3 of picoline), 95.4 (quaternary C of Cp*), 117.5 (*para*-CH of BAr_4^-), 122.8 (q, $^1J_{\text{CF}} = 273$ Hz, CF_3 of

$\text{BAr}^f_4^-$), 127.3 (CH of picoline), 128.7 (q, $^2J_{\text{CF}} = 29$ Hz, *meta*-C of $\text{BAr}^f_4^-$), 134.8 (*ortho*-CH of $\text{BAr}^f_4^-$), 147.0 (quaternary C of picoline), 151.0 (CH of picoline), 161.5 (q, $^1J_{\text{CB}} = 49$ Hz, *ipso*-C of $\text{BAr}^f_4^-$), 215.9 (CO), *ipso* C of 4-picoline not observed. ^{11}B NMR (96 MHz, CD_2Cl_2) : $\delta_{\text{B}} -7.6$ ($\text{BAr}^f_4^-$). ^{19}F NMR (283 MHz, CD_2Cl_2) : $\delta_{\text{F}} -62.8$ (CF_3). IR (thin film CD_2Cl_2 , cm^{-1}) : $\nu(\text{CO})$ 1966, 1932, 1910.

Synthesis of $[\{\text{Cp}^*\text{Fe}(\text{CO})_2\}_2(\mu\text{-InPMe}_3)]^+[\text{BAr}^f_4]^-$ (5.18)

A solution of $[\text{Cp}^*\text{Fe}(\text{CO})_2]_2\text{InBr}$ 5.8 (52 mg, 0.08 mmol) in dichloromethane (10 cm^3) was added to slurry of $\text{Na}[\text{BAr}^f_4]$ (72 mg, 0.08 mmol) in dichloromethane (2 cm^3) at -78°C with vigorous stirring. The reaction was allowed to warm to room temperature and stirred for 2 h; IR sampling at this point revealed bands at 2005, 1983, and 1952 cm^{-1} characteristic of $[\{\text{Cp}^*\text{Fe}(\text{CO})_2\}_2\text{In}]^+[\text{BAr}^f_4]^-$ (5.12). The solution was filtered and a solution of PMe_3 in dichloromethane (1.20 cm^3 of a 0.08 M solution, 0.07 mmol) was added with an immediate colour change to light yellow. The reaction was stirred for 1 h, concentration, layering with hexanes and storage at -30°C yielded $[\{\text{Cp}^*\text{Fe}(\text{CO})_2\}_2(\mu\text{-InPMe}_3)]^+[\text{BAr}^f_4]^-$ (5.18) as pale yellow microcrystalline needles. ^1H NMR (300 MHz, CD_2Cl_2) : $\delta_{\text{H}} 1.40$ (9H, d, $J = 10.11$ Hz, CH_3 of PMe_3), 1.82 (30H, s, CH_3 of Cp^*), 7.48 (4H, s, *para*-H of $\text{BAr}^f_4^-$), 7.64 (8H, s, *ortho*-H of $\text{BAr}^f_4^-$). ^{31}P NMR (MHz, CD_2Cl_2) : $\delta_{\text{P}} 28.9$ (PMe_3). ^{11}B NMR (96 MHz, CD_2Cl_2) : $\delta_{\text{B}} -7.6$ ($\text{BAr}^f_4^-$). ^{19}F NMR (283 MHz, CD_2Cl_2) : $\delta_{\text{F}} -62.8$ (CF_3). IR (thin film CD_2Cl_2 , cm^{-1}) : $\nu(\text{CO})$ 1988, 1959, and 1930 cm^{-1} .

Synthesis of $[\{\text{Cp}^*\text{Fe}(\text{CO})_2\}_2(\mu\text{-Ga.thf})]^+[\text{BAr}^f_4]^-$ (5.19)

A solution of $[\text{Cp}^*\text{Fe}(\text{CO})_2]_2\text{GaCl}$ 5.4 (0.051 g, 0.09 mmol) in dichloromethane (10 cm^3) was added to slurry of $\text{Na}[\text{BAr}^f_4]$ (0.078 g, 0.09 mmol) also in dichloromethane

(2 cm³) at -78°C with vigorous stirring. The reaction was allowed to warm to room temperature and stirred for 2 h; IR sampling at this point revealed bands at 2015, 1994, and 1963 cm⁻¹ characteristic of [$\{\text{Cp}^*\text{Fe}(\text{CO})_2\}_2\text{Ga}\}^+[\text{BAr}_f^4]^-$ (5.5). The solution was filtered and thf (2 cm³) was added with an immediate colour change to light yellow. The reaction was stirred for 1 h, concentration and layering with hexanes yielded [$\{\text{Cp}^*\text{Fe}(\text{CO})_2\}_2(\mu\text{-Ga thf})\}^+[\text{BAr}_f^4]^-$ (5.19) as pale yellow needles. Isolated yield 0.033 g, 35 %. ¹H NMR (400 MHz, CD₂Cl₂) : δ 1.80 (br m, 4H, CH₂ of thf), 1.86 (s, 30H, Cp*), 3.65 (br m, 4H, CH₂ of thf), 7.48 (s, 4H, *para*-CH of BAr_f⁴⁻), 7.65 (s, 8H, *ortho*-CH of BAr_f⁴⁻). ¹³C NMR (76 MHz, CD₂Cl₂) : δ 10.2 (CH₃ of Cp*), 25.5 (CH₂ of thf), 69.0 (CH₂ of thf), 97.4 (quaternary C of Cp*), 117.6 (*para*-CH of BAr_f⁴⁻), 122.8 (q, ¹J_{CF} = 273 Hz, CF₃ of BAr_f⁴⁻), 129.1 (q, ²J_{CF} = 34 Hz, *meta*-C of BAr_f⁴⁻), 134.9 (*ortho*-CH of BAr_f⁴⁻), 160.8 (q, ¹J_{CB} = 53 Hz, *ipso*-C of BAr_f⁴⁻), 211.6 (CO). ¹¹B NMR (96 MHz, CD₂Cl₂) : δ -7.6 (BAr_f⁴⁻). ¹⁹F NMR (283 MHz, CD₂Cl₂) : δ -62.8 (CF₃ of BAr_f⁴⁻). IR (thin film CH₂Cl₂/thf, cm⁻¹) : ν_(CO) 1978, 1962, 1927. MS (ES⁺) : m/z 635.7 (weak) [M]⁺, correct isotope distribution for 2 Fe, 1 Ga atoms, significant fragment ions at m/z 563 (45 %) [M - thf]⁺, 535 (10 %) [M - thf - CO]⁺, 507 (5 %) [M - thf - 2CO]⁺. Exact mass: calc. for [M - thf]⁺ 563.0093, meas. 563.0095.

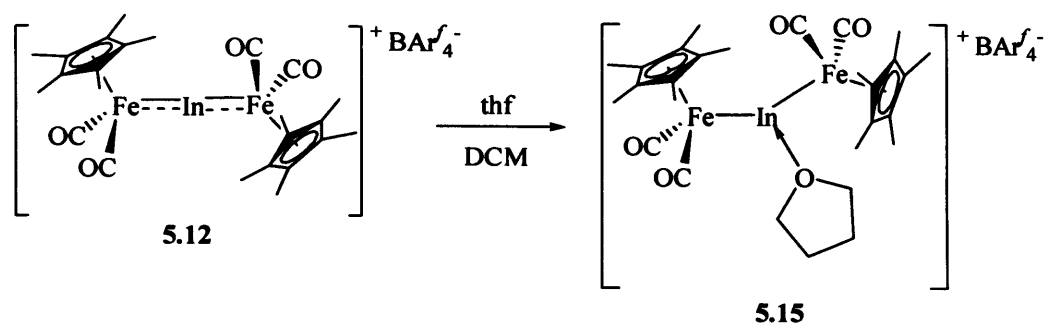
Synthesis of [$\{\text{Cp}^*\text{Fe}(\text{CO})_2\}_2(\mu\text{-Ga 4-pic})\}^+[\text{BAr}_f^4]^-$ (5.20)

A solution of [Cp*Fe(CO)₂]₂GaCl 5.4 (0.161 g, 0.268 mmol) in dichloromethane (10 cm³) was added to slurry of Na[BAr_f⁴⁻] (0.286 g, 0.323 mmol) also in dichloromethane (2 cm³) at -78°C with vigorous stirring. The reaction was allowed to warm to room temperature and stirred for 2 h; IR sampling at this point revealed bands at 2016, 1994, and 1963 cm⁻¹ characteristic of [$\{\text{Cp}^*\text{Fe}(\text{CO})_2\}_2\text{Ga}\}^+[\text{BAr}_f^4]^-$ (5.5). The solution was filtered and a solution of 4-picoline in dichloromethane (3.14 cm³ of a 0.09 M

solution, 0.26 mmol) was added with an immediate colour change to light yellow. The reaction was stirred for 1 h, concentration, layering with hexanes and storage at -30°C yielded $[\{\text{Cp}^*\text{Fe}(\text{CO})_2\}_2(\mu\text{-Ga}4\text{-pic})]^+[\text{BAr}^f_4]^-$ (**5.20**) as yellow crystals suitable for X-ray diffraction. ^1H NMR (300 MHz, CD_2Cl_2) : δ_{H} 1.62 (s, 30H, CH_3 of Cp^*), 2.41 (s, 3H, CH_3 of picoline), 7.42 (d, $J = 5.44$ Hz, 2H, CH of picoline), 7.50 (s, 4H, *para*-H of $\text{BAr}^f_4^-$), 7.58 (s, 8H, *ortho*-H of $\text{BAr}^f_4^-$), 8.68 (d, $J = 6.63$ Hz, 2H, CH of picoline). ^{13}C NMR (76 MHz, CD_2Cl_2) : δ_{C} 8.9 (CH_3 of Cp^*), 20.8 (CH_3 of picoline), 95.1 (quaternary C of Cp^*), 116.7 (*para*-CH of $\text{BAr}^f_4^-$), 122.7 (q, $^1J_{\text{CF}} = 273$ Hz, CF_3 of $\text{BAr}^f_4^-$), 127.1 (CH of picoline), 128.2 (q, $^2J_{\text{CF}} = 29$ Hz, *meta*-C of $\text{BAr}^f_4^-$), 134.0 (*ortho*-CH of $\text{BAr}^f_4^-$), 144.5 (quaternary C of picoline), 151.0 (CH of picoline), 161.2 (q, $^1J_{\text{CB}} = 49$ Hz, *ipso*-C of $\text{BAr}^f_4^-$), 213.8 (CO). ^{11}B NMR (96 MHz, CD_2Cl_2) : $\delta_{\text{B}} -7.6$ ($\text{BAr}^f_4^-$). ^{19}F NMR (283 MHz, CD_2Cl_2) : $\delta_{\text{F}} -62.8$ (CF_3). IR (thin film CD_2Cl_2 , cm^{-1}) : $\nu(\text{CO})$ 1993, 1970, 1924.

5.4.2 Results and Discussion

The reactivity of $[\{\text{Cp}^*\text{Fe}(\text{CO})_2\}_2(\mu\text{-In})]^+[\text{BAr}^f_4]^-$ **5.12** and $[\{\text{Cp}^*\text{Fe}(\text{CO})_2\}_2(\mu\text{-Ga})]^+[\text{BAr}^f_4]^-$ **5.5** toward neutral two electron donors has been investigated. In the presence of tetrahydrofuran, the cationic trimetallic species $[\{\text{Cp}^*\text{Fe}(\text{CO})_2\}_2(\mu\text{-In})]^+[\text{BAr}^f_4]^-$ **5.12** coordinates a single molecule of thf to generate the 1:1 adduct $[\{\text{Cp}^*\text{Fe}(\text{CO})_2\}_2(\mu\text{-In.thf})]^+[\text{BAr}^f_4]^-$ **5.15** (Scheme 5.10).^{3b}



Scheme 5.10 Synthetic route to complex **5.15**.

The 1:1 stoichiometry is implied by integration of the ^1H NMR signals of the thf and Cp* moieties, and coordination of the oxygen donor at the group 13 centre is consistent with the significant shifts to lower wavenumbers in the carbonyl stretching bands (1974, 1958, 1922 vs. 2005, 1983, 1951 cm^{-1} for **5.12**).

Single crystals of **5.15** suitable for X-ray diffraction were accessible by cooling a concentrated solution of **5.15** in dichloromethane to -30°C . The 1:1 binding stoichiometry implied by the spectroscopic data for **5.15** was confirmed by single crystal X-ray diffraction studies and the structure is illustrated in Figure 5.5. Relevant bond lengths and angles are listed in Table 5.6.

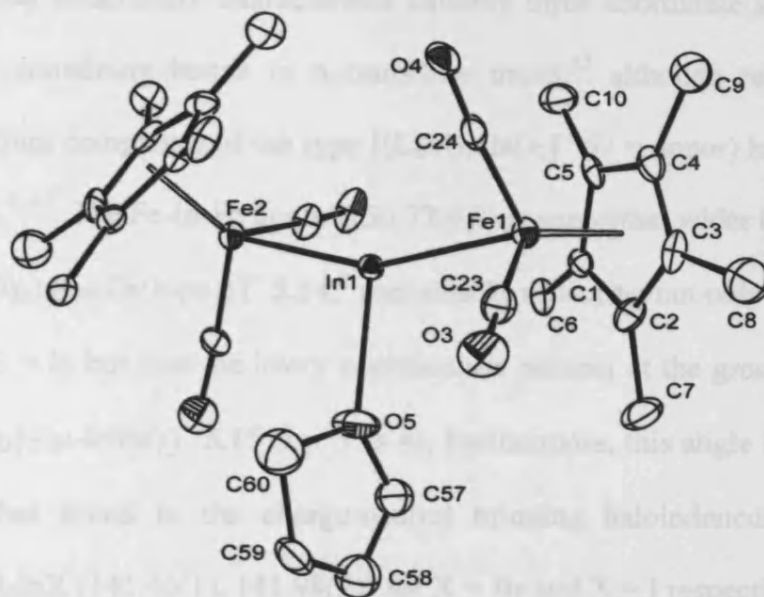


Figure 5.5 The molecular structure of $[\{\text{Cp}^*\text{Fe}(\text{CO})_2\}_2(\mu\text{-Inthf})][\text{BARf}_4]$ **5.15**.

Table 5.6 Selected bond lengths [Å] and angles [°] for **5.15**.

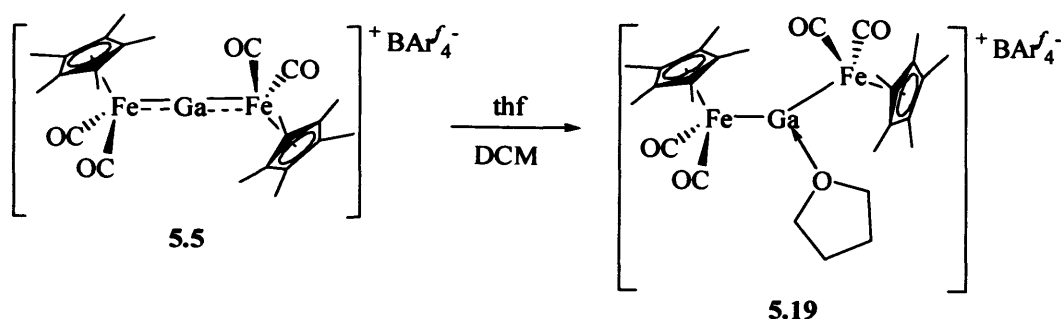
Fe(1)-In(1)	2.498(2)	Fe(1)-C(23)	1.748(13)
Fe(2)-In(1)	2.494(2)	In(1)-O(5)	2.382(8)
Fe(1)-Cp* centroid	1.729(12)		
Fe(1)-In(1)-Fe(2)	156.72(6)	Fe(2)-In(1)-O(5)	103.2(3)
Fe(1)-In(1)-O(5)	100.1(3)		

The indium centre is trigonal planar ($\Sigma(\text{angles at indium}) = 360$ within the standard 3σ limit), and the approximately orthogonal alignment of the Fe_2In and OC_2 planes (torsion $\text{Fe}(1)\text{-In}(1)\text{-O}(5)\text{-C}(57) = 80.0(4)^\circ$) is presumably enforced on steric grounds. As expected, given the relatively small π component determined for the Fe-In bonds in the base free complex $[\{\text{Cp}^*\text{Fe}(\text{CO})_2\}_2\text{In}]^+$, there is only a relatively minor lengthening of these linkages on coordination of the thf molecule (2.498(2), 2.494(2) vs. 2.460(2), 2.469(2) Å for **5.15** and **5.12**, respectively). **5.15** represents

only the second structurally characterised cationic three coordinate indium species and the first containing bonds to a transition metal,¹³ although related N-donor stabilised gallium complexes of the type $[(L_nM)_2GaD_2]^+$ (D = donor) have previously been reported.^{8, 14} The Fe-In-Fe angle ($156.72(6)^\circ$) is somewhat wider than that found in $[\{CpFe(CO)_2\}_2\{\mu-Ga(bipy)\}]^+$ **5.14**,⁸ presumably reflecting not only the longer Fe-E bonds for E = In but also the lower coordination number at the group 13 centre in $[\{Cp^*Fe(CO)_2\}_2\{\mu-In(thf)\}]^+$ **5.15** (*i.e.* 3 vs 4). Furthermore, this angle is significantly wider than that found in the charge-neutral bridging haloindanediyl complexes $[Cp^*Fe(CO)_2]_2InX$ ($141.46(1)$, $141.98(2)^\circ$ for X = Br and X = I respectively),⁵ despite the greater steric demands of thf (*cf.* Br⁻ or I⁻). This phenomenon has previously been observed for a range of group 13 adducts. Thus, for example, the Cl-Ga-Cl angles in $GaCl_3 \cdot thf$ (113.07° (mean)) are significantly wider than those found in the corresponding Cl⁻ adduct $[GaCl_4]^-$ (109.5° (mean)).¹⁵

In a similar fashion, coordination of a single molecule of thf is also observed for $[\{Cp^*Fe(CO)_2\}_2(\mu-Ga)]^+[BARf_4]^-$ **5.5**, generating the three coordinate cationic species $[\{Cp^*Fe(CO)_2\}_2(\mu-Ga \cdot thf)]^+[BARf_4]^-$ **5.19** (Scheme 5.11).⁵ The 1:1 stoichiometry is implied by integration of the ¹H NMR signals 1.80 (CH₂ of thf), 1.86 (CH₃ of Cp*), 3.65 (CH₂ of thf), 7.48 (CH of BARf₄⁻), and 7.65 (CH of BARf₄⁻) with relative intensities of 4:30:4:4:8, respectively. The ¹³C NMR spectrum is consistent with coordination of thf with peaks at 10.2, 25.5, 69.0, 97.4, 117.6, 122.8, 129.1, 134.9, 160.8 and 211.6 corresponding to CH₃ of Cp*, CH₂ of thf, CH₂ of thf, quaternary C of Cp*, *para*-CH of BARf₄⁻, CF₃ of BARf₄⁻, *meta*-C of BARf₄⁻, *ortho*-CH of BARf₄⁻, *ipso*-C of BARf₄⁻, CO respectively. The measured CO stretching bands are consistent with the coordination of thf to the gallium centre with a shift to lower

coordination numbers on coordination (1978, 1962, 1927 vs. 2016, 1994, 1963 cm^{-1} for 5.5) mirroring that found for the indium complexes discussed above.



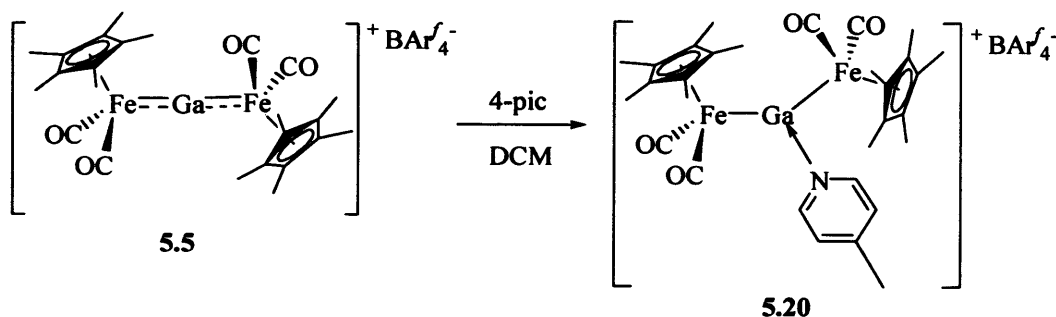
Scheme 5.11 Synthetic route to complex **5.19**.

Unfortunately, attempts to grow single crystals of **5.19** suitable for X-ray diffraction studies were unsuccessful and the formulation of this complex is therefore proposed on the basis of NMR and IR spectroscopic results, from which a similar structure for **5.19** to that obtained for **5.15** can be proposed.

Interestingly, it has been demonstrated that the coordination of the thf donor in **5.15** and **5.19** is reversible. For example, on exposure of **5.15** and **5.19** to prolonged continuous vacuum (10^{-4} Torr), the spectroscopic data obtained for both complexes is consistent with the loss of the coordinated thf. Monitoring this process by IR, and ^1H NMR spectroscopy reveals that in the case of the gallium species **5.19** a mixture of the donor-stabilised and the 'naked' two coordinate species **5.12** is obtained. In the case of indium-containing **5.15** complete loss of thf is observed over a period of 6 h. leading to the regeneration of $[\{\text{Cp}^*\text{Fe}(\text{CO})_2\}_2(\mu\text{-In})]^+[\text{BAr}_4^-]$ **5.12**. This behaviour is consistent with a relatively weak Lewis acid/base interaction in both cases, with the greater ease of removal of the indium-bound thf ligand reflecting previous reports of

the thermodynamics of oxygen donor coordination to gallium- and indium- based Lewis acids.^{16, 17}

The base-stabilised adduct $[\{\text{Cp}^*\text{Fe}(\text{CO})_2\}_2(\mu\text{-Ga}^4\text{pic})]^+[\text{BAr}_4^f]^-$ **5.20** was prepared by reaction of $[\{\text{Cp}^*\text{Fe}(\text{CO})_2\}_2(\mu\text{-Ga})]^+[\text{BAr}_4^f]^-$ **5.5** with 4-picoline in dichloromethane (Scheme 5.12).¹⁸



Scheme 5.12 Synthetic route to complex **5.20**.

The formulation of **5.20** is supported by multinuclear NMR data. Coordination of a single molecule of picoline at the gallium centre is implied by integration of the ^1H NMR signals with peaks being evident at 1.62 (CH_3 of Cp^*), 2.41 (CH_3 of picoline), 7.42 (CH of picoline), 7.50 (*para*-H of BAr_4^f), 7.58 (*ortho*-H of BAr_4^f), 8.68 (CH of picoline). The measured carbonyl stretching frequencies [1993, 1970, 1936 and 1924 cm^{-1}] are intermediate between those found for two-coordinate **5.5** [2015, 1994, and 1963 cm^{-1}]^{3b} and *neutral* three-coordinate **5.4** [1960, 1925 and 1910 cm^{-1}]⁵ species which is consistent with coordination at the gallium centre with the formation of a *cationic* three coordinate species.

Single crystals of **5.20** suitable for X-ray diffraction were accessible by cooling a concentrated solution of **5.20** in dichloromethane to -30°C ; the structure is

illustrated in Figure 5.6. Relevant bond lengths and angles are listed in Table 5.7. The crystallographic study reveals that the solid state structure contains isolated $[\{\text{Cp}^*\text{Fe}(\text{CO})_2\}_2(\mu\text{-Ga}^4\text{pic})]^+$ and $[\text{BAR}^f_4]^-$ ions, thereby confirming the 1:1 ratio of $[\{\text{Cp}^*\text{Fe}(\text{CO})_2\}_2(\mu\text{-Ga})]^+$ and 4-picoline moieties and the trigonal planar coordination geometry at the gallium centre [$\Sigma(\text{angles at gallium}) = 360^\circ$ within the standard 3σ limit]. From a structural point of view important features include the Fe-Ga distances and the Fe-Ga-Fe angle for **5.20**. Both structural parameters [2.328(1), 2.342(1) Å and $139.67(4)^\circ$] are intermediate between those measured for the two- and four-coordinate gallium cations $[\{\text{Cp}^*\text{Fe}(\text{CO})_2\}_2(\mu\text{-Ga})]^+$ **5.5** and $[\{\text{CpFe}(\text{CO})_2\}_2(\mu\text{-Ga}^b\text{bipy})]^+$ [2.266(1), 2.272(1) Å, $178.99(2)^\circ$ and 2.397(2) $^\circ$, 2.404(1) $^\circ$, $132.81(5)^\circ$, respectively].^{3b, 8} Such a trend is expected on the basis of enhanced steric crowding and/or diminished Fe→Ga π backbonding with increasing coordination number at the gallium centre.

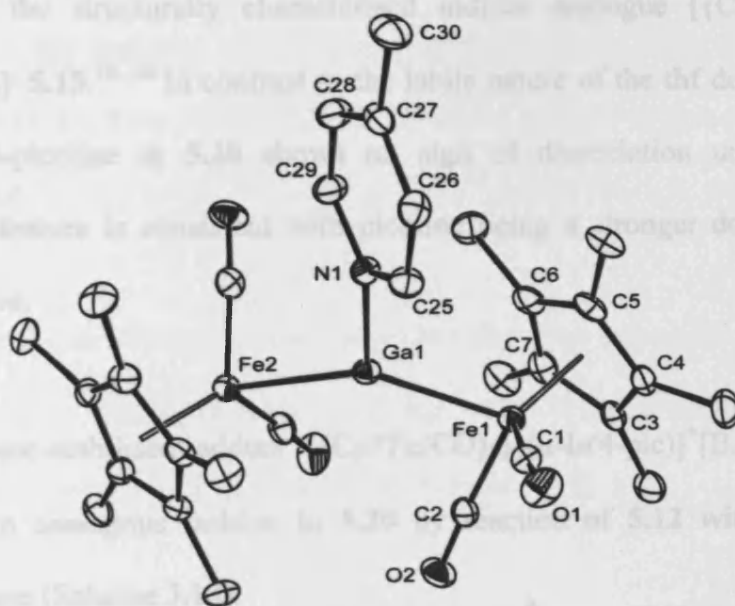


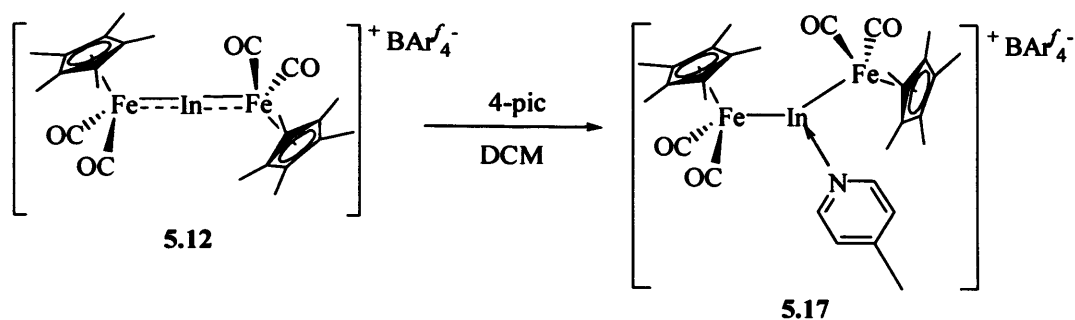
Figure 5.6 The molecular structure of $[\{\text{Cp}^*\text{Fe}(\text{CO})_2\}_2(\mu\text{-Ga}^4\text{pic})]^+[\text{BAR}^f_4]^-$ **5.20**.

Table 5.7 Selected bond lengths [Å] and angles [°] for **5.20**.

Ga(1)-N(1)	2.142(5)	C(1)-O(1)	1.148(7)
Fe(2)-Ga(1)	2.3274(10)	N(1)-C(25)	1.343(7)
Fe(1)-Ga(1)	2.3415(10)	C(27)-C(30)	1.486(9)
Fe(1)-C(1)	1.749(6)	Fe(1)-Cp* centroid	1.727(6)
O(1)-C(1)-Fe(1)	176.2(5)	N(1)-Ga(1)-Fe(1)	109.90(13)
N(1)-C(25)-C(26)	123.1(6)	Fe(2)-Ga(1)-Fe(1)	139.67(4)
C(1)-Fe(1)-Ga(1)	91.36(9)	C(13)-Fe(2)-Ga(1)	86.6(2)
N(1)-Ga(1)-Fe(2)	110.22(12)		

5.20 represents the first cationic three-coordinate gallium-containing system featuring bonds to a transition metal, although a similar structure has been proposed for $[\{\text{Cp}^*\text{Fe}(\text{CO})_2\}_2(\mu\text{-Ga}\cdot\text{thf})]^+[\text{BAr}'_4]^-$ **5.19** on the basis of similar spectroscopic properties to the structurally characterised indium analogue $[\{\text{Cp}^*\text{Fe}(\text{CO})_2\}_2(\mu\text{-In}\cdot\text{thf})]^+[\text{BAr}'_4]^-$ **5.15**.^{18, 3b} In contrast to the labile nature of the thf donor in **5.15**, the coordinated 4-picoline in **5.20** shows no sign of dissociation under continuous vacuum, this feature is consistent with picoline being a stronger donor than thf as discussed above.

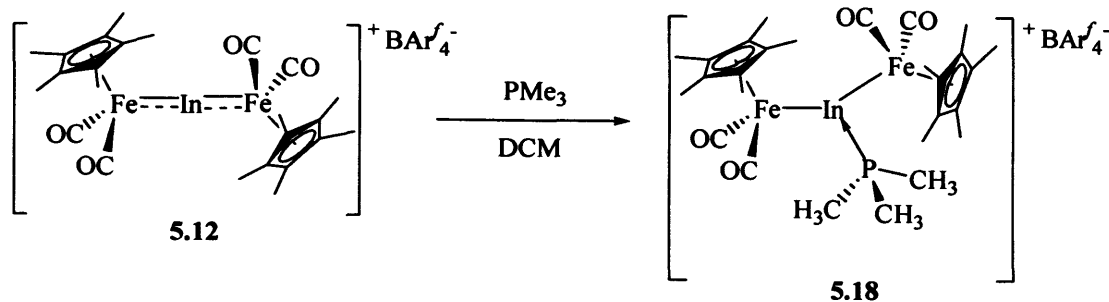
The base-stabilised adduct $[\{\text{Cp}^*\text{Fe}(\text{CO})_2\}_2(\mu\text{-In}\cdot 4\text{-pic})]^+[\text{BAr}'_4]^-$ **5.17** was prepared in an analogous fashion to **5.20** by reaction of **5.12** with 4-picoline in dichloromethane (Scheme 5.13).



Scheme 5.13 Synthetic route to complex 5.17.

The proposed formulation is supported by multinuclear NMR data, in which the 1:1 stoichiometry is implied by integration of the ^1H NMR signals due to the 4-picoline and Cp^* moieties. The coordination of the nitrogen donor at the group 13 centre is consistent with the significant shifts to lower wavenumbers in the carbonyl stretching bands (1966 , 1932 and 1910 cm^{-1}), which are comparable to those found for the thf adduct 5.15 (1974 , 1958 and 1922 cm^{-1}). Unfortunately, attempts to grow single crystals of 5.17 suitable for X-ray diffraction studies were unsuccessful and the formulation of this complex is therefore proposed on the basis of NMR and IR spectroscopic results, from which a similar structure for 5.17 to that obtained for 5.20 can be proposed.

Investigations with phosphine donors has also been examined, reaction of 5.12 with PMe_3 in dichloromethane yielded the PMe_3 coordinated adduct $[\{\text{Cp}^*\text{Fe}(\text{CO})_2\}_2(\mu\text{-In}\cdot\text{PMe}_3)]^+ [\text{BAr}_4]^-$ 5.18 (Scheme 5.14).



Scheme 5.14 Synthetic route to complex **5.18**.

The proposed formulation of **5.18** is supported by multinuclear NMR data in which the 1:1 stoichiometry is implied by integration of the ^1H NMR signals due to the PMe_3 and Cp^* moieties. The formation of the PMe_3 adduct **5.18** is implied by the change in the ^{31}P NMR chemical shifts [δ_{P} -60 for free PMe_3 to δ_{P} 28.9 for **5.18**]. The coordination of the phosphine donor at the group 13 centre is consistent with significant shifts to lower wavenumbers in the carbonyl stretching bands (1988, 1959 and 1930 cm^{-1}) which is comparable to those found for **5.19** and **5.17** (1974, 1958, 1922 and 1966, 1932, 1910 cm^{-1} , respectively). Unfortunately, attempts to grow single crystals of **5.18** suitable for X-ray diffraction studies were unsuccessful and the formulation of this complex is therefore proposed on the basis of multinuclear NMR and IR spectroscopic results.

5.5 Attempted Syntheses of Phosphine Containing Bridging Systems

5.5.1 Experimental

Reaction of $[\text{Cp}^\text{Fe}(\text{CO})_2]_2\text{InBr}$ (**5.8**) with dppe*

To a solution/suspension of $[\text{Cp}^*\text{Fe}(\text{CO})_2]_2\text{InBr}$ **5.8** (0.076 g, 0.110 mmol) in toluene (10 cm^3) was added a solution of dppe (0.045 g, 0.113) in toluene (40 cm^3), the reaction mixture was photolysed for 20 h. with stirring. The brown solution was filtered, concentrated *in vacuo* (*ca.* 10 cm^3), and hexanes (30 cm^3), was added,

however, no tractable compounds were isolated. The ^{31}P NMR revealed a number of phosphorus containing compounds with multiple peaks being present in the spectrum.

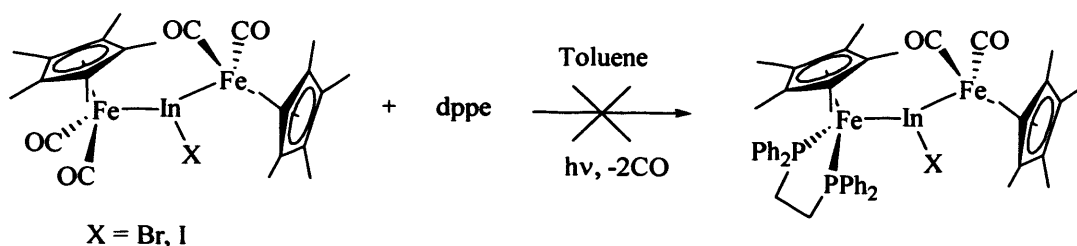
Reaction of $[\text{Cp}^*\text{Fe}(\text{CO})_2]_2\text{InI}$ (5.9) with dppe

To a solution/suspension of $[\text{Cp}^*\text{Fe}(\text{CO})_2]_2\text{InI}$ **5.9** (0.151 g, 0.205 mmol) in toluene (20 cm^3) was added a solution of dppe (0.077 g, 0.194 mmol) in toluene (80 cm^3), the reaction mixture was photolysed for 50 h with stirring. The resulting orange solution was filtered, concentrated *in vacuo* (ca. 15 cm^3), and hexanes (30 cm^3), was added, however, no tractable compounds were isolated. The ^{31}P NMR revealed a number of phosphorus containing compounds with multiple peaks being present in the spectrum.

5.5.2 Results and Discussion

With the aim of varying the degree of the π back-bonding component within complexes of the type $[\{\text{Cp}^*\text{Fe}(\text{L})_2\}_2(\mu\text{-In})]^+$ and $[\{\text{Cp}^*\text{Fe}(\text{L})_2\}_2(\mu\text{-Ga})]^+$, substitution of the carbonyl ligand for less π acidic phosphine ligands was investigated in the precursor complexes **5.8** and **5.9**. It has been previously demonstrated by Ogino that phosphine ligands such as dppe are effective in stabilising highly reactive group 13 species due to the increased π backbonding character to the group 13 centre.²

Reaction of $[\text{Cp}^*\text{Fe}(\text{CO})_2]_2\text{InX}$ (X = Br, or I) with dppe in toluene under photolytic conditions did not yield any tractable phosphine containing compounds. The ^{31}P NMR revealed a number of phosphorus containing compounds with multiple peaks being present in the spectra.



Scheme 5.15

This mixture of intractable products is perhaps unsurprising given the mechanism of photolytic CO substitution reported in the generation of the species $\text{Cp}^*\text{Fe}(\text{CO})_2\text{GaI}_2$ discussed in Chapter 4.

5.6 Conclusions and Suggestions for Further Research

It has been demonstrated that salt elimination and EX insertion are viable synthetic routes to the synthesis of indium halide complexes of the type $[\text{Cp}^*\text{Fe}(\text{CO})_2]_2\text{InX}$ ($X = \text{Br}$ **5.8**; $\text{I} = \text{5.9}$). Furthermore, it has been shown that halide abstraction chemistry offers a viable synthetic route to the formation of cationic two coordinate group 13 complexes of the type $[\{\text{Cp}^*\text{Fe}(\text{CO})_2\}_2(\mu\text{-In})]^+[\text{BARf}_4]^-$ **5.12**, featuring a 'naked' bridging indium centre. **5.12** can be readily synthesised by the reaction of **5.8** with $\text{Na}[\text{BARf}_4]$. Halide abstraction studies have revealed that the product obtained is dependant on the nature of the halide. Thus, reaction of the bromide-containing **5.8** with $\text{Na}[\text{BARf}_4]$ yielded **5.12**, but the analogous reaction with iodide-containing **5.9** yielded instead the bridging iodo complex $[\{\text{Cp}^*\text{Fe}(\text{CO})_2\}_2(\mu\text{-I})][\text{BARf}_4]$ **5.13**. DFT calculations have revealed the Fe-In bond within **5.12** to contain 74 % σ and 26 % π contributions to the covalent bonding density, which is significantly less than that found for **5.5** (61 % σ and 38 % π contributions to the FeGa bonds) and $[\{\text{Cp}^*\text{Mn}(\text{CO})_2\}_2(\mu\text{-Ge})]$ (50 % σ and 49 % π).

Chemical studies have shown complexes **5.5** and **5.12** to be reactive toward neutral nucleophiles. Thus reaction of $[\{\text{Cp}^*\text{Fe}(\text{CO})_2\}_2(\mu\text{-In})]^+$ (**5.12**, E = In; **5.5**, E = Ga) with neutral nucleophiles thf, 4-picoline or PMe_3 , leads to coordination of these species to the group 13 centre generating the base stabilised adducts $[\{\text{Cp}^*\text{Fe}(\text{CO})_2\}_2(\mu\text{-E}\cdot\text{X})]^+[\text{BAR}'_4]^-$ (**5.15**, E = In, X = thf; **5.20**, E = Ga, X = 4-pic). The reversible coordination of thf is indicative of surprisingly weak Lewis acidic behaviour; stronger coordination of 4-picoline reflects the known basicities of these N- and O-donor ligands towards main group electrophiles.

Further investigations involve examining the potential of substituting the CO ligands within $[\{\text{Cp}^*\text{Fe}(\text{CO})_2\}_2\text{M}]^+[\text{BAR}'_4]^-$ (M = Ga, In) for less π acidic fragments such as PR_3 (where R = Me, Ph etc), with the aim of increasing the multiple bond character within the cationic diyl species on halide abstraction.

5.7 References for Chapter Five

1. (a) Braunschweig, H. *Adv. Organomet. Chem.* **2004**, *51*, 2773. (b) Fischer, R. A.; Weiß, J. *Angew. Chem. Int. Ed.* **1999**, *38*, 2830. (c) Linti, G.; Schnöckel, H. *Coord. Chem. Rev.* **2000**, *206-207*, 285. (d) Schebaum, L. O.; Jutzi, P. *ACS Sym. Ser.* **2002**, *822*, 16. (e) Gemel, C.; Steinke, T.; Cokoja, M.; Kempter, A.; Fischer, R. A. *Eur. J. Inorg. Chem.* **2004**, 4161. (f) Cowley, A. H. *J. Organomet. Chem.* **2004**, *689*, 3866. (g) Braunschweig, H.; Colling, M. *J. Inorg. Chem.* **2003**, 383.
2. Ueno, K.; Watanabe, T.; Tobita, H.; Ogino, H. *Organometallics* **2003**, *22*, 4375.
3. Bunn, N. R.; Aldridge, S.; Coombs, D. L.; Rossin, A.; Willock, D. J.; Jones, C.; Ooi, L.-L. *Chem. Commun.* **2004**, 1732. (b) Bunn, N. R.; Aldridge, S.; Kays, D. L.; Coombs, N. D.; Rossin, A.; Willock, D. J.; Day, J. K.; Jones, C.; Ooi, L.-L. *Organometallics* **2005**, *24(24)*, 5891.
4. (a) Braunschweig, H.; Radacki, K.; Scheschkewitz, D.; Whittell, G. R. *Angew. Chem. Int. Ed.* **2005**, *44*, 1658. (b) Braunschweig, H.; Kraft, K.; Kupfer, T.; Radacki, K.; Seeler, F. *Angew. Chem., Int. Ed.*, **2008**, *47*, 4931. (c) Braunschweig, H.; Burzler, M.; Dewhurst, R.; Radacki, K. *Angew. Chem., Int. Ed.*, **2008**, *47*, 5650.
5. Bunn, N. R.; Aldridge, S.; Kays (née Coombs), D. L.; Coombs, N. D.; Day, J. K.; Ooi, L.-L.; Coles, S. J.; Hursthouse, M. B. *Organometallics* **2005**, *24*, 5879.
6. Borovik, A. S.; Bott, S. G.; Barron, A. R. *Organometallics* **1999**, *18*, 2668.
7. Linti, G.; Li, G.; Pritzkow, H. *J. Organomet. Chem.* **2001**, *626*, 82.
8. Ueno, W.; Watanabe, T.; Ogino, H. *Organometallics* **2000**, *19*, 5679.
9. (a) Akita, M.; Terada, M.; Tanaka, M.; Morooka, Y. *J. Organomet. Chem.* **1996**, *510*, 255. (b) Odom, J. D.; Moore, T. F.; Goetze, R.; Nöth, H.; Wrackmeyer, B. *J. Organomet. Chem.* **1979**, *173*, 15. (c) Jacobsen, S. E.; Wojcicki, A. *J. Am. Chem. Soc.* **1973**, *95*, 6962.

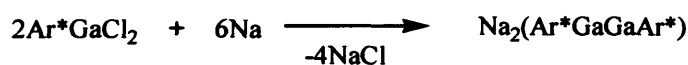
10. Dickinson, A. A. Ph.D. Thesis, Cardiff University, 2003
11. Aldridge, S.; Rossin, A.; Coombs, D. L.; Willock, D. J. *Dalton Trans.* **2004**, 2649
12. (a) Gäde, W.; Weiss, E. *J. Organomet. Chem.* **1981**, *213*, 451. (b) Korp, J. D.; Bernai, I.; Horlein, R.; Serrano, R.; Herrmann, W. A. *Chem. Ber.* **1985**, *118*, 340. (c) Herrmann, W. A.; Kneuper, H. J.; Herdtweck, E. *Chem. Ber.* **1989**, *122*, 437. (d) Ettl, F.; Hüttner, G.; Imhof, W. *J. Organomet. Chem.* **1990**, *397*, 299. (e) Ettl, F.; Hüttner, G.; Zsolnai, L.; Emmerich, C. *J. Organomet. Chem.* **1991**, *414*, 71.
13. Delpéch, F.; Guzei, I. A.; Jordan, R. F. *Organometallics* **2002**, *21*, 1167.
14. Ueno, K.; Watanabe, T.; Ogino, H. *Appl. Organomet. Chem.* **2003**, *17*, 403.
15. (a) Schmidbaur, H.; Thewalt, U.; Zafiropoulos, T. *Organometallics* **1983**, *2*, 1550. (b) Scholz, S.; Lerner, H.-W.; Bolte, M. *Acta Crystallogr. Sect. E* **2002**, *58*, m586.
16. Tuck, D. J. *Chemistry of Aluminium, Gallium, Indium and Thallium*; Downs, A. J. Ed.: Blackie Academic and Professional: London, 1993.
17. Greenwood, N. N.; Earnshaw, A. *Chemistry of the Elements*. Second Edition, Elsevier Butterworth Heinemann; Oxford, 1997.
18. Coombs, N. D.; Bunn, N. R.; Kays (née Coombs), D. L.; Day, J. K.; Ooi, L.-L.; Aldridge, S. *Inorg. Chim. Acta.* **2006**, *359*, 3693.

Chapter Six

Halogallyl Amido Complexes: Synthesis and Reactivity

6.1 Introduction

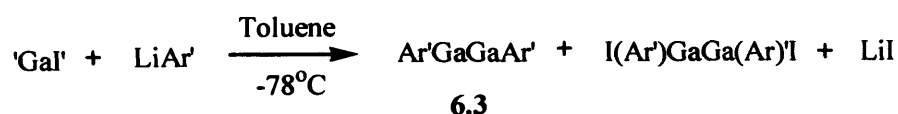
The synthesis and coordination chemistry of neutral low-valent gallium compounds has been the subject of intense research interest.¹⁻³ These compounds typically exist in the solid state as poly- or oligomeric species, such as (weakly) Ga-Ga bonded tetramers or hexamers of the type (GaR)₄ or (GaR)₆, which have the potential to dissociate into monomers either in solution or in the vapour phase. Low-valent gallium species featuring lower aggregation numbers in the solid phase are rare.



Scheme 6.1

In 1997, Robinson reported the synthesis of the complex Na₂(Ar*GaGaAr*) **6.1** in which the bonding between the two gallium centres was controversially described as involving a triple bond (Scheme 6.1).⁴ The multiple bonding within **6.1** was justified on the basis of the short Ga-Ga bond distance (2.319(3) Å) and on similarities between the [Ar*GaGaAr*]²⁻ ion and the neutral germanium species Ar*GeGeAr*, a germanium alkyne analogue.⁵ Although the existence of a GaGa triple bond received support from some calculations, others questioned this view on the basis of (i) the trans-bent structure of the C_{ipso}-Ga-Ga-C_{ipso} framework indicating lone pair character at the gallium centre; (ii) Na-aryl ring and the Na-Ga interactions resulting in shortening of the Ga-Ga distance; and (iii) the role of the *para*-ⁱPr groups

on the flanking rings which cause Ga-Ga-C angular distortions that can strengthen the bond. Several experiments were suggested with the aim of exploring the factors governing the nature of the Ga-Ga bond.⁶⁻⁸ Among these were the investigation of the effects of changing or removing the alkali metal ions and the isolation and characterisation of the neutral ‘digallene’ species, which should contain a Ga-Ga double bond if the assumption of a triple bond in $\text{Na}_2[\text{Ar}^*\text{GaGaAr}^*]$ is correct. Calculations on a variety of model species including HGaGaH , MeGaGaMe and PhGaGaPh , as well as IR measurements on matrix-isolated HGaGaH all indicate weak Ga-Ga bonding. Related studies reported by Power in 2000,^{8a} revealed that reduction of Ar^*GaCl_2 with potassium did not yield $\text{K}_2[\text{Ar}^*\text{GaGaAr}^*]$ but the tetragallium species $\text{K}_2\text{Ar}^*\text{Ga}_4\text{Ar}^*$ **6.2**, which contains a Ga_4 ring (with no Ga-Ga triple bonding) as part of the octahedral K_2Ga_4 core. The isolation of this species underlined the importance of the alkali metal in determining the stability of $\text{Na}_2[\text{Ar}^*\text{GaGaAr}^*]$ **6.1**. It was further postulated that the synthesis of a neutral “digallene” of the type $\text{Ar}^*\text{GaGaAr}^*$ would provide useful information on the Ga-Ga bonding present within the species $\text{Na}_2(\text{Ar}^*\text{GaGaAr}^*)$ **6.1**, as discussed above. However if the species was monomeric, i.e. $:\text{GaAr}^*$, a significantly lower bond order would presumably be implied for $\text{Na}_2(\text{Ar}^*\text{GaGaAr}^*)$ **6.1**. Thus, in 2002 Power reported the synthesis and characterisation of the neutral ‘digallene’ species $\text{Ar}'\text{GaGaAr}'$ **6.3** ($\text{Ar}' = 2,6\text{-Dipp}_2\text{C}_6\text{H}_3$) (Scheme 6.2).⁹



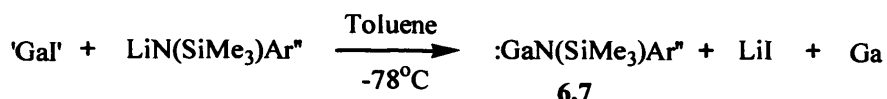
Scheme 6.2

These results revealed that the Ga-Ga bond in the 'digallene' is weak having a bond order less than one. In addition, Power *et al.* sought to further examine the nature of gallium-gallium bonding within the neutral complex $\text{Ar}^*\text{GaGaAr}^*$. This group had previously utilised highly bulky terphenyl ligands in the synthesis of the monomeric indium and thallium compounds of the type $\text{MC}_6\text{H}_3\text{-2,6-Trip}_2$ ($\text{M} = \text{In}$ or Tl), featuring one-coordinate group 13 centres.^{3e, 3f} Extending this methodology to gallium systems it was found that reaction of the corresponding terphenyllithium reagents with 'GaI' yielded the first stable monovalent compounds of the type GaAr^* **6.4** ($\text{Ar}^* = \text{C}_6\text{H}_3\text{-2,6-Trip}_2$) and $\text{GaAr}^\#$ **6.5** ($\text{Ar}^\# = \text{C}_6\text{H}_3\text{-2,6}(\text{tBuDipp})_2$ ($\text{tBuDipp} = \text{C}_6\text{H}_2\text{-2,6-}^i\text{Pr}_2\text{-4-}^t\text{Bu}$), and the dimeric species $(\text{GaAr}')_2$ **6.6** ($\text{Ar}' = \text{C}_6\text{H}_3\text{-2,6-Dipp}_2$).¹⁰

From these results it was concluded that the bonding between the arylgallium(I) fragments is weak and that certain complexes can even exist as monomers in dilute solution. The Ga-Ga bond within the complex $\text{Na}_2(\text{Ar}^*\text{GaGaAr}^*)$ **6.1** was thus described by Power as a single bond being formed by a two-electron reduction of $(\text{GaAr}^*)_{1\text{or}2}$. Thus, the stability of the $\text{Na}_2(\text{Ar}^*\text{GaGaAr}^*)$ **6.1** complex was attributed to the matching size of the Na^+ ions and the presence of Na-Ga and Na-Ar* interactions stabilising the Na_2Ga_2 cluster.

Subsequently in 2006, with the aim of examining the bonding between heavier group 13 atoms and nitrogen, Power reported the synthesis of the first Ga(I) amide $\text{GaN}(\text{SiMe}_3)\text{Ar}''$ **6.7** ($\text{Ar}'' = \text{C}_6\text{H}_3\text{-2,6-(C}_6\text{H}_2\text{-2,4,6-Me}_3)_2$) featuring a one coordinate gallium centre.¹¹ Reaction of $\text{LiN}(\text{SiMe}_3)\text{Ar}''$ with 'GaI' in toluene yielded $\text{GaN}(\text{SiMe}_3)\text{Ar}''$ **6.7** in which the gallium centre is coordinated to a single nitrogen

atom (Scheme 6.3), although there is also the presence of a long interaction between the gallium and the flanking mesityl ring of the terphenyl nitrogen substituent.

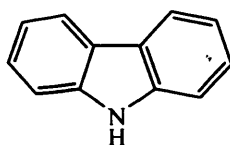


Scheme 6.3

However, it was found that this distance is *ca.* 0.6 Å longer than typical Ga-C single bonds, thus it was concluded that the gallium centre is effectively one coordinate with only a very weak coordination from the mesityl substituent. It was found that the measured Ga-N bond length of 1.980(2) Å is longer than those measured for monomeric three-coordinate gallium(III) amides of the type [R₂NGaR₂] (R = alkyl, aryl, or related species) which range from 1.829 to 1.923 Å,¹² but is shorter than the average Ga-N distances reported within the complexes Ga{(NDippCMe)₂CH} **6.8** (Ga-N = 2.054(2) Å), {DippNC(NCy₂)NDipp}Ga **6.9** (Ga-N = 2.091(2) Å) and TpBu'₂Ga **6.10** (TpBu'₂ = tris(3,5-di-tert-butylpyrazolyl)hydroborato) (Ga-N = 2.230(5) Å) which feature two- and three-coordinate gallium (I) centres.¹³

6.1.1 Aims of Research

We have sought to investigate the potential for bulky carbazole derived amido ligands in stabilising low coordinate group 13 centres.¹⁴



Carbazole

We aim to investigate the synthesis complexes of the type R_2N-EX_2 (where E = Ga, In and X = Cl, Br), and further examine the reduction chemistry of these species. Increasing the steric bulk of the R_2N : substituent will be examined in order to maximise the steric protection afforded to the group 13 centre.

6.2 Synthesis of Halogallyl Amido Complexes

6.2.1 Experimental

Synthesis of (1,8-diphenyl-3,6-dimethylcarbazol-9-yl)gallium dichloride (6.11)

A solution of $GaCl_3$ (0.411 g, 2.33 mmol) dissolved in hexanes (15 cm³) was added dropwise to a suspension of [1,8-diphenyl-3,6-dimethyl-carbazol-9-yl]lithium (0.825 g, 2.33 mmol) in hexane (25 cm³) at $-15^\circ C$. The reaction mixture was allowed to warm slowly to room temperature and stirred for a further 12 h, with the formation of a pale yellow solution and orange precipitate. The precipitate was isolated and dried *in vacuo*. The solid was extracted into the minimum amount of toluene, filtered and hexanes (30 cm³) added. Orange crystals of 6.11 were obtained at $-30^\circ C$. Isolated yield 0.146 g, 13 %. ¹H NMR (300 MHz, C₆D₆) : δ_H 2.34 (s, 6H, CH₃ of carbazole), 6.89 (m, 4H, aromatic CH), 7.26 (m, 8H, aromatic CH), 7.76 (s, 2H, aromatic CH). ¹³C NMR (76 MHz, C₆D₆) : δ_C 20.0 (CH₃), 119.2 (aromatic CH), 124.4 (aromatic CH), 124.8 (aromatic CH), 125.8 (aromatic CH), 126.1 (aromatic CH), 127.8 (aromatic CH), 128.1 (aromatic CH), 128.6 (aromatic CH), 135.0 (aromatic CH), 138.3 (aromatic CH), 141.1 (aromatic CH), 144.1 (aromatic CH). MS EI *m/z* : 347.3 {100 %, [M-GaCl₂]⁺}, calc. 485.0223 [M]⁺, measd. 485.0222 [M]⁺.

Attempted synthesis of (1,8-diphenyl-3,6-dimethylcarbazol-9-yl)indium dibromide

A solution/suspension of [1,8-diphenyl-3,6-dimethylcarbazol-9-yl]lithium (0.563 g, 1.61 mmol) in toluene (60 cm³) was added to a suspension of InBr₃ (0.410 g, 1.61 mmol) in toluene (20 cm³) at -15°C. The reaction was warmed to 20°C, stirred for 12h., filtered, concentrated *in vacuo* and layered with hexanes however, no tractable compounds were isolated.

Synthesis of 1,8-dimesityl-3,6-dimethylcarbazole (6.12)

1,8-dibromo-3,6-dimethylcarbazole (3.184 g, 9.018 mmol) and Pd(PPh₃)₄ (1.068 g, 1.043 mmol) was dissolved in toluene (420 cm³). To this solution was added a solution of mesitylboronic acid (21.024 g, 128.19 mmol) in ethanol (100 cm³), followed by an aqueous solution of 1 M Na₂CO₃ (92.4 cm³), and the resulting yellow suspension degassed in a stream of argon for 30 min. The reaction mixture was then heated to 80°C and stirred for 18 h. After filtration while hot, the filtrate washed with 1M NaOH (2 × 180 cm³) and water (2 × 180 cm³). The resulting dark brown solution was dried over MgSO₄, filtered and volatiles were removed *in vacuo* yielding a dark brown solid. Recrystallization from hot ethanol yielded 6.12 as a beige solid. Isolated yield, 1.655 g, 43 %. Crystals suitable for X-ray diffraction were obtained from a concentrated ethanol solution at -30°C. ¹H NMR (300 MHz, CDCl₃) : δ_H 1.87 (s, 12H, CH₃ of Mes), 2.25 (s, 6H, CH₃ of Mes), 2.51 (s, 6H, CH₃ of carbazole), 6.85 (s, 2H, aromatic CH of carbazole), 6.88 (s, 4H, aromatic CH of Mes), 7.05 (s, 1H, NH of carbazole), 7.78 (s, 2H, aromatic CH of carbazole). ¹³C NMR (76 MHz, CDCl₃) : δ_C 19.2 (CH₃), 20.0 (CH₃), 20.4 (CH₃), 117.8 (aromatic CH), 122.2 (aromatic CH), 122.6 (aromatic CH), 127.0 (aromatic CH), 127.4 (aromatic CH), 127.7 (aromatic CH), 133.6 (aromatic CH), 135.3 (aromatic CH), 136.0 (aromatic CH), 136.1

(aromatic CH). MS EI m/z : 431.3 {100%, $[M]^+$ }. Exact mass, calcd. 431.2608 $[M]^+$, measd. 431.2610 $[M]^+$.

Synthesis of [1,8-dimesityl-3,6-dimethylcarbazol-9-yl]lithium (6.13)

To a solution of 1,8-dimesityl-3,6-dimethylcarbazole (6.12, 1.211 g, 2.81 mmol) in hexanes (100 cm³) was added ⁿBuLi (2.08 cm³ of a 1.6 M solution in hexanes, 3.33 mmol) and the reaction was stirred at room temperature for 3 h. After concentration *in vacuo* (ca. 15 cm³), the resulting residue was isolated and dried *in vacuo* yielding [1,8-dimesityl-3,6-dimethyl-carbazol-9-yl]lithium 6.13 as an off white powder. Isolated yield, 0.905 g, 74 %, which was used in subsequent chemistry without further purification.

Synthesis of (1,8-dimesityl-3,6-dimethylcarbazol-9-yl)gallium dichloride (6.14)

To a suspension of [1,8-dimesityl-3,6-dimethylcarbazol-9-yl]lithium 6.13 (0.700 g, 1.60 mmol) in hexanes (20 cm³) was added a solution of GaCl₃ (0.282 g, 1.60 mmol) also in hexanes (30 cm³) at –30°C. The reaction mixture was warmed slowly to room temperature and stirred for 12 h. The resulting grey precipitate was isolated, extracted into toluene (15 cm³), and filtered. Hexanes (50 cm³) were added to the concentrated toluene solution yielding (1,8-dimesityl-3,6-dimethylcarbazol-9-yl)gallium dichloride 6.14 as a pale purple solid at –30°C. Isolated yield, 0.488 g, 54 %. Crystals suitable for X-ray diffraction were obtained from a concentrated toluene solution layered with hexanes at –30°C. ¹H NMR (300 MHz, CDCl₃) : δ_H 1.75 (s, 12H, *ortho*-CH₃ of Mes), 1.78 (s, 6H, *para*-CH₃ of Mes), 2.13 (s, 6H, CH₃ of carbazolyl), 6.49 (s, 2H, CH of carbazolyl), 6.61 (s, 4H, CH of Mes), 7.59 (s, 2H, CH of carbazolyl). ¹³C NMR (76 MHz, CDCl₃) : δ_C 20.1 (CH₃), 20.9 (CH₃), 21.3 (CH₃), 119.7 (aromatic CH), 123.6

(aromatic CH), 126.1 (aromatic CH), 129.4 (aromatic CH), 131.8 (aromatic CH), 132.8 (aromatic CH), 136.3 (aromatic CH), 140.0 (aromatic CH), 142.8 (aromatic CH). MS EI m/z : 431.2287 {100 %, $[M-GaCl_2]^+$ }, 571.1229 {10 %, $[M]^+$ }. Exact mass. calcd. 569.1168 $[M]^+$, measd. 569.1149 $[M]^+$.

Attempted synthesis of 1,8-bis(triisopropylphenyl)-3,6-dimethylcarbazole

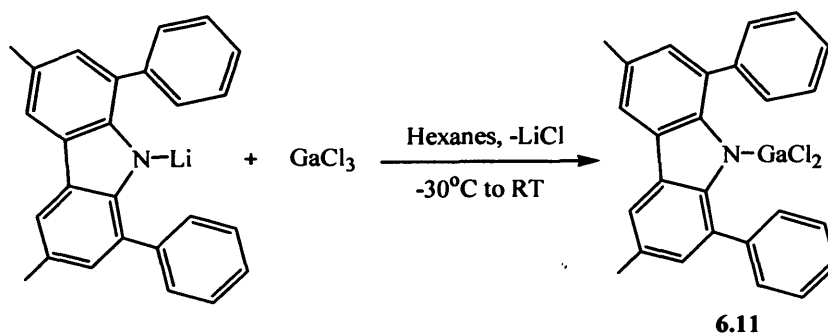
1,8-dibromo-3,6-dimethylcarbazole (0.956 g, 2.708 mmol) and $Pd(PPh_3)_4$ (0.314 g, 0.307 mmol) was dissolved in toluene (420 cm³). To this a solution of triisopropylphenylboronic acid (0.354 g, 1.426 mmol) in ethanol (100 cm³) was added followed by an aqueous solution of 1M Na_2CO_3 (27.17 cm³), and the resulting yellow suspension was degassed in a stream of argon for 30 min. The reaction mixture was then heated to 80°C and stirred for 18 h. The solution was filtered while hot and the filtrate washed with 1M NaOH (2 × 180 cm³) and water (2 × 180 cm³). The dark brown solution was dried over $MgSO_4$, filtered and volatiles were removed *in vacuo* yielding a brown oil. However recrystallisation from hot ethanol yielded only unreacted 1,8-dibromo-3,6-dimethylcarbazole.

6.2.2 Results and Discussion

2,6-Diarylphenyl ligands have been widely exploited in the isolation of complexes containing highly unsaturated metal centres protected, in part, by the large degree of steric shielding afforded by the flanking aryl rings.^{10, 11, 15-17} Given that monoanionic carbazolyl ligands have been reported to act as strong donors in transition metal chemistry,¹⁸ and that the ability to functionalise such ligands at the 1 and 8 positions *via* Suzuki coupling has previously been reported,^{14, 19} we have targeted the 1,8-diarylcarbazol-9-yl framework as the basis for a range of alternative

ligands. Three questions were examined (i) how do the 2,6-diarylphenyl and 1,8-diarylcarbazol-9-yl ligands compare in terms of the spatial and angular extent of the sterically shielded cavity produced, (ii) how are the steric properties of 1,8-diarylcarbazol-9-yl ligand influenced by the bulk of the flanking aryl rings and in particular, (iii) to what extent (as a function of aryl substituent bulk) is the metal coordination sphere likely to be augmented *via* either intra- or intermolecular interactions. As the coordination geometry at the metal centre (and the degree of aggregation) found for complexes of the type 2,6-(2,4,6-R₃C₆H₂)C₆H₃GaCl₂ (for R = Me, ⁱPr),²⁰ is known to be highly sensitive to the bulk of the peripheral R substituents, dichlorogallium complexes of the type (1,8-Ar₂-3,6-Me₂C₁₂H₄N)GaCl₂ were targeted for comparative structural studies.

The halogallyl carbazolyl complex (1,8-diphenyl-3,6-dimethylcarbazol-9-yl)gallium dichloride **6.11** was prepared by addition of GaCl₃ to a suspension of the previously reported compound [1,8-diphenyl-3,6-dimethylcarbazol-9-yl]lithium in hexanes at -30°C, and isolated as an orange crystalline solid in a modest yield (13 %) after recrystallisation from a concentrated toluene solution layered with hexanes (Scheme 6.4).



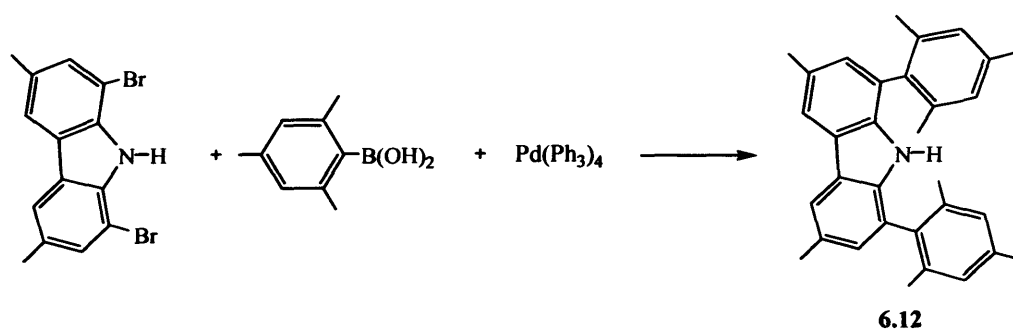
Scheme 6.4 Synthetic route to complex **6.11**.

The proposed formulation of **6.11** is supported by ^1H and ^{13}C NMR measurements. The reaction proceeds with retention of the diphenylcarbazol-9-yl fragment as evident by peaks at chemical shifts of δ_{H} 2.34, 6.89, 7.26, and 7.76 with relative intensities of 6:4:8:2 respectively. The EI mass spectrum also displays weak peaks for the parent $[\text{M}]^+$ ions with the fragment peaks corresponding to the $[\text{M-GaCl}_2]^+$ ion also being evident; the isotope distribution for the $[\text{M}^+]$ ion is as expected for a complex containing one gallium, one nitrogen, and two chlorine atoms. Single crystals of **6.11** suitable for X-ray diffraction were obtained by layering a concentrated solution of **6.11** with hexanes. Crystallographic studies revealed that **6.11** is mononuclear in the solid state, and although the quality of the structure solution is sufficient enough to prove connectivity, pernicious disorder involving carbon atoms of the carbazolyl aromatic system precluded detailed discussion of metrics. That said, it is clear that the least squares planes defined by pendent phenyl rings do not lie perpendicular to that defined by the carbazolyl aromatic ring, with inter-plane angles ranging from 40-60° for the two molecules in the asymmetric unit. It is also apparent that in each independent molecule there is a short secondary contact ($>2.4 \text{ \AA}$) between the gallium centre and one of the *ortho* carbons of one of the phenyl rings that is significantly shorter than the sum of the respective van der Waals radii (*ca.* 3.6 \AA).²¹

With the aim of increasing the steric bulk of the carbazolyl unit attention was switched to the corresponding dimesityl derivatives. The Suzuki coupling reaction of mesitylboronic acid with 1,8-dibromo-3,6-dimethylcarbazole in the presence of the catalyst $\text{Pd}(\text{PPh}_3)_4$, yielded the bis(mesityl) substituted system 1,8-dimesityl-3,6-dimethylcarbazole (**6.12**) as a white microcrystalline solid in 42 % yield (Scheme

6.5). As with previous observations of Suzuki/Miyaura chemistry,²² the yields of the coupling reactions used to generate 1,8-diphenyl-3,6-dimethylcarbazole and 1,8-dimesityl-3,6-dimethylcarbazole are strongly dependent on the steric bulk of the boronic acid. Thus, while 1,8-diphenyl-3,6-dimethylcarbazole has been synthesised in yields of up to 85 % using a Pd(PPh₃)₄/Na₂(CO)₃/10:3 ethanol/water mixture,¹⁴ 1,8-dimesityl-3,6-dimethylcarbazole is synthesised in only 42 % yield.

The Suzuki coupling reaction of triisopropylphenyl boronic acid with 1,8-dibromo-3,6-dimethylcarbazole in the presence of Pd(PPh₃)₄ was also investigated in an analogous fashion. However, it was found that recrystallisation from hot ethanol yielded only the starting material 1,8-dibromo-3,6-dimethylcarbazole as evident from ¹H NMR data (which did not reveal any peaks corresponding to the triisopropylphenyl fragment). This lack of reactivity presumably arises as a result of the greater steric bulk of the triisopropyl fragment compared to mesityl – a phenomenon known to be important in this coupling protocol.²²



Scheme 6.5 Synthetic route to complex **6.12**.

¹H NMR data for **6.12** revealed a broad peak at a chemical shift of 7.05 corresponding to the NH moiety. The ¹H NMR spectrum is consistent with the synthesis of a mesityl-functionalized carbazole fragment with relative peak intensities

of 12:6:6:2:4:1:2. EI mass spectra displays strong peaks for the parent $[M]^+$ ion with the expected isotope distribution.

Confirmation of the nature of the ligand was obtained from crystallographic data. Single crystals of **6.12** suitable for X-ray diffraction were accessible by cooling a saturated solution of **6.12** in ethanol to -30°C . The spectroscopic data for **6.12** was confirmed by single crystal X-ray diffraction studies and the structure is illustrated in Figure 6.1. Relevant bond lengths and bond angles for **6.12** are listed in Table 6.1.

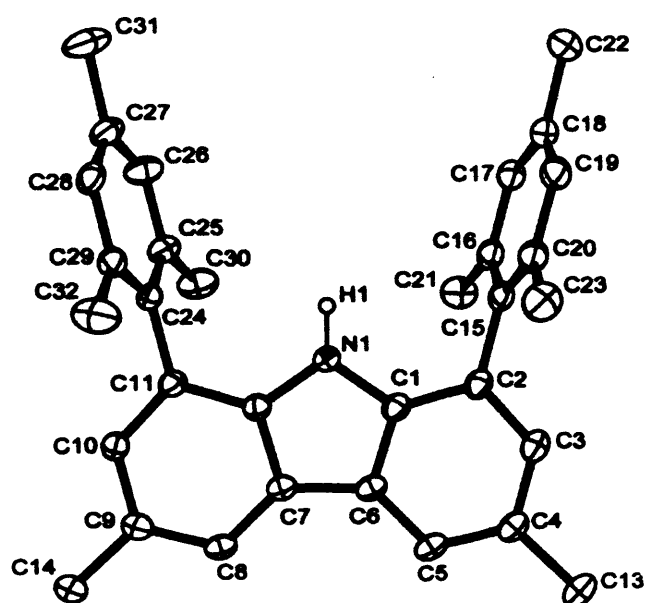


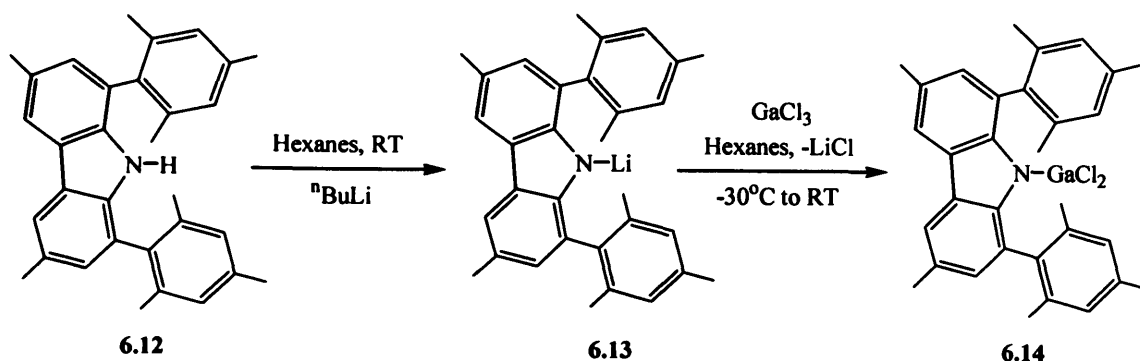
Figure 6.1 The molecular structure of 1,8-dimesityl-3,6-dimethylcarbazole **6.12**.

Table 6.1 Selected bond lengths [Å] and angles [°] for **6.12**.

N(1)-C(12)	1.386(4)	N(1)-C(1)	1.388(4)
C(1)-C(6)	1.411(5)	C(4)-C(13)	1.522(5)
C(7)-C(6)	1.451(5)	C(6)-C(5)	1.391(4)
C(18)-C(22)	1.507(5)	C(2)-C(15)	1.503(5)
C(12)-N(1)-C(1)	108.8(3)	N(1)-C(1)-C(2)	128.3(3)
N(1)-C(1)-C(6)	109.0(3)	C(1)-C(2)-C(15)	120.1(3)
C(1)-C(6)-C(7)	106.4(3)	C(2)-C(15)-C(20)	119.9(3)
C(1)-C(6)-C(5)	119.0(3)		

The crystal structure confirms that the ligand exists as the expected monomeric units; furthermore it is apparent that the 1,8-dimesityl-3,6-dimethylcarbazole fragment provides a more rigid sterically protected 'pocket' than the corresponding diphenyl species. Thus, the solid state of **6.12** features mesityl substituents which, despite the minimal steric demands of the carbazolyl substituent (*i.e.* hydrogen) are inclined at angles with respect to the carbazole backbone which are significantly closer to perpendicular (74.1 - 82.3° for the two independent molecules in the asymmetric unit) than in compounds containing the *diphenyl*carbazole unit.

Lithiation of **6.12** was carried out by reaction with ⁿBuLi in hexanes yielding [1,8-dimesityl-3,6-dimethylcarbazol-9-yl]lithium **6.13** as a pale yellow solid in 74 % yield (Scheme 6.6). Due to the highly reactive nature of **6.13**, spectroscopic confirmation of its identity was not obtainable and the composition of **6.13** is merely inferred from its subsequent reactivity (*vide infra*).



Scheme 6.6 Synthetic route to complex 6.13 and 6.14.

Addition of GaCl_3 to a suspension of 6.13 in hexanes at -30°C yields (1,8-dimesityl-3,6-dimethylcarbazol-9-yl)gallium dichloride 6.14, as a purple microcrystalline solid (Scheme 6.6) in *ca.* 54 % yield after recrystallisation from a concentrated toluene solution layered with hexanes. The proposed formulation is supported by ^1H and ^{13}C NMR spectroscopy; the ^1H NMR spectrum confirms the disappearance of the NH signal and retention of the dimesityl carbazolyl fragment with observed relative peak intensities of 12:6:6:2:4:2. The EI mass spectrum displays moderately strong peaks for the parent $[\text{M}]^+$ ions with fragment peaks corresponding to the $[\text{M-GaCl}_2]^+$ ion also being evident; the isotope distribution for $[\text{M}^+]$ is as expected for a complex containing one gallium, one nitrogen, and two chlorine atoms.

Definitive verification of compound identity for 6.14 and establishment of its state of aggregation were dependant on crystallographic data. Single crystals of 6.14 suitable for X-ray diffraction were obtained from layering a concentrated toluene solution of 6.14 with hexanes and storage at -30°C . The spectroscopic data for 6.14 was confirmed by single crystal X-ray diffraction studies and the structure is

The crystal structure obtained features isolated monomeric (1,8-dimesityl-3,6-dimethylcarbazol-9-yl)gallium dichloride molecules (**6.14**), in which the gallium is bound to the nitrogen centre of the carbazole substituent. The carbazol-9-yl ligand has an approximate two-fold axis of rotation, but the metal atom is displaced from the best plane of the C₄N ring by 0.37 Å and also from the plane of its coordinated N and Cl atoms by 0.15 Å. To our knowledge **6.14** represents the first monomeric amidogallium dihalide to be reported in the literature, although the Ga-N distance [1.852(2) Å] is similar to that reported for other trigonal planar gallium monohalides featuring sterically bulky substituents [1.829(9)-1.937(3) Å].²³ Ga-Cl distances [2.127(1), 2.112(1) Å] are similar to those measured for 2,6-(Trip)₂C₆H₃GaCl₂ [2.113(4), 2.124(3) Å] which also features a trigonal planar gallium centre, and significantly shorter than the terminal Ga-Cl bonds found in dimeric [2,6-(Mes)₂C₆H₃GaCl₂]₂ which features tetra-coordinate gallium [2.172(5), 2.290(4) Å].²⁰ Furthermore it is apparent that the mesityl substituents are inclined at angles (with respect to the carbazolyl backbone), which are even closer to perpendicular (89.0 and 87.7°) than that found in the parent ligand (74.1 and 82.3°). Additionally, and in contrast to [1,8-diphenyl-3,6-dimethylcarbazol-9-yl]gallium dichloride, relatively long Ga-C_{ipso} contacts (2.851 and 3.179 Å) are observed. While the shorter of these distances is actually shorter than that measured by Schmidbaur *et al.* for 1,2,4,5-tetramethylbenzene coordinated to gallium [closest Ga-C contact 2.965(4) Å, albeit for Ga(I) rather than Ga(III)],^{24, 25} much shorter M⁺⋯C_{ipso} contacts have been observed by Power *et al.* for complexes containing 2,6-diarylphenyl ligands [*e.g.* 2.294(1) Å for (2,6-Dipp₂C₆H₃Cr)₂].^{17c} Thus despite the noticeable asymmetry in the positioning of the GaCl₂ unit between the flanking arene ring in **6.14**, the long Ga-C_{ipso} distances and the trigonal planar coordination geometry [sum of angles at gallium = 358.95(8)°] are

consistent with relatively weak secondary interactions for this ligand. Further analyses of the structures of **6.14** and of $[2,6-(\text{Ar})_2\text{C}_6\text{H}_3\text{GaCl}_2]_n$ ($\text{Ar} = \text{Trip}$, $n = 1$; $\text{Ar} = \text{Mes}$, $n = 2$) allows useful comparison of the steric properties of the 1,8-diarylcarbazolyl and 2,6-diarylphenyl ligand classes. Thus, from a superficial perspective the fact that **6.14** is mononuclear, featuring a three-coordinate trigonal planar gallium centre while $2,6\text{-Mes}_2\text{C}_6\text{H}_3\text{GaCl}_2$ dimerises *via* bridging chloride ligands (yielding four-coordinate metal centres) implies that for a given flanking aryl ring (*i.e.* Mes in this case) the carbazolyl framework offers greater bulk in the vicinity of the metal centre.²⁰ Indeed, comparison of the spatial and angular extent of the cavity between the flanking aryl rings confirms this inference. Thus, the separation between the two mesityl ring centroids in **6.14** is 6.53 Å, while the mean distance in $[2,6-(\text{Mes})_2\text{C}_6\text{H}_3\text{GaCl}_2]_2$ is 7.44 Å (7.35 Å for the mononuclear Trip complex); the angle between the two mesityl least squares planes in **6.14** is 35.1°, compared to 58.7° (mean) for $[2,6-(\text{Mes})_2\text{C}_6\text{H}_3\text{GaCl}_2]_2$ and 64.6° for the Trip analogue.²⁰ This geometric data implies a significantly wider cone angle for the 1,8-dimesitylcarbazol-9-yl ligand system than its 2,6-dimesitylphenyl counterpart. This conclusion is confirmed by calculation of the Tollman cone angle (θ) using an established method for ligands of this type (*i.e.* with $\theta > 180^\circ$). Thus a cone angle of 269° is calculated for 1,8-dimesitylcarbazol-9-yl ligand based on the distances measured from the crystal structure of **6.14**, with analogous values of 185.4° and 200.5° being calculated for the 2,6-Mes₂ and 2,6-Trip₂ derivatised phenyl ligands, respectively.^{20, 26}

6.3 Attempted Reduction Chemistry

6.3.1 Experimental

Reaction of (1,8-diphenyl-3,6-dimethylcarbazol-9-yl)gallium dichloride 6.11 with potassium: synthesis of [1,8-diphenyl-3,6-dimethylcarbazol-9-yl]potassium (6.17)

A solution of (1,8-diphenyl-3,6-dimethylcarbazol-9-yl)gallium dichloride 6.11 (0.021 g, 0.04 mmol) dissolved in C₆D₆ (3 cm³) was added to a potassium mirror at room temperature, and the reaction mixture stirred for a further 15 min, with the formation of a light green solution. The solution was layered with hexanes and crystals suitable for X-ray diffraction were obtained at 20°C. Attempts to spectroscopically characterise the complex were unsuccessful due to the extreme sensitivity of the species.

Attempted reduction of (1,8-diphenyl-3,6-dimethylcarbazol-9-yl)gallium dichloride 6.11 with stoichiometric potassium graphite

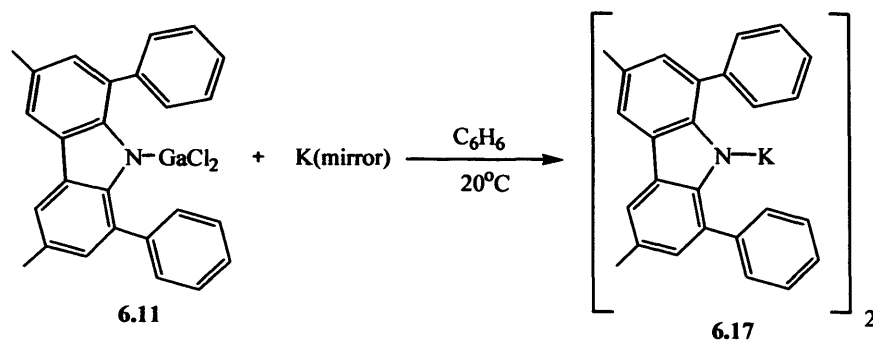
To a suspension of potassium graphite (0.032 g, 0.240 mmol) in toluene (10 cm³) was added a solution of 6.11 (0.057 g, 0.120 mmol) in toluene (20 cm³) at -78°C. The reaction mixture was warmed to room temperature and stirred for an additional 1.5 h with the formation of a green solution. Isolation of the solution was not possible due to the extreme sensitivity of the species. It was not possible to decant or filter the solution through a cannula without the species decomposing, as evident by a change in colour of the solution from pale green to colourless when exposed to the surface of the cannula.

Attempted reaction of (1,8-dimesityl-3,6-dimethylcarbazol-9-yl)gallium dichloride***6.14 with 2 equivalents of potassium graphite***

To a suspension of potassium graphite (0.099 g, 0.73 mmol) in toluene (3 cm³) was added a solution of **6.14** (0.201 g, 0.35 mmol) in toluene (10 cm³) at -40°C with stirring. The reaction mixture was warmed to room temperature and stirred for an additional 72 h, with the formation of a pale lime green solution. The pale green solution was decanted, concentrated *in vacuo*, layered with hexanes, and stored at -30°C, however no tractable compounds were isolated. It was found that after 96 h at -30°C the reaction mixture began to decompose as evident by a change in colour of the solution from pale green to colourless.

6.3.2 Results and Discussion

With the aim of synthesising monovalent gallium compounds of the type (R₂NGa)_x, reduction of the carbazolygallium dichloride complexes **6.11** and **6.14** was examined with a range of reducing agents. Addition of a solution of (1,8-diphenyl-3,6-dimethylcarbazol-9-yl)gallium dichloride **6.11** in C₆D₆ to a potassium mirror at 20°C yielded the potassium salt [1,8-diphenyl-3,6-dimethylcarbazol-9-yl]potassium **6.17** as fluorescent green crystals (Scheme 6.7). Attempts to spectroscopically characterise the complex were unsuccessful due to the extreme sensitivity of the species; it was found that removal of the reaction solvent resulted in immediate decomposition of the complex.



Scheme 6.7 Synthetic route to complex **6.17**.

Identification of **6.17** was therefore dependant on crystallographic data. Single crystals of **6.17** suitable for X-ray diffraction were obtained from a concentrated C_6D_6 solution of **6.17** layered with hexanes at 20°C ; the structure is illustrated in Figure 6.3. Relevant bond lengths and angles for **6.17** are listed in Table 6.3.

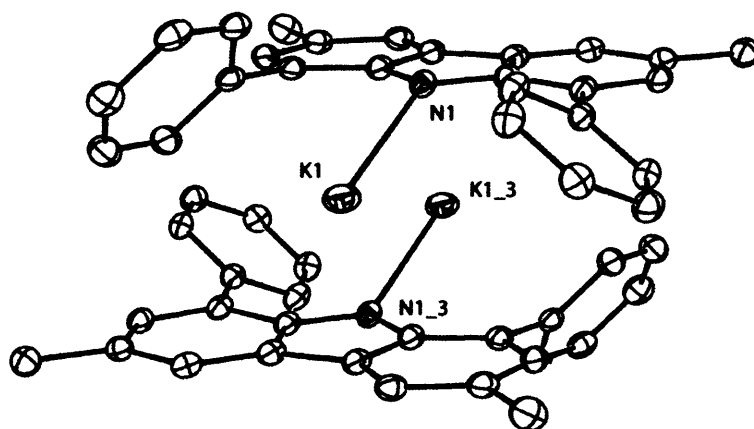


Figure 6.3 The molecular structure of [1,8-diphenyl-3,6-dimethylcarbazol-9-yl]potassium **6.17**.

Table 6.3 Selected bond lengths [Å] and angles [°] for **6.17**.

K(1)-N(1)	2.745(2)	N(1)-C(12)	1.376(2)
N(1)-C(1)	1.380(2)		
C(12)-N(1)-K(1)	129.92(12)	C(1)-N(1)-K(1)	115.72(12)
N(1)-C(1)-C(6)	113.70(17)	N(1)-C(1)-C(2)	126.46(19)

The crystal structure obtained confirms that the complex exists as dimeric units of the potassium carbazolyl species, in which the potassium is coordinated to the nitrogen atom with no additional coordination of solvent at the metal centre. The molecular geometry provides further evidence that rotation of the phenyl rings in the 1,8-diphenyl-3,6-dimethylcarbazol-9-yl ligand about the $C_{ipso}-C_{ipso}$ bonds is sufficiently facile such as to accommodate secondary metal-arene interactions. Each (1,8-Ph₂-3,6-Me₂C₁₂H₄N)K unit features not only a relatively short K-N distance [2.745(2) Å],²⁷ but also intermolecular contacts with the ipso and ortho carbons of both pendant phenyl rings (3.181-3.227 Å) which are also well within the sum of the respective van der Waals radii (*ca.* 4.0 Å). These secondary interactions also fall within the range of previously reported potassium-arene contacts,²⁸ and are presumably responsible for the observed disrotatory rotation of the phenyl substituents about the $C_{ipso}-C_{ipso}$ bonds (*cf.* the observed conrotatory orientation observed (1,8-diphenyl-3,6-dimethylcarbazol-9-yl)gallium dichloride **6.11**). This orientation of the phenyl rings allows for further *intermolecular* interactions involving the potassium centre. Thus, a centrosymmetric dimeric structure is adopted in the solid state through pair-wise interaction of each potassium with C(5) and C(6) of the second carbazolyl ligand (3.059-3.080 Å). These intermolecular contacts lead to significant bending of the K-N vector out of the parent carbazolyl ligand plane; the

angle defined by K(1), N(1) and the centroid of the central five-membered carbazolyl ring is $150.37(5)^\circ$.

Due to the highly reactive nature of **6.17** spectroscopic data was unobtainable without the complex decomposing. In addition it was concluded that use of a reducing agent which could be reacted in a controlled 2:1 stoichiometry with **6.11** and **6.14**, would be desirable in preventing further reduction of the species as seen in the formation of **6.17**. Thus, in an attempt to synthesise the reduced species (1,8-diphenyl-3,6-dimethylcarbazol-9-yl)gallium(I), reaction of a solution of **6.11** with a suspension of two equivalents of KC_8 in toluene at -78°C was examined. It was found that on warming the solution to 20°C a dark green solution resulted. However, attempts to isolate the solution *via* decanting through a cannula were unsuccessful, as the solution immediately turned colourless when exposed to the surface of the cannula. This result emphasises the highly reactive nature of these complexes. From these results it was concluded that the conformational flexibility inherent in diphenyl substituted ligands of this type is likely to be incompatible with the isolation of low coordinate metal systems. Thus reaction of the corresponding dimesityl derivatives was investigated in the hope that the increased steric bulk of the flanking arene rings would lead to less labile products.

Reaction of **6.14** with KC_8 was investigated in the hope that the greater steric bulk provided by the mesityl fragment might stabilise the highly reactive gallium centre produced on reduction. A solution of **6.14** was added to suspension of KC_8 in toluene at -40°C , with the formation of a dark green solution after stirring at 20°C for 3 h. The solution was left undisturbed for 12 h., decanted, concentrated *in vacuo* and

layered with hexanes. Unfortunately, no tractable compounds could be isolated. It was found that over a period of 12 days stored at -30°C the dark green solution progressively turned colourless indicating decomposition of the compound.

6.4 Attempted Synthesis from Metal(I) Halides

6.4.1 Experimental

Attempted reaction of [1,8-dimesityl-3,6-dimethylcarbazol-9-yl]lithium 6.13 with 'GaI'

A solution of [1,8-dimesityl-3,6-dimethylcarbazol-9-yl]lithium 6.13 (0.205 g, 0.47 mmol) in toluene (20 cm^3) was added to a suspension of 'GaI' at -78°C . The reaction mixture was warmed to 20°C and stirred for 17 h. The resulting yellow solution was filtered, concentrated and layered with hexanes. No tractable compounds were isolated.

Attempted reaction of [1,8-dimesityl-3,6-dimethylcarbazol-9-yl]lithium 6.13 with InCl

To a suspension of InCl (0.071 g, 0.47 mmol) in toluene (10 cm^3) was added a solution of 6.13 (0.202 g, 0.46 mmol) also in toluene (60 cm^3) at -78°C with stirring. The reaction was warmed to room temperature, with the formation of a dark brown mixture. The reaction mixture was filtered yielding a lime green solution. Volatiles were removed *in vacuo*, and the resulting yellow/green oil was extracted into hexanes and filtered. However, no tractable compounds were isolated.

6.4.2 Results and Discussion

It has been previously demonstrated by Power *et al.* that reaction of E(I)X (E = group 13 element, X = halide) with ArLi (Ar = terphenyl ligand) has been successful in synthesising complexes of the type ArE featuring a monovalent group 13 centre.¹⁰ We sought to examine this approach in synthesising analogous carbazole complexes of the type R₂NE. The attempted reaction [1,8-dimesityl-3,6-dimethylcarbazol-9-yl]lithium **6.13** with 'GaI' unfortunately resulted in no tractable compounds being isolated. The analogous reaction with InCl yielded some promising results with the formation of a lime solution after filtration. Removal of the volatiles and extraction into hexanes yielded lime green crystals at -30°C. However X-ray crystallography and spectroscopic results revealed the nature of the product as 1,8-dimesityl-3,6-dimethylcarbazole. Very recently the (green) complexes 1,3,6,8-tetra-*tert*-butylcarbazol-9-ylgallium(I) and -indium(I) have been isolated from the reaction of the corresponding lithium salt with 'GaI' and InCl, respectively, and the indium(I) compound structurally characterized (work by Hassanatu Mansaray). The metal coordination environment features η^3 (C,N,C) coordination of the carbazolyl fragment (i.e. an aza-allyl) augmented by weak secondary (intermolecular) metal-arene interactions in the solid state.

6.5 Conclusions and Suggestions for Further Research

The synthesis and preliminary coordination chemistry of a range of sterically bulky carbazolyl ligands has been investigated. A Suzuki coupling protocol was exploited to introduce aryl substituents at the 1 and 8 positions of the parent framework, allowing for variation in the steric bulk of the boronic acid. It was found that the yield obtained was strongly dependant on the nature of the boronic acid, thus

phenyl and mesityl boronic acids yielded 1,8-diphenyl and 1,8-dimesityl-3,6-dimethylcarbazole (**6.12**) in yields of 85 % and 43 %, respectively. However, when triisopropylphenylboronic acid was employed no coupled product could be obtained using standard coupling conditions.

Salt elimination chemistry has proven to be a viable synthetic route to the formation of dihalogallyl complexes; thus (1,8-dimesityl-3,6-dimethylcarbazol-9-yl)gallium dichloride **6.11** and (1,8-dimesityl-3,6-dimethylcarbazol-9-yl)gallium dichloride **6.14** have been synthesized and characterized by standard spectroscopic and crystallographic methods.

Preliminary reduction studies of these species with KC_8 have revealed the formation of dark green solutions on reduction. However, due to the sensitivity of these species isolation was not possible. Unsurprisingly it was found that the reduced phenyl-substituted carbazolyl species was far more reactive than the corresponding mesityl complex, presumably due to the reduced steric protection present. The dimeric potassium salt [1,8-diphenyl-3,6-dimethylcarbazol-9-yl]potassium **6.17** was isolated from the reaction of (1,8-diphenyl-3,6-dimethylcarbazol-9-yl)gallium dichloride **6.11** with an excess of potassium.

6.6 References for Chapter Six

1. (a) Uhl, W. *Coord. Chem. Rev.* **1997**, *163*, 1. (b) Janiak, C. *Coord. Chem. Rev.* **1997**, *163*, 107. (c) Uhl, W. *Rev. Inorg. Chem.* **1998**, *18*, 239. (d) Linti, G.; Schnöckel, H. *Coord. Chem. Rev.* **2000**, *206-207*, 285. (e) Schnöckel, H.; Schnepf, A. *Adv. Organomet. Chem.* **2001**, *47*, 235. (f) Loos, D.; Baum, E.; Ecker, H.; Schnöckel, H.; Downs, A. J. *Angew. Chem. Int. Ed. Engl.* **1997**, *36*, 860. (g) Beachley, O. T.; Churchill, M. R.; Fettinger, J. L.; Pazik, J. C.; Victoriano, L. *J. Am. Chem. Soc.* **1986**, *108*, 4666. (h) Dohmeier, C.; Robl, C.; Tacke, M.; Schnöckel, H. *Angew. Chem. Int. Ed. Engl.* **1991**, *30*, 564.
2. (a) Uhl, W.; Hiller, M.; Layh, M.; Schwarz, W. *Angew. Chem. Int. Ed.* **1992**, *31*, 1364. (b) Schluter, R. O.; Cowley, A. H.; Atwood, D. A.; Jones, R. A.; Atwood, J. L. *J. Coord. Chem.* **1993**, *30*, 25. (c) Uhl, W.; Graupner, R.; Layh, M.; Schütz, U. *J. Organomet. Chem.* **1995**, *493*, C1. (d) Schitter, C.; Roesky, H. W.; Röpken, C.; Herbst-Irmer, R.; Schmidt, H. -G.; Noltemeyer, M. *Angew. Chem. Int. Ed. Engl.* **1993**, *32*, 1729. (e) Uhl, W.; Keimling, S. U.; Klinkhammer, K. W.; Schwarz, W. *Angew. Chem. Int. Ed. Engl.* **1997**, *36*, 64.
3. (a) Schumann, H.; Janiak, C.; Görlitz, F.; Loebel, J.; Dietrich, A. *J. Organomet. Chem.* **1989**, *363*, 243. (b) Schumann, H.; Pickhardt, J.; Börner, U. *Angew. Chem. Int. Ed.* **1987**, *26*, 790. (c) Beachley, O. T.; Noble, M. J.; Allendoerfer, R. D. *J. Organomet. Chem.* **1999**, *582*, 32. (d) Uhl, W.; Cuypers, L.; Harms, K.; Kaim, W.; Wanner, M.; Winter, R.; Koch, R.; Saak, W. *Angew. Chem. Int. Ed.* **2001**, *40*, 566. (e) Haubrich, S. T.; Power, P. P. *J. Am. Chem. Soc.* **1998**, *120*, 2202. (f) Niemeyer, M.; Power, P. P. *Angew. Chem. Int. Ed.* **1998**, *37*, 1277.
4. Su, J.; Li, X. -W.; Crittendon, C.; Robinson, G. H. *J. Am. Chem. Soc.* **1997**, *119*, 5471.

5. Stender, M.; Phillips, A. D.; Power, P. P. *Chem. Commun.* **2002**, 1312.
6. (a) Klinkhammer, K. W. *Angew. Chem. Int. Ed. Engl.* **1997**, *36*, 2320. (b) Klinkhammer, K. W. *Angew. Chem. Int. Ed.* **1997**, *109*, 2414. (c) Xie, Y.; Grev, R. S.; Su, J.; Schaefer, H. F.; Schleyer, P. v. R.; Su, J.; Li, X. -W.; Robinson, G. H. *J. Am. Chem. Soc.* **1998**, *120*, 3773. (d) Bytheway, I.; Lin, Z. *J. Am. Chem. Soc.* **1998**, *120*, 12133. (e) Xie, Y.; Schaefer, H. F.; Robinson, G. H. *Chem. Phys. Lett.* **2000**, *317*, 174. (f) Grützmacher, H.; Fässler, T. F. *Chem. -Eur. J.* **2000**, *6*, 2317. (g) Simons, R. S.; Olmstead, M. M.; Power, P. P. *J. Am. Chem. Soc.* **1997**, *119*, 11705.
7. (a) Cotton, F. A.; Cowley, A. H.; Feng, X. *J. Am. Chem. Soc.* **1998**, *120*, 1795. (b) Allen, T. L.; Fink, W. H.; Power, P. P. *Dalton Trans.* **2000**, 407. (c) Bridgeman, A. J.; Ireland, L. R. *Polyhedron* **2001**, *20*, 2841. (d) Takagi, N.; Schmidt, M. W.; Nagase, S. *Organometallics* **2001**, *20*, 1646. (e) Grunenberg, J.; Goldberg, N. *J. Am. Chem. Soc.* **2000**, *122*, 6045. (f) Köppe, R.; Schnöckel, H. *Z. Anorg. Allg. Chem.* **2000**, *626*, 1095. (g) Himmel, H. -G.; Schnöckel, H. *Chem.-Eur. J.* **2002**, *8*, 10.
8. (a) Twamley, B.; Power, P. P. *Angew. Chem. Int. Ed.* **2000**, *39*, 3500. (i) Power, P. P. *Dalton Trans.* **1998**, 2939.
9. Hardman, N. J.; Wright, R. J.; Phillips, A. D.; Power, P. P. *Angew. Chem. Int. Ed.* **2002**, *41*, 2842.
10. Hardman, N. J.; Wright, R. J.; Phillips, A. D.; Power, P. P. *J. Am. Chem. Soc.* **2003**, *125*, 2667.
11. Wright, R. J.; Brynda, M.; Fettingner, J. C.; Betzer, A. R.; Power, P. P. *J. Am. Chem. Soc.* **2006**, *128*, 12498.
12. (a) Brothers, P. J.; Power, P. P. *Adv. Organomet. Chem.* **1996**, *39*, 1-69. (b) Carmalt, C. J. *Coord. Chem. Rev.* **2001**, *223*, 217. (c) Lappert, M. F.; Sanger, A. R.;

Sriastava, R. C.; Power, P. P. *Metal and Metalloid Amides: Synthesis, Structure, and Physical and Chemical Properties*; Ellis Harwood/Wiley: New York, 1980.

13. (a) Hardman, N. J.; Eichler, B. E.; Power, P. P. *Chem. Commun.* **2000**, 1991. (b)

Kuchta, M. C.; Bonanno, J. B.; Parkin, G. *J. Am. Chem. Soc.* **1996**, *118*, 10914.

14. Spitzmesser, S. K.; Gibson, V. C. *J. Organomet. Chem.* **2003**, *673*, 95.

15. See for example: (a) Power, P. P. *J. Organomet. Chem.* **2004**, *689*, 3904. (b)

Stanciu, C.; Richards, A. F.; Fettingner, J. C.; Brynda, M.; Power, P. P. *J. Organomet. Chem.* **2006**, *691*, 2540.

16. See for example: (a) Power, P. P.; *Organometallics* **2007**, *26*, 4362. (b) Wang, Y.;

Robinson, G. H. *Organometallics* **2007**, *36*, 2. (c) Zhu, Z.; Brynda, M.; Wright, R. J.;

Fischer, R. C.; Merrill, W. A.; Rivard, E.; Wolf, R.; Fettingner, J. C.; Olmstead M. M.;

Power, P. P. *J. Am. Chem. Soc.* **2007**, *129*, 10847. (d) Quillian, B.; Wang, Y.; Wei, P.;

Handy, A.; Robinson, G. H. *J. Organomet. Chem.* **2006**, *691*, 3765. (e) Yang, X. -J.;

Wang, Y.; Quillian, B.; Wei, P.; Chen, Z.; Schleyer, P. v. R.; Robinson, G. H.

Organometallics **2006**, *25*, 925. (f) Wright, R. J.; Brynda, M.; Power, P. P. *Angew.*

Chem., Int. Ed. **2006**, *45*, 5953. (g) Wang, Y.; Quillian, B.; Yang, X. -Y.; Wei, P.;

Chen, Z.; Wannere, C. S.; Schleyer, P. v. R.; Robinson, G. H. *J. Am. Chem. Soc.*

2005, *127*, 7672. (h) Young, J. D.; Khan, M. A.; Wehmschulte, R. J. *Organometallics*

2004, *23*, 1965.

17. See for example: (a) Wolf, R.; Brynda, M.; Ni, C.; Long, G. J.; Power, P. P. *J.*

Am. Chem. Soc., **2007**, *129*, 6076. (b) Kays, D. L.; Cowley, A. *Chem. Commun.*,

2007, 1053. (c) Nguyen, T.; Sutton, A. D.; Brynda, M.; Fettingner, J. C.; Long, G. J.;

Power, P. P. *Science*, **2005**, *310*, 844.

18. For examples of homoleptic main group and transition metal complexes containing the carbazol-9-yl ligand see: (a) Beswick, M. A.; Harmer, C. N.; Raithby,

P. R.; Steiner, A.; Verhorevoort, K. L.; Wright, D. S. *J. Chem. Soc., Dalton Trans.* **1997**, 2029. (b) Barr, D.; Edwards, A. J.; Raithby, P. R.; Rennie, M. –A.; Verhorevoort, K.; Wright, D. S. *Chem. Commun.* **1994**, 1627.

19. For examples of carbazol-9-yl ligands bearing additional donors tethered at the 1 and 8 positions see: (a) Moswer, M.; Wucher, B.; Kunz, D.; Rominger, F. *Organometallics* **2007**, 26, 1204. (b) Gaunt, J. A.; Gibson, V. C.; Haynes, A.; Spitzmesser, S. K.; White, A. J. P.; Williams, D. J. *Organometallics* **2004**, 23, 1015. (c) Gibson, V. C.; Spitzmesser, S. K.; White, A. J. P.; Williams, D. J. *Dalton Trans.* **2003**, 2718. (d) Britovsek, G. J. P.; Gibson, V. C.; Hoarau, O. D.; Spitzmesser, S. K.; White, A. J. P.; Williams, D. J. *Inorg. Chem.* **2003**, 42, 3454.

20. (a) Twamley, B.; Power, P. P. *Chem. Commun.*, **1999**, 1805. (b) Su, J.; Li, X. –W.; Robinson, G. H. *Chem. Commun.* **1998**, 2015. (c) Crittendon, R. C.; Li, X. –W.; Su, J.; Robinson, G. H. *Organometallics* **1997**, 16, 2443.

21. Emsley, J. *The Elements*, OUP, Oxford, 2nd Edition., **1991**.

22. Miyaura, N.; Suzuki, A. *Chem. Rev.* **1995**, 95, 2457.

23. Carmalt, C. J. *Coord. Chem. Rev.* **2001**, 223, 217.

24. Schmidbaur, H.; Nowak, R.; Huber, B.; Müller, G. *Polyhedron* **1990**, 9, 283.

25. Covalent radii for Ga(I) and Ga(III): 1.13 and 0.62 Å, respectively.²¹

26. Tollman, C. A. *Chem. Rev.* **1977**, 77, 313.

27. Related K-N distances in the range: 2.740(7)-3.019(4) Å are listed in the Cambridge Structural Database (27/09/2007) with a bond length of 2.774(2) Å having been determined for the [K(18-crown-6)]⁺ salt of the parent carbazol-9-yl ligand: Esbak, H.; Behrens, U. *Z. Anorg. Allg. Chem.*, **2005**, 631, 1581.

28. See, for example: Junk, P. C.; Cole, M. L. *Chem. Commun.*, **2007**, 1579.

Chapter Seven

DFT Calculations of Group 13 Diyl Complexes: Structure and Bonding

7.1 Introduction

The number of investigations into the coordination chemistry of transition metal complexes featuring group 13 diyl ligands ER (E = B-Tl) has increased dramatically over the last decade as a result of the successful synthesis of a number of transition metal-group 13 diyl species $L_nM(ER)$ where the group 13 centre has a formal oxidation state of +1.¹⁻⁴ Investigation of the bonding within these complexes has generated a large amount of research interest not only from a theoretical perspective but also from the viewpoint of identifying future synthetic targets.⁵⁻⁷ Two fundamental questions have arisen regarding the nature of bonding between the group 13 element and the transition metal centre; (i) the degree of covalent and ionic character of the M-ER bond and (ii) the degree of π back-bonding, within the covalent component of the bond.

Following the successful isolation of $(CO)_4FeGaAr^*$ ^{3a} and the syntheses of the first homoleptic diyl complexes $Ni[EC(SiMe_3)_3]_4$ (E = In⁸ or Ga⁹), a number of quantum chemical studies sought to analyse the nature of the covalent bond in such systems and in particular the possibility for M to E π back-bonding when (i) the diyl substituent R is not a strong π donor, and/or when (ii) there are no competing π acid ancillary ligands at M. A theoretical study by Cotton and Feng^{3b} challenged the suggestion made by Robinson^{3a} that $Fe \rightarrow GaAr^*$ π back donation makes a significant contribution to the bonding in $(CO)_4FeGaAr^*$. Other theoretical studies of the electronic structure of group 13 diyl complexes

$L_nM(ER)$ showed, however, that the $p(\pi)$ atomic orbitals of E have higher populations in the complexes than in the free ligands ER, when R is Ph or Me.^{7c, 14}

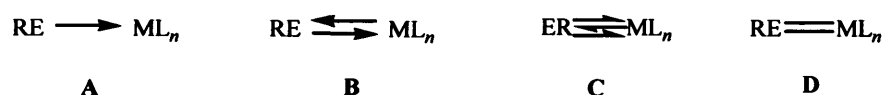


Figure 7.1

A number of bonding models have been proposed to describe the bonding within terminal boranediyl and their heavier congeneric complexes. Macdonald and Cowley¹⁰ sought to resolve this fundamental question by investigating the relative merits of the proposed bonding models shown in Figure 7.1. The primary focus of investigation were the model complexes $(\eta^5\text{-C}_5\text{H}_5)\text{EFe}(\text{CO})_4$ (E = B, Al, Ga, In), the boron system having previously been synthesized by the same group. DFT calculations were also performed on complexes of the type $\text{MeMFe}(\text{CO})_4$ (M = B, Al, Ga, In) to determine if these species are better candidates for E-Fe multiple bonding. The amido-substituted boranediyl complex $(\text{H}_3\text{Si})_2\text{NBFe}(\text{CO})_4$, was also examined to assess the nature of the B-Fe and N-B bonding in light of the reported preparation of $(\text{Me}_3\text{Si})_2\text{NBFe}(\text{CO})_4$ (and the related, crystallographically confirmed complex $(\text{Me}_3\text{Si})_2\text{NBW}(\text{CO})_5$)¹¹. In addition to the work reported by Macdonald and Cowley, other related studies in this area include DFT studies of $\text{PhGaFe}(\text{CO})_4$ ^{3b, 7c} and a series of model bonding complexes of the general type $\text{RBM}(\text{CO})_n$ (R = F, NH_2 , O^- ; $\text{M}(\text{CO})_n = \text{Cr}(\text{CO})_5$, $[\text{Mn}(\text{CO})_5]^+$, $\text{Fe}(\text{CO})_4$, $[\text{Co}(\text{CO})_4]^-$ and $\text{Ni}(\text{CO})_3$)^{6c}. The ground states, frontier orbitals and singlet-triplet energy gaps of the uncoordinated RE ligands (R = $\eta^5\text{-C}_5\text{H}_5$, $(\eta^5\text{-C}_5\text{Me}_5)\text{Me}$, $\text{N}(\text{SiH}_3)_2$; E = B, Al, Ga, In) were first calculated. It

was found that regardless of the substituent R ($R = \eta^5\text{-C}_5\text{H}_5$, $\eta^5\text{-C}_5\text{Me}_5$, Me, $(\text{H}_3\text{Si})_2\text{NB}$) the ground state of each RE fragment is a singlet.

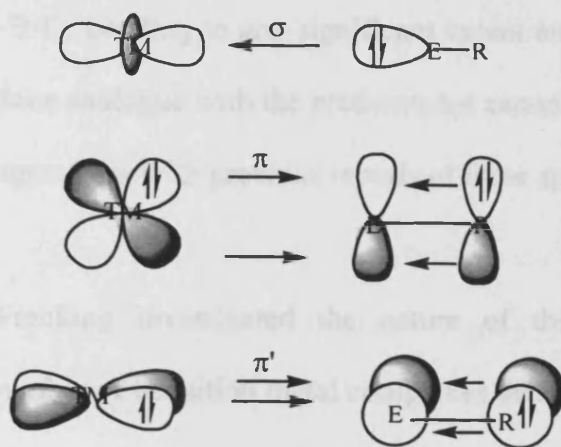


Figure 7.2 Schematic representation of the M-E-R bonding situation when R has occupied $p(\pi)$ -orbitals.

It was further reported that the group RE species with non- π -donating R substituents could have some π -acceptor capability, which is appropriate for metal-ligand back bonding. However, computational evidence of such back-bonding was found only in the case of alkyl-substituted boranediyl complex, $\text{MeBFe}(\text{CO})_4$ and not for the heavier group 13 analogues. On this basis it was proposed that bulky alkyl-substituted boranediyl transition metal carbonyl complexes represent an attractive synthetic target. Overall it was concluded that each boranediyl complex features a stronger E-Fe bond than any of its heavier congeners. Thus from a theoretical standpoint, it was proposed that nearly all of the $\text{REFe}(\text{CO})_4$ complexes are potentially accessible by direct reaction of the isolated RE ligand with $\text{Fe}(\text{CO})_5$; however it was further concluded that the oligomerisation tendency of the monomeric RE species may tend to make this route less synthetically feasible.

Investigations into amido-substituted species revealed that the $(\text{H}_3\text{Si})_2\text{NB}$ ligand is predominately a two-electron donor with a slight capacity for π -acceptor bonding from the transition metal moiety; however it was found that the back-bonding does not contribute to the B-Fe bonding to any significant extent and thus this ligand was described as a vinylidene analogue with the predominant canonical form $(\text{H}_3\text{Si})_2\text{N}=\text{B}-\text{Fe}(\text{CO})_4$ which is in agreement with previous reports of these species.^{12, 6c}

Uddin and Frenking investigated the nature of the metal ligand bond interaction within a number of transition metal complexes featuring terminal group 13 diyl ligands.¹³ Energy partitioning analysis was performed on the complexes $(\text{CO})_4\text{Fe}(\text{ER})$, $\text{Fe}(\text{EMe})_5$ and $\text{Ni}(\text{EMe})_4$ ($\text{E} = \text{B-Tl}$; $\text{R} = \text{Cp}$, $\text{N}(\text{SiH}_3)_2$, Ph , Me) which revealed that the attractive orbital interactions between Fe and ER in $(\text{CO})_4\text{FeER}$ arise mainly from $\text{Fe} \leftarrow \text{ER}$ σ donation. It was found that only the boranediyl complexes $(\text{CO})_4\text{FeBR}$ have significant contributions from $\text{Fe} \rightarrow \text{ER}$ π back donation. However it was reported that even in this case the σ donation remains the dominant orbital interaction term. In addition, calculations revealed that the relative contributions of Fe-ER σ donation and π back donation are only slightly altered when R is changed from a good π donor to a poor π donor. Further investigations revealed that the electrostatic forces between the metal fragment and the diyl ligand are always attractive and are strong. It was reported that these forces arise from the attraction between the local negative charge concentration on the overall positively charged donor atom E of the Lewis base ER and the positive charge of the iron nucleus. It was found that the electrostatic interactions and covalent interactions in $(\text{CO})_4\text{Fe}(\text{ER})$ complexes have similar strength when E is Al-Tl and when R is a good π donor substituent. The Fe-BR bonds of the corresponding boranediyl complexes have

significantly higher ionic character than the heavier group 13 analogues. Calculations showed that weak π donor substituents R enhance the ionic character of the $(\text{CO})_4\text{Fe}(\text{ER})$ bond. By contrast the metal ligand bonds in the homoleptic complexes $\text{Fe}(\text{EMe})_5$ and $\text{Ni}(\text{EMe})_4$ have higher ionic character than that found in $(\text{CO})_4\text{Fe}(\text{ER})$. It was also found that the contribution of $\text{M} \rightarrow \text{ER}$ π back donation to the ΔE_{orb} term is higher, and that this contributes significantly to the total orbital interactions in the homoleptic complexes where no other π acceptor ligands are present. To put these results into context, it was reported that the BMe ligand is nearly as strong a π acceptor in $\text{Fe}(\text{BMe})_5$ as CO is in $\text{Fe}(\text{CO})_5$.

Uddin and Frenking further investigated the bonding within species including $[(\text{CO})_4\text{Fe}-\text{ECp}]$, $[(\text{CO})_4\text{Fe}-\text{EN}(\text{SiH}_3)_2]$, $[(\text{CO})_5\text{W}-\text{EN}(\text{SiH}_3)_2]$, $[(\text{CO})_4\text{Fe}-\text{EPh}]$, and $[\text{M}(\text{ECH}_3)_4]$ ($\text{M} = \text{Ni}, \text{Pd}, \text{Pt}$; $\text{E} = \text{B}, \text{Al}, \text{Ga}, \text{In}, \text{Tl}$).¹⁴ It was concluded that the bonding situation in transition metal complexes with terminal group 13 diyl ligands can be summarised by the following: (i) the M-ER bond dissociation energies are high, and substituents (R) that are weak π donors lead to strong M-ER bonds; calculated bond energies are in the order $\text{B} > \text{Al} > \text{Ga} \approx \text{In} > \text{Tl}$; (ii) the M-ER attractive interaction is mainly caused by charge attraction between the negatively charged M atoms and the positively charged group 13 atoms. Covalent contributions to the M-ER bonds are less important than Coulombic interactions. The M-ER bond order is in all cases < 1 . (iii) The M-ER σ component is larger than the M-ER π -donation when R is a strong π -donor. $\text{M} \rightarrow \text{ER}$ π back-donation becomes larger and may even become bigger than the M-ER σ -donation when R is a weak π -donor. The natural bond orbital (NBO) data revealed that the trend of the M-ER π back-donation is in most cases $\text{B} > \text{Al} > \text{Ga} > \text{In} > \text{Tl}$, while the $\text{M} \leftarrow \text{ER}$ σ -donation has an irregular

sequence. AlR is always the strongest σ -donor and TlR is the weakest σ -donor, while BR, GaR and InR have similar σ -donor strength. Uddin and Frenking summarised that the $M \leftarrow ER$ π back-donation may become significant as the $M \rightarrow ER$ σ -donation, but the sum of the covalent interactions do not even give a bond order of 1. This is different from the bonding situation in the carbyne complexes, where the bond order for the L_nM-ER bond is between 1.7 and 2.1 for Fischer type carbyne complexes, and even as high as 2.3 to 2.5 for Schrock-type carbyne complexes.

7.1.1 Aims of Research

Following the synthesis of the cationic transition metal borylene complex $[\text{CpFe}(\text{CO})_2\text{BMes}]^+[\text{BAr}_4]^-$,² the extension of this approach to heavier group 13 systems was targeted. In addition to synthetic studies, quantum chemical investigation of these species was to be explored with the aim of determining the factors affecting the nature of the M-ER bond. In particular, the method of Frenking¹³ will be employed to probe the extent of π back-bonding. Complexes of the type $[\text{Cp}^*\text{FeL}_2\text{EX}]^+$ (E = B, Ga; L_2 = dmpe, dppe; X = F, Cl, Br, I) will be examined with a view to investigating the multiple bond character within the M-EX bond; in addition isoelectronic Fe-BF, Fe-CO and Fe-N₂ species will be compared. Further calculations involving complexes such as $[(\eta^5\text{-C}_5\text{R}_5)\text{FeL}_2\text{EX}]^+$ (E = B, Ga; R = H, Me; L = CO, PH₃, PMe₃) where X is a bulky amino or alkyl group will also be investigated, as these species represent more synthetically accessible systems (*cf.* when X = halogen) and are closer to those reported within the literature. Base-stabilised species will also be investigated, as these species are also known in the literature. At the outset, preliminary studies will be carried out on the free ligands BX

(X = Cp*, Mes, NCy₂) to confirm the singlet ground states predicted by Cowley and MacDonald¹⁰ and to quantify singlet/triplet energy splittings as a function of X.

7.2 Singlet Versus Triplet States

7.2.1 Results

Table 7.1 Singlet and Triplet States for BR (R = Cp*, Mes, NCy₂)

ER fragment	Singlet (kJ mol ⁻¹)	Triplet (kJ mol ⁻¹)	Energy Diff. (kJ mol ⁻¹)
BCp*	-13605	-13445	-160
BMes	-11384	-11260	-124
BNCy ₂	-18495	-18319	-176

7.2.2 Discussion of Results

Singlet and triplet state energy calculations were performed on the three borylene diyl species BCp*, BMes and BNCy₂ with the aim of establishing the ground state electronic configuration of group 13 diyl systems. Calculations confirmed that each of the group 13 diyl species feature the ligand in a singlet ground state, for example, the calculated energies for BCp* revealed a singlet ground state energy of -13605 and an excited triplet state at -13445 kJmol⁻¹ (Table 7.1). This result is also in agreement with calculations reported by Macdonald and Cowley¹⁰ for RE species (R = η⁵-C₅H₅, η⁵-C₅H₅, Me, (H₃Si)₂NB; E = B, Al, Ga, In), which also predict singlet ground states. However, the singlet-triplet energy gap (ΔE_{S→T}) obtained by Cowley for BCp* (-223 kJmol⁻¹) differs significantly from that obtained in the current study -160 kJmol⁻¹ (Table 7.1). This difference presumably arises as a result of variation in the level of theory and basis sets used in the calculations. Moreover, the current study reveals no apparent systematic trend in ΔE_{S→T} since the order of splitting is NCy₂ > Cp* > Mes, and the order of π donor capacity is Cp* >

$\text{NCy}_2 > \text{Mes}$. However, given the confirmation of singlet ground states for each of the ligands of interest, the likely mode of bonding of these systems to transition metal fragments can then be described by utilizing an electron pair in the group 13 element σ orbital and a formally vacant π orbital (Figure 7.3).

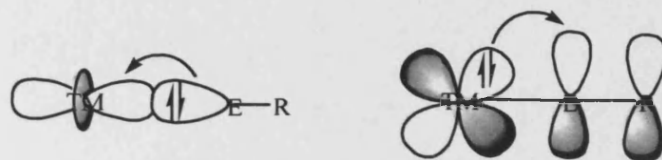


Figure 7.3 Bonding within diyl systems

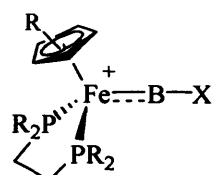
In conclusion calculations have confirmed singlet ground states for the species BCp^* , BMes , BNCy_2 . Thus the relative importance of σ , π -acceptor properties of singlet ligands with respect to transition metal centres will be investigated with the aim of determining the potential for multiple bond character between the transition metal and group 13 centres.

Table 7.3 DFT calculations of the contribution of the ligand to the overall bonding density in $(\text{Cp}^*\text{Ti}(\text{dppf}))\text{B}(\text{X})_2$ ($\text{X} = \text{F}, \text{Cl}, \text{Br}, \text{I}$)

Compound	σ	π	δ	π^*
$(\text{Cp}^*\text{Ti}(\text{dppf}))\text{BF}_2$	55%	42%	18%	15%
$(\text{Cp}^*\text{Ti}(\text{dppf}))\text{BCl}_2$	60%	40%	18%	15%
$(\text{Cp}^*\text{Ti}(\text{dppf}))\text{BBr}_2$	61%	39%	18%	15%
$(\text{Cp}^*\text{Ti}(\text{dppf}))\text{BI}_2$	57%	40%	17%	15%

7.3 EX Complexes (X = F, Cl, Br, I)

7.3.1 Results



X = F, Cl, Br, I

Table 7.2 DFT calculated σ and π contributions to the covalent bonding density in $[\text{Cp}^*\text{Fe}(\text{dppe})\text{BX}]^+$ (X = F, Cl, Br, I)

Compound	Fe-B		B-X	
	σ	π	σ	π
$[\text{Cp}^*\text{Fe}(\text{dppe})\text{BF}]^+$	47 %	53 %	62 %	38 %
$[\text{Cp}^*\text{Fe}(\text{dppe})\text{BCl}]^+$	58 %	42 %	59 %	42 %
$[\text{Cp}^*\text{Fe}(\text{dppe})\text{BBr}]^+$	58 %	42 %	62 %	38 %
$[\text{Cp}^*\text{Fe}(\text{dppe})\text{BI}]^+$	44 %	56 %	53 %	48 %

Table 7.3 DFT calculated σ and π contributions to the covalent bonding density in $[\text{Cp}^*\text{Fe}(\text{dmpe})\text{BX}]^+$ (X = F, Cl, Br, I)

Compound	Fe-B		B-X	
	σ	π	σ	π
$[\text{Cp}^*\text{Fe}(\text{dmpe})\text{BF}]^+$	58 %	42 %	55 %	45 %
$[\text{Cp}^*\text{Fe}(\text{dmpe})\text{BCl}]^+$	60 %	40 %	58 %	42 %
$[\text{Cp}^*\text{Fe}(\text{dmpe})\text{BBr}]^+$	61 %	39 %	60 %	40 %
$[\text{Cp}^*\text{Fe}(\text{dmpe})\text{BI}]^+$	53 %	46 %	51 %	50 %

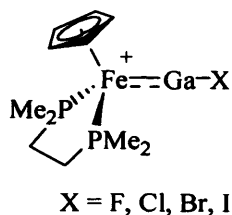


Table 7.4 DFT calculated σ and π contributions to the covalent bonding density in $[\text{Cp}^*\text{Fe}(\text{dmpe})\text{GaX}]^+$ (X = F, Cl, Br, I)

Compound	Fe-Ga		Ga-X	
	σ	π	σ	π
$[\text{CpFe}(\text{dmpe})\text{GaF}]^+$	69 %	30 %	31 %	69 %
$[\text{CpFe}(\text{dmpe})\text{GaCl}]^+$	69 %	31 %	51 %	49 %
$[\text{CpFe}(\text{dmpe})\text{GaBr}]^+$	69 %	31 %	52 %	48 %
$[\text{CpFe}(\text{dmpe})\text{GaI}]^+$	67 %	33 %	48 %	53 %

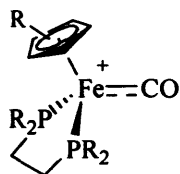


Table 7.5 DFT calculated σ and π contributions to the covalent bonding density in $[\text{Cp}^*\text{FeL}_2\text{CO}]^+$ ($L_2 = \text{dppe}, \text{dmpe}$)

Compound	Fe-C		C-O	
	σ	π	σ	π
$[\text{Cp}^*\text{Fe}(\text{dppe})\text{CO}]^+$	56 %	44 %	40 %	60 %
$[\text{CpFe}(\text{dmpe})\text{CO}]^+$	61 %	39 %	39 %	61 %

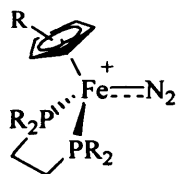


Table 7.6 DFT calculated σ and π contributions to the covalent bonding density in $[\text{Cp}^*\text{FeL}_2\text{N}_2]^+$ ($\text{L}_2 = \text{dppe}, \text{dmpe}$)

Compound	Fe-N		N-N	
	σ	π	σ	π
$[\text{Cp}^*\text{Fe}(\text{dppe})\text{N}_2]^+$	57 %	43 %	40 %	60 %
$[\text{CpFe}(\text{dmpe})\text{N}_2]^+$	61 %	38 %	39 %	61 %

7.3.2 Discussion of results

DFT calculations were performed on a range of cationic borylene and gallylene complexes featuring systematically varied halide substituents of the type $[\text{Cp}^*\text{Fe}(\text{dppe})\text{BX}]^+$, $[\text{CpFe}(\text{dmpe})\text{BX}]^+$, and $[\text{CpFe}(\text{dmpe})\text{GaX}]^+$ ($\text{X} = \text{F-I}$). From a bonding perspective, the π back bonding contribution to the covalent (orbital) components of the metal-ligand bonds of $[\text{CpFe}(\text{dmpe})\text{BX}]^+$ are significant representing 42 (BF), 40 (BCl), 39 (BBr) and 46 % (BI). A similar trend was also calculated for the corresponding $[\text{Cp}^*\text{Fe}(\text{dppe})\text{BX}]^+$ and $[\text{CpFe}(\text{dmpe})\text{GaX}]^+$ species, the latter revealing a breakdown of the covalent (orbital) components of the metal-ligand bonds within $[\text{CpFe}(\text{dmpe})\text{GaX}]^+$ as 30 (GaF), 31 (GaCl), 31 (GaBr), and 33 % π (GaI). As expected the cationic borylene species displayed the greater π backbonding character when compared to the analogous gallylene systems. This presumably arises as a result of the poorer orbital overlap of gallium compared to boron and π back donation being less significant for gallium compared to boron. Essential to a discussion of the nature of the transition metal-ligand bond is the extent of both σ donation from the ER fragment to the metal centre and the π acceptor ability

of E. Well-matched orbital energies from the EX fragment and efficient orbital overlap are essential for the formation of stable metal-ligand bonds. The two main factors which are likely to determine the degree of σ donation and π acceptance within these transition metal-diyl systems are (i) the electronegativity of the EX fragment and (ii) the nature of the orbital overlap. It would be expected that BF would be a poorer σ donor than BCl, BBr or BI due to the electron withdrawing effect of F. From a π backbonding viewpoint in the case of the $[\text{Cp}^*\text{Fe}(\text{dppe})\text{BX}]^+$ and $[\text{CpFe}(\text{dmpe})\text{BX}]^+$ systems, it would be expected that the overlap between E and X would be in the order $\text{B-F} > \text{B-Cl} > \text{B-Br} > \text{B-I}$, with B-F exhibiting the most effective overlap and B-I the least. On this basis the degree of backbonding would be in the order of $\text{B-F} < \text{B-Cl} < \text{B-Br} < \text{B-I}$. However, from an electronegativity perspective the electronegativity difference is greatest for B-F and smallest for B-I. This difference in electronegativity will affect the composition of the π^* antibonding orbital of the ligand (*i.e.* the LUMO). The larger the electronegativity difference, the more the LUMO is polarised towards boron. Thus on this basis it would be expected that the overlap of the iron centre with the LUMO would be greatest for BF and smallest for BI. Hence the orbital overlap and electronegativity contributions oppose each other and thus the trend observed in π backbonding appears to result as a trade off between these two factors.

Density functional theory (DFT) analyses of electronic structure were also carried out using the model systems $[\text{CpFe}(\text{dmpe})\text{CO}]^+$ and $[\text{CpFe}(\text{dmpe})\text{N}_2]^+$ to compare the multiple bonding within these species compared with analogous group 13 halide complexes. Here too, calculations revealed that the orbital interactions of π symmetry are also significant (representing 39 (CO) and 38 % (N_2) of the total

covalent bonding density). Previous computational studies for charge neutral metal complexes have predicted stronger σ donor properties for BX (X = F, NH₂, NMe₂), compared to CO. Baerends *et al.* investigated the bonding within CO and its isolobal analogues such as BF,^{6c} showing that for the formation of stable metal-ligand bonds it is essential to have significant σ donation through the 5 σ orbital, and π acceptance through the 2 π orbitals. It was reported that CO has just the right orbital electronic structure to provide balanced, synergic bonding having a moderately high-energy 5 σ HOMO, largely localised on carbon and directed towards the metal centre, and moderately low-energy 2 π LUMOs which are also localised to a large extent on carbon. It was found that the 5 σ orbitals are at higher energy and the 2 π^* are at lower energy in BF (*cf.* CO). The frontier orbitals of BF are also more strongly localised on the boron atom. Thus, the polar BF molecule was found to bind even better to first row transition metal centres than CO predominately because of its excellent σ donor properties, with its π -acceptor capability only being slightly stronger. Similarly, a comparison of the free ligands BNH₂ and CCH₂ reported by Bickelhaupt, Hoffmann and Baerends,⁶ revealed a greater localisation of the HOMO (σ donor) and LUMO (π acceptor) orbitals on the donor atom in the case of BNH₂. In each case the breakdown of the covalent (orbital) components of the metal-ligand bonds of Fe-GaI, Fe-BF, Fe-CO, Fe-N₂, revealed π symmetry interactions of 33 (GaI), 42 (BF), 39 (CO), and 38 % (N₂) of the total covalent density. This trend presumably arises as a result of the electronegativity of the EX fragment (i.e. the energy of the HOMO) (Figure 7.4), the nature of the orbitals and their interaction with the [CpFe(dmpe)]⁺ fragment. Thus BF comprises a higher π orbital interaction than CO and N₂ due to its greater electronegativity and the effective orbital overlap of the EX ligand with the [CpFe(dmpe)]⁺ fragment. Despite the higher energy of the HOMO for GaI (-6.08 eV

cf. -9.03 eV for CO) and the greater localisation of the LUMO at the donor atom, the weaker orbital contribution for GaI compared to BF, CO and N_2 reflects (at least in part) the more diffuse nature of the 4s/4p derived orbitals at gallium and less effective fragment orbital of $[CpFe(dmpe)]^+$. Thus BF displays the greatest π orbital contribution with GaI displaying the least.

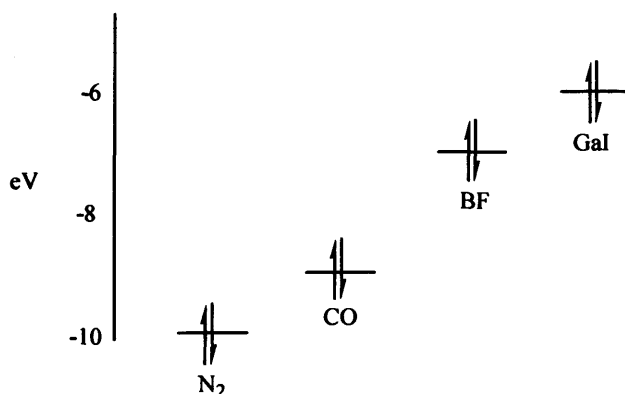


Figure 7.4 Relative energies of the HOMO orbital within N_2 , CO, BF and GaI

Interestingly, calculations revealed that on substitution of the dmpe and Cp ligands on the iron centre for dppe and Cp^* the π backbonding contribution increased for the EX, CO and N_2 species.

7.4 Sterically Demanding Borylene and Gallylene Complexes

7.4.1 Results

Table 7.7 Borylene systems

Compound	Fe-B		B-R	
	σ	π	σ	π
[CpFe(CO) ₂ BNCy ₂] ⁺	71 %	29 %	64 %	36 %
[Cp ⁱ Fe(CO) ₂ BN ⁱ Pr ₂] ⁺	69 %	31 %	60 %	40 %
[CpFe(PMe ₃) ₂ BNCy ₂] ⁺	63 %	37 %	66 %	34 %
[Cp ⁱ Fe(CO) ₂ BN ⁱ Pr ₂] ⁺	70 %	30 %	63 %	37 %
[CpFe(PMe ₃) ₂ BMes] ⁺	60 %	40 %	–	–
[CpFe(CO) ₂ BCp*] ⁺	86 %	14 %	–	–

Table 7.8 Gallylene systems

Compound	Fe-Ga		Ga-R	
	σ	π	σ	π
[CpFe(CO) ₂ GaMes] ⁺	77 %	23 %	–	–
[CpFe(CO) ₂ GaN ⁱ Pr ₂] ⁺	80 %	20 %	60 %	40 %
[CpFe(CO) ₂ GaNCy ₂] ⁺	80 %	19 %	61 %	39 %
[CpFe(PMe ₃) ₂ GaNMe ₂] ⁺	68 %	32 %	–	–
[CpFe(PH ₃) ₂ GaNMe ₂] ⁺	72 %	28 %	–	–
[CpFe(PMe ₃) ₂ GaN ⁱ Pr ₂] ⁺	66 %	34 %	66 %	35 %
[CpFe(PH ₃) ₂ GaNCy ₂] ⁺	69 %	31 %	60 %	40 %
[CpFe(PH ₃) ₂ GaMes] ⁺	70 %	30 %	–	–

Table 7.9 Vinylidene systems

Compound	Fe-C		C-R	
	σ	π	σ	π
[CpFe(CO) ₂ CC ⁱ Pr ₂] ⁺	66 %	34 %	43 %	58 %
[CpFe(CO) ₂ CCMe ₂] ⁺	65 %	35 %	45 %	55 %

7.4.2 Discussion of Results

DFT calculations were performed on a range of cationic borylene and gallylene complexes having varying R substituents with the aim of examining the relative/importance of σ and π contribution to covalent bonding between the group 13 and transition metal centres. By varying the substituents on the group 13 and transition metal centres it was found that the $M \rightarrow E$ π backbonding contribution changes dramatically. In addition, DFT calculations revealed a difference in the covalent (orbital) component of the metal ligand bonds between the boron-based species and the gallium-containing systems. As expected, the borylene compounds exhibited greater π backbonding character than the analogous gallylene species. The calculated σ/π bonding components revealed for $[\text{CpFe}(\text{CO})_2\text{BNCy}_2]^+$ (71 % σ and 29 % π) and for $[\text{CpFe}(\text{CO})_2\text{GaNcy}_2]^+$ (80 % σ and 20 % π). This trend presumably arises as a result of the poorer orbital overlap for gallium due to the more diffuse nature of the orbitals and higher energies of the gallium p orbital.

Varying the R substituents on the group 13 centre was investigated revealing that for both the cationic borylene and gallylene systems the $M \rightarrow E$ π backbonding character was greater when the R fragment was an aryl group compared to an amino group. For example, the calculated π symmetry covalent (orbital) component within the Fe-Ga bond of $[\text{CpFe}(\text{CO})_2\text{GaMes}]^+$ was 23 %; analogous calculations for the related systems $[\text{CpFe}(\text{CO})_2\text{GaNcy}_2]^+$ and $[\text{CpFe}(\text{CO})_2\text{GaN}^i\text{Pr}_2]^+$ revealed π contributions of 20 % and 19 % respectively (Table 7.8). Similarly, the calculated $M \rightarrow E$ π backbonding contribution for the borylene species $[\text{CpFe}(\text{CO})_2\text{BMes}]^+$, $[\text{CpFe}(\text{CO})_2\text{BNCy}_2]^+$ and $[\text{CpFe}(\text{CO})_2\text{BN}^i\text{Pr}_2]^+$ were 34 %, 29 % and 30 %, respectively (Table 7.7). These trends presumably arise as a result of the good π

donating properties of the nitrogen centre compared to carbon. Thus, when the R substituent is an amino group, the nitrogen centre donates electron density to the group 13 metal, as a result the requirement of the transition metal to supplement the electron density at the group 13 centre is less and thus the M→E π backbonding contribution decreases. In addition, the differences on going from mesityl to amino substituents are larger for boron than gallium as π bonding is more relevant for the lighter group 13 element.

The substitution of the CO ligands on the transition metal centre for less π acidic fragments was also investigated. In general the relative contributions from σ and π symmetry covalent interactions to the M-E bond reflect the expected trends in the σ donor/ π acceptor properties of the diyl ligand and in the electronic properties of the metal-ligand fragment. Unlike CO, trialkyl phosphines are strong donors but poor acceptors, and as such it would be expected that substitution of a phosphine ligand for CO would increase the M→E π backbonding component. Calculations revealed that the nature of the ligand at the transition metal centre affects the degree of π backbonding within borylene and gallylene species but not as much as the diyl substituent itself. Thus compared to the model complex $[\text{CpFe}(\text{CO})_2\text{GaMes}]^+$, the significance of π back-bonding is enhanced for phosphine ligated complex $[\text{CpFe}(\text{PH}_3)_2\text{GaMes}]^+$ (30 % of the orbital contribution to the bond, *cf.* $[\text{CpFe}(\text{CO})_2\text{GaMes}]^+$ 23 %) (Table 7.8). Similarly, the borylene complex $[\text{CpFe}(\text{CO})_2\text{BNCy}_2]^+$ revealed σ : π bonding covalent contributions of 71:29 % whereas the analogous phosphine species $[\text{CpFe}(\text{PMe}_3)_2\text{BNCy}_2]^+$ featured σ : π covalent contributions of 63:37 % (Table 7.7). This trend is unsurprising as CO is a stronger π acid and thus is a better electron acceptor. As a result CO directly

competes with the group 13 ER fragment for electron density from the transition metal centre and thus the degree of back donation to the group 13 metal is significantly reduced. In addition, the larger difference in π bonding values on going from PR_3 to CO is greater for boron than gallium, π backbonding being more relevant for boron than gallium. Another interesting feature worth noting is the increase in π back donation on going from $[\text{CpFe}(\text{PH}_3)_2\text{GaNMe}_2]^+$ to $[\text{CpFe}(\text{PMe}_3)_2\text{GaNMe}_2]^+$ (28 % and 32 %, respectively) (Table 7.8) as expected on the basis of the electron donating abilities of PH_3 vs PMe_3 .

7.5 Base Stabilised Adducts

7.5.1 Results

Table 7.10 Base stabilised adducts

Compound	Fe-B		B-N	
	σ	π	σ	π
$[\text{CpFe}(\text{CO})_2\text{BNCy}_2(\text{pic})]^+$	87 %	14 %	83 %	18 %
$[\text{CpFe}(\text{CO})_2\text{BN}^i\text{Pr}_2(\text{imine})]^+$	88 %	12 %	64 %	36 %
$[\text{CpFe}(\text{CO})_2\text{BN}^i\text{Pr}_2(\text{Ph}_3\text{PO})]^+$	90 %	11 %	65 %	35 %
$[\text{CpFe}(\text{CO})_2\text{BN}^i\text{Pr}_2(\text{Ph}_3\text{PS})]^+$	87 %	13 %	64 %	36 %

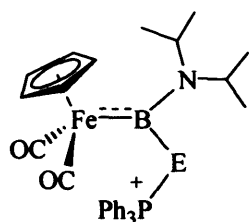
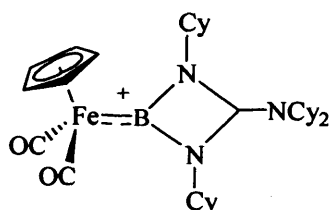


Table 7.11 Ph_3PO adduct $[\text{CpFe}(\text{CO})_2\text{BN}^i\text{Pr}_2(\text{Ph}_3\text{PO})]^+$

Bonding	PO aligned	BO aligned	BFe aligned	BN aligned
σ	45 %	89 %	90 %	65 %
π	55 %	11 %	11 %	35 %

Table 7.12 Ph₃PS adduct [CpFe(CO)₂BNⁱPr₂(Ph₃PS)]⁺

Bonding	PS aligned	BS aligned	BFe aligned	BN aligned
σ	41 %	74 %	87 %	64 %
π	59 %	26 %	13 %	36 %

**Table 7.13** [CpFe(CO)₂B(NCy)₂CNCy₂]⁺

Compound	Fe-E		Total bonding energy kJmol ⁻¹
	σ	π	
[CpFe(CO) ₂ B(NCy) ₂ CNCy ₂] ⁺	83 %	17 %	-47184

7.5.2 Discussion of Results

DFT calculations were also performed on a range of cationic base stabilised diyl adducts. Varying the EPPH₃ (E = O, S) component within CpFe(CO)₂BNⁱPr₂(EPPH₃)⁺ revealed that there was no significance difference in the π back-bonding contribution on coordination of SPPH₃ (13 %) compared to OPPH₃ (11 %). It should be noted that the difference in the covalent (orbital) component of the metal-ligand bond within cationic M-B(R)L systems is significantly less than that found within M-BR cationic species (*cf.* [CpFe(CO)₂BNⁱPr₂]⁺ 30 %, and [CpFe(CO)₂BNCy₂]⁺ 29 %). This trend arises as a result of the lower coordination and hence highly electron deficient nature of the boron centre within MBR cationic species compared to M-B(R)L cationic systems.

DFT calculations involving the base stabilised species $[\text{CpFe}(\text{CO})_2\text{BN}(\text{Cy})_2(\text{picoline})]^+$, $[\text{CpFe}(\text{CO})_2\text{BN}^i\text{Pr}_2(\text{imine})]^+$ and $[\text{CpFe}(\text{CO})_2\text{B}(\text{NCy})_2\text{CNCy}_2]^+$ were investigated. It was found that $[\text{CpFe}(\text{CO})_2\text{BN}(\text{Cy})_2(\text{picoline})]^+$ ($\sigma:\pi$ 86:14 %), $[\text{CpFe}(\text{CO})_2\text{BN}^i\text{Pr}_2(\text{imine})]^+$ ($\sigma:\pi$ 88:12 %) and $[\text{CpFe}(\text{CO})_2\text{B}(\text{NCy})_2\text{CNCy}_2]^+$ ($\sigma:\pi$ 83:17 %) all feature a minor π backbonding component. These results are consistent with those found for $[\text{CpFe}(\text{CO})_2\text{BCp}^*]^+$ ($\sigma:\pi$ 86:14 %), which in effect can be viewed as a base stabilised species in which the Cp^* ring coordinates to the boron centre in an η^5 bonding mode.

7.6 Conclusions and Suggestions for Further Research

At the outset, we sought, through DFT calculations, to characterise the nature of the metal-group 13 element interaction in cationic diyl complexes, to assess the merits of a simple bonding model for complexes of the type $[(\eta^5\text{-C}_5\text{R}_5)\text{Fe}(\text{L})\text{EX}]^+$ ($\text{R} = \text{H}, \text{CH}_3$; $\text{L} = (\text{CO})_2, \text{dppe}, \text{dmpe}$; $\text{E} = \text{B}, \text{Ga}$), comprising $\text{E} \rightarrow \text{Fe}$ σ donation, supplemented by $\text{Fe} \rightarrow \text{E}$ π back donation. Given the calculated data it is now possible to draw a number of conclusions concerning the nature of the metal-ligand bond in the complexes investigated. The relative importance of the π symmetry covalent component for cationic borylene systems is similar to that for carbene type ligands, with π back-donation being less important for cationic gallylene systems. The trend in the orbital interaction of π symmetry observed for $[\text{CpFe}(\text{dmpe})\text{GaI}]^+$ (33 %), $[\text{CpFe}(\text{dmpe})\text{BF}]^+$ (42 %), $[\text{CpFe}(\text{dmpe})\text{CO}]^+$ (39 %), $[\text{CpFe}(\text{dmpe})\text{N}_2]^+$ (38 %) arises as a result of the electronegativity of the EX fragment (*i.e.* the energy of the HOMO) and the nature of the orbitals and their interaction with the $[\text{CpFe}(\text{dmpe})]^+$ fragment. Thus BF comprises a higher π orbital interaction than CO and N_2 due to its greater electronegativity resulting from the fluoride moiety and the effective orbital overlap

of the EX ligand with the $[\text{CpFe}(\text{dmpe})]^+$ fragment. This result is consistent with earlier reports by Baerends *et al.* in which BF was found to bind to first row transition metal complexes even better than CO due to excellent σ donor properties and slightly stronger π acceptor capabilities.^{6c} In the case of GaI it was found that despite the higher energy of the HOMO (-6.03 eV cf. -9.08 eV for CO) and the greater localisation of the LUMO at the donor atom, the weaker orbital contribution was observed (*cf.* BF, CO and N_2) reflecting (at least in part) the more diffuse nature of the 4s/4p derived orbitals at gallium and the less effective interaction with the fragment orbitals of $[\text{CpFe}(\text{dmpe})]^+$. Thus BF displays the greatest π orbital contribution with GaI displaying the least. These results also support experimental studies in which CO readily displaces the GaI fragment within $[\text{Cp}^*\text{Fe}(\text{dppe})\text{GaI}]^+$ yielding $[\text{Cp}^*\text{Fe}(\text{dppe})\text{CO}]^+$, presumably arising as a result of the stronger metal-ligand bond strengths of CO compared to GaI

The significance of π back bonding is enhanced for phosphine ligated (*cf.* carbonyl systems) species reflecting the absence of competing strongly acidic carbonyl ligands. As expected π back donation is significantly reduced on coordination of a base to the group 13 centre.

7.7 References for Chapter Seven

- (a) Cowley, A. H.; Lomeli, V.; Voight, A. *J. Am. Chem. Soc.* **1998**, *120*, 6401. (b) Braunschweig, H.; Kollann, C.; Englert, U. *Angew. Chem. Int. Ed.* **1998**, *37*, 3179. (c) Braunschweig, H.; Colling, M.; Kollann, C.; Stammler, H. G.; Neumann, B. *Angew. Chem. Int. Ed.* **2001**, *40*, 2299. (d) Braunschweig, H.; Colling, M.; Kollann, C.; Merz, K.; Radacki, K. *Angew. Chem. Int. Ed.* **2001**, *40*, 4198. (e) Braunschweig, H.; Colling, M.; Hu, C.; Radacki, K. *Angew. Chem. Int. Ed.* **2003**, *42*, 205. (f) Braunschweig, H.; Colling, M. *Eur. J. Inorg. Chem.* **2003**, 383. (g) Irvine, G. J.; Rickard, C. E. F.; Roper, W. R.; Williamson, A.; Wright, L. J. *Angew. Chem. Int. Ed.* **2000**, *39*, 948. (h) Rickard, C. E. F.; Roper, W. R.; Williamson, A.; Wright, L. J. *Organometallics* **2002**, *21*, 4862. (i) Braunschweig, H. *Adv. Organomet. Chem.* **2004**, *51*, 163.
- (a) Coombs, D. L.; Aldridge, S.; Jones, C.; Willock, D. J. *J. Am. Chem. Soc.* **2003**, *125*, 6356. (b) Aldridge, S.; Rossin, A.; Coombs, D. L.; Willock, D. J. *Dalton Trans.* **2004**, 2649.
- (a) Su, J.; Li, X.-W.; Crittendon, R. C.; Campana, C. F.; Robinson, G. H. *Organometallics* **1997**, *16*, 4511. (b) Cotton, F. A.; Feng, X.; *Organometallics*, **1998**, *17*, 128.
- (a) Jutzi, P.; Neumann, B.; Reumann, G.; Stammler, H.-G. *Organometallics*, **1998**, *17*, 1305. (b) Fischer, R. A.; Schulte, M. M.; Weiss, J.; Zsolnai, L.; Jacobi, A.; Huttner, G.; Frenking, G.; Boehme, C.; Vyboishchikov, S. F. *J. Am. Chem. Soc.* **1998**, *120*, 1237. (c) Reger, D. L.; Garza, D. G.; Rheingold, A. L.; Yap, G. P. A. *Organometallics* **1998**, *17*, 3624. (d) Linti, G.; Köster, W. *Chem. Eur. J.* **1998**, *4*, 942. (e) Uhl, W.; Benter, M.; Melle, S.; Saak, W.; Frenking, G.; Uddin, J. *Organometallics*, **1999**, *18*, 3778. (f) Fölsing, H.; Segnitz, O.; Merz, K.; Winter, M.; Fischer, R. A. *J. Organomet. Chem.* **2000**, *606*, 132. (g) Weiß, W.; Winter, M.; Merz,

K.; Knüfer, A.; Fischer, R. A.; Fröhlich, N.; Frenking, G. *Polyhedron*, **2002**, *21*, 535.

(h) Harman, N. J.; Wright, R. J.; Phillips, A. D.; Power, P. P. *J. Am. Chem. Soc.* **2003**, *125*, 2667. (i) Cokoja, M.; Gemel, C.; Steinke, T.; Schröder, F.; Fischer, R. A. *Dalton Trans.* **2005**, 44. (j) Steinke, T.; Gemel, M.; Cokoja, M.; Winter, M.; Fischer, R. A. *Dalton Trans.* **2005**, 55. (k) Haubrich, S. T.; Power, P. P. *J. Am. Chem. Soc.* **1998**, *120*, 2202.

5. (a) Frenking, G.; Fröhlich, N. *Chem. Rev.* **2000**, *100*, 717. (b) Boehme, C.; Uddin, J.; Frenking, G. *Coord. Chem. Rev.* **2000**, *197*, 249. (c) Uddin, J.; Frenking, G. *J. Am. Chem. Soc.* **2001**, *123*, 1683. (d) Chen, Y.; Frenking, G. *Dalton Trans.* **2001**, 434.

6. (a) Bickelhaupt, F. M.; Radius, U.; Ehlers, A. W.; Hoffmann, R.; Baerends, E. J. *New J. Chem.* **1998**, 1. (b) Radius, U.; Bickelhaupt, F. M.; Ehlers, A. W.; Goldberg, N.; Hoffmann, R. *Inorg. Chem.* **1998**, *37*, 1080. (c) Ehlers, A. W.; Baerends, E. J.; Bickelhaupt, F. M.; Radius, U. *Chem. Eur. J.* **1999**, *4*, 210.

7. (a) Weiss, J.; Stetzkamp, D.; Nuber, B.; Fisher, R. A.; Boehme, C.; Frenking, G. *Angew. Chem. Int. Ed.* **1997**, *36*, 70. (b) Cotton, F. A.; Frenking, G. *Angew. Chem. Int. Ed.* **1997**, *36*, 70. (c) Cotton, F. A.; Feng, X. *Organometallics* **1998**, *17*, 128. (d) Boehme, C.; Frenking, G. *Chem. Eur. J.* **1999**, *5*, 2184. (e) Linti, G.; Schnöckel, H. *Coord. Chem. Rev.* **2000**, *206-207*, 285.

8. Uhl, W.; Pohlmann, M.; Wartchow, R. *Angew. Chem.* **1998**, *110*, 1007; *Angew. Chem. Int.* **1998**, *37*, 961.

9. Uhl, W.; Benter, M.; Melle, S.; Saak, W.; Frenking, G.; Uddin, J. *Organometallics* **1999**, *18*, 3778.

10. Macdonald, C. L. B.; Cowley, A. H. *J. Am. Chem. Soc.* **1999**, *121*, 12113.

11. Braunschweig, H.; Kollan, C.; Englert, U. *Angew. Chem. Int. Ed.* **1998**, *37*, 3179.

12. For recent discussions, see (a) Wrackmeyer, B. *Angew. Chem. Int. Ed.* **1999**, *38*, 771. (b) Murugavel, R.; Chandrasekhar, V. *Angew. Chem. Int. Ed.* **1999**, *38*, 1211.
13. Uddin, J.; Frenking, G. *J. Am. Chem. Soc.* **2001**, *123*, 1683.
14. Uddin, J.; Boehme, C.; Frenking, G. *Organometallics* **2000**, *19*, 571

Appendix One

List of Publications

1. Coombs, Natalie D.; Vidovic, Drasko.; Day, Joanna K; Thompson, Amber L.; Stasch, Andreas.; Clegg, William.; Rosso, Luca.; Male, Louise.; Hursthouse, Micheal B.; Willock, David J.; Aldridge, Simon. **Cationic terminal gallylene complexes by halide abstraction: Coordination chemistry of a valence isoelectronic analogue of CO and N₂**. Submitted.
2. Pierce, Glesni. A.; Vidovic, Drasko.; Kays, Deborah. L.; Coombs, Natalie. D.; Thompson, Amber. L.; Willock, David. J.; Jemmis, E. D.; De, S.; Aldridge, Simon. **Half-sandwich group 8 borylene complexes: Synthetic and structural studies, and oxygen atom abstraction**. Submitted.
3. Pierce, Glesni. A.; Vidovic, Drasko.; Kays, Deborah. L.; Coombs, Natalie. D.; Thompson, Amber. L.; Willock, David. J.; Jemmis, E. D.; De, S.; Aldridge, Simon. **Reactivity of cationic terminal borylene complexes: Novel mechanisms for insertion and metathesis chemistry involving strongly Lewis acidic ligand systems**. Submitted
4. Coombs, Natalie D.; Clegg, William; Willock, David. J.; Aldridge, Simon. **A Group 13/Group 17 analogue of CO and N₂: Coordinative trapping of the GaI molecule**. *Journal of the American Chemical Society*. **2008**, *130*, 5449-5451.*
* This paper was also cited as a highlight from the recent chemical literature *Angew. Chem. Int. Ed.* **2008**, *47*, 2.
5. Coombs, Natalie D.; Stasch, Andreas.; Aldridge, Simon. **Reactions of 'GaI' with organometallic transition metal halides**. *Inorganica Chimica Acta*. **2008**, *361*, 449-456.
6. Coombs, Natalie D.; Stasch, Andreas.; Cowley, Andrew.; Thompson, Amber. E.; Aldridge, Simon. **Bulky aryl functionalised carbazolyl ligands; Amido alternatives to the 2,6-diarylphenyl ligand class?** *Dalton Transactions* **2008**, *3*, 332-337. (selected as a HOT article).
7. Coombs, Natalie. D.; Watkin, David. J.; Aldridge, Simon. **Crystal Structure of $[(\eta^5\text{-C}_5\text{Me}_5)\text{Fe}(\text{CO})_2\text{In}(\text{C}_6\text{H}_2\text{Bu}'_{3-2,4,6})_2(\mu\text{-F})]^+[\text{BF}_4]_3(\text{CH}_2\text{Cl}_2)$** . *Analytical Science*. **2008**, *24*, in press.
8. Coombs, Natalie D.; Aldridge, Simon; Thompson, Amber L.; Male, Louise; Hursthouse, Michael B. **Crystal structures of $[\text{L}_n\text{E}]^+[(\eta^7\text{-C}_7\text{H}_7)\text{Mo}(\text{CO})_2\text{GaI}_3]^-$ ($\text{L}_n\text{E} = (\text{thf})_4\text{Li}$, Cy_3PH)**. *Analytical Sciences: X-Ray Structure Analysis Online* **2007**, *23*, 213-214.
9. Pierce, Glesni A.; Coombs, Natalie D.; Willock, David J.; Day, Joanna K.; Stasch, Andreas; Aldridge, Simon. **Insertion reactions of dicyclohexylcarbodiimide with aminoboranes, -boryls and -borylenes**. *Dalton Transactions* **2007**, *39*, 4405-4412.

10. Coombs, Natalie D.; Aldridge, Simon; Stasch, Andreas. **Crystal structure of $[(\eta^7\text{-C}_7\text{H}_7)\text{Mo}(\text{CO})_2\text{Ga}]_2(\mu\text{-OGaI}_3)\{\mu\text{-OGaI}(\text{OH})_2\}_2\text{3benzene}$** . Analytical Sciences: X-Ray Structure Analysis Online **2007**, *23*, 57-58.
11. Pierce, Glesni A.; Aldridge, Simon.; Jones, Cameron.; Gans-Eichler, Timo.; Stasch, Andreas.; Coombs, Natalie D.; Willock, David J. **Cationic terminal aminoborylene complexes: Controlled stepwise insertion into M=B and B=N double bonds**. Angewandte Chemie, International Edition **2007**, *46*, 2043-2046. (selected as a VIP paper).
12. Coombs, Natalie, D.; Day, Joanna K.; Aldridge, Simon.; Coles, Simon J.; Hursthouse, Micheal B. **Linking of main group metals via bridging halide ligands: Structures of the bromoindanediyl dimer $[(\text{CpFe}(\text{CO})_2)_2\text{InBr}]_2$ and the related lithium bromide adduct $[\text{CpFe}(\text{CO})_2)_2\text{In}(\mu\text{-Br})_2\text{Li}(\text{OEt})_2$** . Main Group Metal Chemistry, **2007**, *30*, 195-198.
13. Aldridge, Simon; Jones, Cameron; Gans-Eichler, Timo; Stasch, Andreas; Kays, Deborah L.; Coombs, Natalie D.; Willock, David J. **Cationic terminal borylene complexes: structure/bonding analysis and [4+1] cycloaddition reactivity of a BN vinylidene analogue**. Angewandte Chemie, International Edition **2006**, *45*, 6118-6122.
14. Coombs, Natalie D.; Bunn, Natalie R.; Kays, Deborah L.; Day, Joanna K.; Ooi, Li-Ling; Aldridge, Simon. **Substitution, abstraction and addition chemistry of low-coordinate gallium and indium ligand systems**. Inorganica Chimica Acta **2006**, *359*, 3693-3698.
15. Aldridge, Simon; Baker, Robert J.; Coombs, Natalie D.; Jones, Cameron; Rose, Richard P.; Rossin, Andrea; Willock, David J. **Complexes of a gallium heterocycle with transition metal dicyclopentadienyl and cyclopentadienylcarbonyl fragments, and with a dialkylmanganese compound**. Dalton Transactions **2006**, *27*, 3313-3320.
16. Aldridge, Simon; Kays, Deborah L.; Bunn, Natalie R.; Coombs, Natalie D.; Ooi, Li-ling. **Structures of the metallated trihalogallate and indate ions $[(\eta^5\text{-C}_5\text{Me}_5)\text{Fe}(\text{CO})_2\text{InI}_3]^-$ and $[(\eta^5\text{-C}_5\text{H}_5)\text{Fe}(\text{CO})_2\text{GaI}_2\text{Br}]^-$** . Main Group Metal Chemistry **2005**, *28*, 201-205.
17. Bunn, Natalie R.; Aldridge, Simon; Kays, Deborah L.; Coombs, Natalie D.; Rossin, Andrea; Willock, David J.; Day, Joanna K.; Jones, Cameron; Ooi, Li-ling. **Halide Abstraction as a Route to Cationic Transition-Metal Complexes Containing Two-Coordinate Gallium and Indium Ligand Systems**. Organometallics **2005**, *24*, 5891-5900.
18. Bunn, Natalie R.; Aldridge, Simon; Kays, Deborah L.; Coombs, Natalie D.; Day, Joanna K.; Ooi, Li-ling; Coles, Simon J.; Hursthouse, Michael B. **Towards Cationic Gallane- and Indanediyl Complexes: Synthetic Approaches to Three-Coordinate Halogallyl and -indyl Precursors**. Organometallics **2005**, *24*, 5879-5890.

